SYNTHESIS AND STRUCTURAL STUDIES OF NOVEL ACYCLIC UNSYMMETRIC FUNCTIONALIZED IMIDES AND MECHANISTIC STUDIES ON E. COLI ASPARAGINE SYNTHETASE B

By

JOSE G. ROSA RODRIGUEZ

A DISSERTATION PRESENTED TO THE GRADUATE SCHOOL
OF THE UNIVERSITY OF FLORIDA IN PARTIAL FULFILLMENT
OF THE REQUIREMENTS FOR THE DEGREE OF
DOCTOR OF PHILOSOPHY

UNIVERSITY OF FLORIDA

1996

To my wife and family.

ACKNOWLEDGMENTS

First I would like to thank my advisor, Dr. Nigel G. J. Richards, for his guidance, patience, support, and valuable input throughout this entire journey. Second, I would like to thank Dr. Sheldon M. Schuster for his advice, input, and useful discussions on enzyme kinetics, and for the excellent food I consumed on Friday afternoons. Third, I want to thank Dr. Susan K. Boehlein for her advice and instructive conversations and for conducting all enzyme assays in this study. I also would like to thank Dr. William Dolbier Jr., Dr. Eric Enholm, and Dr. Gus Palenik for their advice and valuable suggestions. I could not have done it without the help from these important people. They have my appreciation and best wishes for the future.

Next, I would like to thank my colleagues Anthony (Tony) B. Dribben, Yannis (Janice) Karayannis, Nagraj (Nag) Bokinkere, Rajiv (Raju) Moghe, and Susan (Sue) Rasmussen for daily productive and nonproductive conversations in the topics of chemistry and life. Special thanks go to Tony Dribben for useful advice regarding computers and computational chemistry. I wish all of them the best in the future and hope to see them again.

Special thanks go to my wife, Lymari Montalvo, for her company, love, and support throughout these years of graduate study and to her family, Jose A. Montalvo, Carmen Montalvo, and Omar Montalvo, for their support. My personal thanks go to my mother and father, Ana Lydia Rodriguez and Jose L. Rosa, my father's wife, Nancy Rosa, and my brothers and sister, Jose L. Rosa, Ricardo J. Rosa, and Ana B. Del Cueto, for helping me througout these years and throughout my life in one way or another.

Last but not least, I want to thank Dr. John F. Helling and Dr. Michael J. Phillip for giving me the opportunity to develop myself as a professional at this institution. I will always be grateful.

TABLE OF CONTENTS

AKNOWLEDGEMENTS iii

LIST OF FIGURES viii

ABSTRACT xviii

CHAPTERS

1 STRUCTURE AND FUNCTION OF AMIDOTRANSFERASES AND E. COLI ASPARAGINE SYNTHETASE B 1

The Amidotransferases 1
Asparagine Synthetase 6
Structure and Function 6
Reaction Mechanism 10
E. Coli Asparagine Synthetase B 17
Structure and Function 17
Reaction Mechanism 18
Specific Aims 28

2 REVIEW OF ACYCLIC IMIDE SYNTHETIC METHODOLOGY 30

Introduction 30
Imides from Amides or Amines and Acid Anhydrides 32
Imides from Amides or Amines and Acid Chlorides 41
Imides from Nitriles and Carboxylic Acids 53
Imides from Amides 58
Imides from Amide Anions 59
Imides from Amides and Ketenes 62
Imides from Isocyanates and Acid Anhydrides 64
Miscellaneous Methods 65
Concluding Remarks 71

3 SYNTHESIS AND PROPERTIES OF HIGHLY FUNCTIONALIZED UNSYMMETRIC ACYCLIC IMIDES 73

Designing the Enzyme Imide Intermediate 73
Synthesis of Di-protected L-Glutamine Derivatives 76
Synthesis of Di-protected L-Aspartic Acid Derivatives 79
Synthesis of Protected Imide Intermediate 80
Deprotections of Imide Intermediate 85
Other Novel Imide Derivatives of L-Glutamine 86
Deprotections of Novel Nγ-Acylated L-Glutamine

Derivatives 94
Stability Studies of Novel Nγ-Acylated L-Glutamine Derivatives 97
The Structure of Nγ-Acylated L-Glutamine Derivatives 121

4 MECHANISTIC STUDIES OF E. COLI ASPARAGINE SYNTHETASE B 137

Introduction 137
Enzyme Assay Design 139
Reaction of Imide **12** with Wild Type E. Coli Asparagine Synthetase B 144
Studies of Imide **12** with C1A and C1S Mutants of E. Coli Asparagine Synthetase B 146

5 INHIBITION STUDIES OF E. COLI ASPARAGINE SYNTHETASE B 155

Re-engineering the Function of E. Coli Asparagine Synthetase B from Amidohydrolase to Nitrile Hydratase 155
Introduction 155
Rational Design and Synthesis of a Nitrile L-Glutamine Analog 160
Stability Studies of Nitrile L-Glutamine Analog ... 161
Studies of Nitrile L-Glutamine Analog with E. Coli Asparagine Synthetase B 172
Design and Synthesis of Other Potential Inhibitors of E. Coli Asparagine Synthetase B 176
Introduction 176
Rational Design and Synthesis of L-Glutarimide 177
Rational Design and Synthesis Towards an α,β-Unsaturated L-Glutamine Analog 180
Inhibition Studies of Potential Inhibitors with Wild-Type E. Coli Asparagine Synthetase B 183

6 CONCLUSIONS 184

Synthesis and Properties of Acyclic Unsymmetric Functionalized Imides 184
Mechanistic and Inhibition Studies on E. coli Asparagine Synthetase B 185

7 EXPERIMENTAL 188

Materials, Instruments, and Methods 188
Nuclear Magnetic Resonance Experiments 189
Enzymatic Assays 190
Theoretical Calculations 193
Synthetic Procedures and Chemical Data of Compounds 194

APPENDIX 266
LIST OF REFERENCES 267
BIOGRAPHICAL SKETCH 281

LIST OF FIGURES

Figure page

1-1. Transfer of the amido nitrogen from L-glutamine **1** for the biosynthesis of other molecules via pathways **A-F**. 2

1-2. Reaction catalyzed by the synthetase domain of Amidotransferases. 4

1-3. Reaction catalyzed by the glutamine amidotransferase domain (GAT) of Amidotransferases. 4

1-4. Primary sequence alignment of Class II glutamine-dependent amidotransferases. Residue numbers correspond to D-fructose-6-phosphate amidotransferase. Taken from Boehlein, Richards and Schuster (39). 8

1-5. Reactions catalyzed by Asparagine Synthetase; (**iii**) ammonia-dependent activity; (**iv**) glutamine-dependent activity; (**v**) glutaminase activity. 9

1-6. Formation of ^{18}O-β-aspartyl-AMP intermediate **6** and generation of L-asparagine **4** and ^{18}O-AMP in *E. coli* AS. 11

1-7. Proposed mechanism of Asparagine Synthetase based on studies upon glutamine PRPP amidotransferase (8). 13

1-8. Kinetic mechanism showing order of substrate binding, nitrogen transfer, and product release in AS; **A.** glutamine-dependent activity in mouse pancreas AS; **B.** glutamine-dependent activity in beef pancreas AS; **C.** ammonia-dependent activity of beef pancreas AS. 15

1-9. Proposed mechanism for glutamine-dependent nitrogen transfer in *E. coli* AS-B involving acyclic unsymmetric imide **12** as a reaction intermediate. 19

1-10. Kinetic mechanism of *E. coli* AS-B. 22

1-11. Proposed mechanism for nitrogen transfer in *E. coli* AS-B involving tetrahedral intermediate **8**. ...24

1-12. Proposed mechanism for nitrogen transfer in *E. coli* AS-B involving imide intermediate **12**.....25

2-1. Diversity of imidic compounds: **16** = acyclic, **17** = functionalized acyclic, **18** = highly functionalized acyclic, **19** and **20** = cyclic.....31

2-2. Mechanistic pathways for the reaction between amides **43** and acid anhydrides **44** to give imides **49**, nitriles **48**, and acids **47**. 38

2-3. Formation of bisphenylacetimide **57** via phenylacetyl carbonium ion intermediate **53**.....39

2-4. Formation of acetonitrile **64** and benzoic acid **65** from heating acetamide **61** and benzoyl chloride **62**.....41

2-5. Formation of acetylbenzamide via intermediate **75** and acetonitrile and benzoic acid via intermediate **76**.....43

2-6. Mechanistic pathways for the formation of (**a**) nitrile **80** and acid **81**, (**b**) imide **83**, and (**c**) triacylamine **85**.....45

2-7. Synthesis of functionalized symmetric imides **97** and **98** and rearrangement of **98** to amide **99**. 48

2-8. Base promoted rearrangement of unsymmetric imides **103b,c** to amides **104-107**.....49

2-9. Synthesis of functionalized imides **131-133** from nitrile **129** and acid **130**. 54

2-10. Synthesis of functionalized unsymmetric imides **136** and **137**. 55

2-11. Mechanism for nitrile and carboxylic acid group exchange via imide intermediate **144**.....56

2-12. Synthesis of cyclic imides **157** and **159** from diprotected L-asparagines **155** and **156** and L-glutamine **158**.....60

2-13. Formation of imides **173** from isocyanates **170** and acid anhydrides **171** via intermediate **172**. 64

3-1. Retrosynthetic analysis for the formation of imide **12** starting from N-protected-L-glutamine **211** and N-protected-L-aspartic acid **212**. 75

3-2. Synthesis of N,C-diprotected-L-glutamine **213a-c** from N-protected-L-glutamine **211a** and **211b** or C-protected-L-glutamine **217**. Reagents and conditions: **i**; a) Cs_2CO_3, MeOH/H_2O, pH 8, 0 °C-R.T., quant., b) BnBr, DMF/MeOH, R.T., 95%. **ii**; BnOH, TsOH(cat.), benzene reflux, 59%. **iii**; *t*-BuOH, DCC, DMAP(cat.), THF, 0 °C-R.T., 83%. **iv**; **iii**, 85%. **v**; (t-$BuO_2C)_2O$, triethylamine, THF, 0 °C-R.T., 98%. 77

3-3. Synthesis of β-activated N-Carbobenzyloxy-α-benzyl-L-aspartic acid **215a,b** from N-Carbobenzyloxy-L-aspartic acid **212**. Reagents and conditions: **i**; Ac_2O, R.T., 95%. **ii**; BnOH, 80 °C, 61%. **iii**; PCl_5, Et_2O, 0 °C-R.T., 89%. **iv**; DCC, CH_2Cl_2, 0 °C, 90%..... 79

3-4. Acid catalyzed reaction between amide **213a** and acid anhydride **215b** to give new products **220-222**..... 81

3-5. N-acylation of amides **213** by acid chloride **215a** in the presence of pyridine to give unsymmetric imides **216**, N,N-diacylamines **223**, and nitriles **224**..... 82

3-6. Deprotection of imide **216b** to give free acid-imide **225** and amino acid-imide **12**. Reagents and conditions: **i**; TFA, CH_2Cl_2, 0 °C, 94%. **ii**; 10% Pd/C, 1,4-cyclohexadiene, EtOH/THF, reflux, 90%. 86

3-7. Synthesis of electrophiles **228**, **229**, and **231**. Reagents and conditions: **i**; BnOH, 100 °C, 948%. **ii**; PCl_5, Et_2O, 0 °C-R.T.. **iii**; DCC, CH_2Cl_2, 0 °C-R.T., 93%. **iv**; PCl_5, Et_2O, R.T.. 87

3-8. Acid catalyzed N-acylation of amides **213** by acid anhydrides **232** to give unsymmetric imides **233** and by-products **220**, **234**, and **235**..... 89

3-9. N-acylation of amides **213** by acid chlorides **236** in the presence of pyridine to give unsymmetric imides **237**, N,N-diacylamines **238**, and nitriles **239**..... 92

3-10. Synthesis of imides **243** and **245** from L-glutamine derivative **240**. Reagents and conditions: **i**; PCl_5, Et_2O, R.T., 88%. **ii**; **242**, pyridine, $CHCl_3$, R.T. **iii**; a) **244**, CH_2Cl_2, -5 °C-R.T., b) petroleum ether, EtOH, R.T., 61%. 93

3-11. Deprotection of unsymmetric imides **237a,b** to give free acid-imide **246** and amino acid-imide **247**. Reagents and conditions: **i**; TFA, CH_2Cl_2, 0 °C, 94%. **ii**; 10% Pd/C, ammonium formate, EtOH, R.T.. **iii**; **ii**, 86%. 94

3-12. Deprotection of unsymmetric imides **237d,e** to give free acid-imide **248** and amino acid-imide **249**. Reagents and conditions: **i**; TFA, CH_2Cl_2, 0 °C, 47%. **ii**; 10% Pd/C, ammonium formate, EtOH, R.T. **iii**; 10% Pd/C, 1,4-cyclohexadiene, EtOH/THF, R.T, 63%. 95

3-13. Deprotection of unsymmetric imide **237h** to give free acid-imide **250**. Reagents and conditions: **i**; TFA, CH_2Cl_2, 0 °C, 94%. **ii**; 10% Pd/C, 1,4-cyclohexadiene, EtOH, AcOH, R.T. **iii**; 10% Pd/C, 1,4-cyclohexadiene, EtOH/THF, AcOH, R.T, 63%. 96

3-14. ^1H NMR (500 MHz) spectra of imide **12** (4-9 mM) in Bis-tris (100 mM) and Tris (100 mM) buffers in the pH 2-8 range: **A.** no buffer, pH 2.8; **B.** Bis-tris, pH 5.9; **C.** Tris, pH 6.8; **D.** Tris, pH 8.1. Labelled signals **X** correspond to compound **X**. Vertically offscale signals at 4.8 and 3.8 ppm correspond to water and Bis-tris/ Tris protons, respectively. 98

3-15. ^1H NMR (500 MHz) spectra of imide **12** (7-8 mM) in various buffers in the pH 7-8 range: **A.** HEPES (100 mM), pH 7.0 (vertically offscale signals around 2.8, 3.0, and 3.8 correspond to HEPES); **B.** Na_4BO_4 (210 mM), pH 7.9; **C.** NaH_2PO_4 (240 mM), pH 7.7; **D.** $NaHCO_3$ (1.1 M), 8.0. Labelled signals **Y** correspond to compound **Y**.....100

3-16. ^1H NMR (500 MHz) spectra of imide **12** (8 mM) in showing irreversible formation of species **X** from imide **12**: **A.** D_2O, pH 2.8; **B.** D_2O/Tris buffer, pH 8.4 (vertically offscale signals at 3.7 correspond to Tris); **C.** DCl/D_2O/Tris buffer reacidified to pH 5.4. 101

3-17. Possible products arrising from imide **12** at pH > 6.8. 102

3-18. Possible products arrising from imide **12** at pH > 6.8. 103

3-19. Synthesis of dipeptide **255**. Reagents and conditions: **i**; isobutylene, H_2SO_4(cat.), 66%. **ii**; 10% Pd/C, 1,4-cyclohexadiene, EtOH/THF,

reflux, 99%. **iii**; Ac_2O, R.T., 70%; **iv**; BnOH, 100 °C, 17%. **v**; DCC, THF, R.T., 78%. **vi**; TFA, CH_2Cl_2, 0 °C, 80%.....106

3-20. Synthesis of dipeptide **263**. Reagents and conditions: **i**; 10% Pd/C, 1,4-cyclohexadiene, EtOH/THF, reflux, 92%. **ii**; triethylamine, THF, 0 °C-R.T., 81%. **iii**; TFA, CH_2Cl_2, 98%. 107

3-21. Comparison of ^1H NMR (500 MHz) spectra in Tris (100 mM) buffer between possible products arising from imide **12**: **A**. imide **12** (7 mM), pH 8.2; **B**. dipeptide **255** (19 mM), pH 8.1; **C**. dipeptide **263** (15 mM), pH 8.1; **D**. pyrrolidone **265** (12 mM)+ L-asparagine (12 mM), pH 8.1. Vertically offscale signals at 4.8 and 3.7 ppm correspond to water and Tris protons, respectively. 109

3-22. Comparison of ^1H NMR (500 MHz) spectra in $NaHCO_3$ (1 M) buffer between possible products arising from imide **12**: **A**. imide **12** (7 mM), pH 8.0; **B**. L-Gln (16 mM) + L-Asp (16 mM), pH 8.1; **C**. L-Glu (17 mM) + L-Asn (18 mM), pH 8.0. Vertically offscale signals around 4.8 ppm correspond to water protons. 110

3-23. Comparison between imides **103b,c** and imide **12** based on the position of the NH_2 group. 112

3-24. ^1H NMR (500 MHz) spectra of imide **247** (11-21 mM) in Bis-tris (100 mM) and Tris (100 mM) buffers in the pH 6-9 range: **A**. no buffer, pH 6.6; **B**. Bis-tris, pH 6.6; **C**. Tris, pH 7.5; **D**. Tris, pH 8.1; **E**. Tris, pH 8.9. Labelled signals **Z** correspond to compound **Z**. Vertically offscale signals at 4.8 and 3.5-3.8 ppm correspond to water and Bis-tris/Tris protons, respectively. 115

3-25. ^1H NMR spectra of imide **247** (16-21 mM) showing irreversible formation of species **Z**: **A**. D2O, pH 6.5; **B**. D2O/Tris buffer, pH 8.8 (vertically offscale signal at 3.5 ppm correspond to Tris protons); **C**. DCl/D2O/Tris buffer reacidified to pH 6.5. 117

3-26. Comparison of ^1H NMR (500 MHz) spectra in Tris buffer between possible products arising from imide **247**: **A**. imide **247** (18 mM), pH 8.9; **B**. pyrrolidone **265** (39 mM) + acetamide (34 mM), pH 8.5; **C**. L-Glu (27 mM) + acetamide (24 mM), pH

8.9; **D.** L-Gln (190 mM) + acetic acid (170 mM), pH 8.8. Vertically offscale signal at 3.5 ppm correspond to Tris protons. 118

3-27. Formation of pyrrolidone **265** and acetamide **280** from imide **247** at pH > 7.5 via presumed intermediate **279**.....119

3-28. ^{1}H NMR spectra of imide **249** (4-8 mM) in Bis-tris (100 mM) and Tris (100 mM) buffers in the pH 6-8 range: **A.** Bis-tris, pH 6.0; **B.** Tris, pH 7.0; **C.** Tris, pH 8.1. Vertically offscale signals at 4.8 and 3.5-3.8 ppm correspond to water and Bis-tris/Tris protons, respectively. ...120

3-29. Isomerism in acyclic unsymmetric imides: **281**, cis-cis; **282**, cis-trans; **283**, trans-cis; **284**, trans-trans. 122

3-30. Possible configurational isomers of imide **12**.....124

3-31. Possible configurational isomers of imide **247**....124

3-32. Possible configurational isomers of imide **249**....125

3-33. Selected signals from the ^{1}H NMR (500 MHz) spectra of imide **225** (23 mM) in acetone-d_6.over the -85 - 0 °C region: **A.** imide N-H signal; **B.** 2-CH_2 and 2'-CH_2 signals. 129

3-34. Selected signals from the ^{1}H NMR (500 MHz) spectra of imide **237a** (56 mM) in acetone-d_6.over the -85 - 0 °C region: **A.** imide N-H signal; **B.** 2-CH_2 and 2'-CH_2 signals. 130

3-35. Selected signals from the ^{1}H NMR (500 MHz) spectra of imide **248** (53 mM) in acetone-d_6.over the -85 - 0 °C region: **A.** imide N-H signal; **B.** 2-CH_2 and 2'-CH_2 signals. 131

3-36. Lowest energy conformation of each configurational isomer of imide **12**.....133

3-37. Lowest energy conformation of each configurational isomer of imide **247**.....134

3-38. Lowest energy conformation of each configurational isomer of imide **249**.....135

4-1. Reversed Phase HPLC chromatogram of a standard mixture (0.3 mM, 10 mL) of substrates in Bis-tris (100 mM). Peak identity: **a.** ATP; **b.** imide

12; **c**. L-Asp; **d**. L-Glu; **e**. L-Asn; **f**. L-Gln; **g**. Bis-tris. 140

4-2. Standard curve of imide **12** (nmoles) versus area under the peak (mV-sec). 141

4-3. ^{1}H NMR (300 MHz) spectra of **A**. imide **12** (17 mM) and **B**. dipeptide **255** (18 mM) after treatment with DIEA:MeOH (50:50) at ambient temperature for 10 min.. 143

4-4. Reversed Phase HPLC chromatogram of substrates (0.3 mM) in Bis-tris (100mM) after boiling at 100 °C for 1 min.; 10 μL sample: **A**. ATP, imide **12** (**b**), L-Asp (**c**), L-Glu (**d**), L-Asn (**e**), L-Gln (**f**); **B**. imide **12** (**b**). 145

4-5. Reversed Phase HPLC chromatogram of ATP (0.6 mM), AMP (0.2 mM), and imide **12** (0.2 mM) in Bis-tris (100 mM) boiled for 1 minute at 100 °C. **A**. untreated with activated charcoal, **B**. treated with activated charcoal and filtered. Peak identity: **a**. ATP; **b**. imide **12**; **h**. AMP. 147

4-6. Reversed Phase HPLC chromatogram of the reaction mixture with WT AS-B (5 mg) in Bis-tris (100 mM) at pH 6.5: **A** imide **12** (7.5 mM), t = 0; **B**. imide **12** (7.5 mM), t = 15 min., 37 °C. Peak identity: **b**. imide **12**.....148

4-7. Reversed Phase HPLC chromatogram of the reaction mixture incubated at 37 °C for 15 min. with WT AS-B (5 mg) in Bis-tris (100 mM) at pH 6.5: **A** imide **12** (1.5 mM), L-Gln (1 mM); **B**. imide **12** (1.5 mM), ATP (1 mM); **C**. imide **12** (0.3 mM), L-Asp (1 mM), ATP (1 mM). Peak identity: **a**. ATP; **b**. imide **12**; **c**. L-Asp; **d**. L-Glu; **f**. L-Gln. 149

4-8. Reversed Phase HPLC chromatogram of the reaction mixture with WT AS-B (5 mg) in Bis-tris (100 mM) at pH 6.5: **A**. imide **12** (0.3 mM), ATP (1 mM), L-Asp (1 mM), L-Gln (1 mM), t = 0; **B**. imide **12** (0.3 mM), ATP (1 mM), L-Asp (1 mM), L-Gln (1 mM), t = 15 min., 37 °C. Peak identity: **a**. ATP; **b**. imide **12**; **c**. L-Asp; **d**. L-Glu; **e**. L-Asn; **f**. L-Gln. 150

4-9. Reversed Phase HPLC chromatogram of the reaction mixture incubated at 37 °C for 30 min. with C1A AS-B (6.3 nmol) in Bis-tris (100 mM) at pH 6.5. after boiling for 1 min. at 100 °C and subsequent treatment with activated charcoal: **A** ATP (1.2 mM), L-Asp (1.2 mM), L-Gln (1.2 mM); **B**. imide **12**

(0.3 mM), ATP (1.2 mM), L-Asp (1.2 mM), L-Gln (1.2 mM). Peak identity: **a.** ATP; **b.** imide **12**; **c.** L-Asp; **f.** L-Gln.....152

4-10. Relative energies between AS-B enzyme-substrate complexes and transition state for imide **12** formation based on kinetic parameters. TS = transition state; WT AS-B-Gln = enzyme-glutamine complex for WT AS-B; C1S AS-B-Gln = enzyme-glutamine complex for the C1S AS-B mutant; C1A AS-B-Gln = enzyme-glutamine complex for the C1A AS-B mutant. 153

4-11. Reversed Phase HPLC chromatogram of the reaction mixture incubated at 37 °C for 30 min. with C1S AS-B (8.7 nmol) in Bis-tris (100 mM) at pH 6.5. after boiling for 1 min. at 100 °C and subsequent treatment with activated charcoal: **A** ATP (1.2 mM), L-Asp (1.2 mM), L-Gln (1.2 mM); **B.** imide **12** (0.3 mM), ATP (1.2 mM), L-Asp (1.2 mM), L-Gln (1.2 mM). Peak identity: **b.** imide **12**; **c.** L-Asp; **f.** L-Gln.....154

5-1. Currently accepted mechanism of papain leading to the formation of amine **287** and acid **290** from amide **285**.....156

5-2. Reversible formation of enzyme-thioimidate **292** from nitrile **291** in papain.....157

5-3. Proposed mechanism by Dufour, et.al. (209) for the nitrile hydratase activity of Q19E papain mutant showing the formation of amide **295** from nitrile **291**.....159

5-4. Proposed inhibition pathway of *E. coli* AS-B by nitrile **296**.....161

5-5. Synthesis of nitrile **296**. Reagents and conditions: **i**; DCC, pyridine, R.T. **ii**; 1,4-cyclohexadiene, 10% Pd/C, EtOH, reflux, 77%. 161

5-6. ^{1}H NMR (500 MHz) spectra of nitrile **296** (20-34 mM) in Bis-tris (100 mM) and Tris (100 mM) buffers: **A.** Bis-tris, pH 6.3; **B.** Tris, pH 7.3; **C.** Tris , pH 8.2; **D.** Tris, pH 8.7. Vertically offscale signals at 4.8 and 3.6-3.8 ppm correspond to water and Bis-tris/Tris protons, respectively. 163

5-7. ^{1}H NMR (500 MHz) spectra of nitrile **296** in nitrogen buffers: **A.** methylamine, pH 9.0, after 15 hrs. at 4 °C; **B.** HEPES buffer, pH 8.8, after

15 min. at R.T.; **C.** HEPES buffer, pH 8.8, after 24 hrs. at R.T. Signals at 2.6 (offscale), 2.8, 3.1, and 3.7 ppm correspond to HEPES protons. 164

5-8. ^1H NMR (500 MHz) spectra of nitrile **296** in non-nitrogenous buffers: **A.** Na_2HPO_4 buffer, pH 9.0, after 15 min. at R.T.; **B.** Na_2HPO_4 buffer, pH 9.0, after 24 hrs. at R.T.; **C.** $NaHCO_3$ buffer, pH 9.9, after 30 min. at R.T.. 165

5-9. ^1H NMR (500 MHz) spectra of nitrile **296** (30 mM) in **A.** D_2O, pH 6.3, **B.** D_2O/Tris buffer, pH 8.4, and **C.** DCl/D_2O/Tris buffer reacidified to pH 7.1. Vertically offscale signals at 4.8 and 3.6 ppm correspond to water and Tris protons, respectively. 166

5-10. Possible products **299-302** formed from nitrile **296** at high pH.....168

5-11. ^{13}C NMR (500 MHz) spectra of nitrile **296** (94-110 mM) in **A.** D_2O, **B.** Tris buffer, pH 8.9, and **C.** Na_2HPO_4 buffer , pH 8.9. The signal around 40 ppm corresponds to DMSO-d_6 internal standard. 170

5-12. ^1H NMR (500 MHz) spectra of nitrile **296** (94-110 mM) at 70 °C in **A.** D_2O, **B.** Tris buffer, pH 8.9 and **C.** Na_2HPO_4 buffer, pH 8,9. Vertically offscale signals around 4.4 and 3.5 ppm correspond to water and Tris protons, respectively. 171

5-13. Stabilization of tetrahedral intermediate **303** or thioacylenzyme **304** by Asn_{74} upon attack of Cys_1 thiolate anion on L-glutamine in AS-B. 173

5-14. Proposed mechanism for the nitrile hydratase activity of *E. coli* N74D AS-B mutant. 175

5-15. Potential mechanism-based inhibitors **308-311** of *E. coli* AS-B. 177

5-16. Proposed inhibition pathways of *E. coli* AS-B by cyclic imide **308**.....178

5-17. Synthesis of cyclic imide **308**. Reagents and conditions: i; a) Na_2CO_3, MeOH, H_2O, R.T., b) MeI, DMF, R.T., 95%. ii; NaH, THF, R.T., 93%. iii; 31% HBr/AcOH, Et_2O, R.T., 77%.....179

5-18. Proposed inhibition pathway of *E. coli* AS-B by α,β-unsaturated-L-glutamine analog **309**.....180

5-19. Synthetic route towards α,β-unsaturated-L-glutamine analog **309**. Reagents and conditions: **i**; $(Ph)_3P{=}CHCO_2CH_3$, THF, -65 °C-R.T., 90%. **ii**; NH_3, MeOH, -65 °C-R.T., 13%. **iii**; a) KOH, MeOH, H_2O, 0 °C-R.T., b) HCl, pH = 1, 97%. **iv**; a) PCl_5, Et_2O, 0 °C-R.T., b) NH_3, Et_2O, 0 °C-R.T.,68%. **v**; TsOH(cat.), MeOH, R.T., 30%. **vi**; HCl, Et_2O, R.T. **vii**; CH_3CN, MeOH, TsOH, R.T., 60%. **viii**; KOH, MeOH, R.T., 87%. **ix**; CH_3CN, H_2O, TsOH, R.T., 33%. 182

Abstract of Dissertation Presented to the Graduate School of the University of Florida in Partial Fulfillment of the Requirements for the Degree of Doctor of Philosophy

SYNTHESIS AND STRUCTURAL STUDIES OF NOVEL ACYCLIC UNSYMMETRIC FUNCTIONALIZED IMIDES AND MECHANISTIC STUDIES ON E. COLI ASPARAGINE SYNTHETASE B

By

Jose G. Rosa Rodriguez

December, 1996

Chairman: Dr. Nigel G. J. Richards
Major Department: Department of Chemistry

Several new N_γ-acylated L-glutamine derivatives were synthesized in variable yields. The pH-dependent stability of three N_α,C-deprotected-N_γ-acylated L-glutamine imides in various buffers was studied using ^1H NMR spectroscopy. Two of these imides rearranged irreversibly at pH > 7 to form more stable products.

Rotational barriers about the imide nitrogen-carbonyl bond were estimated at 10.1-10.4 kcal/mol for three N_α,C-protected-N_γ-acylated L-glutamine imides using low temperature ^1H NMR spectroscopy. Solid state IR studies for three N_α,C-deprotected-N_γ-acylated L-glutamine imides showed the cis-trans or trans-cis geometry while MOPAC calculations, using AM1 parameters in a water solvation potential, revealed

the cis-trans geometry as the most stable isomer with energies ranging from 0.0-9.4 kcal/mol relative to the other geometrical isomers.

Unsymmetric imide N_{γ}-(β-L-aspartyl)-L-glutamine was tested as an intermediate in glutamine-dependent nitrogen transfer of *E. coli* asparagine synthetase B (AS-B) using wild type and mutant enzymes of asparagine synthetase B. Studies were inconsistent with an imide-mediated nitrogen transfer mechanism in the ATP-dependent nitrogen transfer from L-glutamine to L-aspartate. Incubation of N_{γ}-(β-L-aspartyl)-L-glutamine with wild type AS-B under standard enzyme reaction conditions did not form the usual products L-glutamate and L-asparagine. Moreover, formation of this imide was not detected when incubating L-glutamine, L-aspartate, and ATP with C1A and C1S AS-B mutants under standard conditions.

The function of *E. coli* asparagine synthetase B was re-engineered from amidohydrolase to nitrile hydratase. Incubation of the N74D AS-B mutant with 2-amino-4-cyanobutyric acid under standard conditions generated L-glutamine with no subsequent oxidation to L-glutamate. The pH-dependent stability of this nitrile in various buffers was studied by using ^{1}H and ^{13}C NMR spectroscopy. Studies were inconsistent with the formation of amidines, diketopiperazines, or isoimides at pH 8.

CHAPTER 1
STRUCTURE AND FUNCTION OF AMIDOTRANSFERASES AND E.COLI ASPARAGINE SYNTHETASE B

The Amidotransferases

Amidotransferases are a group of enzymes which catalyze the nitrogen transfer reaction from the glutamine 1 amide functionality to other biomolecules for the biosynthesis of amino acids (1), amino sugars (2), purine and pyrimidine nucleotides (3), coenzymes (4), and antibiotics (5). The fate of the nitrogen atom in some of these biomolecules is illustrated in **Figure 1-1.** This group of enzymes have been reviewed thoroughly both by Buchanan (6) and more recently by Zalkin (7).

Amidotransferases are composed of a *synthetase* domain, capable of utilizing ammonia as the nitrogen source, and a *glutamine amide transfer* (GAT) domain, able to utilize glutamine as the nitrogen source, either fused together and present on a single protein chain, or present as independent subunits (6,7). Based on the conservation of GAT domains, the amidotransferase family has been divided into two subfamilies. The first subfamily was originally designated PurF-type based on the *purF* gene encoding the GAT domain of glutamine phosphoribosyl pyrophosphate amidotransferase (glutamine PRPP amidotransferase) but is now referred to as

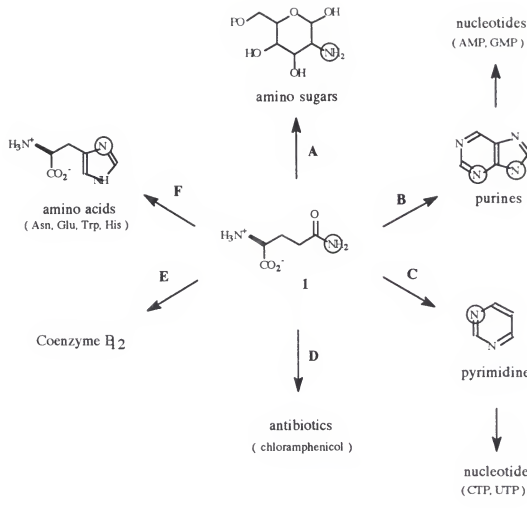

Figure 1-1. Transfer of the amido nitrogen from L-glutamine **1** for the biosynthesis of other molecules via pathways **A-F.**

Class II (8,9). This family includes the enzymes asparagine synthetase (10), glucosamine 6-phosphate synthase (2), glutamate synthase (11), and glutamine PRPP amidotransferase (12). The second subfamily was originally designated TrpG-type based on the *trpG* gene encoding the GAT domain of anthranilate synthase component II but is now Class I. Members of this family include anthranilate synthase (13),

carbamoyl-phosphate synthase (14), CTP synthetase (3), PGAM synthetase (15), GMP synthetase (16), imidazole glycerol-phosphate synthase (1), and aminodeoxychorismate synthase (17). Other amidotransferases which have not yet been classified as Class I or Class II include arylamine synthetase (5), Gln-$tRNA^{Gln}$ amidotransferase (18), NAD synthetase (19), cobyrinic acid *a,c*-diamide synthetase (20), and cobyric acid synthetase (21).

Most amidotranferases catalyze at least three different reactions (6,7). First, they are capable of utilizing ammonia as a nitrogen source in the absence of glutamine (ammonia-dependent activity). Second, these enzymes can use glutamine as the nitrogen source, (glutamine-dependent activity) or hydrolyze it to form glutamic acid **2** and ammonia, (glutaminase activity). The glutamine-dependent and glutaminase activities can be inactivated by alkylating an active site cysteine residue with a glutamine analog, or replacement of the cysteine residue with an alternate amino acid.

These properties are consistent with the presence of two independent domains operating together, namely, the synthetase and the GAT domains. The site of glutamine amide utilization is present in the GAT domain while that of ammonia utilization is present in the synthetase domain (7). The chemical reactions catalyzed by the synthetase domain (**i**) and the GAT domain (**ii**) are illustrated in **Figures 1-2** and **1-3**, respectively.

R = nitrogen acceptor.

L = leaving group.

NH_3^F = free ammonia from ammonium salt source.

Figure 1-2. Reaction catalyzed by the synthetase domain of Amidotransferases.

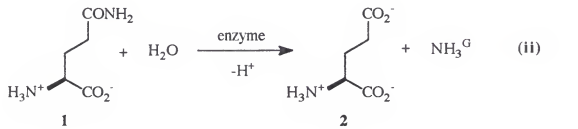

NH_3^G = unidentified form of ammonia derived from glutamine amide nitrogen.

Figure 1-3. Reaction catalyzed by the glutamine amidotransferase domain (GAT) of Amidotransferases.

The mechanism of amide nitrogen transfer from the GAT domain to the synthetase domain was initially investigated by Levitzki and Koshland (22) using the Class I enzyme CTP synthetase from *E.coli*. Using kinetic experiments it was found that any ammonia derived from the glutamine amide functionality (NH_3^G) remains bound to the enzyme. Competition experiments using $(NH_4)_2SO_4$ as the free ammonia (NH_3^F) source demonstrated that NH_3^F from solution competed with NH_3^G for a single site. Later, Zalkin and Truitt (23) conducted similar

experiments of the Class I enzyme GMP synthetase and concluded that $NH_3{}^G$ remains enzyme bound. However, in this study it was found that $NH_3{}^F$ derived from NH_4Cl did not compete with $NH_3{}^G$ for a single site. These authors showed that the results obtained by Levitzki and Koshland showing competence of $NH_3{}^F$ for $NH_3{}^G$ were due to $SO_4{}^{2-}$ inhibition and not to $NH_3{}^F$ inhibition derived from $(NH_4)_2SO_4$. The specific form of $NH_3{}^G$ for these enzymes was not addressed in these studies, however, and remains an open question. Moreover, these experiments were based on Class I enzymes and the same conclusions cannot be extended to include Class II enzymes.

The role of the ammonia-dependent activity has also been studied in other amidotransferases such as anthranilate synthase (24), glutamine (PRPP) amidotransferase (25), and carbamyl-P synthetase (26). In general, it was found that the ammonia-dependent activity of *E.coli* strains in which the GAT domain function has been inactivated by mutagenesis or deletion of the active site cysteine residue, remains unaltered but require large amounts of ammonium salts in the medium. This observation arises from the low concentrations of $NH_3{}^F$ present in solution relative to $NH_4{}^+$ at pH 7.0-7.5 and from the high K_M of $NH_3{}^F$ relative to the glutamine K_M. Two roles for the ammonia-dependent activity were proposed from these studies. One states that ammonia-dependent enzymes existed before the evolution of the GAT domain which expanded the specificity of these enzymes. The other states that ammonia-dependent activity resulted from utilization of an

existing enzyme-bound ammonia site by $NH_3{}^G$. No evidence, however, has been presented to support either of these two proposals.

Asparagine Synthetase

Structure and Function

The amidotransferase Asparagine Synthetase (AS) is a member of the Class II subfamily which are characterized by the location of the GAT domain in their polypeptide chain and an essential N-terminal cysteine residue (8). Asparagine synthetases which strictly use ammonia as the nitrogen source have been found in bacteria (27) whereas asparagine synthetases capable of utilizing both ammonia and glutamine as nitrogen sources have been found in more complex higher organisms. Bacterial AS has been isolated from Streptococcus bovis (28), Escherichia coli (29), Lactobacillus arabinosus (30), and Klebsiella aerogenes (31). AS from fungi such as Neurospora crassa (32), yeast such as Saccharomyces cerevisiae (33), plants (34), and various mammals (10,35-37) has also been purified and isolated.

Coding sequences for AS were first obtained from Chinese hamster (38), and human fibroblasts (10) and found to encode primary sequences of 561 amino acids having 95% identity. Alignment of these sequences with *E. coli* glucosamine 6-phosphate synthase and *E. coli* and yeast glutamine PRPP

amidotransferase sequences confirmed AS as being part of the Class II subfamily with an N-terminal GAT domain followed by a synthetase domain (38).

Primary sequence alignment for several members of the Class II sub-family is shown in **Figure 1-4** (39). From this alignment, at least 11 residues are conserved throughout the GAT domains of all Class II amidotransferases. These correspond to Cys_1, Gly_2, Ile_3, Arg_{30}, Gly_{31}, Asp_{33}, Arg_{49}, Asn_{74}, Gly_{75}, Asn_{79}, and Asp_{98} in *E. coli* asparagine synthetase B (see APPENDIX for amino acid abbreviations). Although the crystal structure for any asparagine synthetase remains to be solved, the crystal structures for Class II enzymes *B. subtillus* glutamine PRPP amidotransferase (40), *E. coli* glutamine PRPP amidotransferase (41), and the GAT domain of glucosamine 6-phosphate synthase (42), as well as Class I enzyme GMP synthetase (43), have been determined.

Asparagine synthetases in both prokaryotes and eukaryotes catalyze the ATP-dependent synthesis of L-asparagine **4** from L-aspartic acid **3** using either ammonia via reaction (**iii**) or L-glutamine via reaction (**iv**) as the nitrogen source (**Figure 1-5**). Reactions (**iii**) and (**iv**) are sometimes referred to as the ammonia-dependent reaction or activity and the glutamine-dependent reaction or activity, respectively. Glutaminase activity (**v**) has also been found in various sources of AS.

```
                01[b]                                                  49
Ham ASase[a] MCGIWALFGS DDCLSVQCL. .SAMKIA... .HRGPDAFRF ENVNGY....
Hum ASase[a] MCGIWALFGS DDCLSVQCL. .SAMKIA... .HRGPDAFRF ENVNGY....
Eco ASase[a] MCSIFGVFDI KTDAVELRK. .KALELSRLM RHRGPD...W SGIYAS....
Pea ASasa[a] MCGILAVLGC SDDSQAKRV. .RILELSRRL KHRGPD...W SGLHQH....
Pea AS II[a] MCGILAVLGC SDPSRAKRV. .RVLELSRRL KHRGPE...W SGLHQH....
Hum GFat[a]  MCGIFAYLNY HVPRTRREIL ETLIKGLQRL EYRGYDSAGV GFDGGNDKDW
Yst GFat[a]  MCGIFGYCNY LVERSRGEII DTLVDGLQRL EYRGYDSTGI AIDGD.....
Rhz NodM[a]  MCGIVGIV.. ....GHQPVS ERLVEALEPL EYRGYDSAGV A.........
PRPP[a]      MCGIVGIAGV M......PVN QSIYDALTVL QHRGQDAAGI ITIDAN....

                50                                                     99
Ham ASase    .......... .......... .......... ......TNCC FGFHRLAVVD
Hum Asase    .......... .......... .......... .. ...TNCC FGFHRLAVVD
Eco ASase    .......... .......... .......... ......DNAI LAHERLSIVD
Pea ASase    .......... .......... .......... ......GDNY LAHQRLAIVD
Pea AS II    .......... .......... .......... ......GDCY LAQQRLAIVD
Hum GFat     EANACKTQLI KKKGKVKALD EEVHKQQDMD LDIEFDVHLG IAHTRWATHG
Yst GFat     ..EADSTFIY KQIGKVSALK EEITK.QNPN RDVTFVSHCG IAHTRWATHG
Rhz NodM     TMDAGTLQRR RAEGKLGNLR EKL....... KEAPLSGTIG IAHTRWATHG
PRPP         ....NCFRLR KANGLVSDVF EARHMQR... ....LQGNMG IGHVRYPTAG

                100                                                    149
Ham ASase    P..LFGMQPI RVKKYPYLWL CYNGEIYNHK ALQQRF.... EFEYQTNVDG
Hum ASase    P..LFGMQPI RVKKYPYLWL CYNGEIYNHK KMQQHF.... EFEYQTKVDG
Eco ASase    V..NAGAQPL YNQQKTHV.L AVNGEIYNHQ ALRAEY..GD RYQFQTGSDC
Pea ASase    P..ASGDQPL FNEDKSII.V TVNGEIYNHE ELRKQL..PN H.KFFTQCDC
Pea AS II    P..ASGDQPL FNEDNPSI.V TVNGEIYNHE DLRKQL..SN H.TFRTGSDC
Hum GFat     EPSPVNSHPQ RSDKNNEFIV IHNGIITNYK DL.KKFLESK GYDFESETDT
Yst GFat     RPEQVNCHPQ RSDPEDQFVV VHNGIITNFR EL.KTLLINK GYKFESDTDT
Rhz NodM     APTERNAHPH FTE...GVAV VHNGIIENFA EL.KDELAAG GAEFQTETDT
PRPP         SSSASEAQPF YVNSPYGITL AHNGNLTNAH ELRKKLFEEK RRHINTTSDS

                150                                                    199
Ham ASase    EIILHLYDK. .......... .....GGIEQ TICMLDGVFA FILLDTANKK
Hum Asase    EIILHLYDK. .......... .....GGIEQ TICMLDGVFA FVLLDTANKK
Eco ASase    EVILALYQE. .......... .....KG.PE FLDDLQGMFA FALYDSEKDA
Pea ASase    DVIAHLYEE. .......... .....HG.EN FVDMLDGIFS FVLLDTRDNS
Pea AS II    DVIAHLYEE. .......... .....YG.ED FVDMLDGIFS FVPLDTRDNS
Hum GFat     ETIAKLVKYM YDN..RESQD TS.FTTLVER VIQQLEGAFA LVFKSVHFPG
Yst GFat     ECIAKLYLHL YNTNLQNGHD LD.FHELTKL VLLELEGSYG LLCKSCHYPN
Rhz NodM     EVVAHLLAKY ......RRDG LG.RREAMHA MLKRVKGAYA LAVLFEDDPS
PRPP         EILLNIFASE LDNFRHYPLE ADNIFAAIAA TNRLIRGAYA CVAMIIGHGM
```

Notes: (a) Ham ASase = Hamster asparagine synthetase (EC 6.3.5.4).
Hum ASase = Human asparagine synthetase (EC 6.3.5.4).
Eco ASase = *E. coli* asparagine synthetase B (EC 6.3.5.4).
Pea ASase = Pea AS1 nodule asparagine synthetase (EC 6.3.5.4).
Pea AS II = Pea AS2 root asparagine synthetase (EC 6.3.5.4).
Hum GFat = Human D-fructose-6-phosphate amidotransferase.
Yst GFat = *S. cerevisiae* D-fructose-6-phosphate amidotransferase.
Rhz NodM = NodM encoded D-glucosamine synthetase (*R. leguminosarum*).
PRPP = *E. coli* purF amidophosphoribosyltransferase (EC 2.4.2.14).
(b) N-terminal methionine is not present in any of the mature proteins. Residue numbers correspond to those of human D-fructose-6-phosphate amidotransferase.

Figure 1-4. Primary sequence alignment of Class II glutamine-dependent amidotransferases. Residue numbers correspond to D-fructose-6-phosphate amidotransferase. Taken from Boehlein, Richards and Schuster (39).

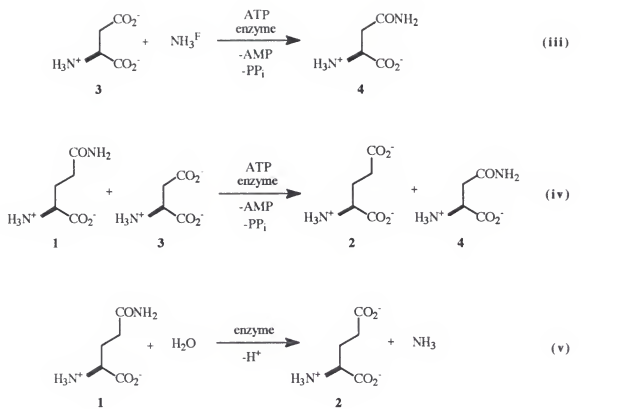

Figure 1-5. Reactions catalyzed by Asparagine Synthetase; **(iii)** ammonia-dependent activity; **(iv)** glutamine-dependent activity; **(v)** glutaminase activity.

While strictly ammonia-dependent enzymes, such as AS-A, can only use ammonia as the only source of nitrogen to produce asparagine, the glutamine-dependent enzymes can use both glutamine and ammonia as the nitrogen source (7). Interestingly, the glutamine-dependent activity of the latter enzymes can be inactivated without affecting their ammonia-dependent activity. Van Heeke and Schuster addressed this problem by expressing and characterizing human AS on *E. coli* (44) and *S. cerevisiae* (45). A mutant enzyme was expressed in which the N-terminal cysteine residue (Cys_1) was replaced

with an alanine residue (C1A mutant). This mutation resulted in the loss of the glutamine-dependent activity and a slight increase in the ammonia-dependent activity. Their results demonstrated the presence of a GAT domain with an N-terminal cysteine residue essential for glutamine-dependent activity and the presence of a synthetase domain responsible for the ammonia-dependent activity. Moreover, Schuster and coworkers demonstrated that these two domains are topographically separated from each other by raising monoclonal antibodies which selectively and specifically inhibited each of the two activities independently (46). Insight into the details or sequence of events involving the interaction between these two domains in the nitrogen transfer reaction at the molecular level is discussed next.

Reaction Mechanism

Cedar and Schwartz demonstrated the presence of a β-aspartyl-AMP intermediate **6** by incubating *E. coli* AS with ^{18}O-labelled aspartic acid **3** and ATP **5** (**Figure 1-6**) (47). These react to form ^{18}O-labelled **6** and release PP_i with no ^{18}O-label. Asparagine **4** can then form by nucleophilic attack of ammonia on **6** to release ^{18}O-AMP **7** as a side product. This scheme of reactions illustrates the events taking place in the ammonia-dependent reaction **(iii)** which occur in the C-terminal synthetase domain of AS.

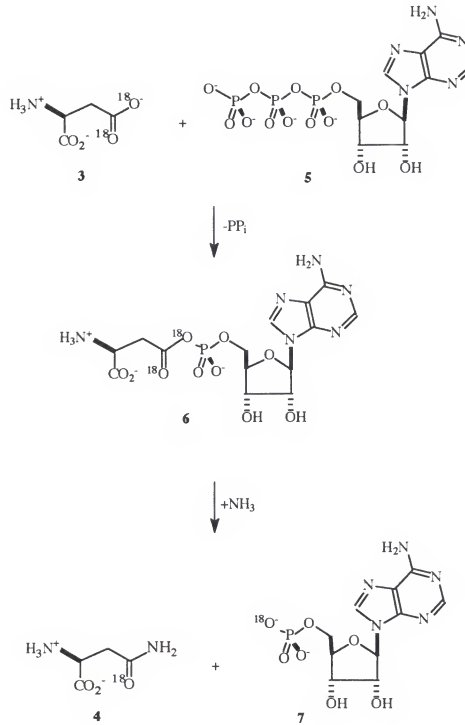

Figure 1-6. Formation of ^{18}O-β-aspartyl-AMP intermediate **6** and generation of L-asparagine **4** and ^{18}O-AMP in *E. coli* AS.

More interesting is the function of the GAT domain. Sequence studies by Tso et al. (48) and Vollmer et al. (49) established the presence of an N-terminal cysteine residue (Cys_1) essential for glutamine-dependent activity on glutamine PRPP amidotransferase. This residue is also conserved in all members of the Class II family. Alkylation of Cys_1 with 6-diazo-5-oxo-L-norleucine (DON) and mutagenesis of histidine (His_{101}) and aspartate (Asp_{29}) residues in glutamine PRPP amidotransferase abolished the glutamine-dependent activity without affecting the ammonia-dependent activity (8). Schuster et al. replaced Cys_1 with alanine (C1A) on human AS and obtained a mutant enzyme with no glutamine-dependent activity and unaffected ammonia-dependent activity (45,50).

Mei and Zalkin (8) have proposed a mechanism for the Class II subfamily based on studies upon glutamine PRPP amidotransferase (**Figure 1-7**). The active site is composed of a Cys_1, His_{101}, and Asp_{29} catalytic triad (glutamine PRPP amidotransferase numbering) which function similar to the Cys-His catalytic diad found in the thiol protease family of enzymes, in which papain (51) has been studied extensively. In this mechanism, His_{101} polarizes or deprotonates Cys_1, increasing the nucleophilicity of the sulphur atom. The thiolate anion formed attacks the amide functionality of glutamine to form tetrahedral intermediate **8**. The primary amine generated abstracts a proton from the imidazolium ion of His_{101} to form intermediate **9**. Breakdown of **9** gives

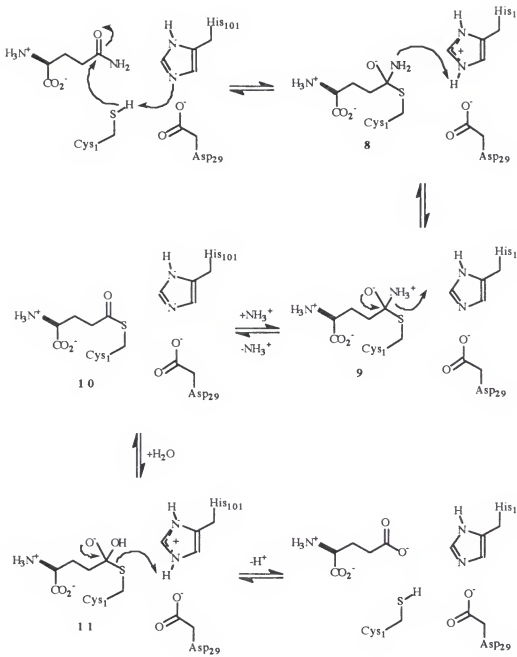

Figure 1-7. Proposed mechanism of Asparagine Synthetase based on studies upon glutamine PRPP amidotransferase (8).

ammonia and γ-glutamylthioester enzyme intermediate **10**. The ammonia generated reacts with β-aspartyl-AMP intermediate **6** to generate asparagine and AMP (**Figure 1-6**). Water, assisted by His_{101}, attacks intermediate **10** to form tetrahedral intermediate **11**. Breakdown of **11** yields glutamate and regenerates the initial state of the enzyme.

Recently, evidence has been obtained which rule out this mechanism. Primary sequence alignment of several Class II amidotransferases have failed to show conserved histidine residues (**Figure 1-4**) (39). Moreover, primary sequence alignment of 20 asparagine synthetases from different sources revealed no histidine residue cognate to His_{101} in glutamine PRPP amidotransferase (52). In addition, the crystal structures of *B. subtillus* glutamine PRPP amidotransferase (40), *E coli* glutamine PRPP amidotransferase (41), and the GAT domain of glucosamine 6-phosphate synthase (42) failed to reveal amino acid residues in close proximity to Cys_1 which can participate in acid-base catalysis. Thus, residues His_{101} and Asp_{29}, implicated as catalytically important residues in glutamine PRPP amidotransferase, do not play a role in catalysis.

Milman et al. (53) kinetically characterized mouse pancreas AS and proposed a uni-uni-bi-ter ping-pong Theorell Chance mechanism (54) (**Figure 1-8A**). In this mechanism, Gln binds first followed by release of Glu. Sequential binding of Asp and ATP follow, at which point nitrogen is transferred. Ordered release of PP_i, AMP, and Asn regenerate the original

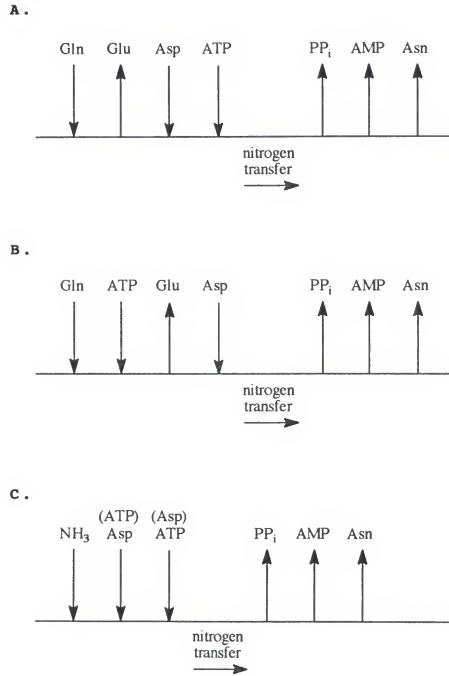

Figure 1-8. Kinetic mechanism showing order of substrate binding, nitrogen transfer, and product release in AS; **A.** glutamine-dependent activity in mouse pancreas AS; **B.** glutamine-dependent activity in beef pancreas AS; **C.** ammonia-dependent activity of beef pancreas AS.

state of the enzyme. Markin et al. (55) kinetically characterized beef pancreas AS and proposed a bi-uni-uni-ter ping-pong mechanism (54) for its glutamine-dependent activity (**Figure 1-8B**). Sequential binding of Gln followed by ATP precedes the release of Glu. Asp binds next, at which point nitrogen becomes transferred. Sequential release of PP_i, AMP, and Asn regenerate the original state of the enzyme. In the ammonia-dependent activity of this enzyme, ammonia binds first followed by random binding of ATP and Asp. Nitrogen transfer occurs next, followed by sequential release of PP_i, AMP, and Asn (**Figure 1-8C**) (55).

The mechanisms shown in **Figure 1-8A** and **Figure 1-8B** have raised important questions regarding the nitrogen transfer step. Both of these mechanisms show hydrolysis of glutamine to glutamate and ammonia before formation of β-aspartyl-AMP **6** (**Figure 1-6**). It is not clear how the enzyme can bind and maintain ammonia nucleophilic enough while binding aspartate and ATP at the same time. In contrast to these results, recent results by H-Tari have shown that glutamine binds last before the nitrogen transfer step (56). In this case, β-aspartyl-AMP formation precedes glutamine hydrolysis.

E.coli Asparagine Synthetase

Structure and Function

Two different AS enzymes have been isolated from *E. coli*, namely, Asparagine synthetase A (AS-A) and Asparagine synthetase B (AS-B) (27,57). AS-A is encoded by the *asnA* gene and strictly catalyzes the ammonia-dependent reaction (iii). In contrast, AS-B is encoded by the *asnB* gene and catalyzes all reactions (iii)-(v) independently. Multiple asparagine synthetases contained in a single organism other than *E. coli* have not been reported however (7).

The primary sequence of *E. coli* AS-A has been determined from the cloned *asnA* gene and found to be composed of 330 amino acids with an M_r of 36,700 (58). Similarly, the primary sequence of *E. coli* AS-B has been determined from the cloned *asnB* gene and found to be composed of 554 amino acids with an M_r of 62,700 (59). Inspection of the N-terminal amino acid sequence of AS-B identified it as being a member of the Class II subfamily. In addition, the primary sequence of AS-B was found to have a high degree of homology (48%) with Human AS and no homology with AS-A. Because of this dissimilarity, it is thought that the *asnA* and *asnB* genes arose independently and the ability of AS-B to possess glutamine-dependent activity did not arise from fusion of an ancestral GAT gene with the *asnA* gene (59).

Site-directed mutagenesis on the GAT domain of AS-B revealed no histidine residues which can participate in glutamine-dependent nitrogen transfer (39). Moreover, crystal structures of other members of the Class II subfamily lacked amino acid residues in close proximity to Cys_1 which may participate in acid-base catalysis. Unfortunately, no crystal structure is available for *E. coli* AS-B or any asparagine synthetase. Thus, revisions regarding the nitrogen transfer step in the mechanism of Class II enzymes and development of new mechanistic pathways have recently been made.

Reaction Mechanism

Richards and Schuster (60) proposed a mechanism for glutamine-dependent nitrogen transfer in *E. coli* AS-B (**Figure 1-9**). In contrast to the mechanism shown in **Figure 1-7**, histidine or aspartate residues do not participate in catalysis. The amide nitrogen attacks β-aspartyl-AMP **6** to form unsymmetric acyclic imide **12** after breakdown of a presumed tetrahedral intermediate. Attack of Cys_1 thiolate anion upon imide **12** generates γ-glutamylthioester **10** and the enol form of asparagine **13** after protonation. Water attacks intermediate **10** to ultimately form glutamate via intermediate **11** (**Figure 1-7**) and regenerate the initial state of the enzyme.

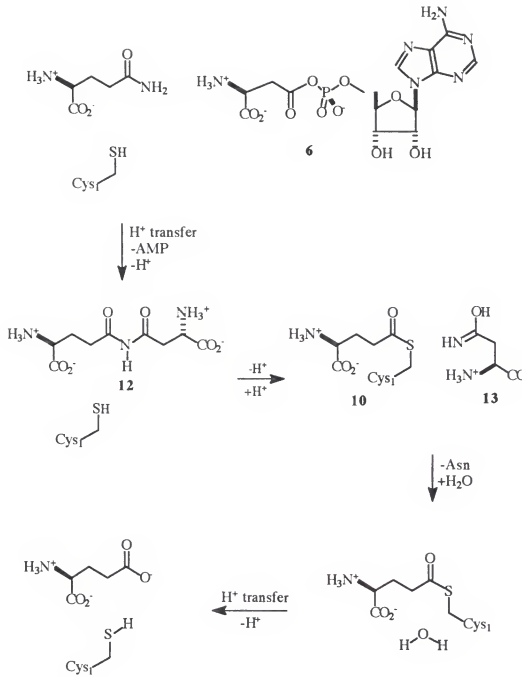

Figure 1-9. Proposed mechanism for glutamine-dependent nitrogen transfer in *E. coli* AS-B involving acyclic unsymmetric imide **12** as a reaction intermediate.

Precedence for this proposal regarding imide formation from primary amides has been obtained for other biological systems and organic compounds (61-63). Gibbs et al. have raised catalytic antibodies which catalyze the rearrangement of an asparaginyl-glycyl peptide sequence to an aspartyl-glycyl and an isoaspartyl-glycyl peptide sequence through the formation of a cyclic succinimide intermediate (61). Solid phase peptide synthesis using certain glutamine derivatives form peptide mixtures arising from coupling at the C_α-carboxyl group and the C_γ-carboxyl group via a cyclic glutarimide intermediate (62,63).

This proposed mechanism can still account for reactions (iii)-(v) (**Figure 1-5**) without the strict requirement of a histidine residue. Moreover this mechanism may have certain advantages over the mechanism proposed by Mei and Zalkin (8) (**Figure 1-7**). First, the role of His_{101} acting as a general acid by protonating and promoting the release of ammonia from tetrahedral intermediate **9** (**Figure 1-7**) is eliminated. The transfer of nitrogen as a resonance stabilized amide anion obviates the strict requirement of general acid catalysis from a histidine residue. Second, the transfer of nitrogen via imide intermediate **12** eliminates the possibility of ammonia diffusing from the active site to form unproductive NH_4^+, as well as, a separate ammonia binding pocket or an NH_3-enzyme complex intermediate.

In a recent study, Boehlein, Richards, and Schuster have investigated the glutamine-dependent nitrogen transfer of *E.*

coli AS-B in more detail (39). Cys_1 to alanine (C1A) and serine (C1S) mutants of AS-B were constructed which had no glutaminase or glutamine-dependent activity. Although the ammonia-dependent activity was unaffected, it was inhibited by glutamine as seen in the case of C1A and C1S mutants of Human AS (51). The C1A mutant inhibition pattern was consistent with the formation of an abortive complex in a similar fashion relative to Human AS C1A mutant. This result is consistent with the mechanism proposed by Richards and Schuster (60) (**Figure 1-9**) where imide intermediate **12** may represent this abortive complex in the C1A mutant.

In the same study, primary sequence alignment showed that Asp_{33} (D33) in AS-B is cognate to Asp_{29} in glutamine PRPP amidotransferase (**Figure 1-4**). Moreover, Asp_{33} is conserved in the Class II subfamily including asparagine synthetases from various sources (39). Asp_{33} to asparagine (D33N) and glutamic acid (D33E) mutants of AS-B had little or no effect, however, on the glutamine and ammonia-dependent activities. Further sequence studies revealed that His_{29} and His_{80} were also conserved in the Class II subfamily (39). His_{29} to alanine (H29A) and His_{80} to alanine (H80A) mutants of AS-B had no effect on the ammonia-dependent activity whereas the glutamine K_M on the glutamine-dependent activity increased by a factor of 4.5 relative to the wild type enzyme.

Kinetic studies conducted by H-Tari (56) on the glutamine-dependent activity of *E. coli* AS-B have revealed a different kinetic order (**Figure 1-10**) relative to previous

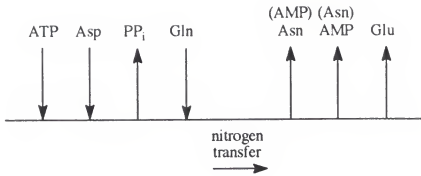

Figure 1-10. Kinetic mechanism of *E. coli* AS-B.

results (**Figure 1-8A,B,C**). These studies showed that ATP binds first followed by sequential binding of Asp and release of PP_i. Gln binds next at which point nitrogen transfer occurs. Random release of AMP and Asn followed by Glu release completes the cycle. In contrast to previous results (**Figure 1-8A,B,C**), this mechanism does not generate free ammonia while interacting with Asp and ATP simultaneously. Moreover, these results are consistent with the mechanism proposed by Richards and Schuster (60) (**Figure 1-9**). The possibility of forming imide intermediate **12** is supported by these studies, since glutamine binds and transfers its amide nitrogen only after formation of β-aspartyl-AMP **6**.

In related studies, Sheng et al. (50) investigated two mutants of human AS by replacing Cys_1 with alanine (C1A) and serine (C1S). Both of these mutants possessed neither glutaminase nor glutamine-dependent activity. Although unaffected, the ammonia-dependent activity was inhibited by glutamine through the formation of an abortive complex.

Moreover, sequence studies (39) carried out by the same group showed that His_{102} in Human AS is not cognate to His_{101} of glutamine PRPP amidotransferase as previously thought. These results introduce the possibility that Human AS could also be operating by a mechanism analogous to the proposed mechanism illustrated in **Figure 1-9.**

Boehlein et al. (64) investigated further the roles of highly conserved residues Arg_{30}, Asn_{74}, and Asn_{79} on the glutamine-dependent activity of *E. coli* AS-B. Sequence studies revealed that these residues were conserved in the entire Class II subfamily of amidotransferases (39). An Arg_{30} to alanine (R30A) mutant of AS-B resulted in a 182-fold increase of K_M for glutamine in the glutamine-dependent activity compared to wild-type AS-B. In addition, the ATP-dependent stimulation of the glutaminase activity was lost or modified, indicating that this residue may be involved in coordinating or synchronizing the synthetase and GAT domain half reactions. Mutants in which Asn_{74} were replaced by alanine (N74A), glutamine (N74Q), and aspartate (N74D), as well as, mutants generated by replacing Asn_{79} by alanine (N79A) were also expressed and assayed. Studies showed that Asn_{79} was not involved in catalysis whereas Asn_{74} played a significant role in glutamine-dependent nitrogen transfer.

These results allowed revision of the proposed mechanism for *E. coli* AS shown on **Figure 1-9.** A modified version of this mechanism consistent with recent results was proposed by Boehlein et al. (64) (**Figures 1-11, 1-12**). In this

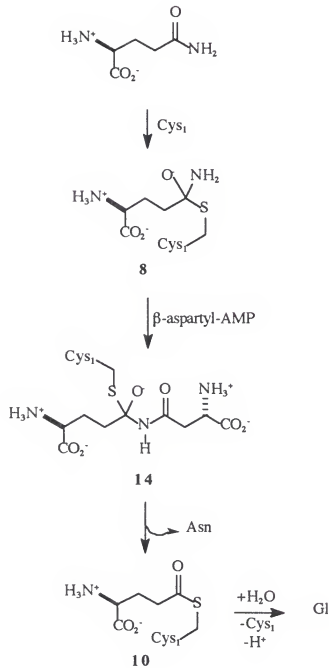

Figure 1-11. Proposed mechanism for nitrogen transfer in *E. coli* AS-B involving tetrahedral intermediate **8**.

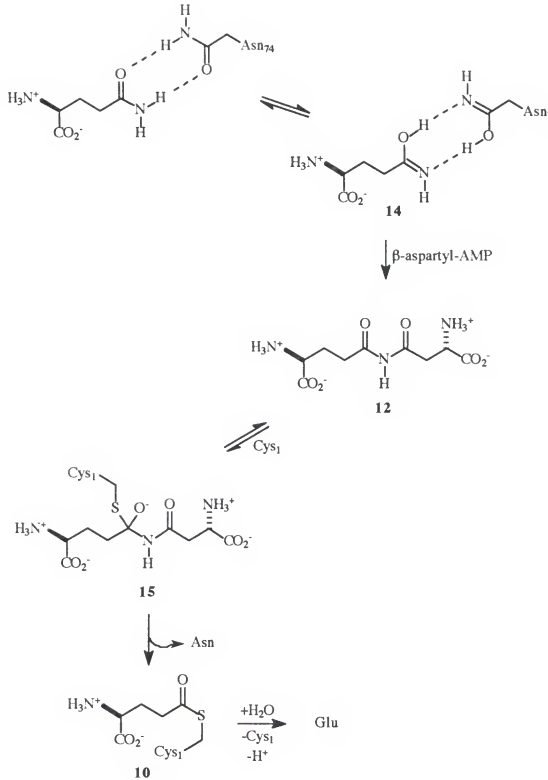

Figure 1-12. Proposed mechanism for nitrogen transfer in *E. coli* AS-B involving imide intermediate **12**.

mechanism, Asn_{74} plays a catalytic role by stabilizing the oxyanion of intermediate **8**. The amide nitrogen of **8**, which is now nucleophilic, can attack β-aspartyl-AMP to form intermediate **14** which ultimately generates asparagine and glutamate as outlined in **Figure 1-9**. Alternately (**Figure 1-12**), Asn_{74} can play a catalytic role by polarizing the amide bond of glutamine to form its hydroxyimine form **15** which now has a nucleophilic nitrogen atom. The nitrogen atom can then attack β-aspartyl-AMP **6** to form imide intermediate **12**. Attack of Cys_1 thiolate anion on imide **12** to form intermediate **14** and subsequent breakdown to give γ-glutamythioester enzyme intermediate **10** can ultimately generate asparagine and glutamate (**Figure 1-9**).

Precedence for this proposal regarding polarization and tautomerization of the glutamine amide group is supported by studies on glycoprotein biosynthesis (65-67). Imperiali et al. synthesized and evaluated conformationally constrained peptides containing the sequence Asn-X-Ser/Thr in which the primay amide nitrogen of the Asn residue becomes N-glycosylated through nucleophilic attack on an electrophilic oligosaccharide. This process is catalyzed by the enzyme oligosaccharyltransferase (65). Their studies indicated that the Ser and Thr residues presumably assist the enolization of the Asn primary amide group, thereby increasing the nucleophilicity of the amide nitrogen atom and its ability to displace leaving groups at the anomeric carbon of oigosaccharides (66,67).

Recently, Stoker et al. determined the amide carbon and nitrogen isotope effects using ^{13}C and ^{15}N labels, respectively, in the glutaminase (**v**) and glutamine-dependent activities (**iv**) of *E. coli* AS-B (68). Carbon and nitrogen isotope effects of 1.0245 and 1.0095, respectively, for the glutaminase reaction and 1.0231 and 1.0222, respectively, for the glutamine-dependent activity indicated that nitrogen transfer does not occur by the formation of free ammonia in the active site. Presumably, nitrogen transfer occurs through a series of intermediates in which glutamine becomes covalently attached to aspartate. These results are also consistent with the mechanisms proposed by Richards and Schuster (60) and Boehlein et al. (64) (**Figures 1-11** and **1-12**).

Boehlein et al. have recently investigated the ability of *E. coli* AS-B to use glutamic acid γ-hydroxamate (LGH) and hydroxylamine as alternate substrates compared to glutamine and ammonia, respectively (69). In these studies, the catalytic efficiency (k_{cat}/K_M) for LGH in the glutaminase and glutamine dependent activities were increased 3-fold and decreased 3-fold, respectively, relative to glutamine. The catalytic efficiency (k_{cat}/K_M) for hydroxylamine in the ammonia-dependent activity increased 2-fold relative to ammonia. In contrast, the catalytic efficiencies (k_{cat}/K_M) for LGH and hydroxylamine in all three reactions (**iii-v**) with the N74A AS-B mutant enzyme remained essentially unchanged compared to glutamine and ammonia, respectively. However,

the catalytic efficiencies (k_{cat}/K_M) in going from WT AS-B to N74A AS-B mutant were reduced 2-fold and 7-fold for glutamine and LGH, respectively. These results provide additional evidence for the involvement of Asn_{74} in catalysis and are still consistent with the mechanisms involving tetrahedral intermediate **8** (**Figure 1-11**) or imide intermediate **12** (**Figure 1-12**).

The major difference between the proposed mechanisms by Richards and Schuster (60) and Boehlein et al. (64) (**Figures 1-11** and **1-12**) and other mechanisms like the one shown in **Figure 1-7**, is the formation and involvement of imide **12** in the formers as a key intermediate in glutamine-dependent nitrogen transfer. In principle, evidence for the imide-mediated mechanism (**Figure 1-12**) can be obtained by proving the existence of imide **12** through detection or isolation. Thus, preparation of authentic acyclic unsymmetric imide **12** is an important step in conducting enzymatic studies to prove its existence and involvement in the nitrogen transfer reaction.

Specific Aims

The first part of the present study involved the design and synthesis of imide **12**, as well as the exploration of its chemical properties in aqueous solution. Due to the lack of previous work on highly functionalized acyclic unsymmetric imides derived from amino acids, such as and including **12**, we

investigated the synthesis of derivatives and the exploration of their chemical properties.

The second part of the present study involved the use of imide **12** to test the mechanism of nitrogen transfer in *E. coli* AS-B proposed by Richards and Schuster (60) and Boehlein et al. (64) (**Figures 1-11** and **1-12**). The third part of this study involved the synthesis and use of rationally designed L-glutamine analogs to obtain structural and mechanistic information on *E. coli* AS-B.

CHAPTER 2
REVIEW OF ACYCLIC IMIDE SYNTHETIC METHODOLOGY

Introduction

The imide functional group can be represented by structure **16** where R_1 = H and R_2 and R_3 can be aromatic or aliphatic and may or may not be equal (**Figure 2-1**). Imides can be either acyclic symmetric (R_2 = R_3) or acyclic unsymmetric ($R_2 \neq R_3$) as well as N-substituted (R_1 = alkyl, Ar). Functionalized acyclic imides are represented by **17**, where R_1 = H and R_2, R_3, and R_4 are different aliphatic or aromatic side chains with at least one functional group (e.g. amino, hydroxy, carboxylate, allyl, vinyl, halide, etc.). These can be either symmetric (R_1 = R_3 = H; R_2 = R_4) or unsymmetric (R_1 = R_3 = H; $R_2 \neq R_4$) as well as N-substituted (R_1 = alkyl or Ar). Highly functionalized imides are represented by **18** where R_1 = H and R_2, R_3, R_4, R_5 are different aliphatic or aromatic side chains with various functional groups. These can also be either symmetric (R_1 = H; R_2 = R_5; R_3 = R_4) or unsymmetric (R_1 = H; $R_2/R_3 \neq R_4/R_5$) as well as N-substituted (R_1 = alkyl or Ar). Imides can also be cyclic, such as **19** and **20**, as well as N-substituted (R_1 = alkyl or Ar). The chemistry of cyclic imides is beyond the scope of this chapter and will not be discussed further. The

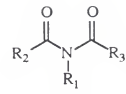

16

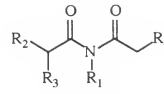

17

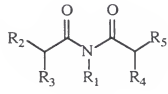

18

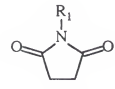

19

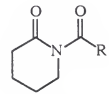

20

Figure 2-1. Diversity of imidic compounds: **16** = acyclic, **17** = functionalized acyclic, **18** = highly functionalized acyclic, **19** and **20** = cyclic.

chemistry of imidic compounds has been well reviewed by Challis and Challis (70) and by Uflyand et al. (71) and that of cyclic imides by Hargreaves, Pritchard, and Dave (72).

Although unimolecular reactions to form cyclic imides occur with great ease (72), bimolecular reactions to give high yields of acyclic imides are more difficult to control (70). In general, the reactions to give acyclic imides involve harsh reaction conditions, and significant formation

of side products. Whereas a large variety of simple acyclic symmetric and unsymmetric imides **16** have been succesfully prepared in reasonable yields, only a small number of functionalized acyclic symmetric and unsymmetric imides **17** have been synthesized in very low yields. Highly functionalized acyclic symmetric and unsymmetric imides **18** are virtually nonexistent in the literature. Moreover, highly functionalized acyclic unsymmetric imides **18** (R_1 = H) containing chiral centers have not yet been reported. The synthesis of imide **12** therefore represents a new extension of the highly functionalized acyclic unsymmetric imide family. We therefore reviewed chemical methods used in the preparation of acyclic imides to their strengths and weaknesses in obtaining highly functionalized acyclic unsymmetric imides. A comprehensive review of these chemical methods is presented here.

Imides from Amides or Amines and Acid Anhydrides

The synthesis and isolation of acyclic N-aryldiacetamides **22** by the action of acetic anhydride on substituted anilides **21** was first reported by Remmers (73). Substituents such as NO_2 and Br were investigated and found to retard acetylation of the anilides. High temperatures and pressures were needed to obtain the desired diacylated products.

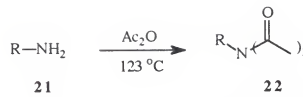

21 **22**

22a; R = $C_6H_2Br_3$
22b; R = $C_6HBr_3NO_2$

A substantial time later, Kay (74,75) reported the synthesis of N-allyl and N-phenyl imides **25** in low yields by heating allylamine and aniline derivatives **23** with acid anhydrides **24**, and Bistrzycki and Ulffers (76) reported the synthesis of N-phenyl diacetamide **25b** by refluxing aniline in acetic anhydride as solvent. Yields as high as 90% could be obtained if the temperature was raised to 200-205 °C for 8-10 hours.

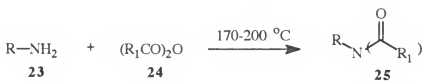

23 **24** **25**

25a; R = Allyl; R_1 = Me
25b; R = Ph; R_1 = Me
25c; R = Ph; R_1 = Et
25d; R = p-toluyl; R_1 = Me
25e; R = Ph; R_1 = Ph

At the same time Ulffers and von Janson (77) reported the synthesis of a variety of N-phenylsubstituted

diacetamides **27** by heating a variety of substituted anilines **26** in acetic anhydride.

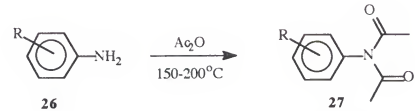

26 **27**

R = H, Br, Me, NO_2

Substituents like Cl, Br, and NO_2 in the ortho-position of the aniline were found to retard the formation of the monoacylated product, but at higher temperatures, this ortho-substituent facilitated the formation of the diacetylated product. The effect of acid catalysts on the acetylation of substituted anilines was then investigated by Smith and Orton (78). It was found that sulphuric acid and temperatures around 70-80 °C accelerated the formation of N-aryl diacetamides **27** from substituted anilines and acetic anhydride.

Subsequently, Sudborough (79) reported the synthesis of additional N-aryl diacetamides **29** by refluxing aniline derivatives **28** with acetic anhydride for one hour. Refluxing was required to obtain diacetylation in yields of 53-81%.

Lindemann (80) reported the synthesis of diacetamide **31** in low yields by heating acetamide **30** and acetic anhydride at 250 °C. Hentschel (81) modified Lindemann's procedure and

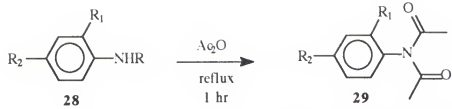

28 29

29a; R = R_1 = R_2 = H; 53%.
29b; R = Ac; R_1 = R_2 = H, 66%.
29c; R = R_2 = H; R_1 = Me, 81%.
29d; R = R_1 = H; R_2 = Me.

increased the yields of diacetamide to 18-29% using lower temperatures (125 °C). Davidson and Karten (82) prepared diacetamide in 36% yield by heating acetamide with acetic anhydride in the presence of ammonium chloride. Polya and Tardrew (83) further improved the yield of diacetamide to 70-76% by passing dry hydrogen chloride to a mixture of acetamide and acetic anhydride. Acetyl chloride also proved to be an effective catalyst for the synthesis of diacetamide.

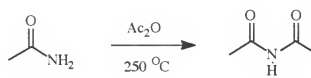

30 31

Polya and Spotswood (84) investigated the reactions between different amides **32** and acid anhydrides **33** to form a wide variety of symmetrical, as well as, the first acyclic unsymmetrical imides **34a-i** in yields ranging from 42-80%. Dunn et al. (85) extended this list further by reporting the

synthesis of acyclic imides **37** and **40** in 11-63% and 37-90% yields by refluxing amides **35** and amines **38** with acid anhydrides **36** and **39**, respectively.

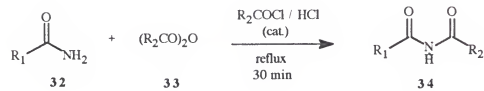

32 **33** **34**

34a,b,c; R_1 = Et, CH_2Cl, Ph; R_2 = Me; 60, 50, 45%.
34d,e,f,g; R_1 = Me, Et, CH_2Cl, Ph; R_2 = Et; 58, 57, 41, 42%.
34h,i; R_1 = CH_2Cl, Ph; R_2 = CH_2Cl, Ph; 65, 80%.

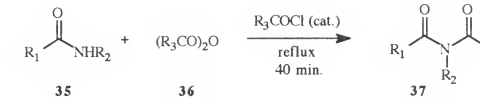

35 **36** **37**

37a,b,c; R_1 = H; R = Ph, Pr, Pr; R_2 = Pr, Me, Pr; 16, 45, 11%.
37d; R = R_2 = Me; R_1 = Ph; 63%.

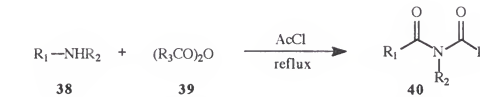

38 **39** **40**

40a,b,c; R = Me; R_1 = H_2Cl; R_2 = Me, Et, Pr; 70, 46, 37%.
40d,e; R = 1-naphthyl, Ph; R_1 = H, Ph; R_2 = Me; 76, 90%.

Wiley et al. (86,87) reported the acetylation of N-alkyl acetamides **41**, derived from glycine and leucine, with acetic anhydride and pyridine to form aliphatic N-substituted

diacetamides **42** in good yields. Later, Cadwallader and LaRocca (88) reported the synthesis of additional new unsymmetrical imides in yields ranging from 3-14%.

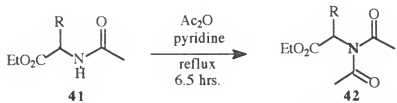

41 **42**

42a; R = H; 88%.
42b; R = i-Bu; 91%.

Davidson and Skovronek (89) investigated the reaction between amides and acid anhydrides in more detail and established the nature of the reaction (**Figure 2-2**). Primary amides **43** react with acid anhydrides **44** to form isoimidinium salt **45** which exists in equilibrum with its isoimide **46** and acid **47** forms. Decomposition to nitrile **48** and acid **47** can take place from **45** via pathway **a** or from **46** via pathway **b**. Rearrangement to imide **49** takes place from **46** via pathway **c**. A three way equilibrium between all of these species is established thermally at about 200 °C. Nitrile and acid formation predominates in the absence or presence of small amounts of acid catalysts such as hydrochloric acid or sulphuric acid and is believed to occur through six membered ring intermediate **50**. As more acid catalyst is added the rearrangement to imide from **46** predominates at the expense of nitrile formation.

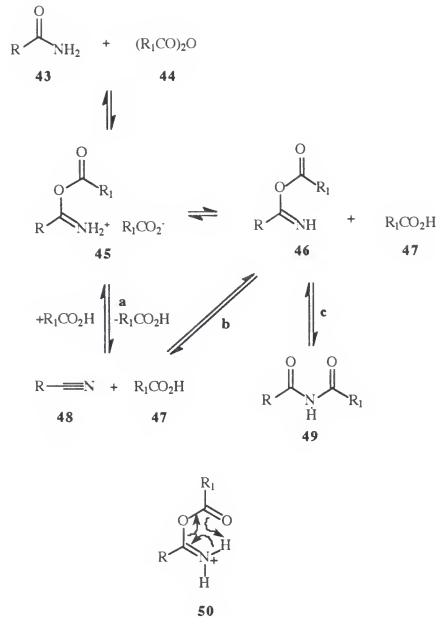

Figure 2-2. Mechanistic pathways for the reaction between amides **43** and acid anhydrides **44** to give imides **49**, nitriles **48**, and acids **47**.

Hurd and Prapas (90) reported the preparation of acyclic unsymmetric imides **52** in moderate yields by heating benzamide and acid anhydrides **51** in the presence of catalytic amounts

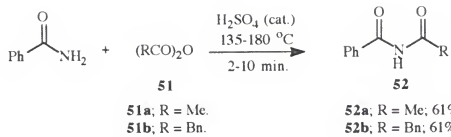

51

51a; R = Me.
51b; R = Bn.

52

52a; R = Me; 61%.
52b; R = Bn; 61%.

of sulphuric acid. Interestingly, bisphenylacetimide **57** (**Figure 2-3**) was obtained by acylating benzamide with either phenylacetic anhydride **51b** or phenylacetyl chloride. The authors rationalized the formation of **57** by assuming that benzamide reacts with phenylacetyl carbonium ion intermediate **53**, arising from the corresponding anhydride or acid chloride, to form the protonated form of unsymmetric imide **54**. This imide breaks down to form phenylacetamide **55** and the more stable phenyl carbonium ion **56**. Phenylacetamide

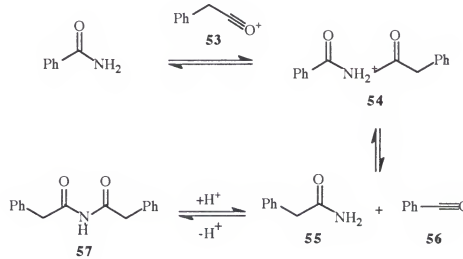

Figure 2-3. Formation of bisphenylacetimide **57** via phenylacetyl carbonium ion intermediate **53**.

reacts with another molecule of anhydride or acid chloride to give the symmetrical imide **57**.

Years later, Barburao et al. (91) reported the synthesis of several new unsymmetric acyclic imides **60** in yields ranging from 12-60% by heating amides **58** with acid anhydrides **59** in the presence of catalytic amounts of sulphuric acid.

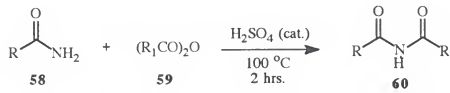

58 **59** **60**

60a,b,c,d,e; R_1 = Me; R = Pr, Bu, C_7H_{15}, $Ph(CH_2)_3$; 49, 57, 54, 58%.
60f,g,h; R_1 = Pr; R = Pr, i-Bu, Ph; 12, 57, 20%.

Although the reaction between amides and acid anhydrides to form imides appears to be general in nature, it is limited by several factors. First, this method generally requires high temperatures to obtain imides allowing the possibility of side reactions. Second, although acid catalysts such as hydrogen chloride, acetyl chloride, and sulphuric acid increased the yields of imides, addition of such catalysts is obviously detrimental to any acid sensitive groups attached to amides or acid anhydrides. In contrast, good yields of imides can be obtained using this method from aliphatic or aromatic amides and anhydrides with no acid or heat sensitive groups.

Imides from Amides or Amines and Acid Chlorides

Early attempts to synthesize imides from amides and acid chlorides were made by Pinner (92). Heating acetamide **61** with benzoyl chloride **62**, however, did not form the desired acetylbenzamide **63** but gave acetonitrile **64** and benzoic acid **65** instead (**Figure 2-4**). At the same time Kay (75) reported the acetylation of N-acetylarylamines **66** with acetyl chloride to give N-aryldiacetamides **67** in good yields.

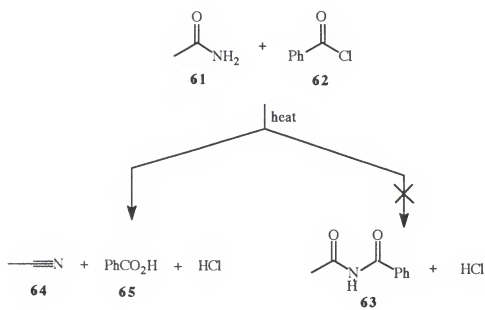

Figure 2-4. Formation of acetonitrile **64** and benzoic acid **65** from heating acetamide **61** and benzoyl chloride **62**.

Titherley (93) also reported the preparation of diacetamide **31** in 30-40% yield by heating acetamide and acetyl chloride in benzene. Kuroda and coworkers (94) improved the synthesis of diacetamide to 80% yield by

66 **67**

67a ; R = Ph ; 51%.
67b ; R = o-toluyl ; 65%
67c ; R = p-toluyl.

refluxing acetamide and acetyl chloride in toluene with catalytic amounts of sulphuric acid. Soon after, Tarbouriech (95,96) reported the synthesis of a series of new aliphatic acyclic unsymmetric imides **70** by heating different amides **68** with various acid chlorides **69**, although yields were not reported.

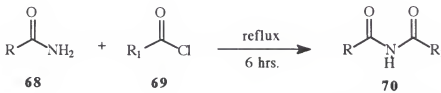

68 **69** **70**

R = Et, Pr, i-Pr, Bu.
R_1 = Pr, i-Pr, Bu, i-Bu.

Titherley and Holden (97) briefly investigated the reaction between primary amides **71** and acid chlorides **72** to give acyclic imides **73**. While heating benzamide with benzoyl chloride at 95 °C gave 22% dibenzamide **73a**, increasing the reaction temperature decreased the yield, producing larger amounts of benzonitrile and benzoic acid. Similar results

were obtained using p-toluamide. Interestingly, heating acetamide with benzoyl chloride produced acetonitrile and benzoic acid exclusively while heating benzamide with acetyl chloride produced acetylbenzamide **73d** in 85% yield.

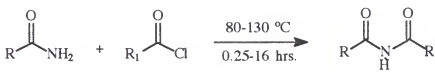

71 **72** **73**

73a; R = R_1 = Ph; 22%.
73b; R = p-toluyl; R_1 = Ph; 22%.
73c; R = Me; R_1 = Ph; 0%.
73d; R = Ph; R_1 = Me; 85%.

Years later, Davidson and Skovronek (89) reproduced these experiments and explained this observation by considering the isoimidinium ions, **74** and **75**, formed for both reactions (**Figure 2-5**). In the case of benzamide with

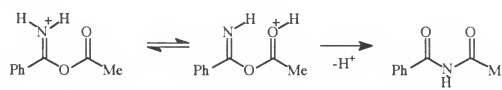

74 **75**

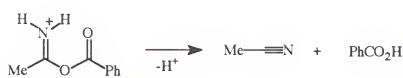

76

Figure 2-5. Formation of acetylbenzamide via intermediate **75** and acetonitrile and benzoic acid via intermediate **76**.

acetyl chloride, the inductive effects of the phenyl and methyl groups of the isoimidinium ion **74** promote proton transfer to form **75**. The newly formed activated carbonyl group and a the ternary nitrogen atom can now rearrange to form the imide product **73d**. In the case of acetamide with benzoyl chloride, the inductive effects of the phenyl and methyl groups of the isoimidinium ion **76** do not promote proton transfer sufficiently enough so breakdown to acetonitrile and benzoic acid predominates.

Davidson and Skovronek (89) also investigated the reaction between amides and acid chlorides in pyridine and established the nature of the reaction (**Figure 2-6**). Primary amides **77** react with acid chlorides **78** to form isoimide **79** and pyridinium chloride. Decomposition to nitrile **80** and acid **81** can take place from **79** via pathway **a**. Acid **81** can further react with another molecule of **78** to give acid anhydride **82**. Rearrangement to imide **83** takes place from **79** via pathway **b**. A third reaction occurs in this system via pathway **c** from **79** with another molecule of **78** forming N-acylisoimide **84** which further rearranges to triacylamine **85**. The distribution of these products depend on a variety of factors such as structure and relative amounts of amides and acid chlorides, order of reagent addition, reaction temperatures, and reaction times.

Dehn (98) acetylated acetamide, acetanilide, and p-toluamide with acetyl chloride in diethyl ether at room temperature to give diacetamides **86**. Although this method

had the advantage of requiring low reaction temperatures, the yields of **86** were not reported for the purpose of comparison.

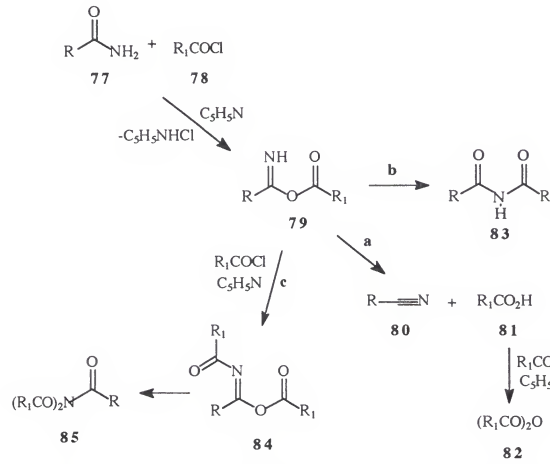

Figure 2-6. Mechanistic pathways for the formation of (**a**) nitrile **80** and acid **81**, (**b**) imide **83**, and (**c**) triacylamine **85**.

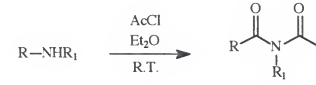

86

86a ; R = Ac ; R_1 = H
86b ; R = Ac ; R_1 = Ph
86c ; R = p-toluyl ; R_1 = H

Titherley (99) prepared dibenzamide in quantitative yield by treating benzamide with benzoyl chloride in pyridine at room temperature, while Freundler (100) reported the preparation of isobutyrylacetamide **87** and isobutyrylacetanilide **88** by treating isobutyryl chloride with acetamide and acetanilide, respectively, in pyridine solution at room temperature.

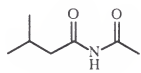

87

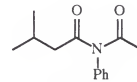

88

Thompson (101) reported the synthesis of several acyclic unsymmetric imides **91** in yields ranging from 5-80% by treating amides **89** with acid chlorides **90** in chloroform/pyridine solutions at temperature ranging from -60 °C to 25 °C. By variation of the experimental conditions, the effect of the substituents on the acyl-chlorine bond, and the structure of the amide, the relative amounts of mono- or di-acylation, and/or dehydration of the amide could be controlled. Generally aromatic amides and acid chlorides gave diacylation while aliphatic amides and acid chlorides gave monoacylation at low temperatures (-60 °C). In all cases, increasing temperatures resulted in increased amounts of dehydration products.

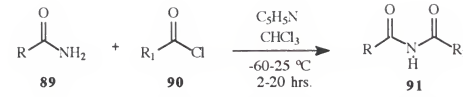

89 90 91

R = Me, Et, i-Bu, furyl, Ph, cinnamyl, m-anisidyl.
R_1 = Et, i-Bu, furyl, Ph, cinnamyl, m and p-anisidyl.

LaLonde and Davis (102) investigated the reaction between aliphatic amides and acid chlorides in the presence of subtituted pyridines, such as 2-methylpyridine and 2,6-dimethylpyridine, in methylene chloride solution. No imides were obtained using these bases but rather diacylation of the amides to form triacylamines took place exclusively in good yields at low temperatures (-20 to -40 °C). Increasing temperatures resulted in lower yields of triacylamines. Factors such as the order of reactant and pyridine mixing, substituents at the α-position of both acid chloride and pyridine, temperature affected the extent of amide acylation.

Cadwallader and LaRocca (88) reported the preparation of several aliphatic acyclic unsymmetric imides **94** in yields ranging from 3-14% by refluxing primary amides **92** with acid chlorides **93**. At the same time, acyclic symmetric imides

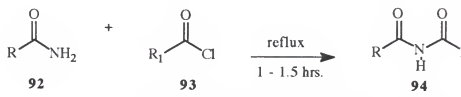

92 93 94

94a,b,c; R = Et; R_1 = t-Bu, 2-Bu, 3-Pentyl; 3, 12, 11%.
94d,e,f; R = i=Pr; R_1 = 2-Bu, t-Bu, 3-Pentyl; 8, 7, 10%.

with amine functionalities were reported by Wieland and Mohr (103) by acylating azido acetamide **95** with azido acetyl chloride **96** to give bis(azidoacetyl)amine **97** (**Figure 2-7**). Further treatment of **97** with HCl gave bis(aminoacetyl hydrochloride)amine **98** in low yields. **98** underwent rearrangement to give diglycinamide **99** in pyridine/water at pH > 5.

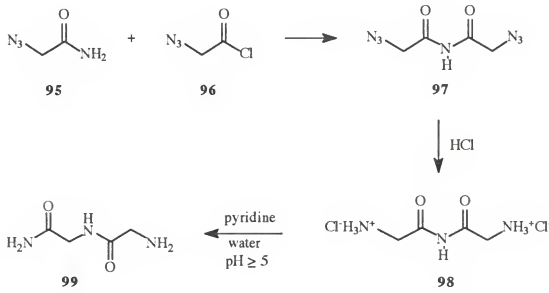

Figure 2-7. Synthesis of functionalized symmetric imides **97** and **98** and rearrangement of **98** to amide **99**.

Wieland and Urbach (104) extended this list of functionalized imides by heating substituted primary amides **100** with substituted acid chlorides **101** to give **102**, which after treatment with HBr afforded imides **103** in variable yields. Treatment of **103b** with traces of triethylamine in ethanol caused rearrangement to diamides **104:105** in a 1.2:1

ratio, respectively, whereas the same treatment on **103c** afforded rearranged products **106:107** in a 15.5:1 ratio, respectively (**Figure 2-8**).

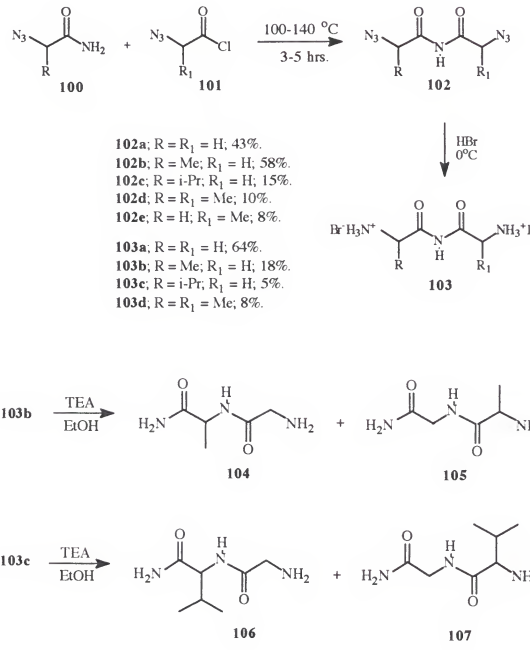

100 **101** **102**

102a; R = R_1 = H; 43%.
102b; R = Me; R_1 = H; 58%.
102c; R = i-Pr; R_1 = H; 15%.
102d; R = R_1 = Me; 10%.
102e; R = H; R_1 = Me; 8%.

103a; R = R_1 = H; 64%.
103b; R = Me; R_1 = H; 18%.
103c; R = i-Pr; R_1 = H; 5%.
103d; R = R_1 = Me; 8%.

103

103b → **104** + **105**

103c → **106** + **107**

Figure 2-8. Base promoted rearrangement of unsymmetric imides **103b,c** to amides **104-107**.

Acid chlorides have also been coupled to aliphatic secondary amides by Tull and coworkers (105). They reported the synthesis of N-benzoyl-ε-caprolactam **109** in excellent yields by heating ε-caprolactam **108** with benzoyl chloride in the presence of N,N-dimethylaniline.

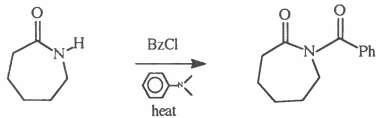

108 **109** (93%)

Weinstock et al. (106) reported the synthesis of several N-alkyl imides **112** in yields ranging from 59-90% by acylating secondary amides **110** with acid chlorides **111** in the presence of N-trimethylsilyl ethylcarbamate.

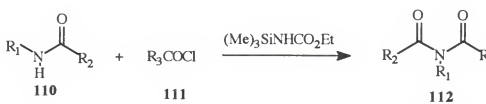

110 **111** **112**

112a; R_1 = i-Pr; R_2 = Me; R_3 = Ph; 53%.
112b; R_1 = i-Pr; R_2 = Ph; R_3 = Me; 96%.
112c; R_1 = Ph; R_2 = R_3 = Me; 77%.
112d; R_1 = R_3 = Ph; R_2 = Me; 95%.
112e; R_1 = i-Pr; R_2 = Me; R_3 = 2-thiazole; 55%.

Mukaiyama et al. (107) also prepared several N-alkyl imides **115** in yields ranging from 82-93% by acylating N-acetylbutylamine **113** with acid chlorides **114** using 1,1'-dimethylstannocene. Davies et al. (108) prepared N-alkyl

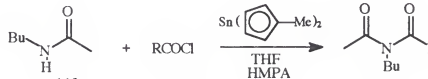

113 **114** **115**

114a,b,c; R_1 = Bu; R_2 = Me; R_3 = Et, i-Pr, Ph; 93, 86, 82%.

imides **118** derived from amino acids in low yields by treating trimethylsilyl amides **116** with acid chlorides **117**. Deprotection under basic conditions caused rearrangement to give amides **119**.

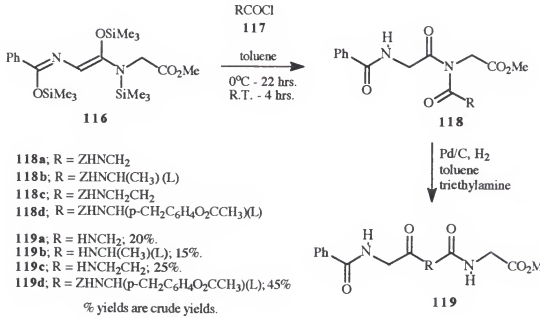

116

118

118a; R = $ZHNCH_2$
118b; R = $ZHNCH(CH_3)$ (L)
118c; R = $ZHNCH_2CH_2$
118d; R = $ZHNCH(p\text{-}CH_2C_6H_4O_2CCH_3)$(L)

119a; R = $HNCH_2$; 20%.
119b; R = $HNCH(CH_3)$(L); 15%.
119c; R = $HNCH_2CH_2$; 25%.
119d; R = $ZHNCH(p\text{-}CH_2C_6H_4O_2CCH_3)$(L); 45%

% yields are crude yields.

119

Bredereck et al. (109) reported the synthesis of N-formyl imides **122** in good yields by treating ditrimethylsilylformamide **120** with acid chlorides **121**. Later, Vederas et al. (110) increased the yields of **122a,b** and further utilized this method to prepare various new N-formyl imides **122c-g** in yields ranging from 59-90%.

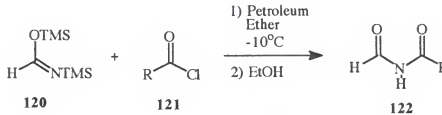

120 **121** **122**

122a,b; R = Me, Et.
122c-g; R = MeO, Ph, Bn, BnO, $BnCH_2$.

One significant advantage of the acid chloride method over the acid anhydride method is that, generally, much lower temperatures are required to form imides. This is not surprising given that acid chlorides are more reactive than the cognate anhydrides (111).

Pyridine bases have been shown to promote reaction between acid chlorides and amides to such an extent that diacylation or dehydration products become significant. This is advantageous in the sense that imides can be synthesized at low temperatures. However, one disadvantage is increased formation of diacylation and dehydration products, decreasing the yield of imide and making purification more difficult.

Imides from Nitriles and Carboxylic Acids

In 1868 Gautier (112,113) reported the preparation of diacetamide **31** in low yields by refluxing acetonitrile and acetic acid. Later, this method was used extensively by

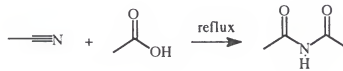

31

various authors to prepare a wide variety of aromatic and aliphatic cyclic imides in variable yields (114-116). Mathews (117) investigated this method further and reported the synthesis of acyclic imides by heating monobasic and polybasic aromatic acids with nitriles. Tarbouriech (95) reported the synthesis of additional aliphatic symmetric acyclic imides **125** by heating nitriles **123** with acids **124**, although the yields were not given. Sumarokova et al. (118) reported the preparation of acyclic symmetric imides **128** by treating dicarboxylic acids **126** with nitrile **127** in the presence of tin(IV)chloride.

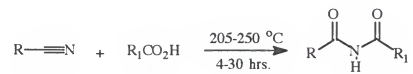

123 **124** **125**

125a; R = R_1 = Pr.
125b; R = R_1 = i-Bu.

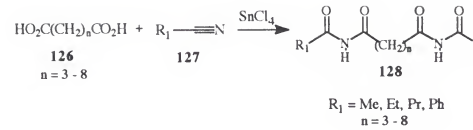

The first synthesis of functionalized aliphatic symmetric acyclic imides using this method was reported by Bergell in 1907 (**Figure 2-9**) (119). Bis(chloroacetyl)amine **131** was obtained in very good yields by heating chloroacetonitrile **129** with chloroacetic acid **130**. Further treatment of **131** with ammonia afforded imide **132** in low yields. Hydrochloride **132** was then treated with silver oxide to give the functionalized imide **133**. Bergell and Feigl (120) extended these studies by reporting the preparation of

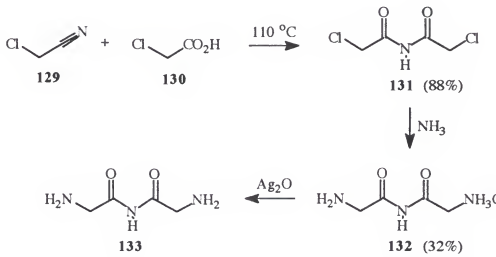

Figure 2-9. Synthesis of functionalized imides **131-133** from nitrile **129** and acid **130**.

the first functionalized unsymmetic acyclic imides **134** by heating **132** with various different reagents. Additional imides **136** and **137** were prepared by heating 2-chloropropionitrile **135** with chloroacetic acid and subsequent treatment with ammonia (**Figure 2-10**).

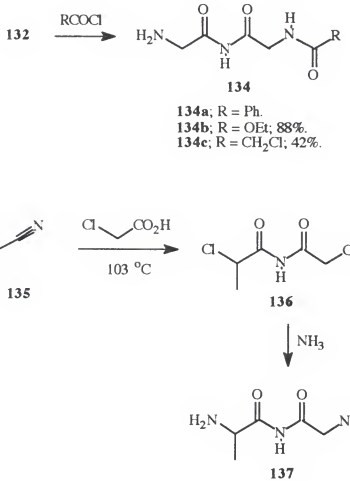

Figure 2-10. Synthesis of functionalized unsymmetric imides **136** and **137**.

Later, Wiley and Guerrant (121) reported the synthesis of symmetric acyclic imides **140a,b** from their correponding

nitriles **138** and acids **139**. Davidson and Skovronek (89) also studied the reaction between nitriles and acids and obtained imides **140c-f** in various yields. Toland and Ferstandig (122) used this method to exchange nitrile and carboxylic acid groups in aromatic compounds (**Figure 2-11**).

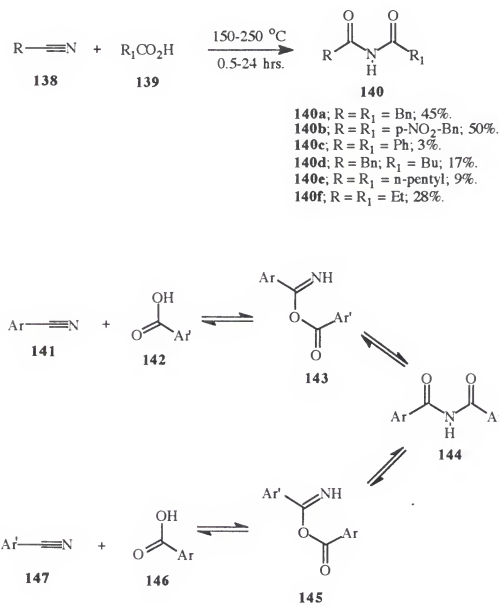

Figure 2-11. Mechanism for nitrile and carboxylic acid group exchange via imide intermediate **144**.

Building on the idea proposed by Davidson and Skovronek (89), they explained their results by assuming the formation of isoimide **143**, arising from nitrile **141** and acid **142**, which can readily rearrange to form imide **144**. The reversibility of this process and the symmetric nature of the imide moiety allows **144** to form another isoimide **145** which ultimately gives rise to new nitriles **146** and acids **147**. Isoimides and imides were not directly observed or isolated in this study.

Although the reaction between nitriles and acids has been used extensively to prepare a wide variety of symmetric and unsymmetric aliphatic and aromatic imides, it suffers from high temperatures and pressures required to drive the reaction forward. Analogous to the acid anhydride method, this method is limited to thermally stable groups.

In contrast, very useful functionalized chloroimides, such as **131** and **136** (**Figure 2-9** and **Figure 2-9**), can be made using this method. These imides can be transformed to more highly functionalized imides by simply substituting the chlorine atom with various nucleophiles. One disadvantage here is that the imide moiety is formed at an early stage of the synthesis. Its stability will thus limit the reaction conditions and reagents used to effect substitutions which could result in imides with high degree of functionality.

Imides from Amides

Early on, Strecker (123) published the synthesis of diacetamide **149a** by heating acetamide at very high temperatures. Titherley and Holden (98) reported the synthesis of symmetric aromatic acyclic imides **149b,c** by heating their corresponding amides in the presence of hydrochloric acid. Hurd and Prapas (90) also described the synthesis of diphenylacetimide **149d** in low yields by heating phenylacetamide in the presence of sulphuric acid. Davidson and Karten (82) reported the synthesis of aliphatic acyclic symmetric imides **149e,f** by heating their corresponding amides at very high temperatures. Nitriles and carboxylic acids were also side products of the reaction.

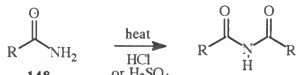

148 **149**

149a; R = Me.
149b; R = Ph.
149c; R = p-toluyl; 0.5%.
149d; R = Bu; 11%.
149e; R = Et; 49%.
149f; R = i-Pr; 12%.

This method of imide synthesis has received very little attention and therefore has not been used by many authors. The high temperatures required to obtain imides permit the significant formation of nitriles and carboxylic acids as

major side products. As expected, this method can only be limited to aliphatic and aromatic amides containing simple heat insensitive groups.

Imides from Amide Anions

The reaction between metallic derivatives of amide anions and acyl halides was first investigated by Titherley (124). The synthesis of several acyclic imides **152** in low yields were reported by heating sodium amides **150** with acid chlorides or bromamides **151**. Rakshit (125) investigated this method further and reported the synthesis of several sodium and potassium imide salts **154** by heating amides **153** with

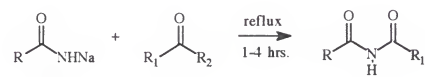

150 **151** **152**

152a; R = R_1 = Ph; R_2 = Cl; 54%.
152b; R = Ph; R_1 = Me; R_2 = Cl.
152c; R = R_1 = Me; R_2 = Cl; 40%.
152d; R = R_1 = Me; R_2 = NHBr.
152e; R = R_1 = Ph; R_2 = NHBr.

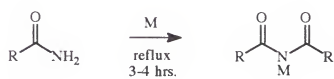

153 **154**

154a,b; R = H; M = Na, K.
154c,d; R = Me; M = Na, K.
154e,f; R = Et; M = Na, K.

sodium or potassium metal in light petroleum or benzene. Treatment of **154c** with hydrochloric acid gave diacetamide in 75% yield.

Sondheimer and Holley (126) reported the synthesis of N-carbobenzyloxy-L-aminosuccinimide **157** by treating N-carbobenzyloxy-L-asparagine methyl ester **155** or N-carbobenzyloxy-L-isoasparagine methyl ester **156** with sodium hydroxide and subsequent acidification with hydrochloric acid (**Figure 2-12**). N-carbobenzyloxy-DL-aminoglutarimide **159**

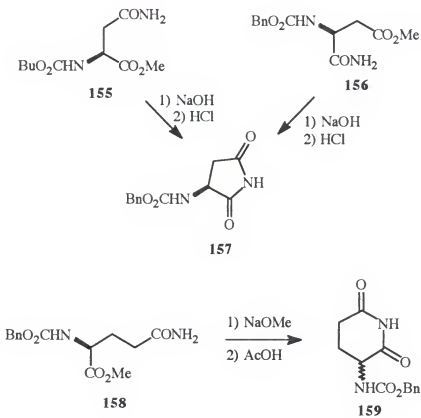

Figure 2-12. Synthesis of cyclic imides **157** and **159** from diprotected L-asparagines **155** and **156** and L-glutamine **158**.

was obtained in a similar fashion by treating N-carbobenzyloxy-L-glutamine methyl ester **158** with sodium methoxide in benzyl alcohol and subsequent acidification with acetic acid, although in this case complete racemization occured. Although **157** and **159** are cyclic imides, **157** was the first example of an optically active imide derived from an amino acid.

Stevens and Munk (127) reported the synthesis of an N-aryl imide **162** in moderate yields by treating amides **160** and **161** with sodium in toluene and subsequent treatment with the corresponding acid chloride. Wolfe and Trimitsis (128) reported the preparation of several β-keto imides **164** in low to excellent yields by treating amides **163** with excess sodium hydride and various aroyl methyl esters in refluxing monoglyme.

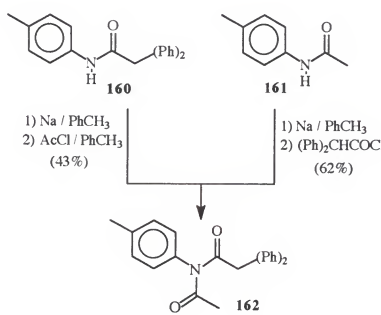

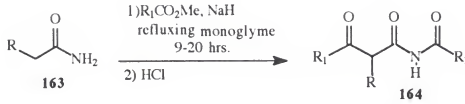

164a,b,c; R = H; R_1 = Ph, anisyl, p-Cl-C_6H_4; 100, 62, 70%.
164d,e,f; R = Ph; R_1 = Ph, anisyl, p-Cl-C_6H_4; 92, 60, 68%.
164g,h; R = Et, Bu; R_1 = Ph; 68, 65%.

Generally, the reaction between amide anions and acyl equivalents gives good yields of imides. The treatment of amides with sodium or potassium metal to give the metallic derivatives of amides possess one major potential disadvantage, however, in that these reactants cannot have functional groups that can react with the metals. The use of sodium hydroxide (126) and sodium hydride (128) to form amide anions involves the use of strongly basic conditions. Such conditions favor side reactions if the amide contains additional functional groups such as esters, aldehydes, halides, etc. Moreover, additional side products can form from direct reaction of these bases with the functional groups themselves. In short, the strongly basic conditions used limits the applicability of this method to simple amides and acyl equivalents.

Imides from Amides and Ketenes

The reaction of ketene **165** with N-arylamides was first investigated by Rice et al. (129) by acetylating N-phenylacetamide **166** with ketene at high temperatures to give

N-phenyldiacetamide **167** in 50% yield. The authors suggested that N-acetyl benzamide was formed similarly from benzamide and ketene, but that the imide decomposed to benzonitrile during the reaction.

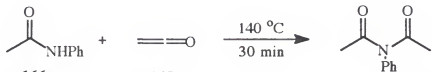

166 **165** **167** (50%)

Padgham and Polya (130) acetylated molten acetamide and benzamide to give diacetamide and N-acetylbenzamide respectively by treatment with ketene. At the same time, Smirnova et al. (131) reported the acetylation of **166** with ketene to give **167** using catalytic amounts of sulphuric acid.

Dunbar and White (132) acetylated various amides **168** with ketene in benzene or ether solutions to give unsymmetric acyclic imides **169** using catalytic amounts of sulphuric acid. Yields of imides were essentially quantitative.

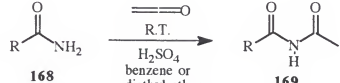

168 **169**

R = Me, vinyl, Ph, p-toluyl, CH_2CN, 2-propene.

In general, this method is limited to amides with heat and acid insensitive functional groups. The use of ketene also limits this method to the synthesis of N-acetyl imides only, unless substituted ketenes are used. Little attention has therefore been given to this method.

Imides from Isocyanates and Acid Anhydrides

Alkyl isocyanates **170** and acid anhydrides **171** react to give imides **173** by way of mixed anhydride **172** (**Figure 2-13**). Hurd and Prapas (90) reported the synthesis of N-substituted imides **176** in good yields by heating isocyanates **174** with acid anhydrides **175**. Later, Kato and Wade (133) applied this method to cyclic anhydrides and reported the synthesis of N-phenylphthtalimide from phenyl isocyanate and phthalic anhydride.

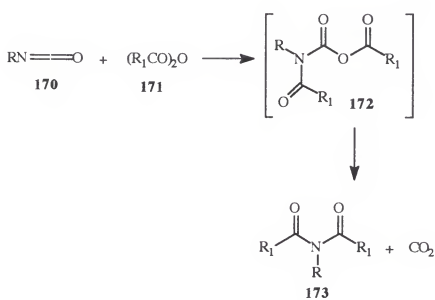

Figure 2-13. Formation of imides **173** from isocyanates **170** and acid anhydrides **171** via intermediate **172**.

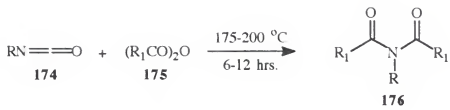

176a; R = Ph; R_1 = Me; 72%.
176b,c,d,e; R = CH_2CO_2Et; R_1 = Me, Et, heptyl, Ph; 74, 37, 70, 70%.

One advantage this method offers is that imide formation occurs presumably via intramolecular rearrangement of **172**. Thus, N-substituted unsymmetric acyclic imides may be synthesized using unsymmetrical acid anhydrides. No such experiments have yet been reported however. In contrast, high temperatures limit the types of substituents allowed on the isocyanate or acid anhydride. In addition, substituents which are incompatible with isocyanates and anhydrides cannot be used.

Miscellaneous Methods

Other methods besides the ones described have been used to prepare imides in good yields. King and Kidd (134) and Baker et al. (135) prepared imides from secondary amides and carboxylic acids under mildly acidic conditions. Other reagents such as phosphorous pentoxide (136), acetyl chloride (137), and thionyl chloride (138) have been used to prepare imides from amides and carboxylic acids.

Hagemeyer (139) reported the synthesis of diacetamide **179a** from acetamide and isopropenyl acetate **178a**. Later,

Rothman et al. (140) reported the synthesis of imides **179b,c** by treating amides **177** with isopropenyl stearate **178b.**

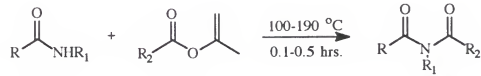

177 **178** **179**

179a; R = R_2 = Me; R_1 = H.
179b; R = Me; R_1 = Ph; R_2 = $C_{19}H_{35}$; 47%.
179c; R = $C_{19}H_{35}$; R_1 = Bu; R_2 = $C_{19}H_{35}$;76%.

Bredereck et al. (141) reported the synthesis of symmetric acyclic imides **181** in variable yields by heating amides **180** with trityl chloride. Krafft and Karstens (142) reported the synthesis of symmetric acyclic aromatic imides **184** via hydrolysis of imidodiamides **183** starting from nitriles **182.**

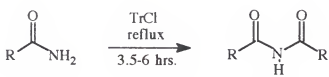

180 **181**

181a,b,c,; R = Me, Et, i-Pr; 17, 73, 83%.

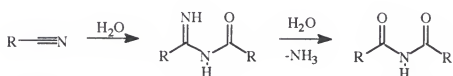

182 **183** **184**

R = o and p-toluyl

Wheeler et al. (143) reported the synthesis of acyclic unsymmetric imides **186** by treating acyl imido esters **185** with hydrochloric acid at room temperature. Later,

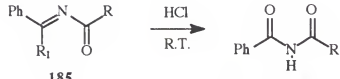

185 **186**

186; R = Me, Et, Pr.
R_1 = Me, Et, Pr.

Gruszecki et al. (144) reported the synthesis of functionalized acyclic unsymmetric N-phenyl imides **189** by treating imidoyl chlorides **188** with N-(tert-Butoxycarbonyl)-amino acids **187**. Yields for **189** were not reported however. Krohn et al. (145) described the synthesis of highly functionalized acyclic unsymmetric imides **192** and **195** in very low yields by treating acyl imido esters **190** with acid chlorides **191** and acyl imido esters **193** with alkyl carbonates **194**, respectively.

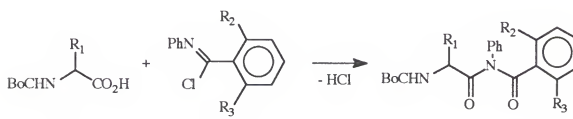

187 **188** **189**

189a,b; R_1 = H, Me; R_2 = NO_2; R_3 = H.
189c,d,e,f,g; R_1 = H, Me, Bn, $(CH_2)_4NHBoc$, CH_2CONH_2; R_2 = R_3 = Cl.

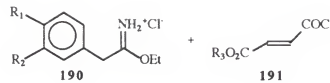

190 191

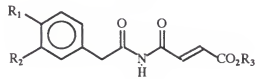

192

192a,b,c,d,e; R_1 = H, OH, OMe, OBn, Cl; R_2 = H; R_3 = Me; 36, 18, 22, 17, 12%.
192f; R_1 = OH; R_2 = Cl; R_3 = Me; 21%.
192g,h; R_1 = R_2 = H; R_3 = n-Bu, n-pentyl; 22, 18%.

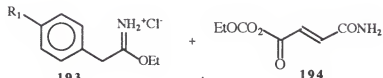

193 194

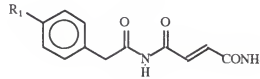

195

195a,b,c; R_1 = H, OMe, Cl; 30, 44, 18%.

Kikukawa et al. (146) prepared N-aryl imides **198** in yields ranging from 50-79% by heating tetrafluoroborate salts **196** with sodium carboxylates **197** and acetonitrile. Bowser (147) reported simple acyclic unsymmetric imides **201** from acid chlorides **199** and N,N-di(trimethylsilyl)amine **200**. Mori et al. (148) have prepared dibenzamide in 1-20% yields by treating benzoyl chloride with a mixture of $TiCl_4$,

nitrogen, magnesium or lithium metal, and trimethylsilyl chloride.

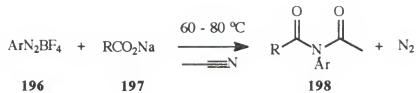

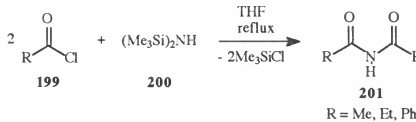

Bates et al. (149) prepared acyclic unsymmetric imides **203** in 50-60% yields by heating acids **202** with acetic anhydride followed by subsequent oxidation. The formation of an acyclic unsymmetric N-alkyl imide from oxidation of an N-alkylcyano amide with sodium hydride in N,N-dimethylformamide (DMF) has been reported by LeBlanc and Gibson (150).

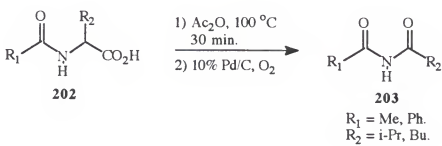

Stevens and Munk (127) prepared acyclic unsymmetric N-aryl imides **206** in 76-80% yields by treating acids **205** with nitrogen ketene analog **204**. MaGee et al. (151) reported the preparation of acyclic unsymetric imide **208** by heating benzamide with ethyl alkynyl ether **207**.

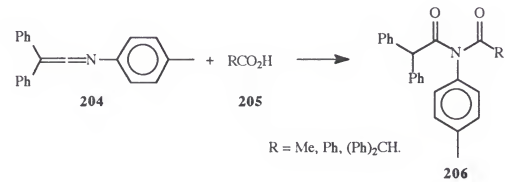

204 **205** **206**

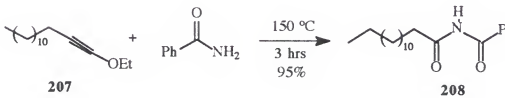

207 **208**

Berkowitz and Rylander (152) reported the oxidation of amides **209a,b** with ruthenium tetroxide to give acyclic symmetric imides **210a,b** in reasonable yields. Years later, Yoshifuji et al. (153) reported the oxidation of unsymmetric acyclic amides **209c-j** with ruthenium tetroxide to give imides **210c-j** in very good yields. Sheehan and Tulis (154) have reported the oxidation of various cyclic amides with ruthenium tetroxide to give cyclic imides in variable yields.

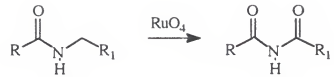

209 **210**

210a,b; R = C_6H_{13}, $(CH_2)_2$; R_1 = C_7H_{15}; 58,49%.
210c-j; R = t-Bu, Ch, Ph, C_9H_{19}, i-Pr, Pr, Me, Cl_3C; R_1 = Et; 89, 96, 67, 92, 92, 81, 0% yields.

Rieche and Schon (155) oxidized ε-caprolactam to the corresponding imide in low yields using oxygen and cobalt nitrate in the presence of ultraviolet light. Needles and Whitfield (156) reported the oxidation of a variety of 5- and 6-membered lactams to their corresponding imides in fair yields by treatment with potassium persulfate.

Concluding Remarks

In general, the methods presented here are limited by a number of factors to the synthesis of fairly simple imides as discussed in each method. The vast majority of known imides are either aromatic and aliphatic cyclic symmetric, or aromatic and aliphatic acyclic symmetric and unsymmetric. Most of these imides, with few exceptions, have no functional groups attached and therefore possess a very low degree of versatility. This lack of functionality places a major limitation if more versatile functionalized imides are demanded.

Imides similar in structure to **12** (**Figure 1-9**) have not been reported. This imide appears unique in that it is aliphatic, unsymmetric, acyclic, and possesses two chiral amino acid centers. A logical approach to obtaining highly functionalized optically pure imides such as **12**, was to begin the synthesis with highly functionalized chiral starting materials. The functional groups could then be protected against a wide variety of reaction conditions using standard protecing groups (157). After formation of the imide bond, deprotection under mild conditions was expected to allow preparation of versatile symmetric or unsymmetric, cyclic or acyclic, highly functionalized chiral imides such as **12**. The next chapter explores the application of imide synthetic methodology to the synthesis of new imides derived from L-glutamine, including imide **12**.

CHAPTER 3
SYNTHESIS AND PROPERTIES OF HIGHLY FUNCTIONALIZED UNSYMMETRIC ACYCLIC IMIDES

Designing The Enzyme Imide Intermediate

Close inspection of imide intermediate **12** reveals certain important features that must be considered before planning out its synthesis. First, it is a highly functionalized unsymmetric acyclic imide. Second, it is tetrafunctionalized derived from glutamine and aspartic acid or glutamic acid and asparagine. Third, it possesses two chiral centers with the (S) configuration (158).

Considering these characteristics and given that in the proposed mechanism by Richards and Schuster (60,64) (**Figures 1-11** and **1-12**) imide **12** is formed from L-glutamine and an activated form of L-aspartic acid, β-aspartyl-AMP, we decided to prepare **12** by forming the imide functional group through reaction between the amide functional group of L-glutamine and the β-carboxyl group of L-aspartic acid. L-glutamine and L-aspartic acid can serve as starting materials which have the correct chirality and functionality required to form imide **12**. Thus, the main problems were the choice of stable protecting groups for the N_{α} and C_{α}-terminals of L-glutamine and L-aspartic acid and an appropriate synthetic method to form the imide functional group.

Our proposed synthetic route for the preparation of imide **12** is illustrated in **Figure 3-1.** This route starts with N-carbobenzyloxy-L-glutamine **211a** or N-*tert*-butoxycarbonyl-L-glutamine **211b** and N-carbobenzyloxy-L-aspartic acid **212** which are commercially available or easily synthesized. Esterification of **211** and **212** applying known procedures (157) was anticipated to give N-protected-α-substituted-L-glutamine esters **213a-c** and N-carbobenzyloxy-α-benzyl-L-aspartic acid **214**, respectively. The purpose of this protection was to isolate the glutamine amide functionality and the β-carboxyl functionality of aspartic acid, and so allow condensation between these two groups to form the imide without reaction of other functional groups in the starting materials. Imide formation can then be accomplished by condensing **213a-c** with an activated form of **215**, namely **215a** or **215b**, to give imide **216**, a tetraprotected form of imide **12**. Recalling the reactions between acid chlorides and amides under mild conditions and acid anhydrides with amides under acid catalysis at reasonable temperatures (Chapter 2), acid chloride **215a** and acid anhydride **215b** were chosen as activated forms of **215**. Problems in this step may arise, however, considering the high degree of functionality involved and the generally variable yields obtained on these methods of imide synthesis.

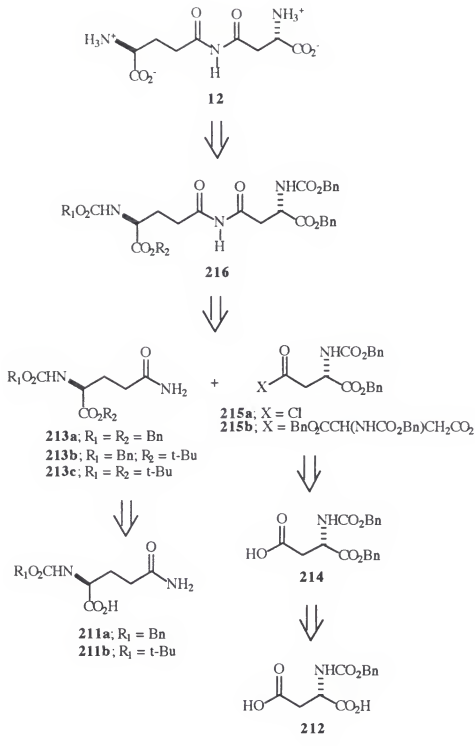

Figure 3-1. Retrosynthetic analysis for the formation of imide **12** starting from N-protected-L-glutamine **211** and N-protected-L-aspartic acid **212**.

Deprotection of **216**, using mild conditions to prevent breakdown of the imide could then allow formation of imide **12**.

Starting with amino acid derivatives **211** and **212** simplified the synthetic route by avoiding the use of asymmetric synthesis (159). In contrast, one disadvantage of choosing these derivatives as starting materials was their lability towards racemization (157,160). Protecting groups which are stable and easily removable under mild conditions were chosen to maximize yields and avoid loss of the imide functionality on the final steps of the synthesis. Reaction conditions for each step of the synthesis were also carefully evaluated so as to avoid partial, or complete racemization, and maximize yields.

Synthesis of Di-protected L-Glutamine Derivatives

Carbobenzyloxy and *tert*-butyloxycarbonyl functional groups for protecting the N-terminal of amino acids have been used extensively in peptide chemistry and can be removed selectively under mild conditions which are not expected to interfere with other moieties introduced into the final products (157,161). Benzyl and *tert*-butyl groups have been used to protect the C-terminal of amino acids and peptides and can also be removed selectively under mild conditions (157,161). A number of different combinations of N_α and C_α-protected L-glutamine derivatives were investigated so as to

introduce versatility into the molecule and increase the chances of obtaining the final product. Three di-protected L-glutamine derivatives **213a-c** were prepared in good yields **(Figure 3-2).**

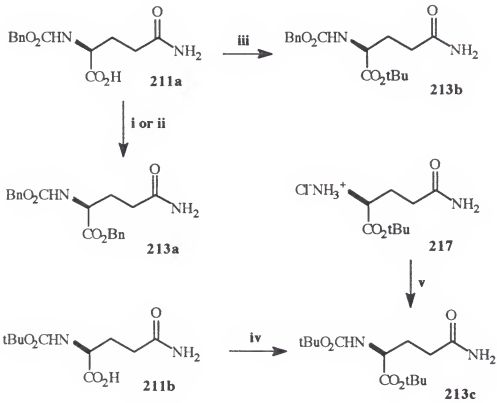

Figure 3-2. Synthesis of N,C-diprotected-L-glutamine **213a-c** from N-protected-L-glutamine **211a** and **211b** or C-protected-L-glutamine **217**. Reagents and conditions: **i**; a) Cs_2CO_3, $MeOH/H_2O$, pH 8, 0 °C-R.T., quant, b) BnBr, DMF/MeOH, R.T., 95%. **ii**; BnOH, TsOH(cat.), benzene reflux, 59%. **iii**; *t*-BuOH, DCC, DMAP(cat.), THF, 0 °C-R.T., 83%. **iv**; **iii**, 85%. **v**; $(t\text{-}BuO_2C)_2O$, triethylamine, THF, 0 °C-R.T., 98%.

Although, N-carbobenzyloxy-L-glutamine **211a** could be purchased from commercial sources, it was also prepared in

76% yield by treatment of L-glutamine **1** with NaOH and benzylchloroformate, followed by subsequent acidification with hydrochloric acid. N-carbobenzyloxy-α-*t*-butyl-L-glutamine **213b** was obtained in 83% yield, after several recrystallizations, by esterification of **211a** with t-butanol and N,N-dicyclohexylcarbodiimide (DCC), following the method of Csanady and Medzihradszky (162). N-carbobenzyloxy-α-benzyl-L-glutamine **213a** was prepared using two methods. In the first, **211a** was refluxed in benzene with benzyl alcohol (BnOH) and catalytic amounts of p-toluenesulfonic acid (TsOH) with azeotropic removal of water to give **213a** in 59% yield. The second method involved isolation of the cesium salt followed by treatment with benzyl bromide (BnBr) in dimethylformamide (DMF)/ methanol (MeOH). This latter method gave **213a** in 95% yield and was used preferentially to the former due to higher yields of product, milder conditions, and ease of product purification.

N-(*tert*-butoxycarbonyl)-L-glutamine **211b** was prepared in 92% yield by treating **1** with sodium hydroxide and di-tert-butyl dicarbonate $(tBuO_2C)_2O$ in cold dioxane/water and subsequent acidification with potassium hydrogen sulfate ($KHSO_4$). Esterification of **211b** with t-butanol and DCC as in **213b** afforded N-(*tert*-butoxycarbonyl)-α-*tert*-butyl-L-glutamine **213c** in 85% yield. Alternately, **213c** could be prepared in 98% yield by treating comercially available α-*tert*-butyl-L-glutamine hydrochloride salt **217** with $(tBuO_2C)_2O$ and triethylamine (TEA) in THF.

Synthesis of Di-protected L-Aspartic Acid Derivatives

The synthesis of acid chloride **215a** and acid anhydride **215b** used as acylating agents to prepare **216** (**Figure 3-1**) is shown in **Figure 3-3.** Commercially available N-carbobenzyloxy-L-aspartic acid **212** was chosen as the starting material for the preparation of **215a** and **215b.** N-

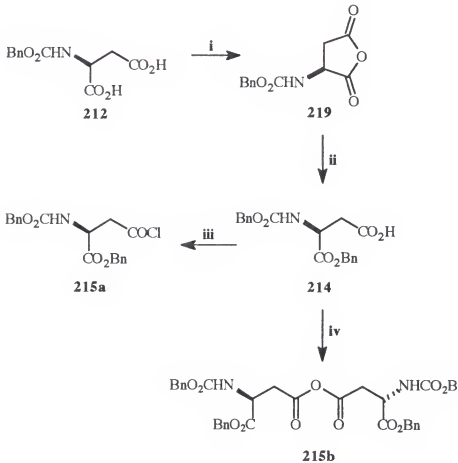

Figure 3-3. Synthesis of β-activated N-Carbobenzyloxy-α-benzyl-L-aspartic acid **215a,b** from N-Carbobenzyloxy-L-aspartic acid **212.** Reagents and conditions: **i;** Ac_2O, R.T., 95%. **ii;** BnOH, 80 °C, 61%. **iii;** PCl_5, Et_2O, 0 °C-R.T., 89%. **iv;** DCC, CH_2Cl_2, 0 °C, 90%.

carbobenzyloxy-L-aspartic anhydride **219** was prepared in 76% yield using the method of Le Quesne and Young (163) by reacting **212** with acetic anhydride. Heating **219** with benzyl alcohol and subsequent fractional extraction following the method of Bergmann, Zervas, Salzmann (164) gave N-carbobenzyloxy-α-benzyl-L-aspartic acid **214** in 61% after recrystallization. Treating **214** with phosphorous pentachloride (PCl_5) afforded acid chloride **215a** in 89% yield after recrystallization from diethyl ether:petroleum ether. Acid anhydride **215b** was prepared in 90% yield from intermolecular condensation of **214** with DCC.

Synthesis of Protected Imide Intermediate

The acid catalyzed condensation between amide **213a** and anhydride **215b** was initially investigated (**Figure 3-4**). For our preliminary experiments, amide **213a** was chosen as one of the starting materials because of its higher stability towards acid compared to **213b** and **213c**. Heating **213a** with **215b** in toluene at high temperatures (70-100 °C) with catalytic amounts of sulphuric acid (0.1-0.2 eq.) did not form the desired imide condensation product. By-products **220**, **221**, and **222**, as well as acid **214**, were only isolated from the reaction mixture. The formation of cyclic imide **220** presumably arose from the acid catalyzed condensation between the N_γ nitrogen with the C_α carbonyl carbon. Cyclic imide

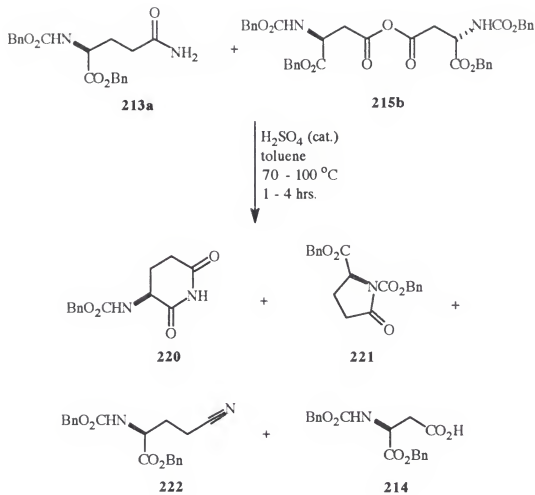

Figure 3-4. Acid catalyzed reaction between amide **213a** and acid anhydride **215b** to give new products **220-222.**

220 has been observed as a by-product from N-carbobenzyloxy-L-glutamine derivatives under basic conditions (126). Pyrrolidone **221** has also been observed and presumably originates from the condensation reaction between the N_{α} nitrogen and the C_{γ} carbonyl carbon (165,166). Nitrile **222** presumably arises from direct dehydration of **213a.** Due to the poor control of reactivity, this route was abandoned and

investigation of the amide/acid chloride method was undertaken.

The condensation reaction between amides **213a-c** and acid chloride **215a** in chloroform and pyridine at room temperature was initially investigated (**Figure 3-5**).

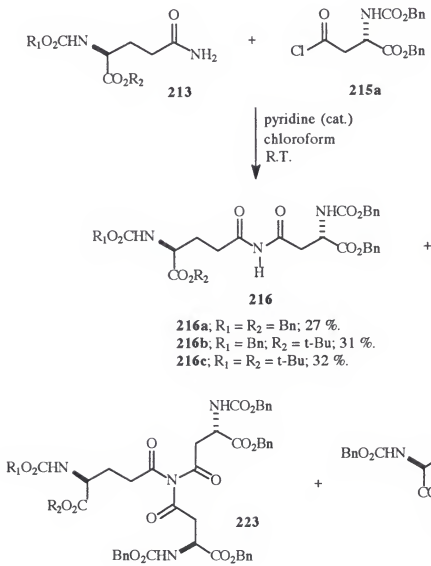

Figure 3-5. N-acylation of amides **213** by acid chloride **215a** in the presence of pyridine to give unsymmetric imides **216**, N,N-diacylamines **223**, and nitriles **224**.

Monoacylation took place to give low yields of the desired imides **216** as well as diacylation products **223** and nitriles **224.** In efforts to optimize the yields of imides **216a-c**, the effects of temperature, solvent, and catalyst concentration were briefly investigated. Amide **213b** was chosen as one of the starting materials for these studies since it was more easily prepared and purified relative to **213a** and **213c.**

When the reaction between amide **213b** and acid chloride **215a** was carried out in chloroform or dichloromethane with pyridine (0.6 eq relative to amide) at -40 °C, the only products obtained were **216b** and **223b.** No significant formation of nitrile **224b** was detected, even after warming up the solution to ambient temperature. Although the yield of **216b** (27%) dropped insignificantly compared to ambient temperature (32%), the **216b/223b** ratio increased from 0.72 at R.T. to 1.4 at -40 °C. These results differ from the findings of Thompson (101) on the pyridine catalyzed condensation between simple amides and acid chlorides where it was generally found that low temperatures decrease the monoacylation/diacylation ratio.

Changing the solvent from dichloromethane to THF at -40 °C resulted in the formation of nitrile **224b** and increased amounts of **223b.** In addition, a significant increase in the **216b/223b** ratio (2.2) was observed. Using an excess of pyridine (10 eq. relative to amide) in dichloromethane at -40 °C resulted in the formation of significant amounts of

nitrile **224b** and complete disappearance of **223b**. This was expected given that using excessive amounts of pyridine should lead to dehydration of the isoimide intermediate (89) to give nitrile **224b** and corresponding acid, rather than its rearrangement to form imide **216b**. This process has been observed with much simpler amides and acid chlorides (89). However, our results are inconsistent with earlier observations by Titherley (99) and Thompson (101) where using excessive amounts of pyridine increased the yield of monoacylated material at the expense of diacylated product. With our starting materials the yield of nitrile, rather than monoacylated material, increased at the expense of diacylated product using excess pyridine.

Changing the catalyst from pyridine to N,N-dimethylaminopyridine (DMAP) in dichloromethane at -40 °C resulted in virtually exclusive formation of nitrile **224b** and **223b** with low amounts of **216b**. Increasing the temperature from -40 °C to ambient temperature in all cases resulted in increased amounts of nitrile **224b** and **223b** with no effect on the yields of **216b**.

Best yields of imide **216b** were obtained using chloroform or dichloromethane as solvent, pyridine (0.4-0.8 eq. relative to amide) as catalyst, and acid chloride/amide molar ratios between 1.3-1.5 at ambient temperature overnight. Nitrile **224b** formation was completely inhibited when using chloroform or dichloromethane as solvent, pyridine (0.6 eq. relative to

amide) as catalyst, and a temperature range of -40 to 23 °C over a period of 24 hours.

The order in which the reagents were added did not affect the product distribution significantly. Due to solubility problems of the amide, the most convenient way to carry out the reaction was to add the base (pyridine) to a mixture of amide and acid chloride in dichloromethane. From our observations, the amount and type of base employed in the coupling reaction are key factors in controlling the distribution of products formed from highly functionalized amides and acid chlorides.

Deprotections of Imide Intermediate

Of all three imides **216a-c** serving as adequate starting materials for the synthesis of imide **12** (**Figure 3-1**), imide **216b** was more easily prepared and purified relative to **216a** and **216c** and therefore was investigated further. Imide **216b** was deprotected to the free acid **225** in excellent yields using TFA in dichloromethane (**Figure 3-6**). Acid **225** was isolated as a stable crystalline solid which was easily purified from several recrystallizations before the final step. Catalytic hydrogen transfer of **225** with 10% Pd/C and 1,4-cyclohexadiene afforded **12** in good yields as a stable hygroscopic solid. Other hydrogen donors such as ammonium formate and formic acid gave mixtures of products. Cyclohexene and hydrogen gas gave only partial conversion to

12. As will be discussed later, imide 12 possesses interesting pH-dependent chemistry in aqueous solutions.

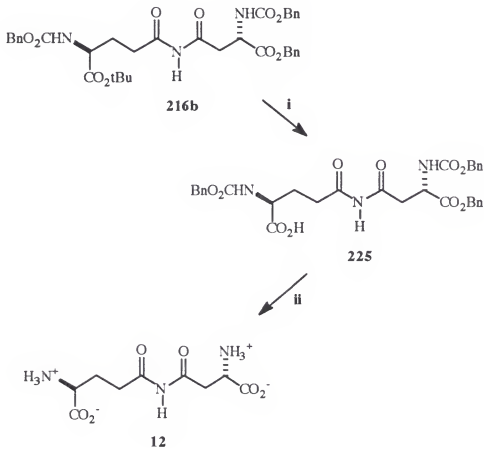

Figure 3-6. Deprotection of imide **216b** to give free acid-imide **225** and amino acid-imide **12**. Reagents and conditions: **i**; TFA, CH_2Cl_2, 0 °C, 94%. **ii**; 10% Pd/C, 1,4-cyclohexadiene, EtOH/THF, reflux, 90%.

Other Novel Imide Derivatives of L-Glutamine

Although **12** is the first acyclic N_γ-acylated-L-glutamine derivative known to date, other novel L-glutamine-derived

imides were prepared for evaluation of their properties and their ability to interact with *E. coli* AS-B. These were also prepared by coupling di-protected L-glutamine derivatives with acid chlorides or acid anhydrides.

While simple acylating agents like acetic anhydride and acetyl chloride were commercially available, more complex acid chlorides and acid anhydrides were prepared as illustrated in **Figure 3-7.** Thus, benzylation of succinic

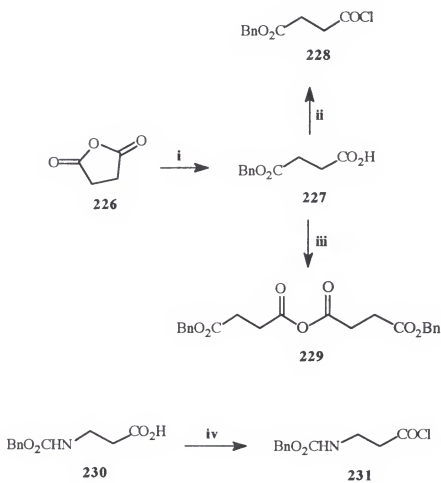

Figure 3-7. Synthesis of electrophiles **228**, **229**, and **231**. Reagents and conditions: **i**; BnOH, 100 °C, 948%. **ii**; PCl_5, Et_2O, 0 °C-R.T.. **iii**; DCC, CH_2Cl_2, 0 °C-R.T., 93%. **iv**; PCl_5, Et_2O, R.T..

anhydride **226** using benzyl alcohol afforded the monoacid **227** in excellent yields. Treatment of **227** with PCl_5 gave acid chloride **228** which was used without further purification. Anhydride **229** was prepared in excellent yields by treatment of **228** with DCC. Acid chloride **231** was also prepared by treating commercially available N-(Benzyloxycarbonyl)-β-alanine **230** with PCl_5 and used without further purification.

Initial experiments were carried out by condensing amides **213a** and **213b** with acetic anhydride or **229** in the presence of catalytic amounts of acid (**Figure 3-8**). Amide **213c** was ignored in these experiments due to its greater lability towards acids relative to **213a** and **213b**. Acylation of **213b** using acetic anhydride and catalytic amounts of sulphuric acid resulted in monoacylation to give imide **233a** in 20% yield with 50% recovered amide after purification (**Table 3-1**). In addition, small amounts of by-products **220**, **234**, **235** and deprotected glutamine were also obtained. Under the same conditions the amide **213a** gave 33% of the desired monoacylation product **233b** with 47% recovered starting material. This increase in yield reflects the greater stability of the benzyl ester over the t-butyl ester of N-carbobenzyloxy-L-glutamine towards acids. Presumably the rate of benzyl ester deprotection is greater than the rate of t-butyl ester deprotection resulting in a greater amount of **213a**, relative to **213b**, available to form imide. More complex acid anhydrides, such as **229**, acylated amide **213b** using catalytic amounts of sulphuric acid to give imide

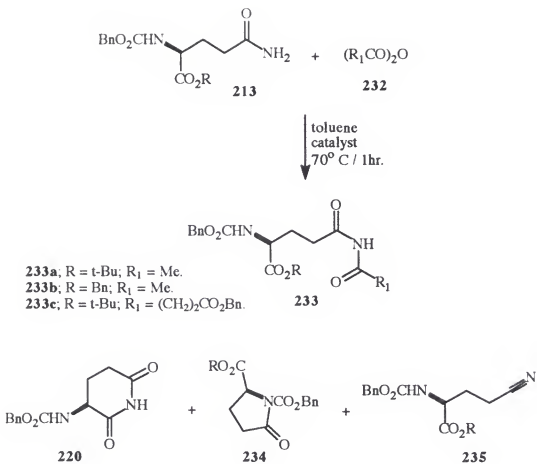

Figure 3-8. Acid catalyzed N-acylation of amides **213** by acid anhydrides **232** to give unsymmetric imides **233** and by-products **220, 234,** and **235.**

233c in 5% yield with the formation of significant amounts of by-products **220, 234,** and **235.** In all cases, temperatures lower than 70 °C did not induce the formation of the desired imides **233a-c** and only caused deprotection of amides **213a** or **213b.**

In efforts to reduce the amount of by-products and deprotection of starting materials to facilitate purification, the weaker acids TsOH and acetic acid were

Table 3-1. Effect of catalyst on the reaction between amides **213** and acid anhydrides **232.**

Entry	R	R_1	catalyst[a]	% yield[b]	by-products observed[c]	% recovered S.M.[d]
233a	tBu	Me	H_2SO_4	20	Y	50
233a	tBu	Me	TsOH	12	N	43
233a	tBu	Me	AcOH	0	N	95
233b	Bn	Me	H_2SO_4	33	Y	47
233c	tBu	$(CH_2)_2CO_2Bn$	H_2SO_4	5	Y	-

[a] approx. 0.1 to 0.2 eq. of catalyst / eq. of amide was used for all reaction:

[b] after column chromatography.

[c] Y = **220,234,235** formed in the reaction : N = **220,234,235** not formed in the reaction.

[d] S.M. refers to di-protected-L-glutamine.

evaluated as catalysts using **213b** as the starting material (**Table 3-1**). In going from sulfuric acid to TsOH the yield dropped from 20 to 12%, respectively, while the amount of recovered amide **213b** remained essentially unchanged. Acetic acid did not induce any reaction and almost all starting amide was recovered. In contrast to H_2SO_4, TsOH and acetic acid inhibited the formation of by-products **220, 234,** and **235,** these being undetected on purification of the reaction mixture. This observation was anticipated given that decreasing the protonating power of the catalyst decreases the protonated forms of **213b** which lead to the formation of these by-products. Because of the generally low yields obtained using this method, further efforts were directed on the acid chloride/amide method.

Amides **213** reacted with acid chlorides **236** in chloroform and pyridine at room temperature to give imides **237** as well as by-products **238** and **239** (**Figure 3-9**). The reaction between amides **213a-c** and acetyl chloride gave imides **237a-c** exclusively in good yields without the formation of by-products **238a-c** or **239a-c**. Relatively similar yields of imides **237d-f** were obtained when acid chloride **228** was used instead of acetyl chloride. In this case, however, significant amounts of the corresponding by-products **238d-f** and **239d-f** were also isolated. Low yields of imides **237g-h**, as well as by-products **238g-h** and **239g-h**, were obtained using acid chloride **231**. From these and previous results (**Figure 3-5**), it is clear that using more complex acid chlorides, relative to acetyl chloride, leads to decreased amounts of monoacylated material and increased amounts by-products.

Additional new unsymmetric acyclic imides **243** and **245** were prepared from L-glutamine derivative **240** (**Figure 3-10**). Imide **243** is part of an alternate route for the synthesis of imide **12** while imide **245** is the first N_γ-formyl L-glutamine derivative. Acid **240** was prepared following the method of Scholtz and Bartlett (167). Acid chloride **241** was obtained in very good yields by treating **240** with PCl_5 in ether. Treating **241** with amide **242**, prepared by esterification of N-carbobenzyloxy-L-asparagine as in **213a** (**Figure 3-2**), in pyridine/chloroform solution afforded imide **243**. Likewise, treating acid chloride **241** with N,N-

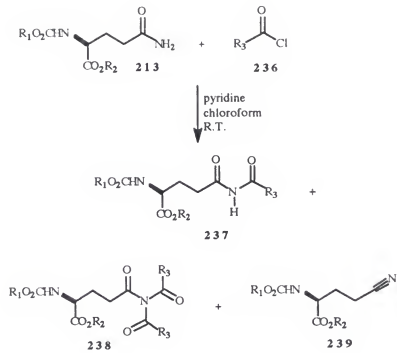

Figure 3-9. N-acylation of amides **213** by acid chlorides **236** in the presence of pyridine to give unsymmetric imides **237**, N,N-diacylamines **238**, and nitriles **239**.

Table 3-2. Identities and percent yields of imides **237a-h** from amides **213a-h** and acid chlorides **236a-h**.

Entry	R_1	R_2	R_3	% yield[a]
237a	Bn	Bn	Me	68
237b	Bn	tBu	Me	66
237c	tBu	tBu	Me	61
237d	Bn	Bn	$CH_2CH_2CO_2Bn$	78
237e	Bn	tBu	$CH_2CH_2CO_2Bn$	60
237f	tBu	tBu	$CH_2CH_2CO_2Bn$	41
237g	Bn	Bn	$CH_2CH_2NHCO_2Bn$	22
237h	Bn	tBu	$CH_2CH_2NHCO_2Bn$	26

[a] Yields obtained after column chromatography.

ditrimethylsilylformamide **244**, prepared following the method of Yoder et al. (168), gave formyl imide **245** in good yields. No further studies were conducted on imides **243** and **245**.

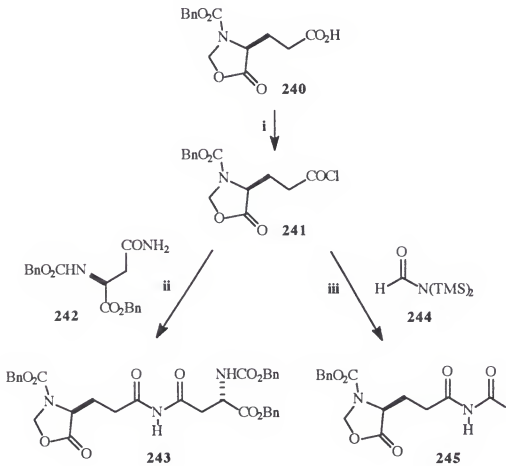

Figure 3-10. Synthesis of imides **243** and **245** from L-glutamine derivative **240**. Reagents and conditions: **i**; PCl_5, Et_2O, R.T., 88%. **ii**; **242**, pyridine, $CHCl_3$, R.T. **iii**; a) **244**, CH_2Cl_2, -5 °C-R.T., b) petroleum ether, EtOH, R.T., 61%.

Deprotection of Novel N_γ-acylated L-Glutamine Imides

Deprotection of **237a-b** to give N_γ-acetyl-L-glutamine **247** is outlined in **Figure 3-11.** Imide **237b** was deprotected to

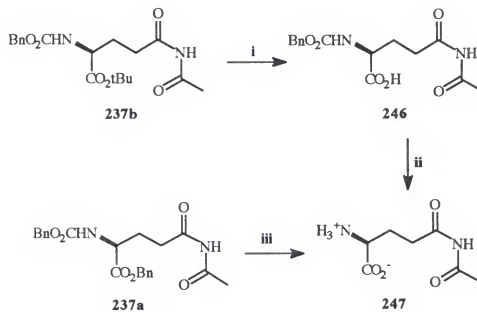

Figure 3-11. Deprotection of unsymmetric imides **237a,b** to give free acid-imide **246** and amino acid-imide **247**. Reagents and conditions: **i**; TFA, CH_2Cl_2, 0 °C, 94%. **ii**; 10% Pd/C, ammonium formate, EtOH, R.T.. **iii**; **ii**, 86%.

give the free acid **246** in good yields using trifluoroacetic acid (TFA) in dichloromethane. Acid **246** was further deprotected to give the free amino acid **247** using 10% Pd/C and ammonium formate as the hydrogen donor. A more efficient route involved treatment of imide **237a** with 10% Pd/C and ammonium formate to give imide **247** directly in very good yields. The advantage of using imide **237a** over imide **237b**

to prepare **247** is that the former is a crystalline stable solid which can be converted very cleanly to **247** in one step, whereas the latter is an oil which lies two steps away from the final product **247**.

The preparation of N_γ-(4-hydroxy-4-oxo-butanoyl)-L-glutamine **249** is illustrated on **Figure 3-12.** Treatment of **237e** with TFA as in **237b** afforded the free acid **248** in good yields as a stable crystalline solid. Hydrogenolysis of **248** using 10% Pd/C and ammonium formate to give **249** suffered from low yields and purification problems. Other hydrogen donors such as formic acid, cyclohexene, and hydrogen gas gave only partial conversion to **249** which was difficult to isolate.

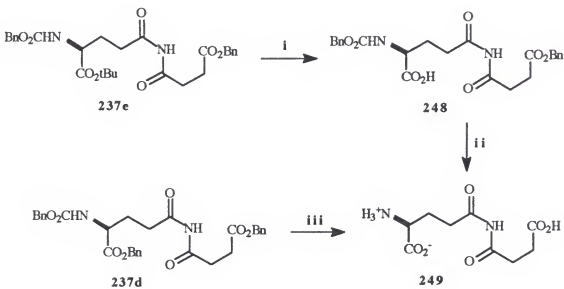

Figure 3-12. Deprotection of unsymmetric imides **237d,e** to give free acid-imide **248** and amino acid-imide **249.** Reagents and conditions: **i**; TFA, CH_2Cl_2, 0 °C, 47%. **ii**; 10% Pd/C, ammonium formate, EtOH, R.T. **iii**; 10% Pd/C, 1,4-cyclohexadiene, EtOH/THF, R.T, 63%.

The easier preparation and purification of imide **237d** over imides **237e,f** (**Figure 3-9** and **Table 3-2**) offered an alternate way to obtain **249** directly in one step. Catalytic hydrogen transfer of **237d** with 10% Pd/C using 1,4-cyclohexadiene as the hydrogen donor afforded **249** as a stable solid in good yields.

Two attempts to deprotect **237g-h** to give N_γ-(β-alanyl)-L-glutamine **251** suffered from purification problems (**Figure 3-13**). Small amounts of acetic acid in the reaction mixture maintained the primary amine in its protonated form to prevent further side reactions. Although the final product

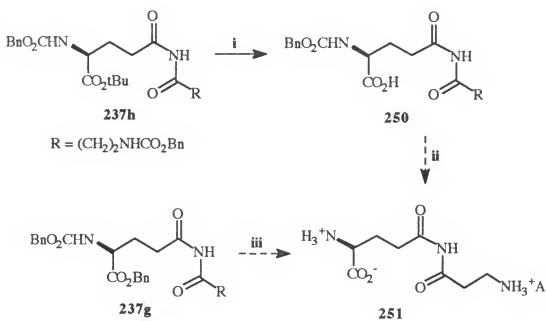

Figure 3-13. Deprotection of unsymmetric imide **237h** to give free acid-imide **250**. Reagents and conditions: **i**; TFA, CH_2Cl_2, 0 °C, 94%. **ii**; 10% Pd/C, 1,4-cyclohexadiene, EtOH, AcOH, R.T. **iii**; 10% Pd/C, 1,4-cyclohexadiene, EtOH/THF, AcOH, R.T, 63%.

251 was not isolated in pure form, the free acid **250** was obtained in excellent yields by treating imide **237h** with TFA in dichloromethane.

Stability Studies of Novel N_γ-acylated L-Glutamine Imides

We next determined the stability of imides **12, 247,** and **249** around physiological pH, in order to establish conditions for their assay with *E. coli* AS-B and selected AS-B mutants. It was imperative that these imides maintain their stability when subjected to enzyme assay conditions. Imide **12** was studied more extensively relative to imides **247** and **249** since the former had been proposed as a possible enzyme intermediate in the mechanism of *E. coli* AS-B (60,64) (**Figure 1-12**).

Stability studies were conducted by monitoring the ^1H NMR (169) spectral changes of the imides at different pH's in Bis-tris or Tris buffer solutions. These buffers were chosen as they are most often used in assays of *E. coli* AS-B. The objective was to determine the stability of imides **12, 247,** and **249** and their decomposition products under standard enzyme assay conditions.

The ^1H NMR spectra of imide **12** in Bis-tris or Tris buffer solutions at pH 2-8 are shown in **Figure 3-14.** These spectra show that imide **12** is stable in the pH 2-6 range. However, between pH 5.9-6.8 range, **12** partly decomposed to form a new compound characterized by the appearance of newly

Figure 3-14. ^{1}H NMR (500 MHz) spectra of imide **12** (4-9 mM) in Bis-tris (100 mM) and Tris (100 mM) buffers in the pH 2-8 range: **A.** no buffer, pH 2.8; **B.** Bis-tris, pH 5.9; **C.** Tris, pH 6.8; **D.** Tris, pH 8.1. Labelled signals **X** correspond to compound **X.** Vertically offscale signals at 4.8 and 3.8 ppm correspond to water and Bis-tris/Tris protons, respectively.

formed signals **X** (referred to from here on as compound **X**). Somewhere between pH 6.8-8.1 range imide **12** decomposes or rearranges completely to the new compound **X**. Other potential buffers such as HEPES, phosphate, and borate gave similar results at pH 7-8 (**Figure 3-15**). Interestingly, bicarbonate buffer resulted in the formation of significant amounts of an additional new compound characterized by the appearance of newly formed signals **Y** (referred to from here on as compound **Y**).

Further studies were conducted to determine if the formation of compound **X** was reversible or irreversible (**Figure 3-16**). Imide **12** was initially dissolved in deuterium oxide to give a pH of 2.8 and the ^1H NMR recorded. This solution was then treated with Tris buffer to a final pH of 8.4. The ^1H NMR of this solution showed the exclusive formation of the new compound **X**. Acidification of this latter solution with deuterium chloride to pH 5.4 produced a ^1H NMR spectrum identical to the spectrum at pH 8.4. These studies clearly show that the formation of compound **X** from imide **12** in the pH 5.9-8.1 range is irreversible. As *E. coli* AS-B is most active between pH 6-8, this placed constraints on the assay conditions involving imide **12**, so as to avoid formation of compound **X** before or during the experiments.

Studies to identify compounds **X** and **Y** were conducted by first analyzing the possible products obtained from imide **12** at high pH (**Figures 3-17** and **3-18**). Possible products L-Gln, L-glutamate, L-Asn, and L-aspartate resulting from

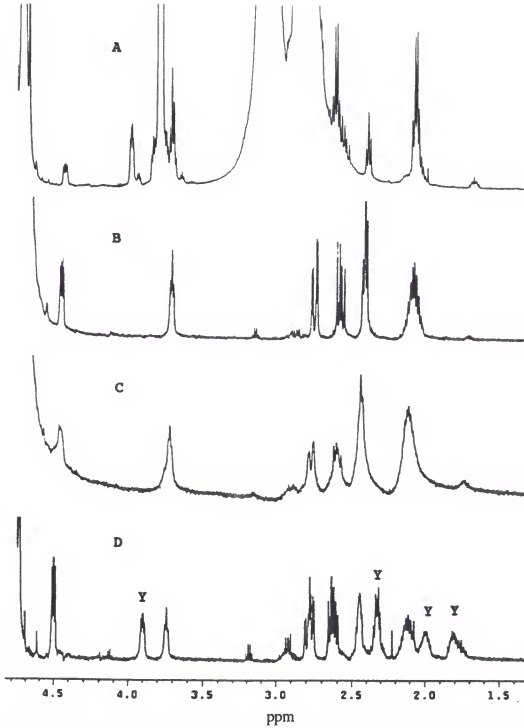

Figure 3-15. ^1H NMR (500 MHz) spectra of imide **12** (7-8 mM) in various buffers in the pH 7-8 range: **A.** HEPES (100 mM), pH 7.0 (vertically offscale signals around 2.8, 3.0, and 3.8 correspond to HEPES); **B.** Na_4BO_4 (210 mM), pH 7.9; **C.** NaH_2PO_4 (240 mM), pH 7.7; **D.** $NaHCO_3$ (1.1 M), 8.0. Labelled signals **Y** correspond to compound **Y**.

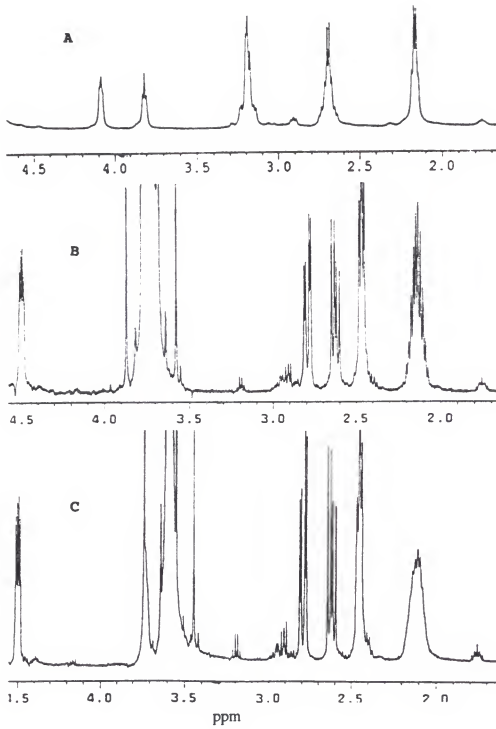

Figure 3-16. ^{1}H NMR (500 MHz) spectra of imide **12** (8 mM) in showing irreversible formation of compound **X** from imide **12**: **A.** D_2O, pH 2.8; **B.** D_2O/Tris buffer, pH 8.4 (vertically offscale signals at 3.7 correspond to Tris); **C.** DCl/D_2O/Tris buffer reacidified to pH 5.4.

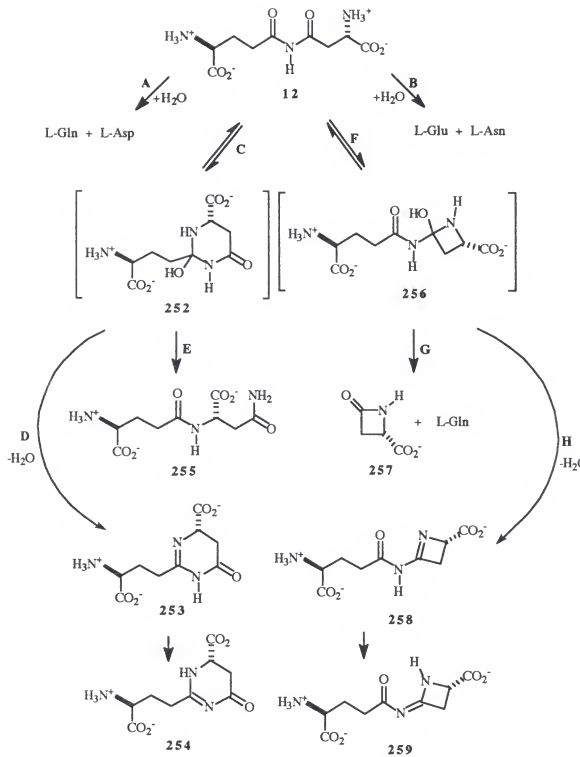

Figure 3-17. Possible products arrising from imide **12** at pH > 6.8.

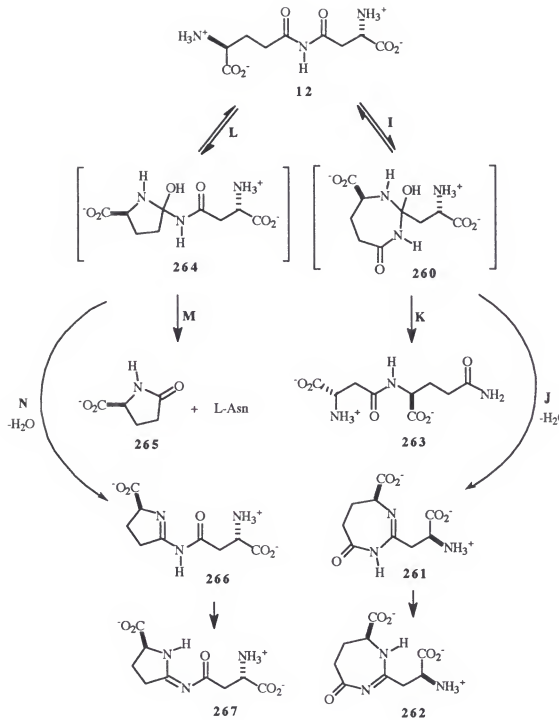

Figure 3-18. Possible products arrising from imide **12** at pH > 6.8.

direct attack of hydroxide ion on the imide functionality of **12** are shown by pathways **A** and **B** (**Figure 3-17**). Likewise, by increasing the pH, deprotonation of either of the two α-amino groups and attack on either of the two C=O groups on the imide functionality of **12** results in the formation of four possible tetrahedral intermediates, **252**, **256**, **260**, and **264**, which can lead to other products. First **252** can loose water to form amidines **253** or **254** via pathway **D** or rearrange through pathway **E** to form dipeptide **255**. Second **256** can breakdown to form β-lactam **257** and L-glutamine via pathway **G** or loose water to form amidines **258** or **259** via pathway **H** (**Figure 3-17**). Third **260** can loose water to form amidines **261** or **262** through pathway **J** or rearrange to form dipeptide **263** through pathway **K** (**Figure 3-18**). Fourth, **264** can breakdown to form γ-lactam **265** and L-asparagine via pathway **M** or lose water to form amidines **266** or **267** via pathway **N**. It is more likely that compounds **X** and **Y** originate from pathways **A**, **B**, **E**, or **M**, rather than pathways **D**, **G**, **H**, **K**, **J**, or **N**, since the former pathways lead to more stable products and intermediates.

By synthesizing dipeptides **255** and **263** and using ^{1}H NMR spectroscopy it was possible to identify compounds **X** and **Y**. Pathways **D** and **E** (**Figure 3-17**) can be distinguished by ^{1}H NMR spectral comparison of dipeptide **255** with imide **12** at high pH. Similarly, pathways **K** and **J** (**Figure 3-18**) can be distinguished by ^{1}H NMR spectral comparison of dipeptide **263** with imide **12**. Lactams **257** and **265** arise from pathways **G**

and **M**, respectively, and can be obtained from commercial sources or by synthesis (170). Pathways **A** and **B** result in the formation of L-glutamine, L-aspartate, L-glutamate, or L-asparagine which are also commercially available. Thus, ^{1}H NMR spectral comparison of **257**, **257** + Gln, **265** + Asn, and **263** with imide **12** at high pH allowed identification of compounds **X** and **Y**, as well as pathways for their formation.

The synthesis of dipeptide **255** is shown in **Figure 3-19.** Commercially available N-(benzyloxycarbonyl)-L-asparagine **268** was esterified in good yields using isobutylene and catalytic amounts of sulphuric acid to give ester **269.** Amine **270** was prepared in quantitative yields by catalytic hydrogen transfer of **269** using 10% Pd/C and 1,4-cyclohexadiene. N-(benzyloxycarbonyl)-α-benzyl-L-glutamic acid **273** was prepared following the method of Bergmann and Zervas (164) with slight modifications starting from N-(benzyloxycarbonyl)-L-glutamic acid **271** via N-(benzyloxycarbonyl)-L-glutamic anhydride **272.** Subsequent coupling of amine **270** with acid **273** to give the protected dipeptide **274** in good yields was accomplished with DCC in THF. The t-butyl group of **274** was removed using TFA to give acid **275** in good yields. Acid **275** was deprotected using 10% Pd/C and 1,4-cyclohexadiene to give the free amino acid dipeptide **255.**

The synthesis of dipeptide **263** is illustratred in **Figure 3-20.** This synthesis begins with hydrochloride **217** or catalytic hydrogen transfer of **213b** to give amine **276.**

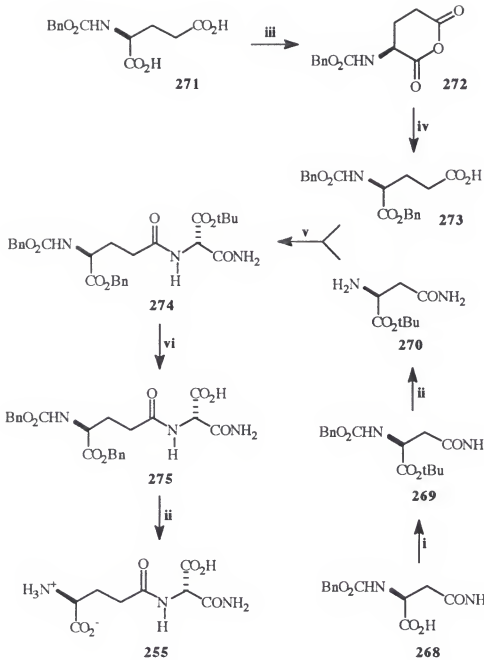

Figure 3-19. Synthesis of dipeptide **255**. Reagents and conditions: **i**; isobutylene, H_2SO_4(cat.), 66%. **ii**; 10% Pd/C, 1,4-cyclohexadiene, EtOH/THF, reflux, 99%. **iii**; Ac_2O, R.T., 70%; **iv**; BnOH, 100 °C, 17%. **v**; DCC, THF, R.T., 78%. **vi**; TFA, CH_2Cl_2, 0 °C, 80%.

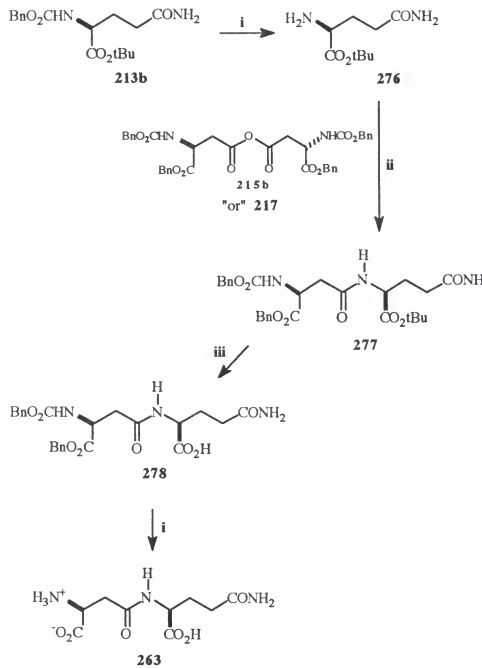

Figure 3-20. Synthesis of dipeptide **263.** Reagents and conditions: **i;** 10% Pd/C, 1,4-cyclohexadiene, EtOH/THF, reflux, 92%. **ii;** triethylamine, THF, 0 °C-R.T., 81%. **iii;** TFA, CH_2Cl_2, 98%.

Coupling between **217** or **276** with anhydride **215b** under basic conditions afforded dipeptide **277** in good yields. Dipeptide **277** was also prepared by coupling acid **214** to amine **276** with DCC or reacting acid chloride **215a** with hydrochloride **217** under basic conditions. These latter two protocols required chromatographic purification and gave lower yields of product relative to the former method. Removal of the t-butyl group to give acid **278** in excellent yields was accomplished using TFA in dichloromethane. Catalytic hydrogen transfer of **278** afforded the free amino acid dipeptide **263** in good yields.

The ^{1}H NMR spectra of **12**, **255**, **263** and **265** + L-asparagine in Tris buffer solution at pH 8 are shown in **Figure 3-21.** It is clear from these spectra that compound **X** is dipeptide **255.** More specifically, imide **12** rearranges exclusively and irreversibly to dipeptide **255** at pH 8 in Tris buffer solution via pathways **C** and **E** (**Figure 3-17**). Imide **12** also rearranges to **255** in HEPES, phosphate, borate, and bicarbonate buffers at this pH.

In bicarbonate buffer, imide **12** forms an additional compound **Y** which does not correspond to dipeptide **255.** **Figure 3-22** shows the ^{1}H NMR of imide **12**, L-Glu + L-Asn, and L-Gln + L-Asp in bicarbonate buffer solution at pH 8. These spectra show that compound **Y** is a mixture of L-Gln + L-Asp. It is noted that these two products can emerge from pathway **A** (**Figure 3-17**) or from hydrolysis of dipeptide **263** (**Figure 3-18**). Since dipeptide **263** was not observed in any buffer and presumably arises from unstable intermediate **260**, it is

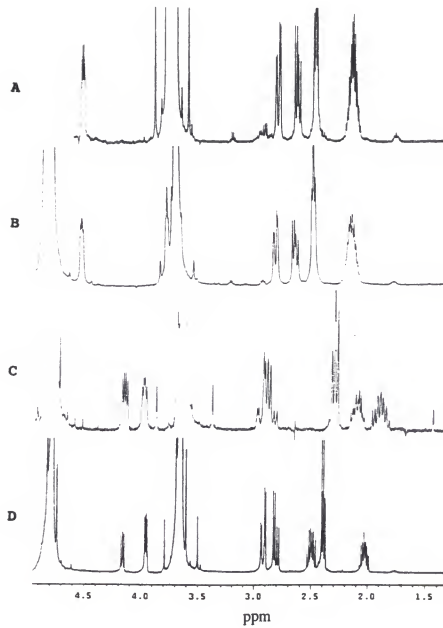

Figure 3-21. Comparison of ^{1}H NMR (500 MHz) spectra in Tris (100 mM) buffer between possible products arising from imide **12: A.** imide **12** (7 mM), pH 8.2; **B.** dipeptide **255** (19 mM), pH 8.1; **C.** dipeptide **263** (15 mM), pH 8.1; **D.** pyrrolidone **265** (12 mM)+ L-asparagine (12 mM), pH 8.1. Vertically offscale signals at 4.8 and 3.7 ppm correspond to water and Tris protons, respectively.

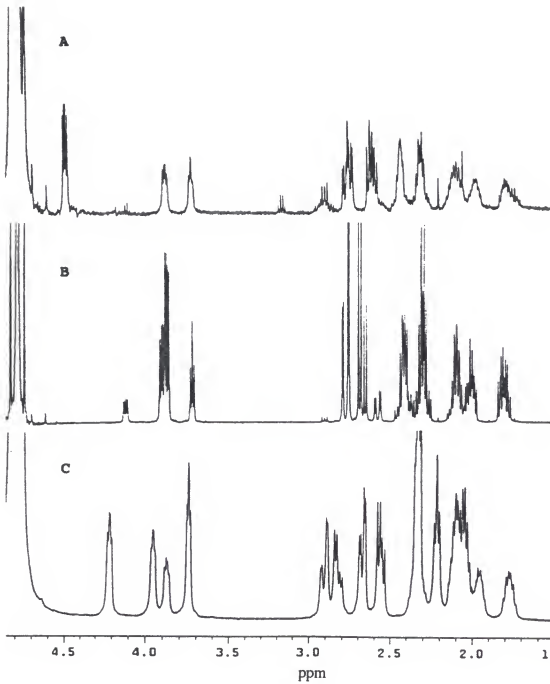

Figure 3-22. Comparison of ^1H NMR (500 MHz) spectra in $NaHCO_3$ (1 M) buffer between possible products arising from imide **12**: **A.** imide **12** (7 mM), pH 8.0; **B.** L-Gln (16 mM) + L-Asp (16 mM), pH 8.1; **C.** L-Glu (17 mM) + L-Asn (18 mM), pH 8.0. Vertically offscale signals around 4.8 ppm correspond to water protons.

more likely that compound **Y** arose from pathway **A**. Thus, in bicarbonate buffer, decomposition of imide **12** to give L-glutamine and L-aspartate competes with rearrangement to dipeptide **255**.

A similar type of rearrangement has been observed by Wieland and Urbach (104) upon treatment of **103b** and **103c** with traces of triethylamine to form the corresponding dipeptides **104**, **105** and **106**, **107**, respectively (see Chapter 2, **Figure 2-8**). These imides are symmetrical with a 2-NH_2 and a 2'-NH_2 group (taking the imide group carbonyls as 1-C and 1'-C) (**Figure 3-23**) and thus can only rearrange to products **104-107** via presumed 3 or 5-membered ring intermediates. In contrast, imide **12** is unsymmetrical having a 4-NH_2 and a 3'-NH_2 group (**Figure 3-23**) and is therefore capable of rearranging through presumed 4, 5, 6, and 7-membered ring intermediates. It is therefore surprising that imide **12** rearranges exclusively to one product while being able to form other stable products, such as dipeptide **263** or pyrrolidone **265** (**Figure 3-18**).

It is interesting to note the preference or selectivity of 3'-N attack versus 4-N attack (**Figure 3-23** for definition) to form the four possible intermediates **252**, **256**, **260**, and **264** from imide **12** (**Figures 3-17** and **3-18**). Presumably the 3'-NH_3^+ group is more acidic than the 4-NH_3^+ group, resulting in a greater population of species containing 3'-NH_2 groups available for nucleophilic attack at the imide carbonyl centers above pH 6.8. In fact, the K_a for

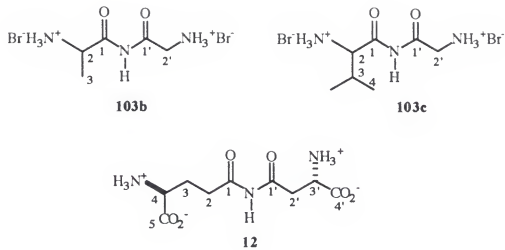

103b **103c**

12

Figure 3-23. Comparison between imides **103b,c** and imide **12** based on the position of the NH_2 group.

the α-NH_3^+ group of L-Asn is 2.1 times larger relative to the corresponding K_a of L-Gln (171). Given that imide **12** could be considered as an N_β-acylated L-Asn derivative or an N_γ-acylated L-Gln derivative where the 3'-NH_3^+ and 4-NH_3^+ correspond to α-NH_3^+ groups, is possible that a similar K_a effect is observed in imide **12**, resulting in a greater population of species containing 3'-NH_2 groups relative to 4-NH_2 groups above pH 6.8. This effect alone cannot rationalize our observations since, presumably at high pH there is a combination of both, 3'-NH_2 and 4-NH_2, amino groups available to form possible intermediates **252**, **256**, **260**, and **264**. Presumably the energies associated with the formation and breakdown of intermediate **252** are lower than the corresponding energies of intermediates **256**, **260**, and **264**, or the stability of product **255** is much greater than the

stability of the products formed from the latter intermediates.

Considering pathway **F** (**Figure 3-17**), the fact that β-lactam **257** + L-Gln were not formed could be attributed to the higher energies associated with both the formation and breakdown of intermediate **256**, relative to **252**, and the instability of lactam **257** relative to dipeptide **255**. In fact, based on MOPAC (172) calculations using AM1 parameters and a water solvation potential, intermediate **252** is more stable than intermediate **256** by 17.2 kcal/mole while dipeptide **255** is more stable than β-lactam **257** + L-glutamine by 25.0 kcal/mole. Amidines **258** and **259** from pathway **H** (**Figure 3-17**) were also expected to be unstable mostly due to ring strain.

In the case of pathway **I** (**Figure 3-18**), that dipeptide **263** was not formed can probably be attributed to the higher energies associated with the formation and breakdown of 7-membered ring intermediate **260** relative to the 6-membered ring intermediate **252** (**Figure 3-17**), since dipeptides **263** and **255** formed from these two intermediates, respectively, should possess similar stability. In fact, MOPAC calculations using AM1 parameters and a water solvation potential showed that intermediate **252** is more stable than intermediate **260** by 6.9 kcal/mol. In contrast, dipeptide **255** is less stable than dipeptide **263** by 2.4 kcal/mol.

Pathways **C** and **L** (**Figures 3-17** and **3-18**) lead to more stable intermediates **252** and **264**, relative to intermediates

256 and **260**, as well as stable products **255** and **265** + L-Asn, respectively. If the energies associated with the formation of **252** and **264** are similar, perhaps a three way equilibrium is established between **252**, imide **12**, and **264** in favor of **252** due to the greater population of 3'-NH_2 groups relative to 4-NH_2 groups at pH 6.8. MOPAC calculations using AM1 parameters in a water solvation potential showed that deprotonation of the 3'-NH_3^+ group relative to 4-NH_2^+ group is favored by 3.4 kcal/mol. In constrast, the 5-membered ring intermediate **264** is more stable than the 6-membered ring intermediate **252** by only 2.1 kcal/mol. In addition, pyrrolidone **265** + L-asparagine are more stable than dipeptide **255** by 2.2 kcal/mol. Based on these calculations and product stability, thermodynamically, intermediate **264** and pyrrolidone **265** and L-asparagine should be favored over intermediate **252** and dipeptide **255** in disagreement with the experimental results. Thus, the exclusive formation of dipeptide **255** from imide **12** seems to be kinetically controlled by the energy barriers associated with the formation and breakdown of intermediates **252** and **264** and the fraction of the 3'-NH_2/4-NH_2 populations. Presumably irreversible rearrangement of imide **12** to dipeptide **255** is faster than irreversible breakdown to pyrrolidone **265** + L-asparagine.

The stability of imide **247** (**Figure 3-11**) was also evaluated in the pH 6-9 range using ^1H NMR spectroscopy (**Figure 3-24**). These spectra show that imide **247** is stable

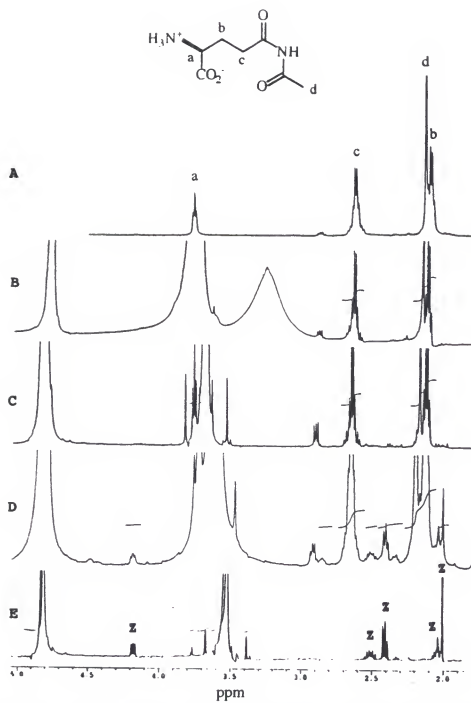

Figure 3-24. ^{1}H NMR (500 MHz) spectra of imide **247** (11-21 mM) in Bis-tris (100 mM) and Tris (100 mM) buffers in the pH 6-9 range: **A.** no buffer, pH 6.6; **B.** Bis-tris, pH 6.6; **C.** Tris, pH 7.5; **D.** Tris, pH 8.1; **E.** Tris, pH 8.9. Labelled signals **Z** correspond to compound **Z**. Vertically offscale signals at 4.8 and 3.5-3.8 ppm correspond to water and Bis-tris/Tris protons, respectively.

below pH 7.5. Between pH 7.5 and 8.1, **247** partly decomposes to form a new compound characterized by the appearance of new signals **Z** (referred to from here on as compound **Z**). Somewhere between pH 8.1 and 9.0, imide **247** decomposes exclusively to compound **Z**.

Further studies were conducted to determine if the formation of compound **Z** was reversible or irreversible (**Figure 3-25**). Imide **247** was initially dissolved in deuterium oxide to give a pH of 6.5 and the ^{1}H NMR recorded. This solution was then treated with Tris buffer to pH 8.8. The ^{1}H NMR of this solution showed partial formation of compound **Z**. Acidification of this latter solution with deuterium chloride to pH 6.5 did not promote the reverse formation of **247** from compound **Z**. These results show that compound **Z** is formed irreversibly from imide **247** in the pH 7.5-9.0 range.

The ^{1}H NMR spectra of imide **247**, pyrrolidone **265** + acetamide, L-Glu + acetamide, and L-Gln + acetic acid in Tris buffer solution at pH 8-9 are shown in **Figure 3-26.** These spectra show that compound **Z** is a mixture of **265** and acetamide. Thus, imide **247** rearranges irreversibly to a mixture of pyrrolidone **265** + acetamide **280** above pH 7.5, presumably through the formation of tetrahedral intermediate **279** (**Figure 3-27**).

Finally, the stability of imide **249** was evaluated in the pH 6-8 range using ^{1}H NMR spectroscopy (**Figure 3-28**). Interestingly, imide **249** is stable throughout this pH range

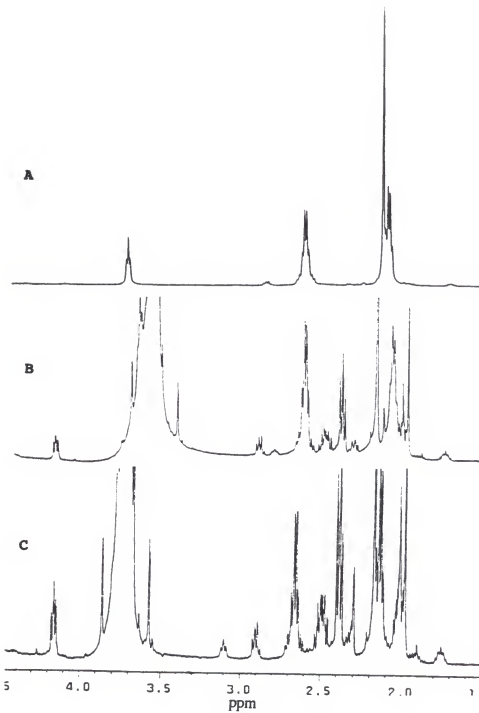

Figure 3-25. ^1H NMR spectra of imide **247** (16-21 mM) showing irreversible formation of compound **Z**: **A.** D_2O, pH 6.5; **B.** D_2O/Tris buffer, pH 8.8 (vertically offscale signal at 3.5 ppm correspond to Tris protons); **C.** DCl/D_2O/Tris buffer reacidified to pH 6.5.

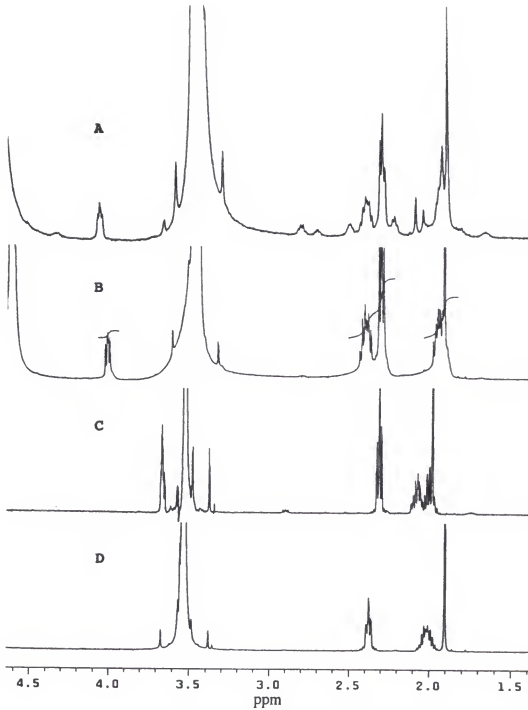

Figure 3-26. Comparison of the ^{1}H NMR (500 MHz) spectra in Tris buffer between possible products arising from imide **247**: **A.** imide **247** (18 mM), pH 8.9; **B.** pyrrolidone **265** (39 mM) + acetamide (34 mM), pH 8.5; **C.** L-Glu (27 mM) + acetamide (24 mM), pH 8.9; **D.** L-Gln (190 mM) + acetic acid (170 mM), pH 8.8. Vertically offscale signal at 3.5 ppm correspond to Tris protons.

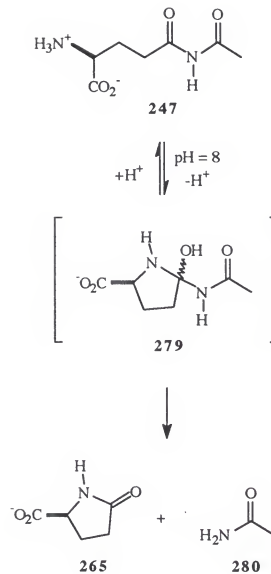

Figure 3-27. Formation of pyrrolidone **265** and acetamide **280** from imide **247** at pH > 7.5 via presumed intermediate **279**.

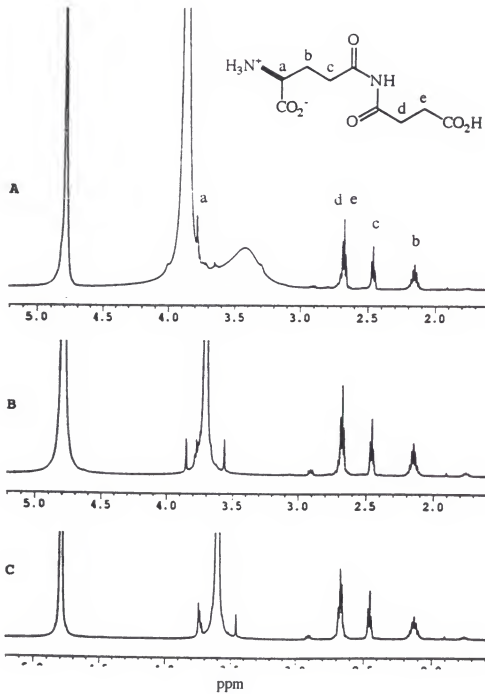

Figure 3-28. ^1H NMR spectra of imide **249** (4-8 mM) in Bis-tris (100 mM) and Tris (100 mM) buffers in the pH 6-8 range: **A.** Bis-tris, pH 6.0; **B.** Tris, pH 7.0; **C.** Tris, pH 8.1. Vertically offscale signals at 4.8 and 3.5-3.8 ppm correspond to water and Bis-tris/Tris protons, respectively.

and does not form any other species as opposed to imides **12** and **247**. Consequently, no equilibrium studies were performed for this imide.

It is worth mentioning the chemical changes that take place in the basic pH limb by substituting the acetyl group of imide **247** with the functionalized succinyl and β-L-aspartyl groups to form imides **249** and **12**, respectively. The acetyl group which possesses no functionality results only in the formation of pyrrolidone **265**. Replacing the acetyl group by a succinyl group completely inhibits the formation of pyrrolidone **265**. In contrast, replacing the acetyl group by a β-L-aspartyl group, which can be thought of as a succinyl group with a 3'-NH_3 group, not only completely inhibits the formation of pyrrolidone **265**, but results in the exclusive formation of dipeptide **255**.

The Structure of N_γ-Acylated L-Glutamine Derivatives

Conjugation between the nitrogen lone pair and the carbonyl π system of the imide functional group, similar to the amide group, introduces a significant barrier to rotation about the C=O and N-H bond in all imides (70). Consequently, acyclic symmetric imides can exist as three different geometric isomers based on the orientation of the C=O groups relative to the N-H group. Acyclic unsymmetric imides, however, can exist as four different geometric isomers, namely, cis-cis (E,E), cis-trans (E,Z), trans-cis (Z,E), and

trans-trans (Z,Z) represented by structures **281**, **282**, **283**, and **284**, respectively (**Figure 3-29**).

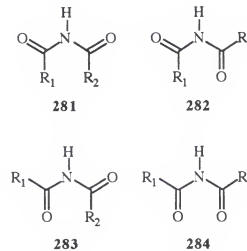

Figure 3-29. Isomerism in acyclic unsymmetric imides: **281**, cis-cis; **282**, cis-trans; **283**, trans-cis; **284**, trans-trans.

Generally, the cis-cis isomer is preferred when R_1 or R_2 are small since the distance between the imide carbonyl oxygen atoms are less, thereby, reducing electrostatic repulsions. When R_1 and R_2 are large, the cis-trans or the trans-cis isomers predominate due to relief of steric repulsions between the R_1 and R_2 groups. The trans-trans isomer is the least favoured due to electrostatic repulsions between the two imide carbonyl oxygen atoms.

Dipole moments (173), X-ray diffraction (174), infrared spectroscopy (175), ^1H NMR and ^{13}C NMR spectroscopy (176,177), microwave spectroscopy (178), and ultraviolet spectroscopy

(179) have been used to differentiate between these different geometrical isomers. Dipole moments have been used as an indication of the relative orientation of the C=O groups and are solvent dependent. High dipole moments are indicative of trans-trans isomers while low dipole moments are indicative of cis-cis isomers (173). Vibrational coupling of the C=O groups gives rise to two bands at 1650-1700 cm^{-1} and 1790-1710 cm^{-1} in the IR spectra of most imides. This vibrational coupling is also dependent on the nature of the substituent on the nitrogen atom (175). In general, acyclic imides exist in the trans-trans isomeric form in the solid state and invert to the trans-cis or cis-trans geometry in non-polar solvents (175). The trans-trans isomer has been characterized by strong absorptions at 3200-3280, 1733-1737, 1503-1505, 1167-1230, and 732-739 cm^{-1} while the cis-trans or trans-cis isomer by absorptions at 3270, 3245, 3190, 1734, 1700, 1659, 1053-1507, 1167-1236, and 816-836 cm^{-1} (70).

The four possible geometric isomers of imides **12**, **247**, and **249** are illustrated in **Figures 3-30**, **3-31**, and **3-32**, respectively. The solid state IR spectrum of imide **12** shows bands at 2000-3200, 1752, 1691, 1610, 1501, 1402, 1350, 1205, and 1140 cm^{-1}. The greater intensity of the lower frequency Imide I band at 1691 cm^{-1} ($\nu_{C=O}$ antisym.) relative to the higher frequency Imide I band at 1752 cm^{-1} ($\nu_{C=O}$ sym.), combined with the presence of the Imide II band at 1501 cm^{-1} (ν_{NH},ν_{CNC} antisym.) provide evidence for the trans-cis or cis-trans geometry on imide **12** in the solid state. In contrast,

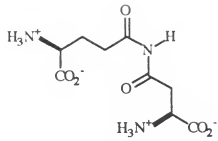

12 cis-trans

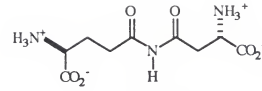

12 trans-trans

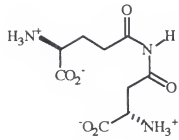

12 cis-cis

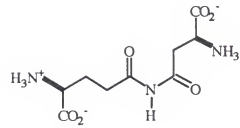

12 trans-cis

Figure 3-30. Possible configurational isomers of imide **12**.

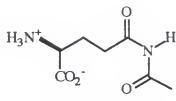

247 cis-trans

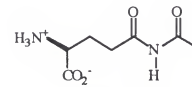

247 trans-trans

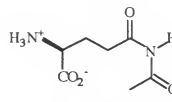

247 cis-cis

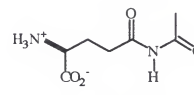

247 trans-cis

Figure 3-31. Possible configurational isomers of imide **247**.

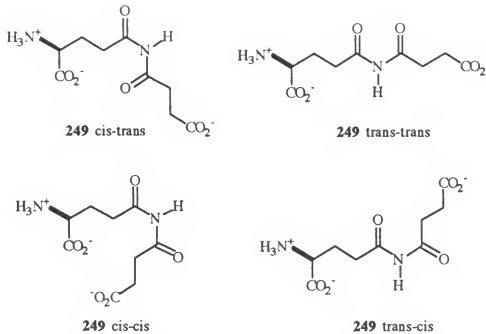

Figure 3-32. Possible configurational isomers of imide **249**.

the Imide II band is not present in cis-cis imides and the lower frequency Imide I band is extremely weak or not present in trans-trans imides (175).

Similarly, the solid state IR spectrum of imide **247** shows carbonyl bands at 2000-3200, 1737, 1648, 1596, 1480, 1385, 1346, 1307, 1206, and 1164 cm^{-1}. The presence of Imide I bands at 1737 and 1648 cm^{-1}, as well as the Imide II band near 1480 cm^{-1} is consistent with the trans-cis or cis-trans geometry for this imide. The solid state IR spectrum of imide **249** shows bands at 2000-3200, 1751, 1670, 1600, 1508, 1410, 1320, 1232, and 1140 cm^{-1}. Again, the presence of Imide I bands at 1751 and 1670 cm^{-1} and the Imide II band near 1508

cm^{-1} comfirms the trans-cis or cis-trans geometry for this imide.

This contrasts with previous findings (175) in which the trans-trans isomer predominates in the solid state of simple non-functionalized acyclic imides. For some imides, however, this isomerism is dependent on the solvent or solvent mixtures used for crystallization. Moreover, the majority of these imides change configurations from trans-trans geometry to cis-trans or trans-cis geometry in going from solid state to solution state, respectively (175). Imides **12**, **247**, and **249** are much different from the imides studied by other authors in the sense that our imides are highly functionalized whereas all other imides studied are nonfunctionalized. In all three imides **12**, **247**, and **249**, the imide functional group is able to form hydrogen bonds with the α-NH_3^+ and α-CO_2^- functional groups of the side chains. This may be responsible for the small shifts of the Imide I and II absorption bands in our imides compared to simple nonfunctionalized imides.

Low temperature ^1H NMR has been used to determine the isomeric configurations of simple nonfunctionalized acyclic symmetric imides in solution (176). The cis-trans geometry is found in virtually all imides studied in solution by this and other methods. At very low temperatures, the two sets of α-protons next to the two imide C=O functional groups in the cis-trans geometry of symmetric imides have different chemical shifts compared to the corresponding cis-cis or

trans-trans geometric forms. At higher temperatures, these two sets of α-protons coalesce to form a single peak resulting from rapid rotation about the C=O and N-H imide bond. Likewise, coalescence of the imide N-H proton can occur. Thus, low temperature ^1H NMR studies could reveal the geometry of imides **12**, **247**, and **249** in solution.

Conformational studies using ^1H NMR at low temperatures were conducted on imides **12**, **247**, and **249**. Since all three imides were only soluble in water, these studies were limited to temperatures greater than 0 °C. The ^1H NMR spectra of **12**, **247**, and **249** at 5 °C in deuterium oxide did not differ from their corresponding spectra at ambient temperature. The lack of α-proton splitting (2-CH_2 and 2'-CH_2 protons in **Figure 3-23**) in the 2.0-3.5 ppm region for all three imides **12**, **247**, and **249** at 0 °C indicated that all geometric isomers were interconverting rapidly. Alternately, only one geometric isomer was present over this temperature range. These two cases might be distinguished by cooling down the solution further to very low temperatures (e.g. -100 to -150 °C). However, temperature limitations impossed by the aqueous solvent did not allow this hypothesis from further exploration. It is noted, however, that energy barriers for the rotation between the C=O and the N-H group of simple non-functionalized acyclic imides in solution lies between 6.9-12.9 kcal/mol (176). Given that rotational barriers lower than 15-20 kcal/mol are easily overcome at ambient

temperature (180), it is likely that imides **12**, **247**, and **249** did not exist as a single geometrical isomer in solution.

Although it was not possible to comfirm this hypothesis by studying these particular imides at very low temperatures, it was possible to study precursor imides **225**, **237a**, and **248** (**Figures 3-6**, **3-9**, and **3-12**, respectively), since these were all soluble in deuterated organic solvents. The low temperature ^{1}H NMR spectra of imides **225**, **237a**, and **248** are shown in **Figures 33**, **34**, and **35**, respectively. The signals corresponding to the imide N-H, 2-CH_2, and 2'-CH_2 protons (see **Figure 3-23** for definition) decoalesce to form two independent signals at -85 °C in all three imides. Therefore, these imides exist as a mixture of two conformational isomers at -85 °C which rapidly interconvert as the temperature increases to 22 °C. Free energies of activation (ΔG^*) for the interconversion of imides **225**, **237a**, and **248** were estimated at 10.4, 10.2, and 10.1 kcal/mol using the imide N-H coalescence temperature of -70, -65, and -65 °C, respectively. Free energies of activation using the 2-CH_2/2'-CH_2 coalescence temperatures of -50/-50, -50/-30, and -55/-55 °C for imides **225**, **237a**, and **248** were also estimated at 10.4/9.4, 10.3/11.5, and 10.7/10.6 kcal/mol, respectively. These energies lie in the range of ΔG^*'s obtained for much simpler imides (176). Imides **225**, **237a**, and **248** therefore exist as mixtures of either cis-trans + trans-cis, cis-trans + trans-trans, or trans-cis +

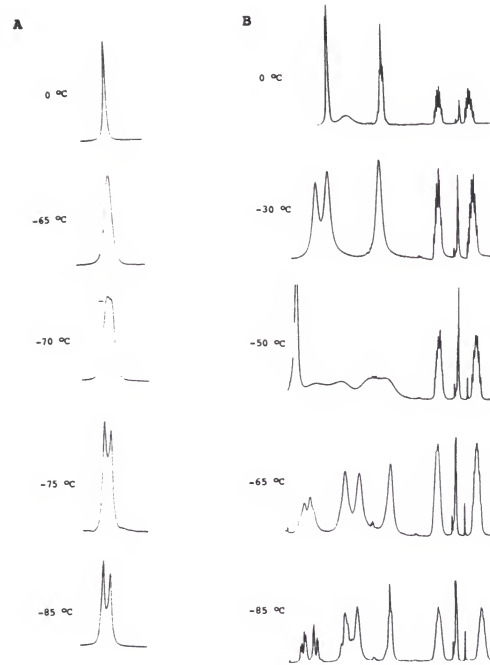

Figure 3-33. Selected signals from the ^1H NMR (500 MHz) spectra of imide **225** (23 mM) in acetone-d_6 over the -85 - 0 °C region: **A.** imide N-H signal; **B.** 2-CH_2 and 2'-CH_2 signals.

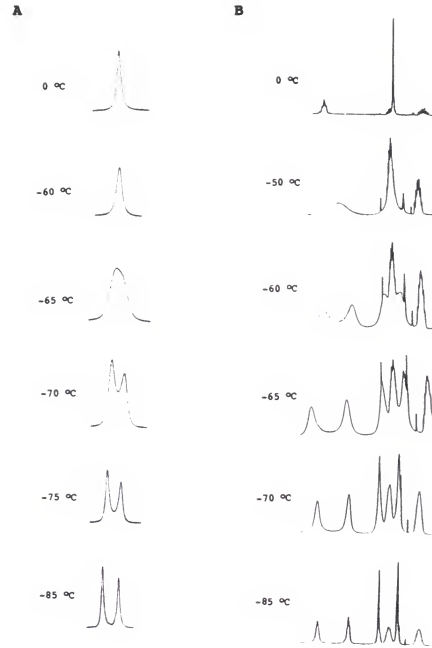

Figure 3-34. Selected signals from the ^1H NMR (500 MHz) spectra of imide **237a** (56 mM) in acetone-d_6 over the -85 - 0 °C region: **A.** imide N-H signal; **B.** 2-CH_2 and 2'-CH_2 signals.

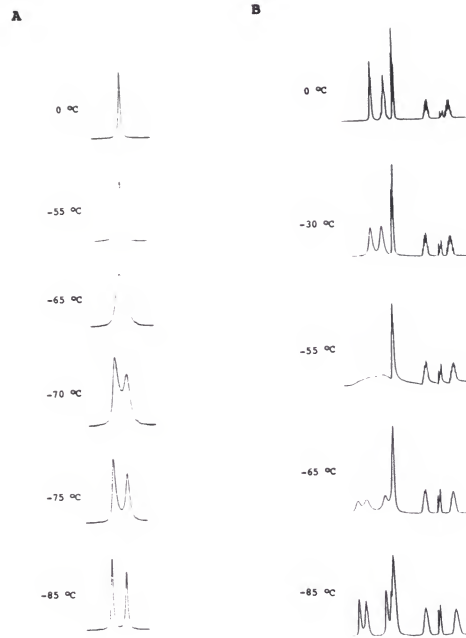

Figure 3-35. Selected signals from the ^1H NMR (500 MHz) spectra of imide **248** (53 mM) in acetone-d_6 over the -85 - 0 °C region: **A.** imide N-H signal; **B.** 2-CH_2 and 2'-CH_2 signals.

trans-trans isomers at low temperatures which rapidly interconvert as the temperature is raised.

Structural information on imides **12**, **247**, and **249** based on theoretical calculations using MOPAC was also obtained. The geometry of several conformations for each geometric isomer of imides **12**, **247**, and **249** was optimized and energy minimized and the heat of formation (ΔH_f) of each conformation was calculated using MOPAC with AM1 parameters in a water solvation potential. **Figures 3-36**, **3-37**, and **3-38** show structures for the most stable conformation of each geometric isomer of imides **12**, **247**, and **249**, respectively. **Tables 3-3**, **3-4**, and **3-5** show relative energies, dihedral angles, and H-bond distances for the structures illustrated in **Figures 3-36**, **3-37**, and **3-38**, respectively.

Figure 3-36 and **Table 3-3** show that the most stable configuration for imide **12** is the cis-trans while the least stable is the cis-cis by 9.4 kcal/mol. This is not surprising since steric repulsions between the 2-C and 2'-C (see **Figure 3-23** for definition) become greater in going from the cis-trans to the cis-cis configuration. The trans-trans isomer is only destabilized by 0.1 kcal/mol relative to the cis-trans isomer. Given that the trans-trans isomer should have a greater dipole moment compared to the cis-trans isomer, a significant part of this small difference in energy between these two isomers could be attributed to the former being preffered in a solvent with a high dielectric constant like water.

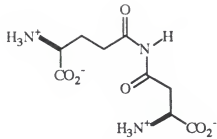

12 ct-1

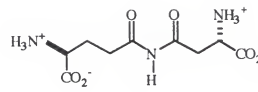

12 tt-1

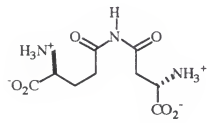

12 cc-1

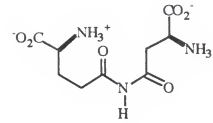

12 tc-1

Figure 3-36. Lowest energy conformation of each configurational isomer of imide **12**.

Table 3-3. Comparison between the relative energies, H-bond distances, and dihedral angles of imide **12** configurational isomers.

Configuration	$\Delta\Delta H_f$ (kcal/mole)[a]	atom distance (A)[b]	dihedral angle (°)[c]
12 ct-1	0.0	4.41, 2.26	-0.64, 178.85
12 tt-1	0.1	4.19, 2.15	178.48, 176.77
12 tc-1	1.4	2.41, 2.24	175.57, -3.33
12 cc-1	9.4	2.17, 2.18	22.84, 5.99

[a]Difference between ΔH_f's relative to the ΔH_f for **12** ct-1.

[b]H_{4N} --- O_{1C}, $H_{3'N}$ --- $O_{1'C}$ atom distances.

[c]O=C_1-N-H, O=$C_{1'}$-N-H dihedral angles.

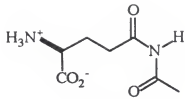

247 ct-1

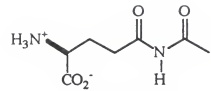

247 tt-1

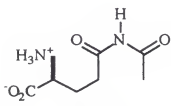

247 cc-1

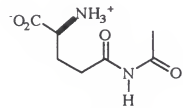

247 tc-1

Figure 3-37. Lowest energy conformation of each configurational isomer of imide **247**.

Table 3-4. Comparison between the relative energies, H-bond distances, and dihedral angles of imide **247** configurational isomers.

Configuration	$\Delta\Delta H_f$ (kcal/mole)[a]	atom distance (A)[b]	dihedral angle (°)[c]
247 ct-1	0.0	4.69, -----	-1.67, 176.96
247 tt-1	0.2	4.26, -----	177.81, 177.94
247 tc-1	1.7	2.34, -----	178.27, -0.75
247 cc-1	6.8	2.28, -----	11.84, 11.73

[a]Difference between ΔH_f's relative to the ΔH_f for **247** ct-1.

[b]H_{4N} --- O_{1C}, $H_{3'N}$ --- $O_{1'C}$ atom distances.

[c]O=C_1-N-H, O=$C_{1'}$-N-H dihedral angles.

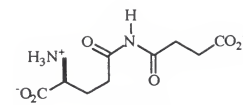

249 ct-1

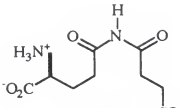

249 cc-1

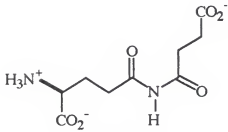

249 tc-1

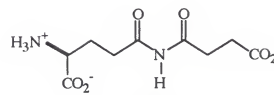

249 tt-1

Figure 3-38. Lowest energy conformation of each configurational isomer of imide **249**.

Table 3-5. Comparison between the relative energies, H-bond distances, and dihedral angles of imide **249** configurational isomers.

Configuration	$\Delta\Delta H_f$ (kcal/mole)[a]	atom distance (A)[b]	dihedral angle (°)[c]
249 ct-1	0.0	2.13, -----	2.50, -179.46
249 tc-1	1.9	4.29, -----	176.29, -2.04
249 tt-1	2.4	3.99, -----	178.86, 179.21
249 cc-1	3.5	2.33, -----	1.02, 1.45

[a]Difference between ΔH_f's relative to the ΔH_f for **249** ct-1.

[b]H_{4N} --- O_{1C}, $H_{3'N}$ --- $O_{1'C}$ atom distances.

[c]O=C_1-N-H, O=$C_{1'}$-N-H dihedral angles.

Figure 3-37 and **Table 3-4** show that the most stable configuration for imide **247** is the cis-trans while the least stable is the cis-cis by 6.8 kcal/mol. Similar to imide **12**, the trans-trans isomer is only destabilized by 0.2 kcal/mol while the trans-cis by 1.7 kcal/mol relative to the cis-trans isomer.

Figure 3-38 and **Table 3-5** show that the most stable configuration for imide **249** is the cis-trans while the least stable is the cis-cis by 3.5 kcal/mol. In this case, the trans-trans isomer is destabilized by 2.4 kcal/mol while the trans-cis by 1.9 kcal/mol relative to the cis-trans isomer.

In general, these calculations show small differences in energy between the four possible isomeric forms for imides **12**, **247**, and **249**. Given such small energy differences, and an estimated imide rotational barrier between 10.1-10.4 kcal/mol from low temperature ^{1}H NMR studies on imides **225**, **237a**, and **248**, it seems reasonable to assume that imides **12**, **247**, and **249**, interconvert between their isomeric forms in solution at ambient temperature. Morever, these calculations are consistent with the predominance of the cis-trans or trans-cis configuration for imides **12**, **247**, and **249** in water, well in agreement with their existence as the cis-trans or trans-cis isomers based on our studies.

CHAPTER 4
MECHANISTIC STUDIES OF E. COLI ASPARAGINE SYNTHETASE B

Introduction

Mechanisms for chemical reactions can be established by demonstrating the presence of kinetically competent intermediates (181). Strong evidence favoring a proposed mechanism for the reaction can be obtained by isolating, trapping, or detecting the intermediate leading to the observed products in the reaction. Alternately, strong evidence for the mechanism is obtained if the same products are observed when either a putative intermediate or the reactants are treated under identical reaction conditions. On the other hand, failure to obtain the usual products from the intermediate provides conclusive evidence to disprove the involvement of the intermediate in the chemical reaction mechanism.

Although these methods have been used succesfully in the study of many chemical reactions, their use in enzymatic reactions can be complicated. First, enzymes catalyze chemical reactions by physically interacting with the reactants. Thus, potential intermediates formed during enzyme catalysis are usually covalently or electrostatically bound to the enzyme, preventing their isolation or detection.

Second, many enzymes upon binding reactants change from a catalytically inactive conformation to a catalytically active conformation which may, or may not, prevent other molecules from reaching the active site until the products are released (182). Moreover, if the active site becomes inaccesible, not only are intermediates formed during enzyme catalysis unable to escape from the active site, but, administration of potential intermediates to test a proposed mechanism may not bind to the enzyme to form products.

The nitrogen transfer step in the glutamine-dependent reaction of *E. coli* AS-B has been proposed to occur via an imide intermediate **12** (Chapter 1, **Figure 1-12**) or the tetrahedral intermediate **8** (Chapter 1, **Figure 1-11**) (60,64). Evidence for either of these two mechanisms can therefore be obtained by isolating or detecting suspected intermediates **12** or **8**. Intermediate **8**, however, is covalently bound to the enzyme and does not exist as an independent entity. In common with other tetrahedral intermediates (183), **8** is also likely to be unstable and difficult to isolate. In contrast, imide **12** is not covalently bound to the enzyme and might be isolable as a stable independent molecule.

Using chemical synthesis, imide **12** was prepared and isolated in pure form (**Figure 3-6**), and its pH-dependent stability in buffer solution studied. This information was used to rationally design experiments aimed to detect and isolate imide **12** during glutamine-dependent nitrogen transfer

in *E. coli* AS-B and selected AS-B mutants, so as to obtain evidence for the imide-mediated nitrogen transfer mechanism (**Figure 1-12**).

Enzyme Assay Design

Based on pH-dependent stability studies of imide **12** (Chapter 3), all enzyme assays were conducted at pH 6.5 in Bis-tris buffer to prevent rearrangement of imide **12** to dipeptide **255**. Detection of imide **12**, reactants, and products from the assay were visualized using derivatives of **12**, **255**, L-Gln, L-Glu, L-Asp, L-Asn, ATP, and AMP. Separation of the components in the reaction mixture was accomplished using reverse phase HPLC (184). **Figure 4-1** shows an optimized HPLC chromatogram of a standard mixture of substrates and products formed during glutamine-dependent asparagine synthesis in *E. coli* AS-B. **Table 4-1** shows retention times and identities of the peaks shown by **Figure 4-1**. The detection limit of imide **12** was lower than 0.6 nmoles. A standard curve correlating nmoles of imide **12** with its chromatogram peak area showed a linear relationship (**Figure 4-2**). Using this curve, we could quantitate the amount of imide **12** produced or consumed during the enzyme assays.

Preliminary studies to determine the stability of imide **12** under derivatization conditions, using phenylisothiocyanate (PITC), showed that derivatized imide **12**

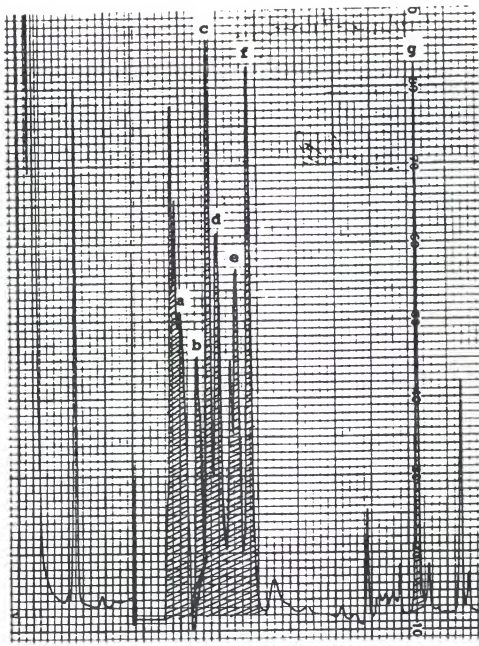

Figure 4-1. Reversed Phase HPLC chromatogram of a standard mixture (0.3 mM, 10 μL) of substrates in Bis-tris (100 mM). Peak identity: **a.** ATP; **b.** imide **12**; **c.** L-Asp; **d.** L-Glu; **e.** L-Asn; **f.** L-Gln; **g.** Bis-tris.

Table 4-1. Retention times (t_R) of substrates in standard mixture.

Peak	Substrate	t_R (min.)[a]
a	ATP	2.5
b	imide **12**	3.5
c	L-Asp	4.0
d	L-Glu	4.4
e	L-Asn	5.5
f	L-Gln	6.0
g	Bis-tris	14.9
—	AMP	3.1
—	dipeptide **255**	3.5

[a]Retention times.

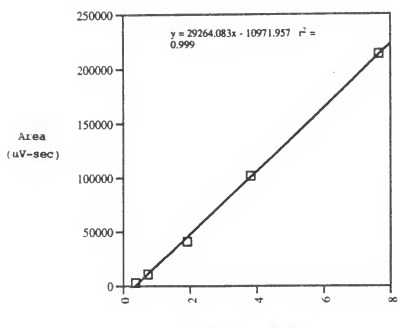

Figure 4-2. Standard curve of imide **12** (nmoles) versus area under the peak (μV-sec).

(PTC-**12**) had the same retention time as derivatized dipeptide **255** (PTC-**255**). Moreover, the ^{1}H NMR spectrum of imide **12** dissolved in derivatization buffer (DIEA/MeOH) was identical to that of dipeptide **255** (**Figure 4-3**). These results are consistent with the idea that rearrangement of imide **12** to dipeptide **255** occurs before reaction with PITC. This was not surprising since this derivatization buffer has a pH between 8-9, a pH region where imide **12** rearranged to dipeptide **255** (**Figure 3-14**).

The observation that imide **12** was not stable under derivatization conditions presented problems in interpretation of experiments aimed at direct detection of imide **12** formation, but not on the experimental features of the enzyme assays themselves. Thus, if imide **12** is a true intermediate and is formed during the enzyme-catalyzed reaction, then, during the subsequent derivatization procedure it will rearrange to dipeptide **255**. Formation of dipeptide **255** during detection should not interfere with enzyme-catalyzed formation of imide **12** during the assay. While this observation does not rule out the enzyme-catalyzed conversion of **255** through a different mechanism, it is inconsistent with the formation of tetrahedral intermediate **8** and the events shown by the mechanism illustrated in **Figure 1-11** (Chapter 1).

Further studies were conducted to determine the stability of imide **12** under enzyme assay quenching conditions. The use of trichloroacetic acid (TCA) caused

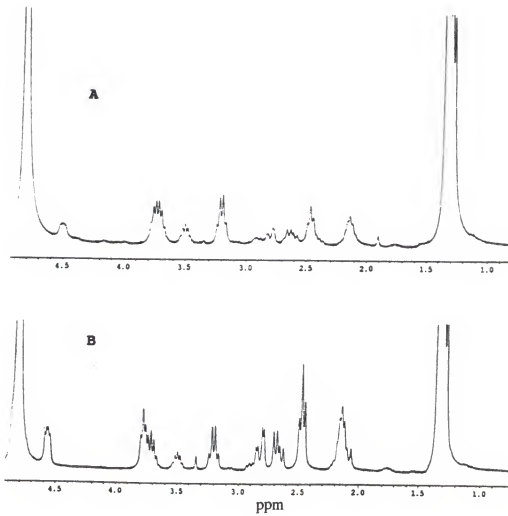

Figure 4-3. ^{1}H NMR (300 MHz) spectra of **A.** imide **12** (17 mM) and **B.** dipeptide **255** (18 mM) after treatment with DIEA:MeOH (50:50) at ambient temperature for 10 min.

decomposition of imide **12** to numerous products, as well as, shifts in the retention times of other substrates. Boiling imide **12** at 100 °C in enzyme buffer for 1 minute did not have any effect on its chromatographic properties nor did facilitate imide decomposition (**Figure 4-4**). Treating a boiled mixture of ATP, AMP, and imide **12** in enzyme buffer with activated charcoal followed by filtration resulted in exclusive removal of ATP and AMP from the reaction mixture without affecting imide **12** (**Figure 4-5**).

Two types of experiments were carried out designed to isolate or detect imide **12** in glutamine-dependent asparagine synthesis by *E. coli* AS-B. The first set of experiments involved incubation of imide **12** with wild type AS-B and detection of products. The second set of experiments involved the use of C1A and C1S AS-B mutants to generate imide **12**.

Reaction of Imide **12** with Wild Type *E. coli* Asparagine Synthetase B

Theoretically, if imide **12** is a true intermediate in glutamine-dependent nitrogen transfer of *E. coli* AS-B, then, incubation of **12** with AS-B might yield L-glutamate and L-Asn under standard enzyme-catalyzed reaction conditions. This hypothesis was tested by incubating imide **12** with wild type AS-B (WT AS-B) in Bis-tris buffer solution at pH 6.5 followed by detection of products by HPLC (**Figures 4-6 to 4-8**). Results showed that L-glutamate (**d**) and L-Asn (**c**) were not

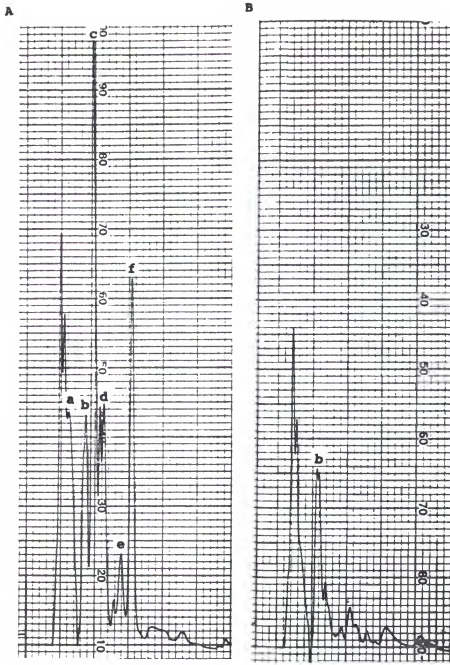

Figure 4-4. Reversed Phase HPLC chromatogram of substrates (0.3 mM) in Bis-tris (100mM) after boiling at 100 °C for 1 min.; 10 µL sample: **A.** ATP, imide **12** (**b**), L-Asp (**c**), L-Glu (**d**), L-Asn (**e**), L-Gln (**f**); **B.** imide **12** (**b**).

formed to any significant extent from imide **12** (**Figures 4-6**). While addition of L-Gln (**f**) resulted in L-Glu (**d**) formation, addition of either ATP (**a**) or ATP (**a**) + Asp (**c**) did not induce the formation of L-Glu (**d**) or L-Asn (**e**) (**Figure 4-7**). The usual products, L-Glu (**d**) and L-Asn (**e**), were formed only when all substrates, L-Gln (**f**), L-Asp (**c**), and ATP (**a**), were present (**Figure 4-8**).

These results did not clearly demonstrate that imide **12** was an intermediate in nitrogen transfer from L-Gln to β-aspartyl-AMP (**Figure 1-12**). It was possible, however, that the enzyme has to undergo a change in conformation from a catalytically inactive, to a catalytically active, form upon binding substrates. In this case, imide **12** cannot interact with AS-B since it cannot induce the conformational change required for binding, and hence cannot be broken down to products.

Studies of Imide **12** with C1A and C1S Mutants of *E. coli* Asparagine Synthetase B

The main difference between the two mechanisms presented by **Figures 1-11** and **1-12** (Chapter 1) is that formation of tetrahedral intermediate **8** requires the essential Cys_1 residue (**Figures 1-11**) whereas imide **12** formation does not (**Figures 1-12**). Thus a stable *E. coli* AS-B mutant in which Cys_1 was replaced by alanine, as in the AS-B C1A mutant, should lead to accumulation of imide **12** if the mechanism illustrated in **Figure 1-12** was correct. Hence, isolation

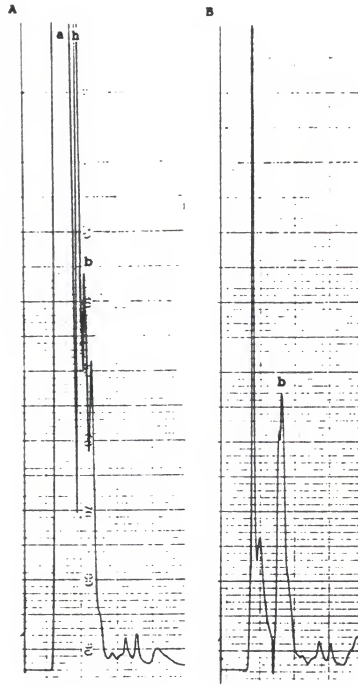

Figure 4-5. Reversed Phase HPLC chromatogram of ATP (0.6 mM), AMP (0.2 mM), and imide **12** (0.2 mM) in Bis-tris (100 mM) boiled for 1 minute at 100 °C. **A.** untreated with activated charcoal, **B.** treated with activated charcoal and filtered. Peak identity: **a.** ATP; **b.** imide **12**; **h.** AMP.

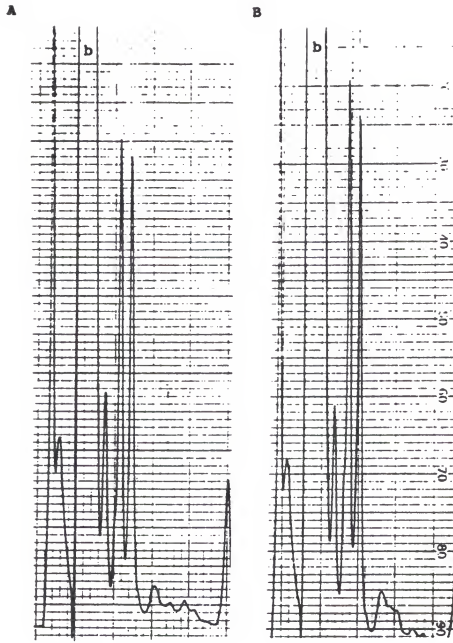

Figure 4-6. Reversed Phase HPLC chromatogram of the reaction mixture with WT AS-B (5 μg) in Bis-tris (100 mM) at pH 6.5: **A** imide **12** (7.5 mM), t = 0; **B.** imide **12** (7.5 mM), t = 15 min., 37 °C. Peak identity: **b.** imide **12.**

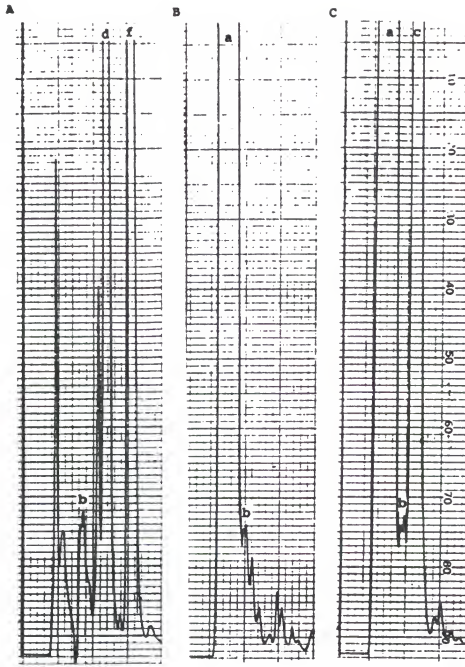

Figure 4-7. Reversed Phase HPLC chromatogram of the reaction mixture incubated at 37 °C for 15 min. with WT AS-B (5 μg) in Bis-tris (100 mM) at pH 6.5: **A** imide **12** (1.5 mM), L-Gln (1 mM); **B.** imide **12** (1.5 mM), ATP (1 mM); **C.** imide **12** (0.3 mM), L-Asp (1 mM), ATP (1 mM). Peak identity: **a.** ATP; **b.** imide **12**; **c.** L-Asp; **d.** L-Glu; **f.** L-Gln.

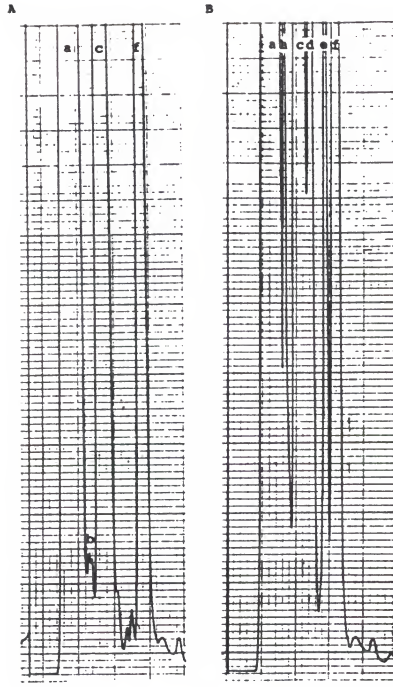

Figure 4-8. Reversed Phase HPLC chromatogram of the reaction mixture with WT AS-B (5 μg) in Bis-tris (100 mM) at pH 6.5: **A.** imide **12** (0.3 mM), ATP (1 mM), L-Asp (1 mM), L-Gln (1 mM), t = 0; **B.** imide **12** (0.3 mM), ATP (1 mM), L-Asp (1 mM), L-Gln (1 mM), t = 15 min., 37 °C. Peak identity: **a.** ATP; **b.** imide **12**; **c.** L-Asp; **d.** L-Glu; **e.** L-Asn; **f.** L-Gln.

and identification of imide **12** from reactions catalyzed by C1A using HPLC and mass spectrometry (185), respectively, would support the imide-mediated nitrogen transfer mechanism (**Figure 1-12**).

The ability of the AS-B C1A mutant to generate imide **12** (**b**) from L-Gln (**f**), L-Asp (**c**), and ATP (**a**) in Bis-tris buffer at pH 6.5 was examined (**Figure 4-9**). No evidence was obtained which showed that imide **12** was being formed from these substrates under these conditions. Control experiments showed that the addition of activated charcoal to remove ATP and AMP did not affect the detection or amounts of imide **12**.

These results are inconsistent with the formation of imide **12** as illustrated in **Figure 1-12**. However, comparison of kinetic parameters for L-Gln [K_M = 660 μM in WT AS-B and K_i = 4 μM in C1A (39)] indicated that the AS-B C1A mutant binds L-Gln tighter than WT AS-B. Ground state stabilization of L-Gln by AS-B C1A relative to WT AS-B could therefore increase the activation energy (E_a) for formation of the transition state leading to imide **12**, making synthesis of imide by the AS-B C1A mutant extremely slow (**Figure 4-10**). Similarly, an AS-B mutant which did not bind L-Gln as tightly as the AS-B C1A mutant might be expected to decrease the activation energy of the reaction yielding imide **12**. Previous studies (39) showed that a stable *E. coli* AS-B mutant where Cys_1 was replaced by Serine (C1S mutant, Ki = 250 μM for L-Gln) binds L-Gln less tightly than the C1A AS-B mutant (**Figure 4-10**).

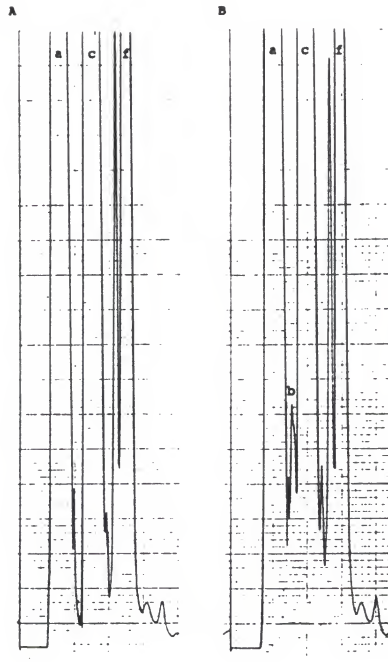

Figure 4-9. Reversed Phase HPLC chromatogram of the reaction mixture incubated at 37 °C for 30 min. with C1A AS-B (6.3 nmol) in Bis-tris (100 mM) at pH 6.5. after boiling for 1 min. at 100 °C and subsequent treatment with activated charcoal: **A** ATP (1.2 mM), L-Asp (1.2 mM), L-Gln (1.2 mM); **B.** imide **12** (0.3 mM), ATP (1.2 mM), L-Asp (1.2 mM), L-Gln (1.2 mM). Peak identity: **a.** ATP; **b.** imide **12**; **c.** L-Asp; **f.** L-Gln.

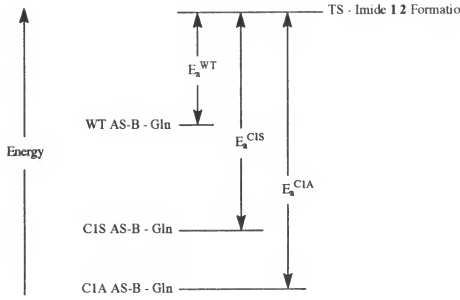

Figure 4-10. Relative energies between AS-B enzyme-substrate complexes and transition state for imide **12** formation based on kinetic parameters. TS = transition state; WT AS-B-Gln = enzyme-glutamine complex for WT AS-B; C1S AS-B-Gln = enzyme-glutamine complex for the C1S AS-B mutant; C1A AS-B-Gln = enzyme-glutamine complex for the C1A AS-B mutant.

We then tested the ability of AS-B C1S mutant to generate imide **12** (**b**) from L-Gln (**f**), L-Asp (**c**), and ATP (**a**) in Bis-tris buffer solution at pH 6.5 (**Figure 4-11**). In contrast to our expectations, C1S AS-B did not generate imide **12** from the normal substrates under these conditions. These results were practically identical to the results obtained using C1A AS-B. Thus, it appears that the lack of imide **12** formation is not due to the changes in the energetics of enzyme-substrate complexes.

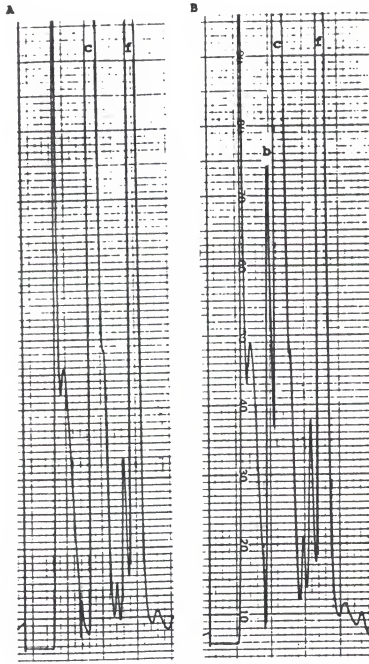

Figure 4-11. Reversed Phase HPLC chromatogram of the reaction mixture incubated at 37 °C for 30 min. with C1S AS-B (8.7 nmol) in BisTris (100 mM) at pH 6.5. after boiling for 1 min. at 100 °C and subsequent treatment with activated charcoal: **A** ATP (1.2 mM), L-Asp (1.2 mM), L-Gln (1.2 mM); **B.** imide **12** (0.3 mM), ATP (1.2 mM), L-Asp (1.2 mM), L-Gln (1.2 mM). Peak identity: **b.** imide **12**; **c.** L-Asp; **f.** L-Gln.

CHAPTER 5
INHIBITION STUDIES OF E. COLI ASPARAGINE SYNTHETASE B

Re-engineering the Function of E. Coli Asparagine Synthetase B from Amidohydrolase to Nitrile Hydratase

Asparagine Synthetase B, and the family of enzymes known as cysteine proteases (186,187), share the ability to hydrolyze amide bonds, i.e. both posses amidohydrolase activity. These two families of enzymes also have a common cysteine residue that is essential for catalysis. Papain, a member of the cysteine protease family, has been well characterized through kinetic (188-191), site-directed mutagenesis (192-194), inhibition (195), and X-ray diffraction (196-198) studies. The accepted mechanism of papain (186,195) (**Figure 5-1**) involves the formation of a Cys_{25}-His_{159} ion pair followed by attack of the thiolate anion upon the amide carbonyl of the substrate **285** to form tetrahedral intermediate **286**. Breakdown of **286** leads to the formation of amine **287** and acyl-enzyme intermediate **288**. Attack of water upon **288** yields a second tetrahedral intermediate **289** which on breakdown gives acid **290** and regenerates the active form of the enzyme.

The ability of papain, as well as other cysteine proteases, to hydrolyze amide bonds has been partly attributed to stabilization of unstable intermediates and

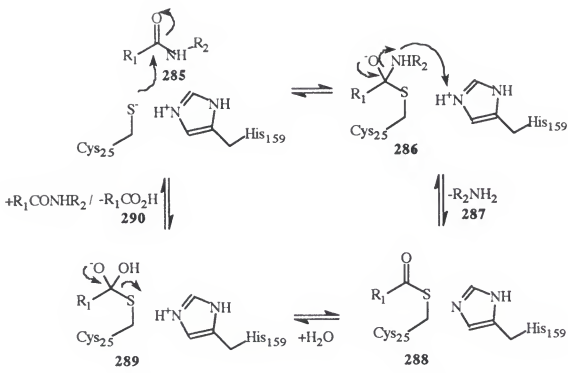

Figure 5-1. Currently accepted mechanism of papain leading to the formation of amine **287** and acid **290** from amide **285.**

transition states involved in the reaction mechanism by a region of the enzyme known as the oxyanion hole (196,199,200). X-ray diffraction (196) studies on papain have shown that this region is comprised of two hydrogen bond donors located on the backbone amide nitrogen of Cys_{25} and the side chain amide nitrogen of Gln_{19}. Site-directed mutagenesis studies (199) on papain by replacing Gln_{19} with Ala and Ser residues have provided evidence for the involvement of the oxyanion hole on transition state stabilization resulting in 60 and 600-fold decrease in k_{cat}/K_M, respectively. Studies on papain mutants by replacing Gln_{19} with Glu resulted in

modulation of the pH dependency of k_{cat}/K_M indicating interactions of the side chain of Gln_{19} with substrates (200).

Further studies upon the role of the oxyanion hole in papain have been conducted using transition state analog inhibitors (201,202) of cysteine proteases such as peptide aldehydes and nitriles (195). Although aldehydes have received considerable attention, the present study focuses on nitrile inhibitors exclusively.

A number of studies have shown that nitriles are good reversible inhibitors of cysteine proteases (203-205). NMR studies on papain (206-208) have shown that nitriles **291** react with Cys_{25} to form enzyme-thioimidate adduct **292** (**Figure 5-2**). Crystal structures of papain-inhibitor complexes representing models of acyl-enzyme intermediate **288**, combined with the structural similarity between thioimidate **292** and **288**, have shown that the thioimidate

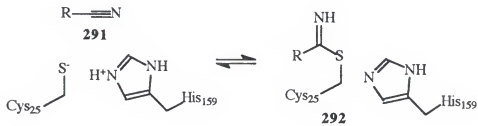

Figure 5-2. Reversible formation of enzyme-thioimidate **292** from nitrile **291** in papain.

nitrogen atom can be stabilized by the oxyanion hole. Evidence in favor of this idea has been obtained by Dufour and coworkers (209) were mutations of Gln_{19} in papain resulted in lower binding affinities for nitriles.

Experimental evidence has shown that hydrolysis of thioimidate **292** to give amides does not occur (204,205,208) unless high concentrations of enzyme are present (210) (**Figure 5-2**). Recent studies by Gour-Salin and coworkers (210) have shown that thioimidate **292** exists in the nonprotonated form favoring back formation of free enzyme and nitrile **291**, consistent with NMR studies (206-208). In contrast, hydrolysis of thioimidates in solution is acid catalyzed (211). Dufour et al. (209) postulated that replacement of Gln_{19} with a residue containing an acidic side chain may lead to hydrolysis of thioimidate **292**, thus changing the activity of papain from amidohydrolase to nitrile hydratase. Replacement of Gln_{19} with Glu (Q19E) afforded a papain mutant with nitrile hydratase activity in addition to amidohydrolase activity, leading to the accumulation of amide and subsequent hydrolysis to the free acid (209). The pH-dependence of the nitrile hydratase activity was consistent with the protonated form of Glu_{19}. A mechanism for the nitrile hydratase activity of this mutant was proposed (**Figure 5-3**). Protonation of thioimidate **292** by Glu_{19} leads to intermediate **293**. Attack of water, assisted by His_{159}, yields tetrahedral intermediate **294** which on breakdown gives amide **295**.

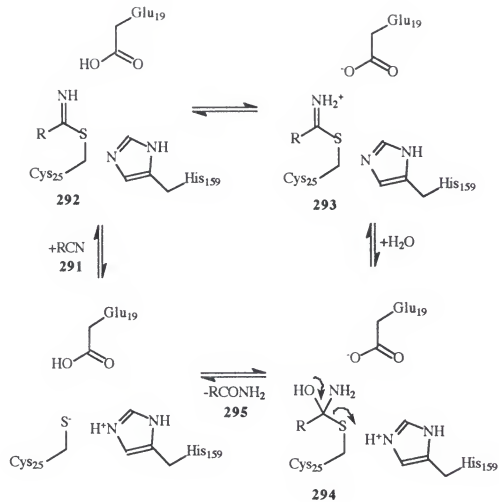

Figure 5-3. Proposed mechanism by Dufour, et.al. (209) for the nitrile hydratase activity of Q19E papain mutant showing the formation of amide **295** from nitrile **291.**

Recent studies on *E. coli* AS-B have shown that the conserved residue Asn_{74} is part of the catalytic machinery in glutamine-dependent nitrogen transfer (64). The AS-B mutant enzymes N74A and N74D possessed a reduced ability and an inability to hydrolyze Gln to glutamate, respectively. Other experiments have also indicated interactions between the side chain amide groups of Asn_{74} and Gln (64,69). Based on the

amidohydrolase activity and the requirement of the essential cysteine residue for both papain and AS-B, it was reasoned that Asn_{74} in AS-B may take a role analogous to Gln_{19} in papain. Thus, a nitrile analog of L-glutamine may serve as a potential candidate to study important active site residues in wild-type and selected mutants of *E. coli* AS-B. The efficient synthesis and chemistry of such nitrile analog follow next.

Rational Design and Synthesis of a Nitrile L-Glutamine Analog

Analogously to papain, we anticipated that L-glutamine nitrile analog **296** would inhibit AS-B by forming thioimidate **297** from attack of Cys_1 thiolate anion upon the CN group of nitrile **296** (**Figure 5-4**). The role of important residues by investigating their interaction with thioimidate **297** could be determined through kinetic studies and site-directed mutagenesis of AS-B.

The synthesis of nitrile **296** is outlined in **Figure 5-5**. Amide **211a** was dehydrated to give the protected nitrile **298** in quantitative yield following the method of Ressler and Ratzkin (212). Deprotection of the amino group using 10% Pd/C and 1,4-cyclohexadiene afforded nitrile **296** in good yields.

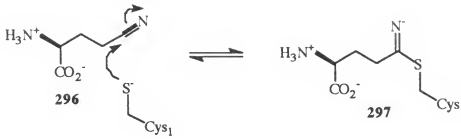

Figure 5-4. Proposed inhibition pathway of *E. coli* AS-B by nitrile **296**.

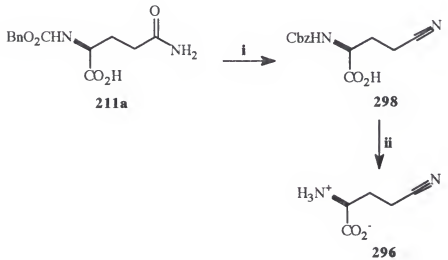

Figure 5-5. Synthesis of nitrile **296**. Reagents and conditions: **i**; DCC, pyridine, R.T. **ii**; 1,4-cyclohexadiene, 10% Pd/C, EtOH, reflux, 77%.

Stability Studies of Nitrile **296**

The stability of nitrile **296** with various buffers in the pH 6-9 range was studied using ^1H NMR spectroscopy (**Figures 5-6** to **5-8**). In Bis-tris or Tris buffer solutions, nitrile **296** was stable in the pH 6.3-7.3 range (**Figure 5-6**).

Between pH 7.3 to 8.2, the α-H triplet centered at 3.79 ppm shifts upfield while the β-H multiplet in the 2.17-2.29 ppm region shifts upfield and splits into two overlapping multiplets. This shifting and splitting increased further in the pH 8.2-8.7 range. Nitrile **296** in methylamine and HEPES buffer at pH 8.8 and 9.0, respectively, gave similar results compared to Tris buffer in the same pH region hours after mixing the components (**Figure 5-7**). HEPES buffer did not induce significant splitting of the multiplet in the 2.17-2.29 ppm region 15 minutes after mixing.

To determine if the shifting and splitting effect was buffer-independent and not caused by nitrogen containing buffers, the stability of nitrile **296** was evaluated in phosphate and carbonate buffers (**Figure 5-8**). Similar results compared to HEPES buffer were obtained for nitrile **296** in phosphate buffer at pH 9.0. Carbonate buffer at pH 9.9 also gave similar results 30 minutes after mixing but caused decomposition of **296** hours after mixing.

Further studies were conducted to determine if the shifting and splitting effect was reversible or irreversible (**Figure 5-9**). Nitrile **296** was initially dissolved in deuterium oxide to give a pH of 6.3 and the ^1H NMR recorded. This solution was then treated with Tris buffer to pH 8.4. The ^1H NMR of this solution showed splitting and shifting of the α and β-protons as before. Acidification of this latter solution with deuterium chloride to pH 7.1 produced a ^1H NMR spectrum identical to the spectrum at pH 6.3. These studies

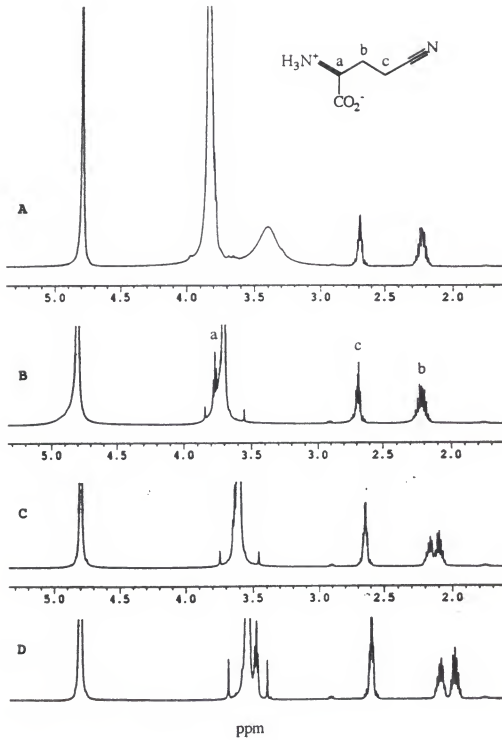

Figure 5-6. ^{1}H NMR (500 MHz) spectra of nitrile **296** (20-34 mM) in Bis-tris (100 mM) and Tris (100 mM) buffers: **A.** Bis-tris, pH 6.3; **B.** Tris, pH 7.3; **C.** Tris , pH 8.2; **D.** Tris, pH 8.7. Vertically offscale signals at 4.8 and 3.6-3.8 ppm correspond to water and Bis-tris/Tris protons, respectively.

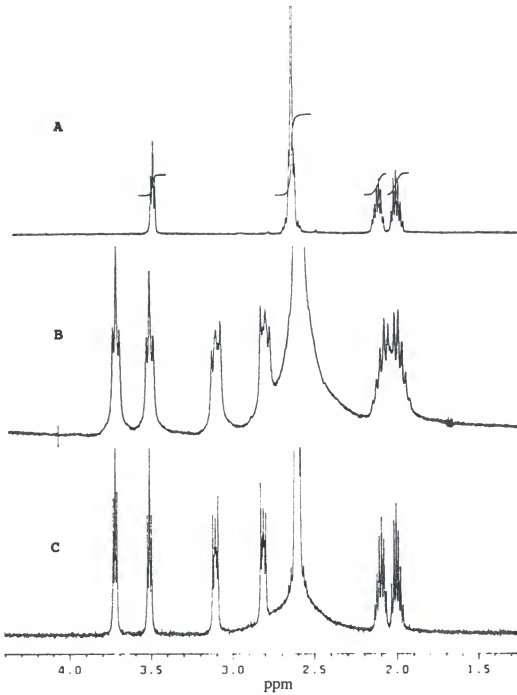

Figure 5-7. ^{1}H NMR (500 MHz) spectra of nitrile **296** in nitrogen buffers: **A.** methylamine, pH 9.0, after 15 hrs. at 4 °C; **B.** HEPES buffer, pH 8.8, after 15 min. at R.T.; **C.** HEPES buffer, pH 8.8, after 24 hrs. at R.T. Signals at 2.6 (offscale), 2.8, 3.1, and 3.7 ppm correspond to HEPES protons.

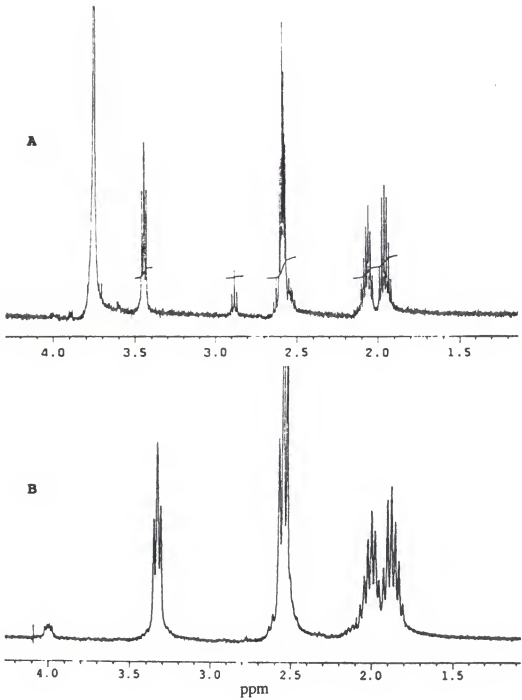

Figure 5-8. ^1H NMR (500 MHz) spectra of nitrile **296** in non-nitrogenous buffers: **A.** Na_2HPO_4 buffer, pH 9.0, after 15 min. at R.T.; **B.** Na_2HPO_4 buffer, pH 9.0, after 24 hrs. at R.T.; **C.** $NaHCO_3$ buffer, pH 9.9, after 30 min. at R.T.

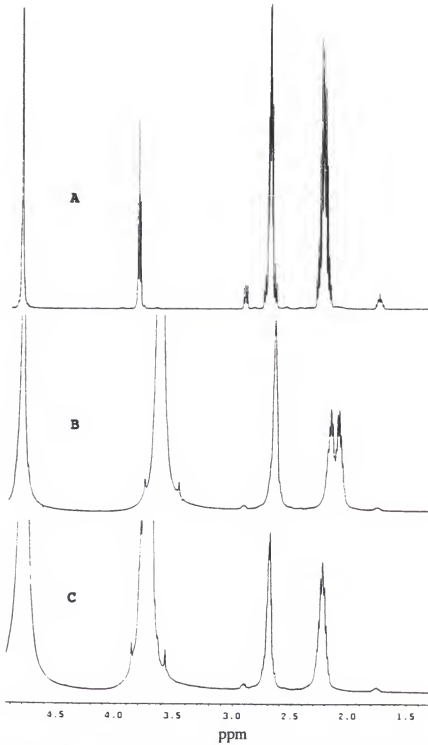

Figure 5-9. ^1H NMR (500 MHz) spectra of nitrile **296** (30 mM) in **A.** D_2O, pH 6.3, **B.** D_2O/Tris buffer, pH 8.4, and **C.** DCl/D_2O/Tris buffer reacidified to pH 7.1. Vertically offscale signals at 4.8 and 3.6 ppm correspond to water and Tris protons, respectively.

showed that the shifting and splitting effects of nitrile **296** are reversible.

The shifting of the α and β-protons is presumably caused by an electronic effect or a change in the electron density of the neighboring atoms. The splitting of the β-protons is more likely to be caused by structural effects around the neighboring atoms which reveal their diastereotopic nature. The lack of appearance of new signals at the expense of the disappearance of signals corresponding to **296** at high pH, in combination with the reversible formation of **296** by decreasing the pH, indicate that the shifting and splitting of the peaks do not correspond to a thermodynamically stable compound.

At high pH, at least four compounds, amidines **299** and **300**, isoimide **301**, and diketopiperazine **302**, could be formed from nitrile **296** (**Figure 5-10**). Amidine **299** should be stable enough to persist in solution without tautomerizing to **300**. However, the formation of amidines similar to **299** and **300** from the reaction of amines and nitriles requires high temperatures (213). The hydrochloride of amidine **300** has also been reported to be stable in DMSO (214). If the stability of **300** does not change between pH 6-9, then, this amidine cannot correspond to the species formed by **296** at high pH's given that this species reverses back to **296** upon acidification. Isoimide **301** is expected to be unstable, since isoimides have been rarely isolated (215). Diketopiperazine **302** should be a stable compound and is

expected to form irreversibly which is also inconsistent with our observations (216).

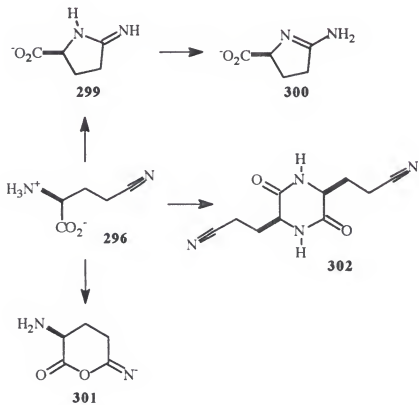

Figure 5-10. Possible products **299-302** formed from nitrile **296** at high pH.

In principle, the formation of compounds **299-302** could be detected using ^{13}C NMR given that the hibridization of the nitrile carbon changes from sp to sp^2 in going from nitrile **296** to amidines **299** or **300** and isoimide **301**, respectively. In the case of diketopiperazine **302**, the CO_2^- group of nitrile **296** is replaced by a CONH group, both of which have different ^{13}C chemical shifts.

The ^{13}C NMR spectra of nitrile **296** in D_2O, Tris buffer at pH 8.9, and phosphate buffer at pH 8.9 is illustrated on **Figure 5-11.** These spectra show that the shifting and splitting effects of the α and β-protons of nitrile **296** were not caused by nitrogen-containing buffers. The formation of amidines **299** or **300**, isoimide **301**, and diketopiperazine **302** were ruled out since formation of the N-C=N, O-C=N, or N-C=O carbons signals, expected around 150-180 ppm, were not detected and disappearance of the corresponding nitrile carbon signal at 121.6 ppm was not observed. However, small downfield peak shifts in the average of 2.45, 1.02, 0.83, and 5.63 ppm corresponding to C_β, C_α, CN, and CO_2^-, respectively, were noted.

Studies to determine if the splitting of the β-protons was due to a configurationally stable rotamer of nitrile **296** at high pH were conducted (**Figure 5-12**). The ^1H NMR spectra of nitrile **296** in Tris and phosphate pH 8.9 buffer solutions at 70 °C were identical to their corresponding ^1H NMR spectra at ambient temperature. Thus, it appears that the splitting of the β-protons at high pH is not due to a configurationally stable rotamer of nitrile **296.** In our favor, pH-dependent shifts and proton splitting similar to ours have been observed in L-Asp (217). These studies indicate that the shifting of the α-proton and the splitting of the β-protons are caused by a pH effect and do not represent the formation of a new stable compound.

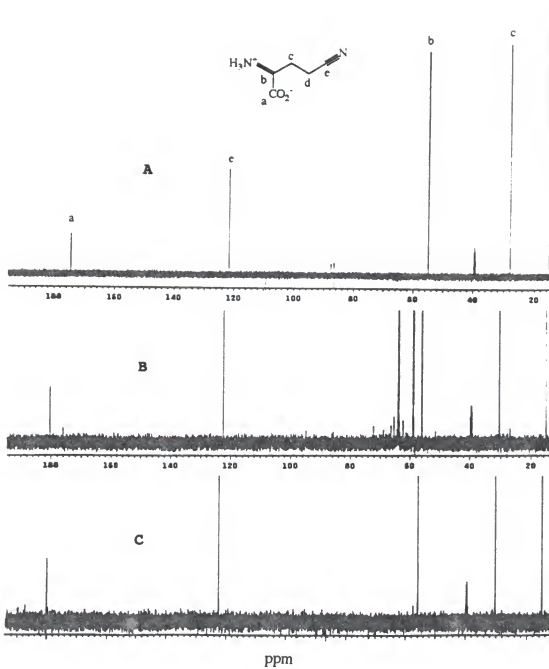

Figure 5-11. ^{13}C NMR (500 MHz) spectra of nitrile **296** (94-110 mM) in **A.** D_2O, **B.** Tris buffer, pH 8.9, and **C.** Na_2HPO_4 buffer, pH 8.9. The signal around 40 ppm corresponds to DMSO-d_6 internal standard.

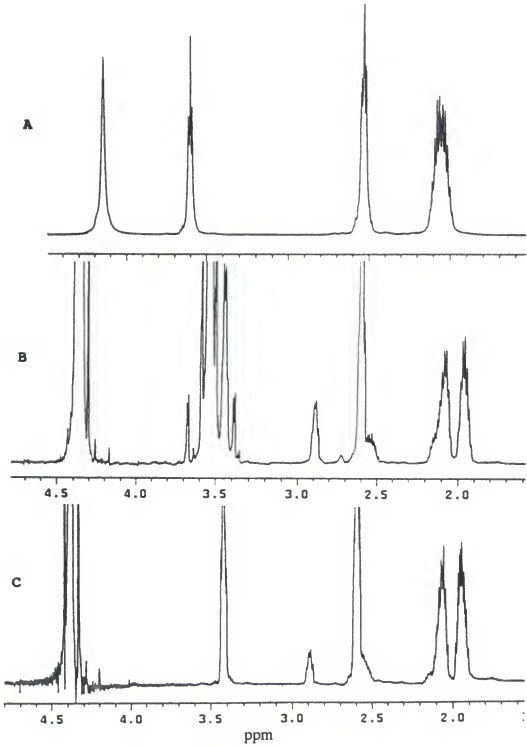

Figure 5-12. ^{1}H NMR (500 MHz) spectra of nitrile **296** (94-110 mM) at 70 °C in **A.** D_2O, **B.** Tris buffer, pH 8.9 and **C.** Na_2HPO_4 buffer, pH 8,9. Vertically offscale signals around 4.4 and 3.5 ppm correspond to water and Tris protons, respectively.

Although the stability of nitrile **296** at high pH presents a problem of scientific interest, for our studies with *E. coli* AS-B it was sufficient that **296** retained its stability near physiological pH. We then studied the ability of nitrile **287** to inhibit wildtype and mutants of AS-B at pH 7. The details of these studies are presented next.

Studies of Nitrile L-Glutamine Analog with *E. coli* Asparagine Synthetase B

Studies of nitrile **296** with WT AS-B revealed a non-competitive inhibition pattern for the glutaminase activity (**Table 5-1**). Moreover, a competitive inhibition pattern was obtained for nitrile **296**, relative to L-glutamine, with the N74A AS-B mutant. These results demonstrated the involvement of Asn_{74} in the catalytic mechanism of AS-B. It appears that this residue mediates the attack of the Cys_1 thiolate anion on the CN group of nitrile **296**. The ability of **296** to competitively inhibit N74A, combined with the reduced glutaminase activity for this enzyme, indicate that Asn_{74} may stabilize either tetrahedral intermediate **303** or thioacylenzyme **304** (**Figure 5-13**).

Based on similarities between the function of Asn_{74} in AS-B and Gln_{19} in papain it was reasoned that replacing Asn_{74} with an acidic residue may lead to hydration of nitrile **296**. We anticipated that the N74D AS-B mutant should possess nitrile hydratase activity analogously to the Q19E papain mutant (209).

Table 5-1. Inhibition parameters for nitrile **296** in the amidohydrolase activity of WT AS-B and N74A AS-B mutant.

Enzyme	Inhibition Pattern[a]	K_{is} (mM)[b]	K_{ii} (mM)[c]
WT AS-B	NC	0.36	0.51
N74A AS-B	C	0.70	-----

[a]C = competitive; NC = non-competitive.
[b]Determined from the slope.
[c]Determined from the intercept.

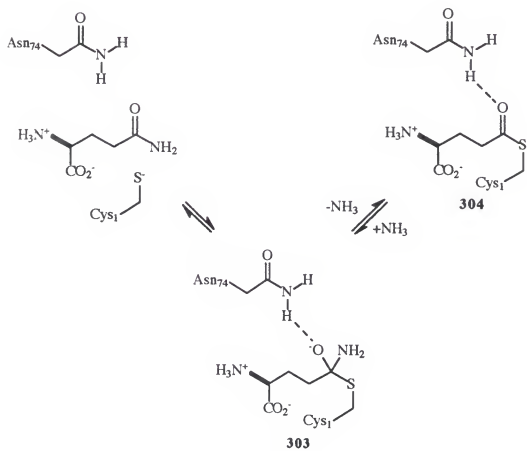

Figure 5-13. Stabilization of tetrahedral intermediate **303** or thioacylenzyme **304** by Asn_{74} upon attack of Cys_1 thiolate anion on L-glutamine in AS-B.

Studies on nitrile **296** with the N74D AS-B mutant showed that it underwent hydration to give L-glutamine. The lack of glutaminase activity for the N74D AS-B mutant enzyme allowed detection of L-glutamine by HPLC. This reaction exhibited Michaelis-Menten kinetics with parameters K_M = 0.86 mM, k_{cat} = 0.02 s^{-1}, and k_{cat}/K_M = 22.7 $M^{-1}s^{-1}$. Further studies on the pH-dependent hydration of **296** by the N74D AS-B mutant were not conducted. These results indicate similarities between the catalytic machinery of papain and AS-B. However, the presence of a histidine residue required for catalysis in papain establishes structural and functional differences between these two enzymes.

From our results, a mechanism was proposed which illustrates the hydratase activity of the N74D AS-B mutant (**Figure 5-14**). Assuming that Asp_{74} is on its protonated form on N74D AS-B, analogously to Glu_{19} in papain (209), attack of the Cys_1 thiolate anion upon nitrile **296** should form thioimidate anion **305**. Protonation of **305** by Asp_{74} to give intermediate **306**, followed by water attack, would yield tetrahedral intermediate **307**. Breakdown of **307** via C-S cleavage results in L-glutamine **1** formation whereas breakdown of **307** via C-N cleavage results in thioacylenzyme **304** and ammonia generation. The incapacity of the N74D AS-B mutant to cleave L-glutamine reflects its inability to stabilize thioacylenzyme **304**. Thus, C-N cleavage to form **304** and ammonia is disfavored resulting in C-S cleavage to give L-glutamine **1**.

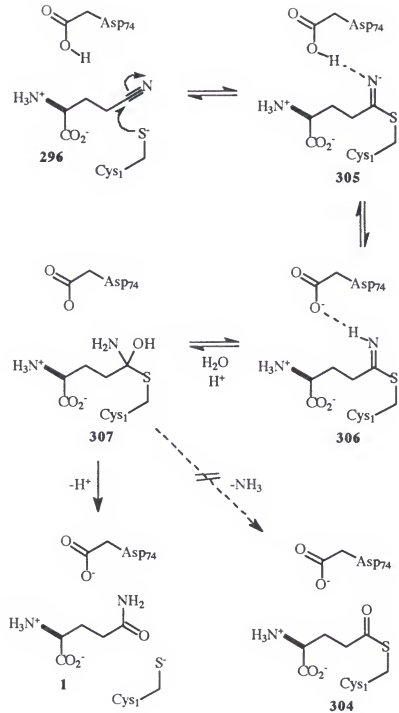

Figure 5-14. Proposed mechanism for the nitrile hydratase activity of *E. coli* N74D AS-B mutant.

Design and Synthesis of Other Potential Inhibitors of *E. coli* Asparagine Synthetase B

Although crystal structures for other members of the Class II subfamily of amidotransferases have been obtained (40-42), crystal structures for any member of the asparagine synthetase group of enzymes remain to be solved. The use of enzyme-inhibitor complexes to reveal the identity of catalytically critical residues has recently received enormous attention. The lack of structural information for *E. coli* AS-B focused our attention to design and synthesize potential mechanism-based inhibitors which may form stable enzyme-inhibitor complexes with AS-B. The crystal structure of these complexes should reveal information on the identity of critically important residues in AS-B which can be used to gain insight into the mechanism of nitrogen transfer.

From studies which showed the requirement of Cys_1 for glutamine-dependent nitrogen transfer in AS-B (39), we rationally designed inhibitors capable of covalently binding to the Cys_1 thiol group, either reversibly or irreversibly. These inhibitors must also be similar in structure to L-glutamine so to favorably interact with the active site of AS-B. To maximize their potency as inhibitors, potential candidates should not be too reactive nor too stable to enzyme assay conditions. Several potential candidates which fit into these categories are illustrated in **Figure 5-15.** The efficient synthesis of L-glutarimide **308** and synthetic

studies towards the synthesis of α,β-unsaturated L-glutamine **309** are presented next.

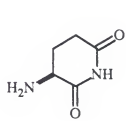

308

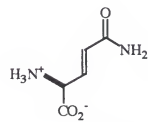

309 cis and trans

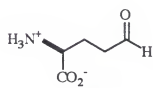

310

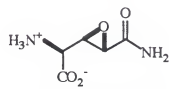

311 cis and trans
syn and anti

Figure 5-15. Potential mechanism-based inhibitors **308-311** of *E. coli* AS-B.

Rational Design and Synthesis of L-Glutarimide

Two possible inhibition routes of AS-B by L-glutarimide **308** are illustrated in **Figure 5-16.** Attack of the Cys_1 thiolate anion on the C_5=O group of **308** via pathway **A** should give rise to a series of intermediates which ultimately form acylenzyme intermediate **312.** This intermediate is not capable of transferring nitrogen but could possibly hydrolyze to form L-isoglutamine. Alternately, attack of the Cys_1

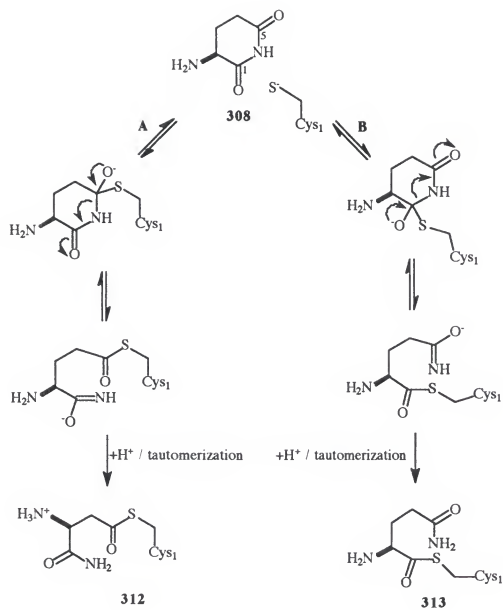

Figure 5-16. Proposed inhibition pathways of *E. coli* AS-B by cyclic imide **308**.

thiolate anion on the C_1=O group of **308** via pathway **B** should give rise to a series of intermediates which ultimately form acylenzyme intermediate **313**. This intermediate is incapable of transferring nitrogen, unless it is hydrolyzed to form L-

glutamine which can react further to form L-glutamate and ammonia. Pathway **B** should therefore present a potential problem since it may show initial inhibition, followed by recovery of activity from L-glutamine hydrolysis (glutaminase activity). We expect that pathway **A** should be preferred over pathway **B** since AS-B normaly attacks the C_5=O functional group of L-glutamine. In either case, inhibition should be observed if **308** can favorably bind and interact with AS-B.

The synthesis of **308** is shown in **Figure 5-17.** The sodium salt of amide **211a** was esterified using methyl iodide in DMF to give the methyl ester **314** in excellent yields.

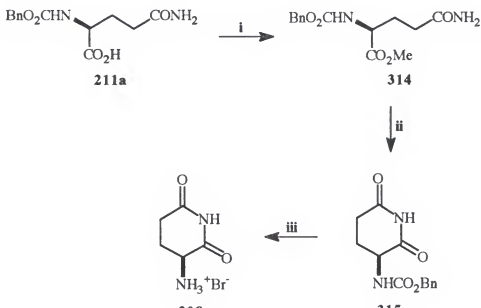

Figure 5-17. Synthesis of cyclic imide **308.** Reagents and conditions: **i;** a) Na_2CO_3, MeOH, H_2O, R.T., b) MeI, DMF, R.T., 95%. **ii;** NaH, THF, R.T., 93%. **iii;** 31% HBr/AcOH, Et_2O, R.T., 77%.

Treatment of **314** with sodium hydride in THF promoted cyclization to give cyclic imide **315** in excellent yields. Deprotection of **315** using 31% HBr in acetic acid afforded cyclic imide **308** in good yields.

Rational Design and Synthesis Towards an α,β-Unsaturated L-Glutamine Analog

A proposed inhibition pathway of AS-B by L-glutamine analog **309** is illustrated in **Figure 5-18.** Michael-type addition (218) of the Cys_1 thiolate anion on **309** should give

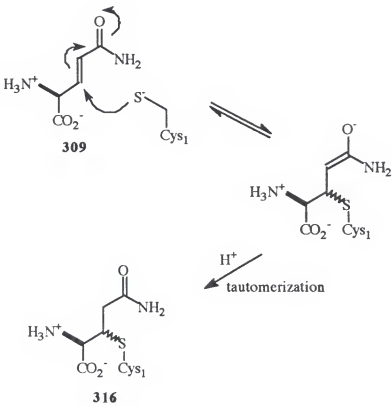

Figure 5-18. Proposed inhibition pathway of *E. coli* AS-B by α,β-unsaturated-L-glutamine analog **309.**

rise to acylenzyme intermediate **316**. This intermediate is incapable of transferring nitrogen, thus, inhibition of the glutaminase and glutamine-dependent activity of AS-B should occur.

Our route towards the synthesis of **309** is shown in **Figure 5-19**. Aldehyde **317** was prepared in four steps (60% overall yield), following the methods of Garner and Park (219) and McKillop et al. (220). Treatment of **317** with $(Ph)_3P{=}CHCO_2CH_3$ gave α,β-unsaturated ester **318** in excellent yields. Further treatment of **318** with ammonia in methanol afforded the α,β-unsaturated amide **319** in low yields. Alternately, good yields of amide **319** were obtained by first hydrolyzing **318** to give α,β-unsaturated acid **320** in excellent yields. Subsequent treatment of **320** with phosphorous pentachloride followed by ammonia in ether afforded amide **319**. This amide was further deprotected using TsOH in methanol to give alcohol **321** in low yields, or hydrogen chloride in ether to give amino-alcohol **322** in good yields. Attempts to oxidize alcohol **321** with pyridinium chlorochromate (PCC) and ruthenium tetroxide (RuO_4) were unsuccesful. No further experiments to oxidize alcohol **321** or amino-alcohol **322** to the final product L-glutamine analog **309** were carried out. Potential precursors of α,β-unsaturated-L-glutamic acid, **323** and **324**, were also synthesized in good yields from **318** and **319**, respectively. Moreover, ester **323** was converted into acid **324** in excellent yields from hydrolysis of the former with KOH.

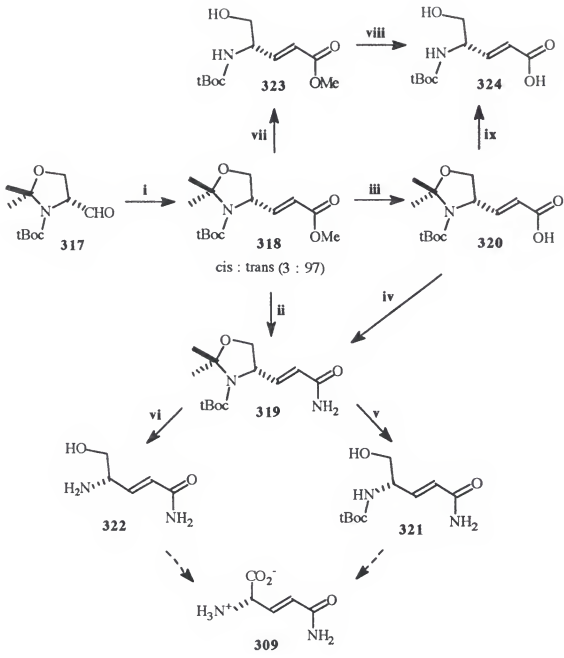

Figure 5-19. Synthetic route towards α,β-unsaturated-L-glutamine analog **309**. Reagents and conditions: **i**; $(Ph)_3P{=}CHCO_2CH_3$, THF, -65 °C-R.T., 90%. **ii**; NH_3, MeOH, -65 °C-R.T., 13%. **iii**; a) KOH, MeOH, H_2O, 0 °C-R.T., b) HCl, pH = 1, 97%. **iv**; a) PCl_5, Et_2O, 0 °C-R.T., b) NH_3, Et_2O, 0 °C-R.T.,68%. **v**; TsOH(cat.), MeOH, R.T., 30%. **vi**; HCl, Et_2O, R.T. **vii**; CH_3CN, MeOH, TsOH, R.T., 60%. **viii**; KOH, MeOH, R.T., 87%. **ix**; CH_3CN, H_2O, TsOH, R.T., 33%.

Inhibition Studies of Potential Inhibitors with Wild Type *E. Coli* Asparagine Synthetase B

The ability of L-glutarimide **308** to inhibit the glutamine-dependent activity of *E. coli* AS-B and C1A AS-B mutant was estimated using the method of Dixon (221) (**Table 5-2**). Imide **12** (**Figure 3-6**) and dipeptide **255** (**Figure 3-17**) were also tested as inhibitors of these enzymes. These studies show that neither **308**, **12**, nor **255** were good inhibitors of WT AS-B. Interestingly, the inhibition curve (1/V vs. [I]) for imide **12** with WT AS-B and C1A AS-B mutant was nonlinear, this deviation resulting in increased inhibition at high concentrations of **12**. In contrast, **308** and **255** did not exhibit this non-linear behavior.

Table 5-2. Inhibition constants of imide **12**, dipeptide **255**, and L-glutarimide **308** with WT AS-B (7.5 μg) and C1A AS-B (34 μg) in Bis-tris (100 mM) at pH 6.5.

Inhibitor	K_i (mM)[a]	
	WT AS-B	C1A AS-B
12	4.3	7.9
255	15.6	-----
308	19.6	13.9

[a]Determined by plotting 1/V vs. [Inhibitor] using the method of Dixon.

CHAPTER 6
CONCLUSIONS

Synthesis and Properties of Acyclic Unsymmetric Functionalized Imides

Several diprotected L-glutamine derivatives were acylated at the N_{γ}-position to give 13 new highly functionalized unsymmetric acyclic imides **216a-c**, **237a-h**, **243**, and **245** in variable yields. Four of these imides **216b**, **237b**, **237e**, and **237h** were partly deprotected in excellent yields to give the new free acids **225**, **246**, **248**, and **250** respectively. Three imides **225**, **237a**, and **237d** were fully deprotected to give the corresponding free amino acid imide derivatives of L-glutamine **12**, **247**, and **249** in good yields. Dipeptides **255** and **263** were also efficiently synthesized. The imides **12**, **247**, and **249**, as well as free acids **225**, **246**, **248**, and **250**, are novel derivatives of L-glutamine with potential applications in the fields of peptide and medicinal chemistry.

The stability of imides **12**, **247**, and **249** was studied using ^{1}H NMR spectroscopy in the pH 6-8 range using Bis-tris and Tris buffers. Imide **247** forms pyrrolidone **265** and acetamide **280** irreversibly at high pH within this range. Imide **249** is stable in this pH range without the detectable formation of new products. Imide **12** forms dipeptide **255**

exclusively and irreversibly in this pH range. Dipeptide **255** is also formed in HEPES, phosphate, borate, and bicarbonate buffers at pH 8. In bicarbonate buffer at pH 8, imide **12** breaks down to a mixture of L-Gln, L-aspartate, and dipeptide **255**.

IR studies showed the cis-trans or trans-cis geometry for all three imides **12**, **247**, and **249** in the solid state. Based on theoretical calculations, the relative energies of the four different conformational isomers of imides **12**, **247**, and **249** lie between 0.0 and 9.4, 6.8, and 3.5 kcal/mole, respectively, the cis-trans isomer being the most stable isomer for all three imides. Low temperature ^1H NMR studies on imides **225**, **237a**, and **248** in acetone-d_6 showed preference for two conformational isomers which rapidly interconvert at ambient temperature. Rotational barriers for interconversion about the imide C=O and N-H bond on imides **225**, **237a**, and **248** were estimated at 10.4, 10.2, and 10.1 kcal/mol, respectively.

Mechanistic and Inhibition Studies on E. coli Asparagine Synthetase B

Incubation of imide **12** with WT AS-B in Bis-tris buffer at pH 6.5 did not form the usual products L-glutamate and L-Asn . Incubation of L-Gln, L-Asp, and ATP with either AS-B C1A or AS-B C1S mutant enzymes in Bis-tris buffer at pH 6.5 did not generate imide **12** as well. Both results are inconsistent with the imide-mediated nitrogen transfer

mechanism (**Figure 1-12**) in glutamine-dependent asparagine synthesis by *E. coli* AS-B. Studies with WT AS-B do not necessarily rule out the possibility of imide **12** as an intermediate in glutamine-dependent nitrogen transfer from L-Gln to β-aspartyl-AMP. Studies with C1A and C1S AS-B mutants indicated that the lack of imide **12** formation was not dependent on the energetics of enzyme-substrate complexes.

These results neither support an imide-mediated nitrogen transfer mechanism in glutamine-dependent asparagine synthesis by *E. coli* AS-B (**Figure 1-12**) nor imide **12** as an intermediate of this reaction. These results, however, do not disprove the mechanism involving tetrahedral intermediate **8** illustrated by **Figure 1-11**.

Nitrile **296** was synthesized efficiently. This compound is stable in Bis-tris and Tris buffer solutions at pH 6.3-7.3. The exclusive buffer-independent formation of a new form of nitrile **296** is observed at pH 7.3-8.7. This form reverses back to nitrile **296** upon acidification to pH 6.3. ^{13}C NMR and ^{1}H NMR studies showed that this form does not correspond to amidines **299** and **300**, isoimide **301**, or diketopiperazine **302**, nor a configurationally stable rotamer of nitrile **296**.

Studies on nitrile **296** with WT AS-B revealed non-competitive inhibition of the glutaminase activity with a K_i = 0.36 mM. Nitrile **296** was a competitive inhibitor of the N74A AS-B mutant, relative to L-glutamine, in the glutaminase activity with a K_i = 0.70 mM. The N74D AS-B mutant hydrated

nitrile **296** to give L-glutamine exhibiting Michaelis-Menten kinetics with parameters K_M = 0.86 mM, k_{cat} = 0.02 s^{-1}, and k_{cat}/K_M = 22.7 $M^{-1}s^{-1}$. The function of *E. coli* AS-B was engineered from amidohydrolase to nitrile hydratase by a single-point mutation of the catalytically essential Asn_{74} residue.

A new and efficient route for preparing L-glutarimide **308** was developed. L-glutarimide **308** was a poor inhibitor of WT AS-B and ClA AS-B mutant with K_i's of 19.6 and 13.9 mM, respectively. Imide **12** and dipeptide **255** were also poor inhibitors of these enzymes. Potential precursors of α,β-unsaturated-L-glutamine and α,β-unsaturated-L-glutamic acid, **321**, **322** and **323**, **324**, respectively, were also synthesized in good yields.

CHAPTER 7
EXPERIMENTAL

Materials, Instruments, and Methods

L-aspartic acid, L-asparagine, L-glutamic acid, L-glutamine, t-butyl-L-glutamine hydrochloride, N-Cbz-L-glutamine, N-Cbz-L-aspartic acid, N-Cbz-L-asparagine, (S)-2-pyrrolidone-5-carboxylic acid, β-alanine, D-serine, Bis-tris, Tris, and HEPES, were obtained from Sigma Chemical Co. and used without further purification. Succinic anhydride, anhydrous pyridine (99 + %) and redistilled trifluoroacetic acid (99 + %) were obtained from Aldrich Chemical Co. and used without further purification. All other reagents were obtained from Aldrich Chemical Co. or Fisher Scientific and were used without further purification unless otherwise specified. Tetrahydrofuran and diethyl ether were distilled from sodium/benzophenome and used immediately prior to reaction. Methylene chloride and t-butanol were distilled from calcium hydride prior to use. Chloroform was distilled from phosphorous pentoxide prior to use. TLC analysis was performed on Whatman silica gel 60 A F-254 nm plates with either aluminum or polyester backing and visualized by charring with (A) 4% ninhydrin in ethanol or (B) ceric sulfate/sulfuric acid (aq) solution. Column chromatography

was performed on Davisil^{R} silica gel (Fisher) 60 A^{o}-200-425 Mesh. Derivatization of amino acids and derivatives were performed using a Applied BioSystems 428A Derivatizer. Separation of derivatized products were conducted using reversed phase HPLC in a Applied BioSystems 130A Separation System. Melting points were obtained using a Fisher-Johns Melting Point Apparatus. pH 4, 7, and 10 buffer solutions were obtained from Fisher Scientific. pH measurements were recorded using a ORION Model 250A pH Meter and a Mettler Toledo Process Analytical, Inc. Model 6030-M3/180/1M/BNC pH electrode. IR spectra were recorded on a Perkin-Elmer 1600 FTIR spectrophotometer. Optical rotations were determined at ambient temperature using a Perkin-Elmer 241 polarimeter. ^{1}H NMR spectra were recorded at 300 and 500 MHz with a Varian VXR-300 spectrometer and Varian Unity-500 spectrometer, respectively, using deuterated chloroform / 0.3 % TMS, deuterium oxide with DSS or DMSO-d_6, acetone-d_6, or methanol-d_4. ^{13}C NMR spectra were recorded at 75.4 and 125.7 MHz with a Varian VXR-300 spectrometer or a Varian Unity-500 spectrometer.

Nuclear Magnetic Resonance Experiments

All NMR experiments were conducted at ambient temperature (22-23 ^{o}C) unless otherwise specified. Buffer solutions of BisTris, Tris, HEPES, Na_2HPO_4/Na_3PO_4, Na_4BO_4, and $NaHCO_3/Na2CO_3$ in D_2O were prepared at ambient temperature and

the pH adjusted to pH 8 with DCl. Stability studies were carried out by adding the buffer solution to a known amount of imide in an NMR tube and readjusting the pH to the desired value if needed. ^{1}H or ^{13}C NMR spectra were recorded at ambient temperature within 30 min. Equillibrium studies were performed by cooling a solution of imide in D_2O to the desired temperature and recording the ^{1}H NMR spectra after 30 min. Low and high temperature ^{1}H NMR studies were conducted by setting the NMR probe to the desired temperature and allowing sufficient time for temperature equillibration of the sample (30 min.) followed by aquisition of the spectra. Rotational barriers (ΔG^{*}) were obtained using the equation ΔG^{*} (kJ/mole) = 8.3 X $10^{-3}T_c(23 + 2.3[\log_{10}(T_c/\Delta v)])$ (222) were Tc = coalescense temperature (K) and Δv = difference between the two coalescing signals (Hz) and converting to kcal/mole (1 kcal/ 4.187 kJ). Chemical shifts in D_2O were reported relative to DSS or DMSO-d_6 internal standards for all ^{1}H and ^{13}C NMR experiments, respectively.

Enzymatic Assays

Detection of reaction products from enzymatic assays was conducted by derivatizing the reaction mixture (20 μL) with PITC and separating the products by reversed phase HPLC detecting at 254 nm. Optimized separation of derivatized products was obtained using the following solvent A (0.5 M sodium acetate in water, pH 5.4):solvent B (0.5 M sodium

acetate in 30:70 water:acetonitrile at pH 6.1):time (min.) gradient; 94:4:0, 94:4:7, 75:25:10, 37:63:20, 0:100:25, 0:100:30, 94:4:31. This procedure was used for separating and detecting all standard mixtures and enzyme assay products. Standard mixtures were prepared from stock solutions of each substrate ATP (2 mM), AMP (2 mM), L-Asp (2 mM), L-Asn (2 mM), L-Glu (2 mM), L-Gln (2 mM), imide **12** (3-30 mM), dipeptide **255** (3-30 mM), and BisTris (500 mM). The standard curve for imide **12** was developed by derivatizing and separating 10 μL of 3.83, 0.76, 0.38, 0.19, 0.08, and 0.04 mM solutions of imide **12**, quantitating the area under its peak using RAININ™ Data Aquisition Program, and plotting Area (μV-sec) vs. imide **12** (nmoles) using linear regression analysis with Cricket Graph™. Retention times were calculated by measuring distance (mm) from the origin (t = 0) to the top of the peak and caculating the average of three runs. Distance units (mm) were converted into time units (min.) using the chart recorder conversion factor of 5 mm/min.

Experiments upon the ability of WT AS-B to employ imide **12** as a substrate were performed by incubating **12** (1.5 mM, 6 μL) with enzyme (5 μg) and different combinations of ATP (37.5 mM, 1 μL), L-aspartate (37.5 mM, 1 μL), L-glutamine (37.5 mM, 1 μL), and $MgCl_2$ (75 mM, 1 μL) in BisTris (500 mM, 6.6 μL) buffer at pH 6.5 (33 μL total volume) for 30 min at 37 °C. The mixture was boiled at 100 °C for 1 min. and filtered to remove denatured enzyme. Treatment with activated charcoal (< 0.5 mg) followed by filtration afforded

a clear colorless solution. Products from the reaction mixture were characterized by derivatizing this solution (20 μL) followed by reversed phase HPLC as described above.

Experiments upon the ability of C1A or C1S AS-B to produce imide **12** were performed by incubating enzyme (C1A = 6.3 nmoles/50 μL; C1S = 8.8 nmoles/50 μL) with ATP (1.5 mM), L-aspartate (1.5 mM), L-glutamine (1.5 mM), and $MgCl_2$ (1.5 mM) in BisTris buffer at pH 6.5 (50 μL total volume) for 30 min at 37 °C. The mixture was boiled at 100 °C for 1 min. and filtered to remove denatured enzyme. Treatment with activated charcoal (< 0.3 mg) followed by filtration, derivatization, and separation as described above allowed characterization of the reaction mixture.

Initial velocities (V) for imide **12**, dipeptide **255**, nitrile **296**, and cyclic imide **308** were determined by incubation with WT AS-B (7.5 μg) or C1A AS-B (34 μg), ATP, L-Asp, and L-Gln and measuring the amount of pyrophosphate released spectrophotometrically using a coupled assay system (Sigma Technical Bulletin #B1-100). Inhibition constants (K_i) for inhibitors **12**, **255**, and **308** were determined by plotting 1/V (nmole/sec/μg) vs. [inhibitor] (mM) using the method of Dixon (221).

The ability of WT AS-B to synthesize L-asparagine using nitrile **296** as a substrate was determined by incubating **296** (10 mM) with WT AS-B (5.6 μg), ATP (5 mM), $MgCl_2$ (8 mM) in HEPES buffer (100 mM) at pH 7.0 for 15 min. at 37 °C and measuring the amount of pyrophosphate released

spectrophotometrically after terminating the reaction by boiling at 100 °C for 1 min.. Inhibition of L-glutamate synthesis by nitrile **296** for WT AS-B or N74A AS-B was determined by incubating **296** with WT AS-B (1.5 μg) or N74A AS-B (14.7 μg), $MgCl_2$ (8 mM), and HEPES buffer (100 mM) at pH 7.0 for 15 min. at 37 °C and measuring the amount of L-glutamate produced by HPLC or standard colorimetric methods (223) after terminating the reaction by boiling at 100 °C for 1 min.. The ability of N74D AS-B mutant to use nitrile **296** as a substrate was determined in a similar fashion. The identity of the reaction products were determined by HPLC.

Theoretical Calculations

All molecular structures were constructed using CAche™ Molecular Modeling system Editor™ program and energy minimized using the Dynamics™ program. Heats of formation (ΔH_f) were calculated using the MOPAC™ program (172) with AM1 parameters (224), CONH corrections, and water solvation potential. Energies reported correspond to the lowest energy conformation from at least three different conformers unless otherwise specified. Relative energies ($\Delta\Delta H_f$) correspond to the difference between the questioned structure and its lowest energy conformer or isomer.

Synthetic Procedures and Chemical Data of Compounds

N-(carbobenzyloxy)-L-glutamine (**211a**); L-glutamine (10.0 g, 68 mmol) was suspended in water (5 ml) and cold 2 M NaOH (30 ml, 6 mmol) slowly added at 5 °C. Benzyl chloroformate (16 ml, 110 mmol) was added in six portions along with 2 M NaOH so as to always maintain the pH > 8. After about 2 hrs. at R.T., the pH did no longer change. 2 M NaOH was added to bring the pH 9.5. Diethyl ether (20 ml) was added and the layers separated. To the aqueous layer was added ethyl acetate (50 ml) and acidified with concentrated HCl to pH=2.5. After several extractions of the aqueous layer, the combined ethyl acetate fractions were combined and the solvent removed under reduced pressure to yield a thick clear paste which soon turned white. Scratching the flask with a stirring rod induced crystallization to yield white crystals. Recrystallization from water gave product as a white solid (71% yield): m.p.=139-140 °C [lit. (225) m.p.= 133-137 °C]; ^{1}H NMR (DMSO-d_6, 300 MHz) δ 1.73 (1 H, m), 1.94 (1 H, m), 2.13 (2 H, t), 3.93 (1 H, m), 5.02 (2 H, s), 6.75 (1 H, s), 7.24-7.37 (6 H, m), 7.57 (1 H, d), 12.07 (1 H, s); ^{13}C NMR (DMSO-d_6, 75.4 MHz) δ 26.93 (t), 31.78 (t), 65.81 (t), 128.13 (d), 128.21 (d), 128.76 (d), 128.83 (d), 173.85 (s).

N-(*tert*-butoxycarbonyl)-L-glutamine (**211b**); L-glutamine (1.0 g, 6.8 mmol) was dissolved in ice cold 1 M NaOH (13.7 ml, 13.7 mmol). A solution of di-t-butyldicarbonate (1.7 g,

7.8 mmol) in dioxane (6.5 ml) was added and the resulting emulsion warmed up to R.T. over a period of 30 min. at which point the pH = 7-8. The reaction mixture was further stirred at R.T. for 72 hrs. After evaporating the organic solvents under reduced pressure the resulting aqueous solution was acidified with concentrated HCl. The mixture was extracted with ethyl acetate (3 X 50 ml) and the organic fractions combined and dried ($MgSO_4$). The solvent was removed under reduced pressure to give a foamy colorless gel (1.56 g, 92%).

N-(carbobenzyloxy)-α-Bn-L-glutamine (**213a**); Method A: N-(carbobenzyloxy)-L-glutamine (7.0 g, 25 mmol) was dissolved in benzene (40 ml) and p-toluenesulfonic acid monohydrate (0.390 g, 2.1 mmol) added followed by benzyl alcohol (4.2 g, 39 mmol). After about 1 hr. of reflux, the benzene/water azeotrope was distilled off under reduced pressure. More benzyl alcohol and benzene were added and reflux was continued until TLC (75:25; ethyl acetate:petroleum ether) showed almost complete disappearance of starting material at the origin. At this time, the excess BnOH was vacuum distilled under high vacuum (bath temperature never exceeded 95 °C) to yield a thick paste. This paste was dissolved in ethyl acetate and extracted with 5% sodium bicarbonate solution. The organic layer was evaporated at reduced pressure to give white flakes. Further removal of the solvent at high vacuum gave almost pure product. Washing with a mixture of methanol/ethyl acetate/petroleum ether and

filtration gave about 59% yield of product. Method B: N-(carbobenzyloxy)-L-glutamine (8.4814 g, 30.3 mmol) was dissolved in methanol (50ml) and a solution of cesium carbonate (4.93 g, 15.1 mmol) in water (60 ml) added at room temperature. After stirring at this temperature for 30 min. the methanol was evaporated under reduced pressure and the aqueous layer freeze dried overnight to give a white solid. DMF (100 ml) was added followed by benzyl bromide (4.5 ml) and the resulting solution stirred for 3 hrs. The precipitated solids were filtered off and washed with DMF. The solvent was removed under reduced pressure at 55 °C to give a white solid. The solid was washed with petroleum ether, ethyl acetate:petroleum ether (25:75), and water, then dried under nitrogen to afford 10.9053 g (97%) of product: m.p.=123-124 °C [lit. (164) m.p.= 123 °C]; $[\alpha]_D$ -17.9° (c 1.12, acetone); ^{1}H NMR (acetone-d_6, 500 MHz) δ 1.94-2.02 (1 H, m), 2.13-2.20 (1 H, m), 2.33-2.36 (2 H, m), 4.30 (1 H, dt, J = 8.5, 5.0 Hz), 5.08 (2 H, d, J = 2.5 Hz), 5.17 (2 H, s), 6.22 (1 H, s), 6.79 (1 H, s), 6.94 (1 H, d, J = 7.0 Hz), 7.29-7.41 (10 H, m); ^{13}C NMR (acetone-d_6, 75.4 MHz) δ 27.64 (t), 31.91 (t), 54.98 (d), 66.71 (t), 67.02 (t), 128.59 (d), 128.78 (d), 128.84 (d), 129.15 (d), 129.25 (d), 137.12 (s), 138.09 (s), 157.07 (s), 172.79 (s), 174.42 (s); IR (KBr) ν 3437, 3322, 3200, 3068, 3032, 2956, 2895, 1741, 1686, 1653.4, 1546, 1451, 1420, 1384, 1341, 1303, 1266, 1243, 1206, 1184, 1067, 1043, 991, 948, 911, 756, 738, 696, 634, 579 cm^{-1}; HRMS (FAB: H^+) exact mass calc. for $C_{20}H_{23}N_2O_5$ requires 371.1607,

found 371.1590; m/e (relative intensity) 371 (64), 327 (10), 235 (7), 167 (8), 91 (100); Anal. Calcd. for $C_{20}H_{22}N_2O_5$: 64.85% C, 5.99% H, 7.56% N; found 64.51% C, 5.82% H, 7.56% N.

N-(carbobenzyloxy)-α-tBu-L-glutamine **(213b)**; N-(carbobenzyloxy)-L-glutamine (25.8568 g, 92.35 mmol) was suspended in dichloromethane (90 ml) and t-BuOH (12.5 ml) under positive nitrogen pressure. The mixture was cooled to 0 °C in an ice bath and a solution of DCC (20.006 g, 96.96 mmol) in dichloromethane (100 ml) was slowly added in three portions followed by DMAP (0.113 g,0.92 mmol). After 15 hrs. at 0 °C TLC (100% ethyl acetate; ninhydrin stain) showed the formation of product (R_f = 0.38) at the expense of starting material (R_f = 0.16). No change in product composition was observed after warming up to R.T. over a period of 8 hrs. The mixture was filtered and washed with dichloromethane. The solvent was removed under reduced pressure and the remaining oil dissolved in ethyl acetate (310 ml). After cooling the solution in an ice-salt bath glacial acetic acid (3.2 ml) was added and stirring continued for and additional 2 hrs. at approx. -10 °C The mixture was filtered and the resulting solution extracted several times with 5% $NaHCO_3$. The organic layer was dried ($MgSO_4$) and the solvent removed under reduced pressure to give a light yellow oil which was precipitated by adding ethyl acetate:petroleum ether. The crude product was further purified by several recrystallizations from ethyl acetate:petroleum ether to give

a white solid. Further purification was achieved by chromatography on silica gel (100% ethyl acetate eluent; ninhydrin stain) (25.7634 g, 83%): m.p. = 114-118 °C [lit. (226) m.p.= 94-95 °C]; $[\alpha]_D$ -15.6° (c 2.73, acetone); ^1H NMR (acetone-d_6, 500 MHz) δ 1.44 (9 H, s) 1.89-1.97 (1 H, m), 2.07-2.13 (1 H, m), 2.32-2.35 (2 H, m), 4.10 (1 H, dt, J = 4.7, 8.5 Hz), 5.07 (2 H, d, J = 4.0 Hz), 6.24 (1 H, s), 6.73 (1 H, d, J = 7.0 Hz), 6.82 (1 H, s), 7.29-7.39 (5 H, m); ^{13}C NMR ($CDCl_3$, 75.4 MHz) δ 27.87 (q), 28.12 (t), 31.66 (t), 54.24 (d), 66.78 (t), 82.14 (s), 127.91 (d), 128.01 (d), 128.14 (d), 128.40 (d), 136.35 (s), 156.34 (s), 171.24 (s), 175.12 (s); IR (KBr) ν 3386, 3150, 2977, 1716, 1670, 1626, 1586, 1500, 1457, 1407, 1368, 1338, 1278, 1258, 1221, 1166.8, 1090, 1048, 1025, 962, 932, 847, 814, 771, 732, 692, 649, 574, 471 cm^{-1}; HRMS (FAB: H^+) exact mass calc. for $C_{17}H_{25}N_2O_5$ requires 337.1763, found 337.1759; *m/e* (relative intensity) 337 (53), 281 (100), 237 (57), 91 (78); Anal. Calcd. for $C_{17}H_{24}N_2O_5$: 60.70% C, 7.19% H, 8.33% N, found 60.45% C, 7.22% H, 8.29% N.

N-(*tert*-butoxycarbonyl)-α-tBu-L-glutamine **(213c)**; Method A. N-(*tert*-butoxycarbonyl)-L-glutamine (5.032 g, 20.46 mmol) was dissolved in THF (50 ml) under positive nitrogen pressure. t-butanol (19.5 ml, 205 mmol) was added and the resulting solution cooled to 0 °C. A solution of DCC (4.59 g, 22.5 mmol) in THF (15 ml) was added followed by DMAP (0.255 g, 2.05 mmol). After stirring for 5 hrs. at 0 °C

glacial acetic acid (1 ml) was added and the mixture warmed up to R.T. over a period of 20 min. Precipitated solids were filtered off and washed with ethyl acetate. After removal of the solvent under reduced pressure, the residual oil was dissolved in ethyl acetate and washed with 10% citric acid, water, saturated $NaHCO_3$ (aq), water, dried ($MgSO_4$), filtered, and evaporated under reduced pressure to give a white solid 5.2 g (85%) which was recrystallized from ethyl acetate/petroleum ether. Method B. α-tBu-L-glutamine hydrochloride (0.877 g, 3.67 mmol) was suspended in THF (12 ml) and cooled to -0 °C under positive nitrogen pressure. Triethylamine (1.0 ml, 7.2 mmol) was added followed by a solution of di-*tert*-butyldicarbonate (0.84 g, 3.85 mmol) in THF (6 ml). After stirring the solution at R.T. for 20 hrs., TLC (70:30 ethyl acetate:petroleum ether; ninhydrin stain) showed the clean formation of product (R_f = 0.21) at the expense of starting material. The solvents were evaporated under reduced pressure to give a white solid which was dissolved in ethyl acetate. Dilute HCl was added and the aqueous solution extracted with ethyl acetate (3 X 75 ml). The organic layers were combined, dried ($MgSO_4$), and evaporated under reduced pressure to give a white solid. Recrystallization from ethyl acetate/petroleum ether afforded pure product (1.08 g, 98%): m.p. 115-116 °C; $[\alpha]_D$ -17.3° (c 1.14, ethyl acetate); ^1H NMR ($CDCl_3$, 500 MHz) δ 1.45 (9 H, s), 1.47 (9 H, s), 1.83-1.91 (1 H, m), 2.13-2.20 (1 H, m), 2.26-2.38 (2 H, m), 4.19 (1 H, dt, J = 8.6, 3.4 Hz), 5.32 (1 H, d, J = 8.5 Hz), 5.70 (1 H,

s), 6.37 (1 H, s) ; ^{13}C NMR ($CDCl_3$, 75.4 MHz) δ 27.73 (q), 28.06 (q), 29.08 (t), 31.77 (t), 53.23 (d), 79.73 (s), 82.08 (s), 155.73 (s), 171.17 (s), 174.64 (s); IR ($CHCl_3$) ν 3529, 3478, 3413, 3338, 3192, 3009, 2983, 2935, 1702, 1593, 1504, 1455, 1394, 1369, 1311, 1236, 1155, 1058, 1028, 844 cm^{-1}; HRMS (FAB: H^+) exact mass calc. for $C_{14}H_{27}N_2O_5$ requires 303.1920, found 303.1950; *m/e* (relative intensity) 303 (50), 247 (48), 191 (100), 147 (61), 130 (28), 57 (21); Anal. Calcd. for $C_{14}H_{26}N_2O_5$: 55.61% C, 8.67% H, 9.26% N; found 55.42% C, 8.71% H, 9.16% N.

N-(carbobenzyloxy)-L-aspartic anhydride (**219**); Prepared following the procedure of Bergmann and Zervas (227). Recrystallization from diethyl ether: dichloromethane: petroleum ether afforded product as white crystals (95 %): m.p.=106-107 °C [lit. (227) m.p.=84 °C]; $[\alpha]_D$ -32.7° (c 1.81, acetone); ^1H NMR (acetone-d_6, 500 MHz) δ 3.11 (1 H, dd, *J* = 18.3, 6.6 Hz), 3.40 (1 H, dd, *J* = 18.6, 10.3 Hz), 4.93 (1 H, dt, *J* = 10.0, 7.0 Hz), 5.12 (2 H, s), 7.32-7.39 (5 H, m), 7.43 (1 H, d, *J* = 7.0 Hz); ^{13}CNMR (acetone-d_6, 75.4 MHz) δ 34.63 (t), 50.93 (d), 66.74 (t), 127.92 (d), 128.04 (d), 128.30 (d), 128.39 (d), 136.51 (s), 156.18 (s), 169.04 (s), 171.44 (s) ; IR (mineral oil) ν 3320, 2923, 2854, 1860, 1809, 1686, 1533, 1456, 1298, 1218, 1082, 996, 906, 746 cm^{-1}; HRMS (FAB: H^+) exact mass calc. for $C_{12}H_{12}NO_5$ requires 250.0715, found 250.0703; m/e (relative intensity) 250.0703 (7), 224 (4), 154 (37), 107 (14), 91 (100); Anal. Calcd. for $C_{12}H_{11}NO_5$

: 57.83% C, 4.45% H, 5.62% N; found 57.79% C, 4.64% H, 5.59% N.

N-(carbobenzyloxy)-α-Bn-L-aspartic acid (**214**); N-(carbobenzyloxy)-L-aspartic anhydride (22.093 g, 88.73 mmol) was dissolved in BnOH (13.5 ml, 130 mmol) and heated at 80 °C for 4 hrs. under a continuous positive nitrogen pressure. After cooling to R.T. the oil was dissolved in diethyl ether (100ml) and fractionally extracted with 2 % sodium bicarbonate (15 X 25 ml) and 5 % sodium bicarbonate (3 X 30 ml) The fractions were acidified with concentrated HCl and placed at 4 °C overnight. Fractions containing solids were combined, filtered, and dissolved in ethyl acetate. The organic layer was dried ($MgSO_4$) and the solvent removed under reduced pressure to give a colorless oil which solidified on standing at R.T. The solid was recrystallized from ethyl acetate:petroleum ether: m.p.= 81-82 °C [lit. (164) m.p.=84-85 °C]; $[\alpha]_D$ -41.0° (c 4.56, ethyl acetate); ^1H NMR ($CDCl_3$, 500 MHz) δ 2.91 (1 H, dd, J = 17.6, 4.4 Hz), 3.10 (1 H, dd, J = 17.3, 4.6 Hz), 4.69 (1 H, dt, J = 8.8, 4.6 Hz), 5.12 (2 H, dd, J = 2.0 Hz), 5.18 (2 H, d, J = 2.4 Hz), 5.82 (1 H, d, J = 8.8 Hz), 7.31-7.35 (10 H, m), 9.78 (1 H, bs); $^{13}CNMR$ ($CDCl_3$, 75.4 MHz) δ 36.39 (t), 50.37 (d), 67.32 (d), 67.66 (d), 127.08 (d), 127.66 (d), 128.10 (d), 128.20 (d), 128.22 (d), 128.44 (d), 128.54 (d), 128.58 (d), 135.13 (s), 136.01 (s), 156.20 (s), 170.51 (s), 175.49 (s); IR ($CHCl_3$) ν 3433, 3033, 2959, 1720, 1509, 1456, 1405, 1338, 1293, 1228, 1198, 1065,

1039, 986, 909, 824 cm^{-1}; HRMS (FAB: H^+) exact mass calc. for $C_{19}H_{20}NO_6$ requires 358.1290, found 358.1236; m/e (relative intensity) 358 (31), 314 (28), 224 (11), 181 (22), 91 (100); Anal. Calcd. for $C_{19}H_{19}NO_6$: 63.86% C, 5.36% H, 3.92% N; found 63.31% C, 5.30% H, 3.87% N.

N-(carbobenzyloxy)-α-Bn-aspartyl chloride (**215a**); N-(carbobenzyloxy)-α-Bn-aspartic acid (0.4740 g, 1.33 mmol) was dissolved in dry diethyl ether (4.5 ml) under a continuous positive nitrogen pressure and the resulting solution cooled to 0 °C in an ice bath. Phosphorous pentachloride (0.2771 g, 1.33 mmol) was added in two portions and the ice bath removed. The resulting mixture was stirred at R.T. for 1.5 hrs. under a blanket of nitrogen. Petroleum ether (2 ml) was added and the precipitated solution placed in an ice bath for 30 min. The white crystalline product was filtered off and washed several times with petroleum ether:diethyl ether (75:25) solution (0.4431 g, 89%): m.p. = 74-76 °C [lit. (164) m.p.=81-82 °C]; $[\alpha]_D$ -16.24° (c 1.52, acetone); ^1H NMR ($CDCl_3$, 500 MHz) δ 3.54 (2 H, ddd, J = 18.3, 14.2, 4.6 Hz), 4.64 (1 H, dt, J = 4.9, 7.3 Hz), 5.12 (2 H, s), 5.20 (2 H, s), 5.75 (1 H, d, J = 7.3 Hz), 7.32-7.39 (10 H, m); ^{13}C NMR ($CDCl_3$, 75.4 MHz) δ 48.82 (t), 50.86 (d), 67.43 (t), 68.12 (t), 128.09 (d), 128.30 (d), 128.37 (d), 128.55 (d), 128.68 (d), 128.69 (d), 134.69 (s), 135.85 (s), 155.72 (s), 169.16 (s), 171.73 (s); IR ($CHCl_3$) 3430, 3034, 2954, 1786, 1723, 1508, 1456, 1400, 1336, 1280, 1198, 1068, 1027, 984, 907 cm^{-1}; HRMS

(FAB: H^+) exact mass calc. for $C_{19}H_{19}NO_5Cl$ requires 376.0952, found 376.0972; m/e (relative intensity) 376 (44), 358 (17), 342 (13), 152 (12), 91 (100); Anal. Calcd. for $C_{19}H_{18}NO_5Cl$: 60.72% C, 4.83% H, 3.73% N; found 60.39% C, 4.90% H, 3.61% N.

N-(carbobenzyloxy)-α-Bn-β-L-asparic anhydride (**215b**); N-(carbobenzyloxy)-α-Bn-L-aspartic anhydride (2.6954 g, 7.55 mmol) was dissolved in dichloromethane (4.0 ml) and the resulting mixture cooled to 0 °C in an ice bath under positive nitrogen pressure. A solution of N,N-dicyclohexylcarbodiimide (0.7633 g, 3.70 mmol) in dichloromethane (4 ml) was added over a period of 2 min. The resulting mixture was stirred at 0 °C for 1 hr. at which point TLC (60:40 ethyl acetate:petroleum ether; ninhydrin stain) showed the clean formation of product (R_f = 0.68) at the expense of starting material (R_f = 0.53). The mixture was filtered and diluted with dichloromethane (20 ml). The resulting solution was quickly washed with ice cold 5% $NaHCO_3$ (25 ml) and 1.5 M HCl (100 ml). The organic layer was dried ($MgSO_4$) and the solvent evaporated at R.T. under reduced pressure to afford a white solid (2.3312 g, 89%): m.p. = 108-110 °C; $[\alpha]_D$ +12.93 (c 3.81, CH_2Cl_2); ^1H NMR ($CDCl_3$, 500 MHz) δ 2.98 (2 H, dd, J = 17.8, 4.7 Hz), 3.08 (2 H, dd, J = 17.6, 4.9 Hz), 4.70 (2 H, dt, J = 7.8, 4.4 Hz), 5.11 (4 H, s), 5.18 (4 H, s), 5.89 (2 H, d, J = 7.3 Hz), 7.31-7.35 (20 H, m); ^{13}C NMR ($CDCl_3$, 75.4 MHz) δ 37.80 (t), 50.16 (d), 67.28 (t), 67.91 (t), 128.11 (d), 128.18 (d), 128.25 (d),

128.32 (d), 128.39 (d), 128.54 (d), 128.60 (d), 128.65 (d), 134.89 (s), 135.97 (s), 155.89 (s), 165.87 (s), 169.80 (s); IR ($CHCl_3$) ν 3432, 3034, 3013, 2940, 1825, 1724, 1509, 1456, 1404, 1384, 1337, 1225, 1198, 1055, 911 cm^{-1}; HRMS (FAB: H^+) exact mass calc. for $C_{38}H_{37}N_2O_{11}$ requires 697.2397, found 697.2301; *m/e* (relative intensity) 697 (2), 448 (7), 358 (6), 225 (12), 181 (17), 91 (100); Anal. Calcd. for $C_{38}H_{36}N_2O_{11}$: 65.51% C, 5.21% H, 4.02% N, found 65.17% C, 5.31% H, 4.09% N.

(*S*)-N-(carbobenzyloxy)-[5-(benzyloxy)-5-oxo]-2-pyrrolidone (**221**); N-(carbobenzyloxy)-α-Bn-L-glutamic acid (0.5 g, 1 mmol) was dissolved in thionyl chloride (2 ml) and stirred at R.T. under a continuous positive nitrogen pressure. After bubbles were no longer seen (20 min.) the solvent was removed at R.T. with high vacuum to give a yellow oil. Acetonitrile was added and the mixture refluxed for 2.5 hrs. (mixture now brownish-red) and quenched with ice which on contact formed brownish white crystals. These were washed with water followed by ethyl acetate. Recrystallization from ethyl acetate afforded pure product (65% yield): m.p. = 107-108 °C ; $[\alpha]_D$ - 44.7° (c 1.1, $CHCl_3$); ^1H NMR ($CDCl_3$, 500 MHz) δ 2.01-2.06 (1 H, m), 2.27-2.36 (1 H, m), 2.48 (1 H, ddd, *J* = 17.5, 9.0, 3.0 Hz), 2.57-2.64 (1 H, dt, *J* = 17.5, 9.9 Hz), 4.70 (1 H, dd, *J* = 9.3, 2.4 Hz), 5.11 (2 H, s), 5.20 (2 H, s), 7.26-7.35 (10 H, m) ; ^{13}C NMR ($CDCl_3$, 75.4 MHz) δ 21.53 (t), 30.76 (t), 58.52 (d), 67.20 (t), 68.11 (t), 127.93 (d), 128.07 (d), 128.22 (d), 128.35 (d), 128.39 (d), 128.46 (d),

134.75 (s), 150.59 (s), 170.61 (s), 172.63 (s); IR ($CHCl_3$) 3029, 2962, 1797, 1750, 1499, 1456, 1384, 1362, 1304, 1259, 1224, 1188, 1146, 1040, 971 cm^{-1}; HRMS (EI) exact mass calc. for $C_{20}H_{19}NO_5$ requires 353.1263, found 353.1260; m/e (relative intensity) 353 (4), 262 (3), 174 (4), 107 (25), 91 (100); Anal. Calcd. for $C_{20}H_{19}NO_5$: 67.98% C, 5.42% H, 3.96% N; found 67.67% C, 5.43% H, 3.86% N

N_α(carbobenzyloxy)-N_γ[N-(carbobenzyloxy)-α-Bn-β-L-aspartyl]-α-tBu-L-glutamine (**216b**); To a mixture of N-(carbobenzyloxy)-α-Bn-L-aspartyl chloride (2.80 g, 7.5 mmol) and N-Cbz-α-tBu-L-glutamine (1.67 g, 5.0 mmol) was added chloroform (30 ml) followed by pyridine (0.17 ml, 2.1 mmol) and the resulting mixture stirred at R.T. overnight. At this time TLC (55:45 ethyl acetate:petroleum ether; ninhydrin) showed the formation of four major products (R_f = 0.74, diacyl; R_f = 0.67, nitrile; R_f = 0.58, monoacyl; R_f = 0.47) and almost no starting material (amide) left. The mixture was taken up in ethyl acetate and washed with aqueous potassium bisulfate, aqueous $NaHCO_3/Na_2CO_3$ (pH = 9-10) solution, and water. The organic layer was dried ($MgSO_4$) and the solvent removed under reduced pressure to give an orange oil. Chromatography on silica gel (55:45 ethyl acetate: petroleum ether; ninhydrin stain) afforded pure monoacylated product as a pale yellow oil (0.911 g, 28%): **216b**; $[\alpha]_D$ -8.6° (c 5.78, acetone); ^1H NMR ($CDCl_3$, 500 MHz) δ 1.44 (9 H, s), 1.90 (1 H, dt, J = 14.7, 7.3 Hz), 2.15 (1 H, dt, J = 13.1,

7.82 Hz), 2.50 (2 H, m), 3.17 (1 H, dd, J = 17.7, 3.1 Hz), 3.37 (1 H, d, J = 17.6 Hz), 4.27 (1 H, dt, J = 8.3, 4.9 Hz), 4.72 (1 H, dt, J = 8.8, 3.9 Hz), 5.07 (2 H, s), 5.09 (2 H, s), 5.15 (2 H, s), 5.60 (1 H, d, J = 7.8 Hz), 5.95 (1 H, d, J = 8.8 Hz), 7.26 - 7.34 (15 H, m), 9.03 (1 H, s); ^{13}CNMR ($CDCl_3$, 75.4 MHz) δ 27.38 (t), 27.92 (q), 33.14 (t), 39.70 (t), 50.20 (d), 53.68 (d), 67.04 (t), 67.39 (t), 128.03 (d), 128.09 (d), 128.31 (d), 128.47 (d), 135.30 (s), 136.20 (s), 156.13 (s), 156.21 (s), 170.78 (s), 170.91 (s), 172.82 (s); IR ($CHCl_3$) ν 3429, 3020, 2983, 1719, 1508, 1456, 1372, 1338, 1211, 1156, 1048 cm^{-1}; HRMS (FAB: H^+) exact mass calc. for $C_{36}H_{42}N_3O_{10}$ requires 676.2870, found 676.2865; *m/e* (relative intensity) 676 (11), 658 (16), 620 (22), 576 (39), 558 (30), 468 (28), 181 (66), 91 (100); Anal. Calcd. for $C_{36}H_{41}N_3O_{10}$: 63.99% C, 6.12% H, 6.22% N found 64.08% C, 6.11% H, 6.11% N: **223b**, 1.86 g, 37%, oil; ^{1}H NMR ($CDCl_3$, 500 MHz) δ 1.45 (9 H, s), 2.26 (1 H, m), 2.37-2.44 (1 H, m), 2.56-2.59 (1 H, m), 3.14-3.21 (4 H, m), 4.19 (1 H, t, J = 7.1 Hz), 4.74 (2 H, m), 4.95-5.08 (6 H, m), 5.13 (4 H, s), 5.43 (1 H, d, J = 7.3 Hz), 6.05 (2 H, d, J = 8.3 Hz), 7.27-7.31 (25 H, m); ^{13}C NMR ($CDCl_3$, 75.4 MHz) δ 27.96 (q), 34.17 (t), 40.46 (t), 51.03 (d), 52.94 (d), 67.16 (t), 67.34 (t), 67.50 (t), 82.67 (s), 128.20 (d), 128.36 (d), 128.43 (d), 128.50 (d), 128.59 (d), 128.70 (d), 135.25 (s), 136.03 (s), 136.16 (s), 156.09 (s), 156.09 (s), 170.69 (s), 170.80 (s), 174.76 (s), 175.81 (s); IR ($CHCl_3$) ν 3430, 3331, 3020, 2983, 1725, 1509, 1456, 1370, 1341, 1211, 1157, 1061 cm^{-1}; HRMS (FAB: H^+) exact mass calc.

for $C_{55}H_{59}N_4O_{15}$ requires 1015.3977, found 1015.3859; *m/e* (relative intensity) 1015 (21), 881 (5), 697 (4), 521 (6), 414 (6), 181 (11), 91 (100); Anal. Calcd. for $C_{55}H_{58}N_4O_{15}$: 65.08% C, 5.76% H, 5.52% N found 64.73% C, 5.76% H, 5.43% N: **224b**; oil; $[\alpha]_D$ -9.0° (c 0.97, acetone); ^1H NMR ($CDCl_3$, 500 MHz) δ 1.48 (9 H, s), 1.96-2.03 (1 H, m), 2.27-2.31 (1 H, m), 2.35-2.48 (2 H, m), 4.31 (1 H, dt, *J* = 7.0, 5.0 Hz), 5.12 (2 H, s), 5.46 (1 H, d, *J* = 7.0 Hz), 7.32-7.37 (5 H, m); ^{13}C NMR ($CDCl_3$, 75.4 MHz) δ 13.39 (t), 27.70 (q), 28.83 (t), 53.17 (d), 66.98 (t), 83.19 (s), 118.60 (s), 127.98 (d), 128.10 (d), 128.28 (d), 128.36 (d), 155.70 (s), 169.56 (s); IR ($CHCl_3$) ν 3423, 3027, 2959, 2933, 2873, 2251, 1724, 1505, 1456, 1396, 1372, 1348, 1249, 1155, 1050, 909, 841 cm^{-1}; HRMS (FAB: H^+) exact mass calc. for $C_{17}H_{23}N_2O_4$ requires 319.1658, found 319.1613; *m/e* (relative intensity) 319 (3), 289 (3), 263 (25), 91 (100).

N_α(carbobenzyloxy)-N_γ[N-(carbobenzyloxy)-α-Bn-β-L-aspartyl]-α-Bn-L-glutamine (**216a**); This compound was synthesized following the procedure of **216b** from N-(carbobenzyloxy)-α-Bn-L-aspartyl chloride (0.361 g, 0.96 mmol) and N-(carbobenzyloxy)-α-Bn-L-glutamine (0.297 g, 0.80 mmol). Spectroscopic data: **216a**, 0.152 g, 27%, oil; ^1H NMR ($CDCl_3$, 300 MHz) δ 1.91-2.00 (1 H, m), 2.12-2.23 (1 H, m), 2.40-2.52 (2 H, m), 2.50 (2 H, m), 3.11 (1 H, dd, *J* = 17.9, 3.5 Hz), 3.34 (1 H, dd, *J* = 19.0, 4.7 Hz), 4.38-4.47 (1 H, m), 4.70 (1 H, dt, *J* = 7.8, 3.9 Hz), 5.08 (2 H, s), 5.10 (2

H, s), 5.15 (4 H, s), 5.54 (1 H, d, J = 8.1 Hz), 5.85 (1 H, d, J = 8.7 Hz), 7.27 - 7.34 (20 H, m), 8.47 (1 H, s); ^{13}CNMR ($CDCl_3$, 75.4 MHz) δ 27.41 (t), 33.10 (t), 39.75 (t), 50.08 (d), 53.13 (d), 67.25 (t), 67.51 (t), 128.08 (d), 128.15 (d), 128.19 (d), 128.27 (d), 128.42 (d), 128.51 (d), 128.54 (d), 128.61 (d), 128.67 (d), 135.99 (s), 135.19 (s), 156.06 (s), 170.58 (s), 171.50 (s), 172.07 (s); IR ($CHCl_3$) ν 3430, 3030, 2955, 1720, 1509, 1456, 1385, 1338, 1217, 1198, 1062, 909, 698 cm^{-1}; HRMS (FAB: H^+) exact mass calc. for $C_{39}H_{40}N_3O_{10}$ requires 710.2714, found 710.2727; *m/e* (relative intensity) 710 (4), 91 (100); **223a**; oil; ^{1}H NMR ($CDCl_3$, 500 MHz) δ 2.23-2.60 (4 H, m), 3.10-3.19 (4 H, m), 4.33-4.39 (1 H, m), 4.68-4.76 (2 H, m), 5.00 (4 H, s), 5.13 (4 H, s), 5.17 (2 H, m), 5.42 (1 H, d, J = 8.7 Hz), 5.97 (2 H, d, J = 9.0 Hz), 7.26-7.36 (30 H, m); ^{13}C NMR ($CDCl_3$, 75.4 MHz) δ 27.79 (t), 33.88 (t), 40.45 (t), 50.94 (d), 52.39 (d), 67.18 (t), 67.53 (t), 82.67 (s), 128.18 (d), 128.34 (d), 128.41 (d), 128.46 (d), 128.54 (d), 128.64 (d), 134.94 (s), 135.08 (s), 135.73 (s), 135.98 (s), 155.98 (s), 170.59 (s), 171.46 (s), 174.73 (s), 175.53 (s); IR ($CHCl_3$) ν 3431, 3034, 2959, 1726, 1509, 1456, 1375, 1339, 1216, 1196, 1061, 909, 698 cm^{-1}; HRMS (FAB: H^+) exact mass calc. for $C_{58}H_{57}N_4O_{15}$ requires 1049.3820, found 1049.3896; *m/e* (relative intensity) 1049 (1), 91 (100).

N_α(*tert*-butoxycarbonyl)-N_γ[N-(carbobenzyloxy)-α-Bn-β-L-asparty1]-α-tBu-L-glutamine (**216c**); This compound was synthesized following the procedure of **216b** from N-

(carbobenzyloxy)-α-Bn-L-aspartyl chloride (0.346 g, 0.92 mmol) and N-(*tert*-butoxycarbonyl)-α-tBu-L-glutamine (0.094 g, 0.31 mmol). Spectroscopic data: **216c**, 0.064 g, 32%, oil; ^{1}H NMR ($CDCl_3$, 500 MHz) δ 1.42 (9 H, s), 1.45 (9 H, s), 1.82-1.91 (1 H, m), 2.09-2.17 (1 H, m), 2.46-2.53 (2 H, m), 3.18 (1 H, d, J = 17.8 Hz), 3.39 (1 H, d, J = 17.1 Hz), 4.15-4.20 (1 H, m), 4.72 (1 H, dt, J = 8.7, 4.0 Hz), 5.10 (2 H, s), 5.16 (2 H, s), 5.26 (1 H, d, J = 7.4 Hz), 5.93 (1 H, d, J = 8.4 Hz), 7.27-7.34 (10 H, m), 9.15 (1 H, s); ^{13}CNMR ($CDCl_3$, 75.4 MHz) δ 27.94 (q), 28.27 (q), 33.42 (t), 39.78 (t), 50.22 (d), 50.26 (d), 67.05 (t), 67.40 (t), 127.97 (d), 128.07 (d), 128.29 (d), 128.44 (d), 128.50 (d), 135.31 (s), 136.20 (s), 170.62 (s), 170.07 (s), 171.54 (s), 172.43 (s); IR ($CHCl_3$) ν 3432, 3020, 2981, 1716, 1506, 1456, 1370, 1336, 1214, 1155, 1062, 929, 754, 669 cm^{-1}; HRMS (FAB: H^+) exact mass calc. for $C_{33}H_{44}N_3O_{10}$ requires 642.3027, found 642.3009; *m/e* (relative intensity) 642 (3), 542 (4), 468 (12), 357 (9), 91 (100); Anal. Calcd. for $C_{33}H_{43}N_3O_{10}$: 61.77% C, 6.75% H, 6.55% N found 61.09% C, 5.60% H, 6.53% N: **223c**, 0.104 g, 34%, oil; ^{1}H NMR ($CDCl_3$, 500 MHz) δ 1.37 (9 H, s), 1.46 (9 H, s), 1.63-1.72 (1 H, m), 2.14-2.22 (1 H, m), 2.52 (1 H, t, J = 7.3 Hz), 2.56 (1 H, t, J = 6.3 Hz), 3.14-3.25 (4 H, m), 4.10-4.16 (1 H, m), 4.69-4.73 (2 H, m), 5.10 (2 H, s), 5.11 (2 H, s), 5.16 (2 H, s), 5.17 (2 H, s), 5.79 (2 H, d, J = 8.2 Hz), 7.28-7.33 (20 H, m); ^{13}C NMR ($CDCl_3$, 75.4 MHz) δ 27.96 (q), 28.26 (q), 34.65 (t), 40.75 (t), 50.70 (d), 67.18 (t), 67.56 (t), 82.67 (s), 128.10 (d), 127.99 (d), 128.14 (d), 128.23 (d), 128.35

(d), 128.46 (d), 128.56 (d), 135.16 (s), 136.13 (s), 170.41 (s), 174.29 (s), 175.93 (s); IR ($CHCl_3$) ν 3433, 3020, 2981, 1725, 1506, 1456, 1370, 1337, 1211, 1155, 1061, 909, 762, 669 cm^{-1}; HRMS (FAB: H^+) exact mass calc. for $C_{52}H_{60}N_4O_{15}$ requires 981.4133, found 981.4102; *m/e* (relative intensity) 981 (0.2), 91 (100); Anal. Calcd. for $C_{52}H_{59}N_4O_{15}$: 63.66% C, 6.16% H, 5.71% N found 63.94% C, 6.37% H, 5.26% N.

N_α(carbobenzyloxy)-N_γ[N-(carbobenzyloxy)-α-Bn-β-L-aspartyl]-L-glutamine **(225)**; N_α(carbobenzyloxy)-N_γ[N-(carbobenzyloxy)-α-Bn-β-L-aspartyl)-α-tBu-L-glutamine (2.433 g, 3.60 mmol) was dissolved in methylene chloride (40 ml) and cooled to -78 °C under a slow stream of nitrogen. Trifluoroacetic acid (8.5 ml, 110 mmol) was added and the resulting solution warmed up to 0 °C and stirred for 15 hrs. At this time TLC (55:45 ethyl acetate:petroleum ether; ninhydrin) showed the formation of product (R_f = 0.12 to 0.31) and very little unreacted starting material (R_f = 0.56). Additional methylene chloride (20 ml) and trifluoroacetic acid (5 ml, 65 mmol) were added at 0 °C and the solution stirred for an additional 40 hrs. At this time TLC showed only traces of starting material. The excess trifluoroacetic acid was evaporated through a high pressure blanket of nitrogen at 0 °C and then at high vacuum at R.T. to give an oil. The crude oil was crystallized from ethyl acetate/chloroform/petroleum ether to give a white solid (2.104 g, 94%): m.p. = 160-162 °C; $[\alpha]_D$ -7.9° (c 0.64,

acetone); ^{1}H NMR (acetone-d_6, 500 MHz) δ 1.96-2.03 (1 H, m), 2.22-2.29 (1 H, m), 2.75 (2 H, t, J = 7.5 Hz), 3.25 (2 H, d, J = 5.4 Hz), 4.32 (1 H, dt, J = 8.8, 4.7 Hz), 4.77 (1 H, dt, J = 9.1, 5.7 Hz), 5.08 (2 H, s), 5.09 (2 H, s), 5.17 (2 H, s), 6.61 (1 H, d, J = 8.3 Hz), 6.68 (1 H, d, J = 8.3 Hz), 7.29-7.39 (15 H, m), 9.82 (1 H, s); ^{13}C NMR (acetone-d_6, 75.4 MHz) δ 25.83 (t), 32.82 (t), 38.79 (t), 49.95 (d), 52.87 (d), 65.73 (t), 66.19 (t), 127.42 (d), 127.52 (d), 127.67 (d), 127.99 (d), 128.06 (d), 135.79 (s), 136.87 (s), 155.68 (s), 155.94 (s), 170.58 (s), 170.68 (s), 172.48 (s); IR (KBr) ν 3313, 1741, 1696, 1647, 1542, 1498, 1453, 1400, 1347, 1265, 1219, 1140, 1071, 1020, 947, 901, 846, 750, 697 cm^{-1}; HRMS (FAB: H^+) exact mass calc. for $C_{32}H_{34}N_3O_{10}$ requires 620.2244, found 620.2225; *m/e* (relative intensity) 620 (6), 576 (2), 358 (5), 289 (7), 181 (6), 136 (55), 91 (100); Anal. Calcd. for $C_{32}H_{33}N_3O_{10}$: 62.03% C, 5.37% H, 6.78% N found 61.74% C, 5.29% H, 6.60% N.

N_γ(β-L-asparty1)-L-glutamine (**12**); To a solution of N_α(carbobenzyloxy)-N_γ[N_α(carbobenzyloxy)-α-Bn-β-L-asparty1]-L-glutamine (1.280 g; 2.07 mmol) in THF/EtOH (7 ml/15 ml) was added 10% Pd in carbon (2.7 g) followed by 1,4-cyclohexadiene (6 ml; 64mmol) and the resulting mixture warmed with a heating gun. After the exothermic reaction the mixture was stirred at R.T. for 1 hr.. The solvents were removed under reduced pressure and the residue filtered through a bed of celite eluting with water. The filtrate was freeze dried

overnight to give product as a white solid (0.381g, 90%): m.p. = 136-138 °C; $[\alpha]_D$ +22.4° (c 2.62, 1 M AcOH); ^1H NMR (D_2O, 500 MHz) δ 2.16 (2 H, q, *J* = 7.2 Hz), 2.64-2.75 (2 H, m), 3.16 (1 H, dd, *J* = 11.5, 6.8 Hz), 3.22 (1 H, dd, *J* = 14.0, 4.3 Hz), 3.81 (1H, t, *J* = 6.5 Hz), 4.16 (1 H, dd, *J* = 6.5, 4.0 Hz); ^{13}C NMR (D_2O, 75.4 MHz) δ 24.33 (t), 32.26 (t), 36.56 (t), 49.94 (d), 53.37 (d), 171.68 (s), 173.89 (s); IR (KBr) ν 3135, 1752, 1686, 1637, 1508, 1400 cm^{-1}; MS (ES: H^+) exact mass calc. for $C_9H_{16}N_3O_6$ requires 262.104, found 262.142; *m/e* (relative intensity) 262 (21), 244 (100), 230 (11), 227 (10), 205 (18), 133 (58).

4-benzyloxy-4-oxo-butanoic acid (**227**); Succinic anhydride (5.2460 g, 52.4 mmol) was dissolved in benzyl alcohol (25.2 ml, 244 mmol) and heated at 100 °C under positive nitrogen pressure in a water bath for 8 hrs. TLC (30:70 ethyl acetate:petroleum ether) at this time showed the formation of product (R_f = 0.28). The resulting solution was cooled at R.T. overnight. The solid residue was taken up in diethyl ether (200 ml) and extracted several times with 5% $NaHCO_3$. After separation of the two layers, the aqueous layer was acidified with concentrated HCl to pH=1. The resulting mixture was extracted with diethyl ether, dried ($MgSO_4$), and evaporated under reduced pressure to obtain crude product which was recrystallized from ethyl acetate/petroleum ether to afford pure product as colorless sheets (10.6825 g, 98%): m.p. = 58-58.5 °C; ^1H NMR ($CDCl_3$,

500 MHz) δ 2.67-2.73 (4 H, m), 5.16 (2 H, s), 7.31-7.39 (5 H, m), 9.47 (1 H, bs); ^{13}C NMR ($CDCl_3$, 75.4 MHz) δ 28.90 (t), 28.93 (t), 66.64 (t), 128.16 (d), 128.26 (d), 128.55 (d), 136.70 (s), 171.95 (s), 178.19 (s); IR ($CHCl_3$) ν 3514, 3037, 2960, 2674, 3514-2674 (broad), 1715, 1434, 1388, 1356, 1258, 1215, 1170 cm^{-1}; HRMS (FAB: H^+) exact mass calc. for $C_{11}H_{13}O_3$ requires 209.0814, found 209.0876; *m/e* (relative intensity) 209 (39), 107 (14), 91 (100); Anal. Calcd. for $C_{11}H_{12}O_3$: 63.45% C, 5.81% H, found 63.32% C, 5.73% H.

4-chloro-4-oxo-butanoic acid (**228**); 4-benzyloxy-4-oxo-butanoic acid (0.6532 g, 3.14 mmol) was dissolved in dry diethyl ether (6.0 ml) and the resulting solution cooled in an ice-salt bath under positive nitrogen pressure. Phosphorous pentachloride (0.6547 g, 3.14 mmol) was added in two portions and the ice-salt bath removed. The resulting mixture was stirred at R.T. for 1 hr. under a blanket of N_2. The solvent was removed at R.T. under high vacuum to give a colorless oil which was used for further reactions: ^1H NMR ($CDCl_3$, 500 MHz) δ 2.72 (2 H, t, J = 6.6 Hz), 3.22 (2 H, t, J = 6.6 Hz), 5.16 (2 H, s), 7.34 - 7.40 (5 H, m); ^{13}C NMR ($CDCl_3$, 75.4 MHz) δ 29.37 (t), 41.73 (t), 66.95 (t), 128.18 (d), 128.30 (d), 128.45 (d), 128.63 (d), 135.46 (s), 170.75 (s); IR ($CHCl_3$) ν 3068, 3033, 2954, 1868, 1790, 1736, 1498, 1456, 1410, 1389, 1356, 1344, 1302, 1263, 1224, 1199, 1173, 1059, 990, 964, 909 cm^{-1}; HRMS (FAB: H^+) exact mass calc. for

$C_{11}H_{12}O_3Cl$ requires 227.0475, found 227.0622; *m/e* (relative intensity) 227 (1), 209 (2), 181 (29), 91 (100).

4-benzyloxy-4-oxo-butyric anhydride (**229**); 4-benzyloxy-4-oxo-butanoic acid (50.9468 g, 244.94 mmol) was dissolved in dichloromethane (100 ml) and the resulting mixture cooled to 0 ^{o}C in an ice bath under positive nitrogen pressure. A solution of N,N-dicyclohexylcarbodiimide (24.7629 g, 120.02 mmol) in dichloromethane (100 ml) was added over a period of 15 min. The resulting mixture was stirred at 0 ^{o}C for 2 hrs., warmed up to R.T. and stirred for an additional 2 hrs. At this time TLC (30:70 ethyl acetate:petroleum ether; ninhydrin stain) showed the clean formation of product (R_f = 0.40) at the expense of starting material (R_f = 0.23). After storing the mixture at -22 ^{o}C overnight it was filtered and diluted with dichloromethane. The resulting solution was quickly washed with ice cold 5% $NaHCO_3$ (150 ml) and 3 M HCl (100 ml). The organic layer was dried ($MgSO_4$) and the solvent evaporated at R.T. under reduced pressure to afford a white solid (45.952 g, 94%): m.p. = 68-69 ^{o}C; ^{1}H NMR ($CDCl_3$, 500 MHz) δ 2.71 (4 H, m), 2.78 (4 H, m), 5.15 (4 H, s), 7.32-7.39 (10 H, m); ^{13}C NMR ($CDCl_3$, 75.4 MHz) δ 28.57 (t), 30.20 (t), 66.75 (t), 128.26 (d), 128.32 (d), 128.58 (d), 135.63 (s), 167.81 (s), 171.38 (s); IR ($CHCl_3$) ν 3033, 2936, 1824, 1736, 1498, 1456, 1413, 1390, 1352, 1312, 1262, 1225, 1175, 1054, 962, 909 cm^{-1}; HRMS (FAB: Na^{+}) exact mass calc. for $C_{22}H_{22}O_7Na$ requires 421.1263, found 421.1268; *m/e* (relative

intensity) 421 (2), 299 (7), 225 (19), 181 (19), 91 (100); Anal. Calcd. for $C_{22}H_{22}O_7$: 66.32% C, 5.57% H, found 66.40% C, 5.62% H.

N_α(carbobenxyloxy)-N_γ(acetyl)-α-tBu-L-glutamine (**237b**); Anhydride Method: N-(carbobenzyloxy)-α-tBu-L-Gln (1.9262 g, 5.73 mmol) was dissolved in toluene (10 ml) and the resulting mixture heated to 40 °C under positive nitrogen pressure. Acetic anhydride (0.56 ml, 5.9 mmol) was then added followed by concentrated sulfuric acid (0.04 ml, 0.72 mmol). The solution was heated at 75-85 °C for 1 hr. at which point TLC (60:40 ethyl acetate:petroleum ether) showed the formation of product (R_f = 0.52). The crude mixture was taken up in ethyl acetate and extracted with 5% $NaHCO_3$ solution so as to obtain an aqueous layer of pH = 7. The organic layer was dried ($MgSO_4$) and evaporated under reduced pressure to obtain a light yellow oil (2.298 g) which was chromatographed on silica gel (55:45 ethyl acetate:petroleum ether) to obtain the desired product as a colorless oil (0.432 g; 20%). Acid Chloride Method: N-(carbobenzyloxy)-α-tBu-glutamine (0.2013 g, 0.60 mmol) was dissolved in chloroform (0.5 ml). Acetyl chloride (0.07 ml, 0.984 mmol) was added followed by pyridine (0.02 ml, 0.247 mmol). The resulting solution was heated at 60 °C for 15 min. under positive nitrogen pressure. Additional pyridine (0.06 ml, 0.742 mmol) was added and the solution heated to 70 °C for 10 min. At this time TLC (55:45 EA:PE; ninhydrin) showed the formation of one major

product (R_f = 0.42) and one minor product (R_f = 0.64) at the expense of starting material. The solution was cooled down to R.T. and diluted ethyl acetate:water (50 ml :50 ml). The aqueous layer was extracted with ethyl acetate (30 ml), dried ($MgSO_4$), and evaporated under reduced pressure to give a yellow oil. The crude oil was chromatographed on silica gel (50:50 ethyl acetate:petroleum ether; ninhydrin stain) to afford the monoacylated product (0.1489 g, 68%), and diacylated product (0.0285 g, 11%): oil; $[\alpha]_D$ +6.42° (c 1.84, $CHCl_3$); ^1H NMR ($CDCl_3$, 500 MHz) δ 1.43 (9 H, s), 1.90-1.97 (1 H, m), 2.11-2.19 (1 H, m), 2.27 (3 H, s), 2.58-2.62 (2 H, m), 4.25 (1 H, dt, *J* = 4.9, 8.3 Hz), 5.06 (2 H, s), 5.70 (1 H, d, *J* = 8.3 Hz), 7.25-7.33 (5 H, m), 9.43 (1 H, s); ^{13}C NMR ($CDCl_3$, 75.4 MHz) δ 24.87 (q), 27.45 (t), 27.89 (q), 33.18 (t), 53.82 (d), 66.96 (t), 82.41 (s), 127.97 (d), 128.06 (d), 128.42 (d), 136.25 (s), 156.12 (s), 170.88 (s), 171.87 (s), 172.95 (s); IR ($CHCl_3$) ν 3399, 3277, 3022, 1711, 1508, 1467, 1371, 1271, 1223, 1155, 1057 cm^{-1}; HRMS (FAB: H^+) exact mass calc. for $C_{19}H_{27}N_2O_6$ requires 379.1869, found 379.1788; *m/e* (relative intensity) 379 (33), 323 (52), 220 (69), 91 (100); Anal. Cald. for $C_{19}H_{27}N_2O_6$: 60.30% C, 6.93% H, 7.40% N, found 59.97% C, 7.01% H, 7.22% N: **238b**; oil; ^1H NMR ($CDCl_3$, 500 MHz) δ 1.47 (9 H, s), 1.91-2.00 (1 H, m), 2.27-2.31 (1 H, m), 2.35 (6 H, s), 2.72 (2 H, t, *J* = 7.6 Hz), 4.29 (1 H, dt, *J* = 4.5, 8.2 Hz), 5.10 (2 H, d, *J* = 6.0 Hz), 5.40 (1 H, d, *J* = 7.5 Hz), 7.32-7.37 (5 H, m); ^{13}C NMR ($CDCl_3$, 75.4 MHz) δ 13.58 (q), 22.01 (t), 27.83 (q), 28.67 (t), 53.49 (d), 67.11

(t), 128.07 (d), 128.20 (d), 128.48 (d), 156.09 (s), 166.40 (s), 169.92 (s); IR ($CHCl_3$) ν 3425, 3020, 2983, 1721, 1508, 1455, 1370, 1348, 1214, 1156, 1058 cm^{-1}; HRMS (FAB: H^+) exact mass calc. for $C_{21}H_{29}N_2O_7$ requires 421.1975, found 421.1969; *m/e* (relative intensity) 421 (10), 365 (6), 264 (5), 220 (21), 91 (100); Anal. Calcd. for $C_{21}H_{29}N_2O_7$: 59.99% C, 6.71% H, 6.66% N, found 59.60% C, 6.65% H, 6.56% N.

N_α(carbobenzyloxy)-N_γ(acetyl)-α-Bn-L-glutamine (**237a**); N-(carbobenzyloxy)-α-Bn-L-glutamine (6.507 g, 17.6 mmol) was suspended in dry chloroform (50 ml). Acetyl chloride (1.9 ml, 26.4 mmol) and dry pyridine (2.1 ml, 26.4 mmol) were added simultaneously at R.T. to form a pale yellow solution under positive nitrogen pressure. After approx. 30 min. TLC (55:45 ethyl acetate:petroleum ether; ninhydrin stain) showed the formation of products (R_f = 0.36, monoacyl) and (R_f = 0.60, diacyl) at the expense of starting material (R_f = 0.07). After stirring the solution at room temperature overnight the solvent was evaporated and the resulting oil taken up in ethyl acetate:water. The layers were separated and the aqueous layer extracted with ethyl acetate (2 X 100 ml), dried (magnesium sulfate), filtered, and evaporated under reduced pressure to give a yellow oil (8.043 g). The oil was taken up in ethyl acetate:petroleum ether (55:45) and cooled in ice for 1 hr. The product was filtered off and washed with cold ethyl acetate:petroleum ether (55:45). Recrystallization from hot ethyl acetate:petroleum ether

afforded product as a white solid 4.92 g (68%): m.p. = 104-105 °C; $[\alpha]_D$ -12.6° (c 4.22, acetone); ^{1}H NMR ($CDCl_3$, 500 MHz) δ 1.95-2.04 (1 H, m), 2.20 (1 H, m), 2.25 (3 H, s), 2.59 (2 H, dt, *J* = 12.1, 7.7 Hz), 4.46 (1 H, dt, *J* = 8.4, 5.0 Hz), 5.07 (2 H, s), 5.15 (2 H, s), 5.77 (1 H, d, *J* = 6.0 Hz), 7.26 - 7.35 (10 H, m), 9.27 (1 H, s); ^{13}C NMR ($CDCl_3$, 75.4 MHz) δ 24.84 (q), 27.00 (t), 33.05 (t), 53.44 (d), 67.09 (t), 67.31 (t), 127.98 (d), 128.13 (d), 128.22 (d), 128.34 (d), 128.47 (d), 128.59 (d), 135.21 (s), 136.19 (s), 156.15 (s), 171.75 (s), 171.89 (s), 173.04 (s); IR ($CHCl_3$) ν 3427, 3397, 3279, 3216, 3020, 1709, 1509, 1456, 1377, 1342, 1267, 1210, 1057, 1028, 909, 762 cm^{-1}; HRMS (FAB: H^+) exact mass calc. for $C_{22}H_{25}N_2O_6$ requires 413.1713, found 413.1724; *m/e* (relative intensity) 413 (26), 310 (9), 181 (13), 91 (100); Anal. Calcd. for $C_{22}H_{24}N_2O_6$: 64.07% C, 5.87% H, 6.79% N found 64.03% C, 5.85% H, 6.71% N.

N_α(*tert*-butoxycabonyl)-N_γ(acetyl)-α-tBu-L-glutamine (**237c**); This compound was prepared following the procedure of **237a** from N-(*tert*-butoxycabonyl)-α-tBu-L-glutamine (0.143 g, 0.47 mmol) and acetyl chloride (0.05 ml, 0.7 mmol). Spectroscopic data: **237a**, 0.099 g, 61%, oil; ^{1}H NMR ($CDCl_3$, 500 MHz) δ 1.44 (9 H, s), 1.47 (9 H, s), 1.90-1.97 (1 H, m), 2.14-2.21 (1 H, m), 2.35 (3 H, s), 2.59-2.68 (2 H, m), 4.27 (1 H, dt, *J* = 8.1, 4.8 Hz), 5.32 (1 H, d, *J* = 7.3 Hz), 9.51 (1 H, s); ^{13}C NMR ($CDCl_3$, 75.4 MHz) δ 24.91 (q), 27.60 (t), 27.91 (q), 28.23 (q), 33.29 (t), 53.28 (d), 79.75 (s), 82.11

(s), 155.58 (s), 171.25 (s), 172.06 (s), 173.12 (s); IR ($CHCl_3$) ν 3431, 3399, 3274, 3214, 3020, 2982, 2934, 1707, 1502, 1456, 1370, 1220, 1164, 1060, 1029, 844, 766, 669 cm^{-1}; HRMS (FAB: H^+) exact mass calc. for $C_{16}H_{29}N_2O_6$ requires 345.2026, found 345.2029; *m/e* (relative intensity) 345 (28), 289 (31), 233 (100), 130 (54); Anal. Calcd. for $C_{16}H_{28}N_2O_6$: 55.80% C, 8.19% H, 8.13% N found 55.10% C, 8.19% H, 7.63% N: **238c**, 0.028 g, 15%, oil; ^1H NMR ($CDCl_3$, 500 MHz) δ 1.44 (9 H, s), 1.48 (9 H, s), 1.86-1.94 (1 H, m), 2.23-2.30 (1 H, m), 2.39 (6 H, s), 2.71-2.75 (2 H, m), 4.21 (1 H, dt, J = 8.3, 4.4 Hz), 5.12 (1 H, d, J = 7.4 Hz); ^{13}C NMR ($CDCl_3$, 75.4 MHz) δ 26.18, 27.93, 28.24, 34.81, 82.35, 173.70, 176.38; IR ($CHCl_3$) ν 3431, 3020, 2981, 2934, 1723, 1500, 1454, 1370, 1214, 1155, 1049, 1029, 929, 845, 750, 669 cm^{-1}; HRMS (FAB: H^+) exact mass calc. for $C_{18}H_{31}N_2O_7$ requires 387.2131, found 387.2122; *m/e* (relative intensity) 387 (14), 331 (19), 275 (74), 233 (36), 215 (68), 130 (100), 102 (97), 84 (44); Anal. Calcd. for $C_{18}H_{30}N_2O_7$: 55.95% C, 7.82% H, 7.25% N found 56.35% C, 7.97% H, 7.09% N.

(*S*)-3-benzyloxycarbonyl-5-oxo-4-oxazolidinepropanoic acid (**240**); Prepared as described by Scholtz and Bartlett (167); colorless gel (quant. yield): ^1H NMR ($CDCl_3$, 500 MHz) δ 2.15-2.38 (2 H, m), 2.44-2.56 (2 H, m), 4.40 (1 H, t, J = 5.9 Hz), 5.18 (2 H, s), 5.22 (1 H, d, J = 4.5 Hz), 5.53 (1 H, s), 7.35-7.38 (5 H, m), 8.81 (1 H, bs); ^{13}C NMR ($CDCl_3$, 75.4 MHz) δ 25.49 (t), 28.91 (t), 53.68 (d), 67.99 (t), 77.66

(t), 128.12 (d), 128.43 (d), 128.48 (d), 134.99 (s), 152.93 (s), 171.58 (s), 177.56 (s); IR ($CHCl_3$) ν 3030, 2922, 1803, 1716, 1499, 1452, 1417, 1357, 1313, 1236, 1167, 1130, 1056, 917, 611, 575 cm^{-1}; HRMS (FAB: H^+) exact mass calc. for $C_{14}H_{16}NO_6$ requires 294.0978, found 294.0965; *m/e* (relative intensity) 294 (8), 250 (15), 91 (100).

(*S*)-3-benzyloxycarbonyl-5-oxo-4-oxazolidinepropionyl chloride (**241**); (*S*)-3-benzyloxycarbonyl-5-oxo-4-oxazolidinepropanoic acid (1.292 g, 4.41 mmol) was dissolved in dry diethyl ether (15 ml) and cooled to 0 °C under positive nitrogen pressure. Phosphorous pentachloride (1.0 g, 4.9 mmol) was added and the resulting mixture warmed up to R.T. over a period of 1 hr. at which point a white solid precipitated out of solution. Dry petroleum ether was added and the product filtered and washed once with petroleum ether. The product was dried under a strong blanket of nitrogen to give a white solid (1.21g, 88%): m.p. = 73-74 °C ; ^1H NMR ($CDCl_3$, 500 MHz) δ 2.24 (1 H, m), 2.35 (1 H, m), 3.07 (2 H, m), 4.36 (1 H, t, J = 6.3 Hz), 5.20 (2 H, s), 5.22 (1 H, d, J = 5.0 Hz), 5.53 (1 H, bs), 7.35-7.41 (5 H, m); ^{13}C NMR ($CDCl_3$, 75.4 MHz) δ 26.05 (t), 42.05 (t), 53.18 (d), 68.20 (t), 77.60 (t), 128.30 (d), 128.56 (d), 128.59 (d), 134.80 (s), 152.85 (s), 170.97 (s), 172.60 (s); IR ($CHCl_3$) ν 3032, 2923, 1802, 1720, 1499, 1454, 1414, 1356, 1228, 1168, 1130, 1055, 1004, 972, 938, 698, 611, 575 cm^{-1}; HRMS (EI: M^+-HCl) exact mass calc. for $C_{14}H_{13}NO_5$ requires 275.0794, found

271.0778; *m/e* (relative intensity) 275 (1), 189 (2), 140 (6), 107 (4), 91 (100); Anal. Calcd. for $C_{14}H_{14}NO_5Cl$: 53.94% C, 4.53% H, 4.49% N; found 53.85% C, 4.55% H, 4.45% N.

N_{α}-(carbobenzyloxy)-α-Bn-L-asparagine (**242**); N-(carbobenzyloxy)-L-asparagine (5.202 g, 19.56 mmol) was suspended in MeOH (70 ml) and a solution of Cs_2CO_3 in water (40 ml) added at R.T. The solution was stirred for 30 min. and the solvents removed to give a white solid. The solid was dissolved in DMF:MeOH (50 ml:50 ml) and heated to 65 °C. Benzyl bromide (2.5 ml, 21 mmol) was added and the resulting solution stirred at R.T. overnight to give a white precipitate. At this time TLC (72:25 ethyl acetate:petroleum ether, ninhydrin) showed the formation of product (R_f = 0.42). The solvents were removed under reduced pressure and the residue dissolved in ethyl acetate:water (100 ml:100 ml). The organic layer was washed with 5% sodium bicarbonate solution (2 X 100 ml), dried ($MgSO_4$), and filtered. The solvent was removed under reduced pressure to give a white solid (3.78 g, 55%): m.p. = 128-129 °C; ^1H NMR ($CDCl_3$, 500 MHz) δ 2.72 (1 H, dd, J = 16.2, 3.8 Hz), 2.92 (1 H, dd, J = 15.7, 4.7 Hz), 4.61 (1 H, dt, J = 8.5, 4.3 Hz), 5.09 (2 H, s), 5.16 (2 H, s), 5.69 (1 H, s), 5.74 (1 H, s), 6.11 (1 H, d, J = 8.5 Hz), 7.28-7.34 (10 H, m); ^{13}C NMR ($CDCl_3$, 75.4 MHz) δ 36.92 (t), 50.58 (d), 66.83 (t), 67.25 (t), 127.77 (d), 127.94 (d), 128.14 (d), 128.29 (d), 128.34(d), 135.08 (s), 135.95 (s), 156.00 (s), 170.80 (s), 171.90 (s); IR

($CHCl_3$) ν 3411, 3013, 2957 , 1718, 1689, 1592, 1508, 1456, 1404, 1338, 1274, 1227, 1196, 1063, 909, 757, 698, 669 cm^{-1}; HRMS (FAB: H^+) exact mass calc. for $C_{19}H_{21}N_2O_5$ requires 357.1450, found 357.1446; *m/e* (relative intensity) 357 (87), 313 (16), 91 (100); Anal. Calcd. for $C_{19}H_{20}N_2O_5$: 64.04% C, 5.66% H, 7.86% N; found 64.01% C, 5.65% H, 7.68% N.

N_α-(carbobenzyloxy)-N_β-[(*S*)-3-benzyloxycarbonyl-5-oxo-4-oxazolidinepropionyl]-α-Bn-L-asparagine (**243**); N-(carbobenzyloxy)-α-Bn-L-asparagine (0.513 g, 1.44 mmol) was dissolved in dry chloroform (5 ml) under positive nitrogen pressure. (*S*)-3-benzyloxycarbonyl-5-oxo-4-oxazolidinepropionyl chloride (0.538 g, 1.73 mmol) followed by pyridine (0.12 ml, 1.5 mmol) were added and the resulting solution stirred at R.T. for 30 min. At this time, TLC (55:45 ethyl acetate:petroleum ether, ninhydrin) showed the formation of products (R_f = 0.61, diacyl; R_f = 0.43, monoacyl). After 24 hrs. at R.T. the solvent was removed via nitrogen pressure and the residue dissolved in ethyl acetate (100 ml). The organic solution was washed with 5% sodium bicarbonate solution (2 X 75ml), 10% citric acid, dried ($MgSO_4$), and filtered. Removal of the solvent under reduced pressure afforded a crude oil. Chromatography on silica gel (55:45 ethyl acetate:petroleum ether, ninhydrin) gave pure product as a colorless oil: $[\alpha]_D$ +39.1° (c 2.85, acetone); ^1H NMR ($CDCl_3$, 500 MHz) δ 2.10-2.32 (4 H, m), 3.11 (1 H, d, J = 15.5 Hz), 3.24-3.34 (1 H, m), 4.35 (1 H, t, J = 6.2 Hz), 4.72

(1 H, dt, J = 4.4, 8.5 Hz), 5.08 (2 H, d, J = 3.0 Hz), 5.15-5.19 (4 H, m), 5.50 (2 H, bs), 5.96 (1 H, d, J = 8.5 Hz), 7.28-7.36 (15 H, m), 9.23 (1 H, bs); ^{13}C NMR ($CDCl_3$, 75.4 MHz) δ 25.10 (t), 28.88 (t), 39.49 (t), 50.06 (d), 50.49 (d), 53.86 (d), 65.76 (t), 67.03 (t), 67.37 (t), 68.06 (t), 127.93 (d), 128.04 (d), 128.24 (d), 128.27 (d), 128.41 (d), 128.44 (d), 128.57 (d), 128.61 (d), 135.13 (s), 136.00 (s), 153.04 (s), 156.09 (s), 170.67 (s), 171.79 (s); IR ($CHCl_3$) ν 3436, 3032, 1802, 1717, 1501, 1456, 1416, 1358, 1224, 1171 1131, 1056, 909, 698, 669 cm^{-1}; HRMS (FAB: H^+) exact mass calc. for $C_{33}H_{34}N_3O_{10}$ requires 632.2244, found 632.2260: diacyl product; $[\alpha]_D$ +49.1° (c 2.20, acetone); IR ($CHCl_3$) ν 3436, 3033, 2924, 1803, 1721, 1502, 1454, 1415, 1358, 1220, 1169, 1131, 1056, 914, 698 cm^{-1}; HRMS (FAB: H^+) exact mass calc. for $C_{47}H_{47}N_4O_{15}$ requires 907.3038, found 907.3026.

N-[(*S*)-3-benzyloxycarbonyl-5-oxo-4-oxazolidinepropionyl]-formamide (**245**); N,N-ditrimethylsilyl formamide (168) (0.376 g, 2.0 mmol) was dissolved in dry dichloromethane (5 ml) under positive nitrogen pressure and cooled to -5 °C. (*S*)-3-benzyloxycarbonyl-5-oxo-4-oxazolidinepropionyl chloride (0.62 g, 2 mmol) was added and the resulting solution stirred at this temperature for 30 min. and warmed up to R.T. over a period of 30 min. At this time, TLC (50:50 ethyl acetate:petroleum ether, ninhydrin) showed the formation of product (R_f = 0.32). The solvents were removed under reduced pressure and the residue dissolved

in petroleum ether:ethanol (50:50, 20ml) and stirred at R.T. for 30 min. The solvents were removed and the residue dissolved in ethyl acetate (30ml). The organic layer was washed with 5% sodium bicarbonate (2 X 50ml), 10% citric acid (25ml), water (50ml),dried ($MgSO_4$), and filtered. Removal of the solvent under reduced pressure afforded crude product as a colorless oil. Chromatography on silica gel (50:50 ethyl acetate:petroleum ether, ninhydrin) afforded pure product as a colorless oil (0.232g, 61%): $[\alpha]_D$ +94.2 ^{o} (c 10.2, acetone); ^{1}H NMR ($CDCl_3$, 300 MHz) δ 2.19-2.33 (2 H, m), 2.48-2.64 (2 H, m), 4.39 (1 H, t, J = 6.3 Hz), 5.17 (2 H, s), 5.22 (1 H, d, J = 4.5 Hz), 5.52 (1 H, bs), 7.32-7.37 (5 H, m); ^{13}C NMR ($CDCl_3$, 75.4 MHz) δ 25.03 (t), 31.30 (t), 53.66 (d), 68.04 (t), 77.70 (t), 128.08 (d), 128.51 (d), 128.55 (d), 135.03 (s), 153.06 (s), 162.70 (s), 171.77 (s), 172.17 (s); IR ($CHCl_3$) ν 3400, 3026, 2922, 2359, 1803, 1750, 1703, 1602, 1455, 1416, 1359, 1225, 1174, 1129, 1056, 698, 652 cm^{-1}; HRMS (FAB: H^+) exact mass calc. for $C_{15}H_{16}N_2O_6$ requires 321.1008, found 321.1005.

N_α(carbobenxyloxy)-N_γ(acetyl)-L-glutamine (**246**); N_α(carbobenzyloxy)-N_γ(acetyl)-α-tBu-L-glutamine (1.1837 g, 3.13 mmol) was dissolved in methylene chloride (3 ml) and cooled to 0 ^{o}C under a slow stream of nitrogen. Trifluoroacetic acid (4.8 ml, 62.3 mmol) was added and the resulting solution stirred at 0 ^{o}C for 24 hrs. under positive nitrogen pressure. At this time TLC (55:45 ethyl

acetate:petroleum ether; ninhydrin stain) showed the formation of product (R_f = 0.09) and some unreacted starting material (R_f = 0.42). Additional methylene chloride (3 ml) and trifluoroacetic acid (7.8 ml, 101 mmol) were added at 0 °C and the solution stirred for 2 hrs. At this time TLC showed large formation of product and traces of starting material. The excess trifluoroacetic acid was evaporated through a high pressure blanket of nitrogen at 0 °C to give an oil; ^{1}H NMR ($CDCl_3$, 500 MHz) δ 1.98-2.05 (1 H, m), 2.20-2.30 (4 H, m), 2.60-2.68 (2 H, m), 4.38-4.43 (1 H, m), 5.06 (2 H, s), 6.03 (1 H, d, J = 7.5 Hz), 7.28-7.29 (5 H, m), 9.73 (1 H, s), 10.32 (1 H, s); ^{13}CNMR ($CDCl_3$) δ 24.73 (q), 26.56 (t), 33.03 (t), 53.13 (d), 67.58 (t), 128.01 (d), 128.35 (d), 128.55 (d), 135.64 (s), 156.78 (s), 173.61 (s), 174.02 (s), 175.38 (s); IR ($CHCl_3$) ν 3400, 3284, 3030, 1710, 1510, 1455, 1377, 1272, 1228, 1204, 1058 cm^{-1}.

N_γ-acetyl-L-glutamine (**247**); N_α(carbobenzyloxy)-N_γ(acetyl)-α-Bn-L-glutamine (2.27 g, 6.14 mmol) was suspended in ethanol (30 ml). Ammonium formate (0.869 g, 13.8 mmol) was added followed by 10% Pd/C (0.47 g) and the resulting mixture warmed with the heating gun and stirred at R.T. for 30 min under positive nitrogen pressure. At this time TLC (80:20 ethyl acetate:petroleum ether; ninhydrin stain) showed the clean formation of product at the origin and no starting material at R_f = 0.77. The solvent was removed under reduced pressure and the resulting gray solid dissolved in ice cold

water and filtered several times through filter paper and celite. The aqueous solutions were freeze dried to afford product as a white solid (0.8911 g, 86%). Recrystallization by dissolving in minimum amount of water and precipitating with ethanol (adding small amount of ether if necessary) affords very pure product: m.p. = 164-165 °C; $[\alpha]_D$ +34.8° (c 1.88, 1 M AcOH); ^1H NMR (D_2O, 500 MHz) δ 2.00 (2 H, q, J = 7.00 Hz), 2.04 (3 H, s), 2.52 (2 H, q, J = 7.00 Hz), 3.63 (1 H, t, J = 6.00 Hz); ^{13}C NMR (D_2O, 75.4 MHz) δ 23.657 (q), 24.378 (t), 32.183 (t), 53.487 (d), 173.537 (s), 173.724 (s), 173.958 (s); IR (KBr) ν 3350, 3104, 1737, 1648, 1596, 1480, 1385, 1346, 1307, 1207, 1154, 1027, 560, 535 cm^{-1}; HRMS (FAB: H^+) exact mass calc. for $C_7H_{13}N_2O_4$ requires 189.0875, found 189.0870; *m/e* (relative intensity) 189 (24), 148 (25), 134 (33), 102 (64); Anal. Calcd. for $C_7H_{12}N_2O_4$: 44.68% C, 6.43% H, 14.89% N, found 44.35% C, 6.55% H, 14.71% N.

N_α(carbobenzyloxy)-N_γ(4-benzyloxy-4-oxo-butanoic acid)-α-Bn-L-glutamine (**237d**); 4-benzyloxy-4-oxo-butanoic acid (3.409 g, 16.4 mmol) was dissolved in dry diethyl ether (40 ml) and cooled to 0 °C under a slow stream of nitrogen. Phosphorous pentachloride (3.752 g, 18.0 mmol) was added the solution allowed to warmed up to R.T. over a period of 2 hrs. The solvent was removed at R.T. via positive nitrogen pressure to give a white pasty solid which was used without further purification. N-(carbobenzyloxy)-α-Bn-L-glutamine (4.0 g, 11 mmol) was added to the crude acid chloride

followed by dry chloroform (40 ml). Dry pyridine (1.35 ml, 17 mmol) was added to the solution at R.T. at which point the white suspension became a homogeneous purple brown solution. After approx. 2 hrs. at R.T., TLC (55:45 ethyl acetate:petroleum ether; ninhydrin stain) showed the formation of products (R_f = 0.64, diacyl; 0.53, nitrile; 0.36, monoacyl) and some unreacted starting material (R_f = 0.07). After stirring at room temperature overnight the solvent was removed under reduced pressure and the residual oil dissolved in ethyl acetate. The mixture was washed with aqueous potassium bisulfate, aqueous $NaHCO_3/Na_2CO_3$ (pH = 9-10) solution, and water. The organic layer was dried ($MgSO_4$) and the solvent removed under reduced pressure to give an orange-brown oil (7.158 g). Chromatography on silica gel (50:50 ethyl acetate:petroleum ether; ninhydrin stain) afforded pure monoacylated product as a pale yellow oil (3.455 g, 78%): **237d**; $[\alpha]_D$ -10.8° (c 6.70, acetone); ^1H NMR ($CDCl_3$, 500 MHz) δ 1.93-2.00 (1 H, m), 2.15-2.21 (1 H, m), 2.55-2.62 (2 H, m), 2.62 (2 H, t, J = 6.5 Hz), 2.84 (2 H, t, J = 6.0 Hz), 4.45 (1 H, dt, J = 8.0, 5.0 Hz), 5.07 (2 H, s), 5.09 (2 H, s), 5.14 (2 H, s), 5.77 (1 H, d, J = 8.5 Hz), 7.26-7.33 (15 H, m), 9.35 (1H, s); ^{13}C NMR ($CDCl_3$, 75.4 MHz) δ 26.97 (t), 28.68 (t), 33.33 (t), 33.93 (t), 52.93 (d), 66.49 (t), 66.84 (t), 67.13 (t), 127.90 (d), 127.94 (d), 127.98 (d), 128.05 (d), 128.10 (d), 128.26 (d), 128.30 (d), 128.36 (d), 128.43 (d), 128.54 (d), 135.05 (s), 135.50 (s), 136.02 (s), 155.93 (s), 171.49 (s), 171.94 (s), 175.58 (s), 175.85 (s); IR ($CHCl_3$) ν

3428, 3392, 3032, 3013, 2959, 1796, 1732, 1500, 1456, 1386, 1351, 1303, 1226, 1167, 1058, 1003 cm^{-1}; HRMS (FAB: H^+) exact mass calc. for $C_{31}H_{33}N_2O_8$ requires 561.2237, found 561.2228; *m/e* (relative intensity) 561 (5), 310 (6), 208 (5), 181 (10), 91 (100); Anal. Calcd. for $C_{31}H_{32}N_2O_8$: 66.42% C, 5.75% H, 5.00% N, found 66.16% C, 5.73% H, 4.59% N: **238d**; oil; $[\alpha]_D$ -8.0° (c 1.228, $CHCl_3$); ^1H NMR ($CDCl_3$, 500 MHz) δ 1.99-2.06 (1 H, m), 2.24 (1 H, m), 2.67 (2 H, t, *J* = 6.3 Hz), 2.71 (4 H, t, *J* = 7.3 Hz), 2.90 (4 H, t, *J* = 6.3 Hz), 4.48 (1 H, dt, *J* = 8.5, 4.5 Hz), 5.06 (2 H, s), 5.08 (2 H, s), 5.11 (2 H, s), 5.15 (2 H, s), 5.67 (1 H, d, *J* = 8.5 Hz), 7.24-7.34 (20 H, m); ^{13}C NMR ($CDCl_3$, 75.4 MHz) δ 26.59 (t), 28.12 (t), 31.87 (t), 32.95 (t), 53.23 (d), 66.35 (t), 66.85 (t), 67.13 (t), 127.84 (d), 127.97 (d), 128.06 (d), 128.26 (d), 128.32 (d), 128.36 (d), 128.43 (d), 135.05 (s), 135.61 (s), 136.04 (s), 156.09 (s), 171.77 (s), 172.182 (s), 172.856 (s), 173.284 (s); IR ($CHCl_3$) ν 3428, 3033, 2960, 1729, 1509, 1456, 1410, 1388, 1351, 1263, 1228, 1159, 1059, 1002 cm^{-1}; HRMS (FAB: H^+) exact mass calc. for $C_{42}H_{43}N_2O_{11}$ requires 751.2867, found 751.2854; *m/e* (relative intensity) 181 (16), 91 (100); Anal. Calcd. for $C_{42}H_{42}N_2O_{11}$: 67.19% C, 5.64% H, 3.73% N, found 66.76% C, 5.99% H, 3.83% N: **239d**; oil; $[\alpha]_D$ -13.6° (c 3.20, acetone); ^1H NMR ($CDCl_3$, 500 MHz) δ 1.88-1.96 (1 H, m), 2.12-2.19 (1 H, m), 2.20-2.28 (2 H, m), 4.40 (1 H, dt, *J* = 8.0, 4.50 Hz), 5.06 (2 H, s), 5.12 (2 H, d, *J* = 5.5 Hz), 5.87 (2 H, d, *J* = 8.00 Hz), 7.25-7.32 (10 H, m); ^{13}C NMR ($CDCl_3$, 75.4 MHz) δ 13.31 (t), 28.26 (t), 52.75 (d), 67.11 (t), 67.63 (t),

118.50 (s), 127.96 (d), 128.14 (d), 128.28 (d), 128.38 (d), 128.54 (d), 128.57 (d), 134.57 (s), 135.71 (s), 155.77 (s), 170.47 (s); IR ($CHCl_3$) ν 3423, 3029, 2960, 2251, 1723, 1506, 1455, 1387, 1346, 1317, 1228, 1193, 1055, 1029, 955, 910, 825 cm^{-1}; HRMS (FAB: H^+) exact mass calc. for $C_{20}H_{21}N_2O_4$ requires 353.1501, found 353.1507; *m/e* (relative intensity) 181 (9), 91 (100); Anal. Calcd. for $C_{20}H_{20}N_2O_4$: 68.15% C, 5.72% H, 7.95% N, found 67.56% C, 5.62% H, 7.64% N.

N_α(carbobenzyloxy)-N_γ(4-benzyloxy-4-oxo-butanoyl)-α-tBu-L-glutamine (**237e**); 4-benzyloxy-4-oxo-butanoic acid (0.467 g, 2.25 mmol) was dissolved in dry diethyl ether (10 ml) and the resulting solution cooled in an ice-salt bath. Phosphorous pentachloride (0.571 g, 2.74 mmol) was added in two portions and the resulting mixture stirred at 0° C for 45 min. The mixture was filtered and washed with dry diethyl ether. The decanted solution was evaporated at < R.T. under high vacuum to give a white powder. N-(carbobenzyloxy)-α-tBu-L-glutamine (0.503 g, 1.50 mmol) was added to the crude acid chloride followed by chloroform (1.5 ml) and the resuling mixture stirred at R.T. Pyridine (0.18 ml) was slowly added at which point the mixture became hot and changed from a white clowdy mixture to a reddish brown homogeneous solution. After stirring at R.T. for 5 min., TLC (55:45 ethyl acetate:petroleum ether; ninhydrin) showed the formation of two major products (R_f = 0.71 and R_f = 0.56) and almost no starting material left remaining. The solution was

heated at 45° C for 15 min., cooled down to R.T., and taken up in ethyl acetate (50 ml) to form a prepcipitate. Water was added (50 ml) to dissolve the precipitate and solution extracted with ethyl acetate (2 X 50 ml), dried ($MgSO_4$), and rotovaped to give a reddish orange oil (0.9952 g). The crude oil was chromatographed on silica gel (55:45 ethyl acetate:petroleum ether; ninhydrin stain) to afford the monoacylated product (0.232 g, 30%), and diacylated product (0.401 g, 37%): **237e**: oil; $[\alpha]_D$ -19.0° (c 9.27, acetone); ^1H NMR ($CDCl_3$, 500 MHz) δ 1.46 (9 H, s), 1.90-1.97 (1 H, m), 2.17-2.22 (1 H, m), 2.56-2.65 (2 H, m), 2.69 (2 H, t, *J* = 6.8 Hz), 2.92 (2 H, t, *J* = 6.0 Hz), 4.28 (1 H, dt, *J* = 8.3, 4.4 Hz), 5.09 (2 H, s), 5.13 (2 H, s), 5.52 (1 H, d, *J* = 7.5 Hz), 7.29-7.37 (10 H, m), 8.71 (1 H, s); ^{13}C NMR ($CDCl_3$, 75.4 MHz) δ 27.45 (t), 27.93 (q), 28.37 (t), 32.16 (t), 33.27 (t), 53.76 (d), 66.53 (t), 66.97 (t), 82.47 (s), 128.02 (d), 128.11 (d), 128.20 (d), 128.39 (d), 128.46 (d), 128.51 (d), 135.79 (s), 136.26 (s), 156.18 (s), 170.94 (s), 172.23 (s), 172.73 (s), 173.07 (s), 173.13 (s); IR ($CHCl_3$) ν 3425, 3394, 3281, 3214, 2983, 2937, 1716, 1508, 1456, 1371, 1351, 1221, 1158, 1057 cm^{-1}; HRMS (FAB: H^+) exact mass calc. for $C_{28}H_{35}N_2O_8$ requires 527.2393, found 527.2399; *m/e* (relative intensity) 527 (7), 471 (5), 220 (10), 208 (13), 169 (9), 91 (100); Anal. Calcd. for $C_{28}H_{35}N_2O_8$: 63.85% C, 6.51% H, 5.32% N, found 63.98% C, 6.60% H, 5.10% N: **238e**: oil; $[\alpha]_D$ -6.3° (c 3.86, acetone); ^1H NMR ($CDCl_3$, 500 MHz) δ 1.48 (9 H, s), 1.95-2.02 (1 H, m), 2.22-2.29 (1 H, m), 2.70-2.76 (6 H, m),

2.95 (4 H, t, J = 6.4 Hz), 4.33 (1 H, dt, J = 8.3, 4.9 Hz), 5.10 (2 H, s), 5.12 (4 H, s), 5.54 (1 H, d, J = 8.3 Hz), 7.29-7.35 (15 H, m); ^{13}C NMR ($CDCl_3$, 75.4 MHz) δ 27.52 (t), 27.96 (q), 28.90 (t), 33.54 (t), 34.29 (t), 53.56 (d), 66.67 (t), 66.93 (t), 82.40 (s), 128.09 (d), 128.25 (d), 128.29 (d), 128.41 (d), 128.48 (d), 128.56 (d), 135.72 (s), 136.35 (s), 156.11 (s), 170.88 (s), 172.08 (s), 176.01 (s); IR ($CHCl_3$) ν 3427, 3020, 2982, 1728, 1509, 1456, 1371, 1351, 1210, 1156, 1057 cm^{-1}; HRMS (FAB: H^+) exact mass calc. for $C_{39}H_{45}N_2O_{11}$ requires 717.3023, found 717.3067; *m/e* (relative intensity) 717 (2), 501 (2), 486 (4), 398 (6); Anal. Calcd. for $C_{39}H_{45}N_2O_{11}$: 65.35% C, 6.19% H, 3.91% N, found 64.96% C, 6.15% H, 3.78% N.

N_α(*tert*-butoxycarbonyl)-N_γ(4-benzyloxy-4-oxo-butanoyl)-α-tBu-L-glutamine (**237f**); This compound was prepared following the method of **237e** from 4-benzyloxy-4-oxo-butanoic acid (1.024 g, 4.92 mmol) and N-(*tert*-butoxycarbonyl)-α-tBu-L-glutamine (1.145 g, 3.79 mmol). Spectroscopic data: **237f**, 0.77 g, 41%, oil; $[\alpha]_D$ -13.1° (c 1.56, acetone); ^1H NMR ($CDCl_3$, 500 MHz) δ 1.43 (9 H, s), 1.46 (9 H, s), 1.88-1.96 (1 H, m), 2.12-2.19 (1 H, m), 2.60-2.73 (4 H, m), 2.90-2.98 (2 H, m), 4.20 (1 H, dt, J = 7.0, 4.5 Hz), 5.12 (2 H, s), 5.30 (1 H, d, J = 8.0 Hz), 7.31-7.36 (5 H, m), 9.34 (1 H, s); ^{13}C NMR ($CDCl_3$, 125.7 MHz) δ 27.83 (t), 27.94 (q), 28.26 (q), 28.35 (t), 32.22 (t), 33.50 (t), 53.17 (d), 66.56 (t), 79.98 (s), 82.40 (s), 128.12 (d), 128.16 (d), 128.22 (d), 128.52

(d), 135.71 (s), 155.72 (s), 170.34 (s), 171.17 (s), 172.22 (s), 172.46 (s), 173.55 (s); IR ($CHCl_3$) ν 3428, 3029, 2983, 2935, 1788, 1729, 1710, 1502, 1453, 1370, 1310, 1230, 1156, 1060, 909, 843 cm^{-1}; HRMS (FAB: H^+) exact mass calc. for $C_{25}H_{35}N_2O_8$ requires 493.2550, found 493.2620; *m/e* (relative intensity) 493 (14), 437 (16), 381 (20), 319 (18), 208 (35), 91 (100): **238f**: oil; $[\alpha]_D$ -10.7° (c 4.15, acetone); ^1H NMR ($CDCl_3$, 500 MHz) δ 1.42 (9 H, s), 1.47 (9 H, s), 1.87-1.95 (1 H, m), 2.16-2.24 (1 H, m), 2.70-2.75 (6 H, m), 2.95 (4 H, t, *J* = 6.1 Hz), 4.23 (1 H, dt, *J* = 8.0, 4.5 Hz), 5.13 (4 H, s), 5.19 (1 H, d, *J* = 8.0 Hz), 7.30-7.35 (10 H, m); ^{13}C NMR ($CDCl_3$, 125.7 MHz) δ 27.46 (t), 27.81 (q), 28.15 (q), 28.76 (t), 33.36 (t), 34.28 (t), 53.94 (d), 66.51 (t), 79.56 (s), 81.99 (s), 128.10 (d), 128.14 (d), 128.41 (d), 135.56 (s), 155.39 (s), 171.11 (s), 171.86 (s), 175.76 (s), 176.06 (s); IR ($CHCl_3$) ν 3434, 3032, 2982, 2935, 1728, 1500, 1454, 1370, 1352, 1230, 1156, 1060, 1029, 995, 844 cm^{-1}; HRMS (FAB: H^+) exact mass calc. for $C_{36}H_{47}N_2O_{11}$ requires 683.3180, found 683.3259; *m/e* (relative intensity) 683 (2), 569 (2), 415 (2), 398 (7), 285 (17), 229 (77), 173 (100), 91 (40).

N_α(carbobenzyloxy)-N_γ(4-benzyloxy-4-oxo-butanoyl)-L-glutamine (**248**); N_α(carbobenzyloxy)-N_γ(4-benzyloxy-4-oxo-butanoyl)-α-tBu-L-glutamine (2.9635 g, 5.63 mmol) was dissolved in methylene chloride (11 ml) and cooled to -78 °C under a slow stream of nitrogen. Trifluoroacetic acid (22 ml, 286 mmol) was added and the resulting solution stirred at

0 °C for 15 hrs. At this time TLC (55:45 ethyl acetate:petroleum ether; ninhydrin stain) showed the formation of product (R_f = 0.12 to 0.17) and very little unreacted starting material (R_f = 0.58). Additional methylene chloride (3 ml) and trifluoroacetic acid (8 ml, 104 mmol) were added at 0 °C and the solution stirred for 6 hrs. After letting the solution warm up to R.T. over a period of 15 min., TLC showed almost complete disappearance of starting material. The excess trifluoroacetic acid was evaporated through a high pressure blanket of nitrogen at 0 °C to give an oil. The crude product was crystallized from a mixture of chloroform:petroleum ether to give a white solid (0.778 g, 29%). The mother liquor was chromatographed on silica gel (100% ethyl acetate eluant; ninhydrin stain) to give additional pure product (1.25 g, 47%). The product was further recrystallized from chloroform:petroleum ether: m.p. = 130-131 °C; $[\alpha]_D$ -4.5° (c 0.97, acetone); ^{1}H NMR (acetone-d_6, 500 MHz) δ 1.96-2.06 (1 H, m), 2.23-2.29 (1 H, m), 2.66 (2 H, t, J = 6.1 Hz), 2.77 (2 H, t, J = 6.5 Hz), 2.94 (2 H, t, J = 6.0 Hz), 4.32 (1 H, dt, J = 8.5, 5.0 Hz), 5.08 (2 H, s), 5.11 (2 H, s), 6.62 (1 H, d, J = 7.5 Hz), 7.27-7.39 (10 H, m), 9.73 (1 H, s); ^{13}C NMR (acetone-d_6, 75.4 MHz) d 25.84 (t), 31.528 (t), 32.824 (t), 52.906 (d), 65.351 (t), 65.605 (t), 127.416 (d), 127.569 (d), 127.990 (d), 128.050 (d), 136.242 (s), 136.876 (s), 155.944 (s), 171.654 (s), 172.081 (s), 172.161 (s), 172.388 (s), 172.475 (s); IR (KBr) ν 3299, 2956, 1735, 1670, 1555, 1497, 1421, 1380, 1336, 1290, 1242,

1201, 1064, 908, 797, 776, 736, 695 cm^{-1}; HRMS (FAB: H^+) exact mass calc. for $C_{24}H_{27}N_2O_8$ requires 471.1767, found 471.1769; *m/e* (relative intensity) 471 (12), 220 (5), 208 (11), 91 (100); Anal. Calcd. for $C_{24}H_{26}N_2O_8$: 61.27% C, 5.57% H, 5.95% N found 61.31% C, 5.55% H, 5.84% N.

N_γ(4-hydroxy-4-oxo-butanoyl)-L-glutamine (**249**); To a solution of N_α(carbobenzyloxy)-N_γ(4-benzyloxy-4-oxo-butanoyl)-α-Bn-L-glutamine (0.439 g ; 0.78 mmol) in THF/EtOH (3 ml/3 ml) was added 10% Pd in carbon (1.01 g) followed by 1,4-cyclohexadiene (2.2 ml; 23 mmol) and the resulting mixture warmed with a heating gun. After the exothermic reaction the mixture was stirred at R.T. for 1hr. The solvents were removed under reduced pressure and the residue filtered through a bed of celite eluting with water. The filtrate was freeze dried overnight to give product as a white solid (0.12 g, 63%): m.p. = 160-162 ^oC; $[\alpha]_D$ +92.4^o (c 0.45, AcOH/ NaAc, pH = 4.4); ^1H NMR (D_2O, 500 MHz) δ 2.11-2.19 (2 H, m), 2.58 (2 H, t, *J* = 6.5 Hz), 2.68 (2 H, q, *J* = 7.0 Hz), 2.74 (2 H, t, *J* = 6.8 Hz), 3.78 (1 H, t, *J* = 6.2 Hz); ^{13}C NMR (D_2O, 75.4 MHz) δ 24.56 (t), 31.01 (t), 32.38 (t), 32.99 (t), 53.65 (d), 173.64 (s), 174.17 (s), 175.07 (s), 180.58 (s); IR (KBr) ν 3333, 2964, 1751, 1654, 1560, 1508, 1410, 1320, 1232, 1140, 704, 670, 538 cm^{-1}; HRMS (CI: H^+) exact mass calc. for $C_9H_{15}N_2O_6$ requires 247.093, found 247.093; *m/e* (relative intensity) 247 (15), 129 (94), 100

(100); Anal. Calcd. for $C_9H_{15}N_2O_6$: 43.89% C, 5.73% H, 11.38% N, found 42.77% C, 5.68% H, 10.97% N.

N_α(carbobenzyloxy)-N_γ[N-(carbobenzyloxy)-β-alanyl]-α-tBu-L-glutamine (**237h**); N-(carbobenzyloxy)-β-alanine (1.542 g, 6.91 mmol) was dissolved in a mixture of diethyl ether/THF (20 ml/7 ml). After cooling the solution to -20 °C, phosphorous pentachloride (1.58 g, 7.6 mmol) was added and the resulting solution warmed up to R.T. over a period of 1.5 hrs. The solvents were removed under high vacuum to give a colorless oil. N-(carbobenzyloxy)-α-tBu-L-glutamine (1.856 g, 5.52 mmol) was added followed by dichloromethane (20ml) at -78 °C. Pyridine (0.5 ml, 6 mmol) was added and the resulting solution warmed up to R.T. over a period of 24 hrs. At this time, TLC (55:45 ethyl acetate:petroleum ether; ninhydrin) showed the formation of two major products (R_f = 0.37, monoacyl; R_f = 0.57, diacyl) with significant amounts of starting material (amide) remaining. The solvents were removed under reduced pressure to give an orange oil. Ethyl acetate was added and the resulting solution washed succesively with 5% sodium bicarbonate and 10% citric acid. The organic layer was dried ($MgSO_4$) and the solvent removed under reduced pressure to give a yellow-orange oil. Chromatography on silica gel (55:45 ethyl acetate:petroleum ether) afforded pure product as a colorless oil (0.957 g, 26%): **237h**; $[\alpha]_D$ -8.6° (c 3.48, acetone); ^1H NMR ($CDCl_3$, 500 MHz) δ 1.45 (9 H, s), 1.89-1.97 (1 H, m), 2.17-2.20 (1 H, m),

2.50 (1 H, m), 2.55-2.67 (2 H, m), 2.81 (2 H, m), 3.45-3.47 (2 H, m), 4.27 (1 H, dt, J = 8.1, 4.7 Hz), 5.07 (2 H, s), 5.07 (2 H, s), 5.48 (1 H, t, J = 5.8 Hz), 5.63 (1 H, d, J = 8.0 Hz), 7.28 - 7.34 (10 H, m), 9.14 (1 H, s); ^{13}CNMR ($CDCl_3$, 75.4 MHz) δ 27.37 (t), 27.81 (q), 33.18 (t), 35.93 (t), 37.45 (t), 53.64 (d), 66.53 (t), 66.88 (t), 82.43 (s), 127.88 (d), 127.93 (d), 128.04 (d), 128.36 (d), 128.37 (d), 136.09 (s), 136.38 (s), 156.15 (s), 156.34 (s), 170.91 (s), 173.03 (s), 173.11 (s); IR ($CHCl_3$) ν 3448, 3031, 2984, 1715, 1511, 1456, 1371, 1347, 1229, 1155, 1062, 1003, 909, 842 cm^{-1}; HRMS (FAB: H^+) exact mass calc. for $C_{28}H_{36}N_3O_8$ requires 542.2502, found 542.2495; *m/e* (relative intensity) 542 (5), 486 (3), 442 (2), 223 (10), 181 (4), 91 (100): **238h**; oil; $[\alpha]_D$ -10.34° (c 5.0, acetone); ^{1}H NMR ($CDCl_3$, 500 MHz) δ 1.46 (9 H, s), 1.79-1.83 (1 H, m), 2.26-2.31 (1 H, m), 2.61-2.71 (2 H, m), 2.84-2.84 (4 H, m), 3.43-3.52 (4 H, m), 4.25 (1 H, dt, J = 8.3, 4.2 Hz), 5.05 (2 H, s), 5.07 (4 H, s), 5.38 (2 H, m), 5.49 (1 H, d, J = 6.5 Hz), 7.30-7.33 (15 H, m); ^{13}C NMR ($CDCl_3$, 75.4 MHz) δ 27.81 (q), 34.53 (t), 36.41 (t), 38.73 (t), 53.20 (d), 66.63 (t), 66.94 (t), 82.62 (s), 127.92 (d), 128.01 (d), 128.08 (d), 128.20 (d), 128.38 (d), 128.40 (d), 136.03 (s), 136.32 (s), 156.22 (s), 170.63 (s), 175.72 (s); IR ($CHCl_3$) ν 3453, 3032, 2984, 1720, 1512, 1455, 1370, 1348, 1229, 1173, 1156, 1063, 1003, 910, 842 cm^{-1}; HRMS (FAB: H^+) exact mass calc. for $C_{39}H_{47}N_4O_{11}$ requires 747.3241, found 747.3257; *m/e* (relative intensity) 747 (2), 428 (3), 206 (4), 181 (5), 91

(100); Anal. Calcd. for $C_{39}H_{46}N_4O_{11}$: 62.72% C, 6.21% H, 7.50% N found 62.92% C, 6.20% H, 7.71% N.

N_α(carbobenzyloxy)-N_γ[N-(carbobenzyloxy)-β-alanyl]-L-glutamine (**250**); N_α(carbobenzyloxy)-N_γ[N-(carbobenzyloxy)-β-alanyl)-α-tBu-L-glutamine (0.794 g, 1.47 mmol) was dissolved in dichloromethane (13 ml) and cooled to -78 °C. Trifluoroacetic acid (3.4 ml, 44 mmol) was added and the resulting mixture placed at 0 °C for 24 hrs. Additional Trifluoroacetic acid (3 ml) and dichloromethane (8 ml) were added and stirring continued at 0 °C for an additional 24 hrs. At this time TLC (100% ethyl acetate; ninhydrin) showed the clean formation of product (R_f = 0.36 streak) and traces of starting material (R_f = 0.68). The solvent was evaporated under high vacuum at R.T. Ethyl acetate was added and the solution extracted with saturated sodium bicarbonate. The layers were separated and the aqueous layer acidified with dilute HCl to pH = 2. Extraction of the aqueous layer with ethyl acetate followed by drying ($MgSO_4$) and removal of the solvent under reduced pressure gave product as a foam. Recrystallization from ethyl acetate/chloroform/petroleum ether afforded pure product as a white solid (0.705 g, 99%): m.p. = 54-56 °C; $[\alpha]_D$ -4.43 (c 5.74, acetone); ^1H NMR ($CDCl_3$, 500 MHz) δ 2.04-2.08 (1 H, m), 2.21-2.25 (1 H, m), 2.56-2.60 (2 H, m), 2.80 (2 H, m), 3.43-3.44 (2 H, m), 4.39-4.40 (1 H, m), 5.05 (2 H, s), 5.07 (2 H, s), 5.47 (1 H, m), 5.84 (1 H, d, J = 8.0 Hz), 7.31-7.34 (10 H, m), 9.44 (1 H,

s); ^{13}C NMR ($CDCl_3$, 75.4 MHz) δ 26.71 (t), 32.97 (t), 36.05 (t), 37.46 (t), 53.05 (d), 66.88 (t), 67.20 (t), 128.09 (d), 128.13 (d), 128.21 (d), 128.50 (d), 135.98 (s), 136.22 (s), 156.44 (s), 156.78 (s), 173.60 (s), 174.67 (s) ; IR ($CHCl_3$) ν 3436, 3281, 3031, 2958, 1712, 1513, 1455, 1409, 1381, 1343, 1227, 1200, 1142, 1063, 1004, 909 cm^{-1}; HRMS (FAB: H^+) exact mass calc. for $C_{24}H_{28}N_3O_8$ requires 486.1876, found 486.1844; *m/e* (relative intensity) 486 (13), 460 (10), 120 (50), 107 (93), 91 (100).

N_α(carbobenzyloxy)-N_γ[N-(carbobenzyloxy)-β-alanyl]-α-Bn-L-glutamine (**237g**); N-(carbobenzyloxy)-β-alanine (2.01 g, 9.0 mmol) was dissolved in diethyl ether (30 ml) and phosphorous pentachloride (1.37 g, 6.6 mmol) added at R.T. After stirring for 1 hr. the solvents were removed under high vacuum to give a colorless oil. N-(carbobenzyloxy)-α-Bn-L-glutamine (2.22 g, 6.0 mmol) and dichloromethane (35 ml) were added at R.T. followed pyridine (0.75 ml, 9.3 mmol) and the resulting solution stirred at R.T. for 24 hrs. At this time, TLC (55:45 ethyl acetate:petroleum ether; ninhydrin) showed the formation of three major products (R_f = 0.31, monoacyl; R_f = 0.52 diacyl; R_f = 0.63, nitrile) with significant amounts of starting material (amide) remaining. The solvents were removed under reduced pressure to give an orange oil. Ethyl acetate was added and the resulting solution washed succesively with 5% sodium bicarbonate and 10% citric acid. The organic layer was dried ($MgSO_4$) and the solvent removed

under reduced pressure to give a yellow-orange oil. Chromatography on silica gel (55:45 ethyl acetate:petroleum ether) afforded pure imide as a colorless oil (0.957g, 22%): **237g**; $[\alpha]_D$ -9.58° (c 5.98, acetone); ^{1}H NMR ($CDCl_3$, 500 MHz) δ 1.92-1.99 (1 H, m), 2.16-2.21 (1 H, m), 2.54-2.64 (2 H, m), 2.74 (2 H, m), 3.40-3.44 (2 H, m), 4.43 (1 H, dt, *J* = 8.3, 4.5 Hz), 5.05 (2 H, s), 5.06 (2 H, s), 5.13 (2 H, s), 5.49 (1 H, t, *J* = 6.0 Hz), 5.79 (1 H, d, *J* = 7.5 Hz), 7.27 - 7.31 (15 H, m), 9.26 (1 H, s); ^{13}CNMR ($CDCl_3$, 75.4 MHz) δ 26.73 (t), 33.01 (t), 35.89 (t), 37.31 (t), 53.21 (d), 66.55 (t), 66.94 (t), 67.21 (t), 127.84 (d), 127.92 (d), 128.02 (d), 128.07 (d), 128.32 (d), 128.34 (d), 128.45 (d), 134.98 (s), 135.94 (s), 136.28 (s), 156.14 (s), 156.36 (s), 171.72 (s), 173.06 (s); IR ($CHCl_3$) ν 3448, 3032, 1717, 1512, 1456, 1379, 1342, 1226, 1193, 1064, 1003, 909 cm^{-1}; HRMS (FAB: H^+) exact mass calc. for $C_{31}H_{34}N_3O_8$ requires 576.2346, found 576.2330; *m/e* (relative intensity) 576 (4), 107 (37), 91 (100): **238g**; oil; $[\alpha]_D$ -17.35° (c 6.76, acetone); ^{1}H NMR ($CDCl_3$, 500 MHz) δ 1.88-1.91 (1 H, m), 2.27-2.31 (1 H, m), 2.63-2.68 (2 H, m), 2.80 (4 H, m), 3.43-3.48 (4 H, m), 4.42 (1 H, dt, *J* = 8.5, 4.0 Hz), 5.06 (6 H, s), 5.16 (2 H, s), 5.38 (2 H, m), 5.61 (1 H, d, *J* = 7.5 Hz), 7.28-7.34 (20 H, m); ^{13}C NMR ($CDCl_3$, 75.4 MHz) δ 27.31 (t), 34.40 (t), 36.38 (t), 38.74 (t), 52.78 (d), 66.65 (t), 67.05 (t), 67.37 (t), 127.94 (d), 128.02 (d), 128.12 (d), 128.22 (d), 128.38 (d), 128.42 (d), 128.45 (d), 128.54 (d), 134.95 (s), 135.93 (s), 136.30 (s), 156.23 (s), 171.44 (s), 175.64 (s); IR ($CHCl_3$) ν 3452, 3033, 2957, 1720,

1512, 1455, 1368, 1341, 1224, 1178, 1063, 1003, 909 cm^{-1}; HRMS (FAB: H^+) exact mass calc. for $C_{42}H_{45}N_4O_{11}$ requires 781.3007, found 781.2937; *m/e* (relative intensity) 781 (4), 107 (44), 91 (100).

N-carbobenzyloxy-L-glutamic anhydride (**272**); Prepared following the procedure of Bergmann and Zervas. The product was further recrystallized from diethyl ether and petroleum ether (70% yield): m.p. 92-93 °C [lit. (225) m.p.= 93-94 °C]; ^1H NMR (acetone-d_6, 300 MHz) δ 2.20-2.23 (1 H, ddd, *J* = 2.5, 5.5, 12.0 Hz), 2.24-2.33 (1 H, ddd, *J* = 5.5, 12.7, 26.5 Hz), 2.96-3.02 (1 H, ddd, *J* = 2.5, 5.5, 18.0 Hz), 3.06-3.14 (1 H, ddd, *J* = 6.7, 12.7, 18.7 Hz), 4.73 (1 H, dt, *J* = 6.0, 13.0 Hz), 5.12 (2 H, s), 7.05 (1 H, d, *J* = 8.0 Hz), 7.31-7.40 (5 H, m); ^{13}C NMR ($CDCl_3$, 75.4 MHz) δ 23 (t), 29 (t), 52 (d), 68 (t), 128 (d) 155 (s), 169 (s); IR (mineral oil) ν 3304, 2923, 2853, 1815, 1760, 1697, 1538, 1457, 1378, 1267, 1071, 1023 cm^{-1}; MS (EI) exact mass calc. for $C_{13}H_{13}NO_5$ requires 263, found 263; m/e (relative intensity) 263 (5), 130 (14), 107 (36), 91 (100); Anal. Calcd. for $C_{13}H_{13}NO_5$: 59.31 % C, 4.98 % H, 5.32 % N, found 59.29 % C, 5.14 % H, 5.27 % N.

N-carbobenzyloxy-α-Bn-L-glutamic acid (**273**); Prepared following the method of Bergmann and Zervas (17% yield) (164): m.p. = 95-97 °C [lit. (228) m.p. = 95-96 °C]; ^1H NMR ($CDCl_3$, 500 MHz) δ 1.93-2.00 (1 H, m), 2.18-2.25 (1 H, m), 2.33-2.46 (2 H, m), 4.47 (1 H, dt, *J* = 7.8, 5.4 Hz), 5.09 (2

H, s), 5.16 (2 H, s), 5.50 (1 H, d, J = 8.3 Hz), 7.30-7.37 (10 H, m), 9.45 (1 H, bs); ^{13}CNMR ($CDCl_3$, 75.4 MHz) δ 27.23 (t), 29.55 (t), 53.04 (d), 66.97 (d), 67.25 (d), 127.88 (d), 128.02 (d), 128.12 (d), 128.32 (d), 128.35 (d), 128.44 (d), 134.80 (s), 155.81 (s), 171.44 (s), 177.48 (s); IR (mineral oil) ν 3317, 3201, 2925, 2854, 1730, 1686, 1542, 1457, 1378, 1350, 1264, 1171, 1070, 819, 740 cm^{-1}; HRMS (FAB: H^+) exact mass calc. for $C_{20}H_{22}NO_6$ requires 372.1447, found 372.1499; m/e (relative intensity) 372 (61), 328 (23), 238 (6), 91 (100); Anal. Calcd. for $C_{20}H_{21}NO_6$: 64.68% C, 5.70% H, 3.77% N; found 64.66% C, 5.74% H, 3.74% N.

N_{α}-(carbobenzyloxy)-α-tBu-L-asparagine (**269**); N-(carbobenzyloxy)-L-asparagine (4.67 g, 17.6 mmol) was suspended in dioxane (50 ml) and cooled to -78 °C under positive nitrogen pressure. Cold isobutylene (50 ml) was added followed by dropwise addition of concentrated sulfuric acid (36 M, 4ml) at -78 °C. The resulting mixture was allowed to warm up to R.T. over a period of 4.5 hrs. in a closed vessel. Diethyl ether (150 ml) was added and the organic layer washed with 10% sodium bicarbonate (390 ml), saturated sodium bicarbonate,dried ($MgSO_4$), and filtered. The solvent was removed under reduced presure to give a colorless oil. The product was crystallized from ethyl acetate/petroleum ether to give a white solid (3.75 g, 66%): m.p. = 103-104 °C; $[\alpha]_D$ -10.0° (c 3.41, acetone); ^{1}H NMR ($CDCl_3$, 300 MHz) δ 1.43 (9 H, s), 2.67-2.73 (1 H, dd, J =

15.9, 4.1 Hz), 2.82-2.89 (1 H, dd, J = 16.1, 5.3 Hz), 4.45 (1 H, dt, J = 8.8, 4.8 Hz), 5.10 (2 H, s), 5.92 (1 H, s), 5.98 (1 H, s), 6.06 (1 H, d, J = 8.1 Hz), 7.29-7.36 (5 H, m); ^{13}C NMR ($CDCl_3$, 75.4 MHz) δ 27.75 (q), 37.38 (t), 51.24 (d), 66.86 (t), 82.41 (s), 127.92 (d), 128.06 (d), 128.44 (d), 136.21 (s), 156.22 (s), 170.08 (s), 172.43 (s); IR ($CHCl_3$) ν 3492, 3411, 3012, 2983, 1717, 1690, 1592, 1508, 1456, 1396, 1371, 1342, 1228, 1156, 1063, 1028, 845, 698 cm^{-1}; HRMS (FAB: H^+) exact mass calc. for $C_{16}H_{23}N_2O_5$ requires 323.1607, found 323.1638; *m/e* (relative intensity) 323 (45), 267 (65), 223 (53), 91 (100); Anal. Calcd. for $C_{16}H_{22}N_2O_5$: 59.62% C, 6.88% H, 8.69% N, found 59.65% C, 6.87% H, 8.60% N.

α-tBu-L-asparagine (**270**); N_α(carbobenzyloxy)-α-tBu-L-asparagine (1.235 g, 3.84 mmol) was dissolved in THF (16 ml) under positive nitrogen pressure. 10% Pd/C was added followed by 1,4-cyclohexadiene (3.6 ml). The mixture was warmed until a spontaneous exothermic reaction took place. After approximately 5 min. from this exotherm TLC (100% ethyl acetate, ninhydrin stain) showed the clean formation of product (R_f = 0.05) at the expense of starting material (R_f = 0.45). The solvent was removed and the residue filtered through a bed of celite eluting with methanol. Removal of the solvent under reduced pressure afforded product as a light yellow oil which crystallized on standing at R.T. (0.715g, 99%): m.p. = 91-93 °C; $[\alpha]_D$ -159.2° (c 1.12, acetone); ^1H NMR (CD_3OD, 300 MHz) δ 1.46 (9 H, s), 2.52-2.59

(1 H, dd, J = 15.6, 6.9 Hz), 2.60-2.67 (1 H, dd, J = 15.6, 5.1 Hz), 3.65-3.67 (1 H, dt, J = 6.9, 5.1 Hz); ^{13}C NMR (CD_3OD, 75.4 MHz) δ 28.25 (q), 39.90 (t), 52.72 (d), 82.55 (s), 174.49 (s), 175.37 (s); IR ($CHCl_3$) ν 3475, 3410, 3303, 3008, 2984, 2936, 1727, 1678, 1589, 1394, 1370, 1283, 1253, 1156, 958, 905, 844 cm^{-1}; HRMS (FAB: H^+) exact mass calc. for $C_8H_{17}N_2O_3$ requires 189.1239, found 189.1261; *m/e* (relative intensity) 189 (100), 133 (65), 107 (39); Anal. Calcd. for $C_8H_{16}N_2O_3$: 51.03% C, 8.57% H, 14.88% N, found 49.91% C, 8.45% H, 14.40% N.

N_α-[N-(carbobenzyloxy)-α-Bn-γ-L-glutamyl]-α-tBu-L-asparagine (**274**); A mixture of N_α(carbobenzyloxy)-α-Bn-L-glutamic acid (0.98 g, 2.6 mmol) and α-tBu-L-asparagine (0.50 g, 2.6 mmol) were dissolved in THF (12 ml) and cooled to -78 °C under positive nitrogen pressure. A solution of DCC (0.54 g, 2.6 mmol) in THF (7 ml) was added and the resulting solution warmed up to 0 °C over a period of 2 hrs. and then to R.T. over a period of 10 hrs. At this time TLC (100% ethyl acetate, ninhydrin stain) showed the formation of product (R_f = 0.38) and some remaining starting material (R_f = 0.02 amine). Ethyl acetate was added followed by glacial acetic acid (5 drops) and the resulting mixture stirred at R.T. for 10 min. The solids were filtered off and washed with ethyl acetate. The organic layer was washed with 10% potassium bisulfate, saturated sodium bicarbonate, and dried ($MgSO_4$). The solvent was removed under reduced pressure to

give a colorless oil. The product was crystallized from ethyl acetate/petroleum ether to afford a colorless solid (1.17 g, 78%): m.p. = 143-144 ^{o}C; $[\alpha]_D$ -8.4^{o} (c 2.04, acetone); ^{1}H NMR ($CDCl_3$, 500 MHz) δ 1.43 (9 H, s), 1.92-1.99 (1 H, m), 2.18-2.24 (1 H, m), 2.28 (2 H, t, J = 6.8 Hz), 2.69-2.73 (1 H, dd, J = 15.9, 4.2 Hz),), 2.77-2.81 (1 H, dd, J = 15.9, 5.1 Hz), 4.39-4.43 (1 H, dt, J = 7.8, 4.4 Hz), 4.61-4.64 (1 H, dt, J = 7.3, 4.6 Hz), 5.07 (2 H, d, J = 4.9 Hz), 5.15 (2 H, s), 5.75 (1 H, s), 6.02-6.15 (3 H, m), 6.98 (1 H, d, J = 7.8 Hz), 7.27-7.40 (10 H, m); ^{13}C NMR ($CDCl_3$, 75.4 MHz) δ 27.72 (t), 27.80 (q), 31.75 (t), 37.20 (t), 49.57 (d), 53.50 (d), 66.93 (t), 67.18 (t), 82.36 (s), 128.05 (d), 128.11 (d), 128.21 (d), 128.40 (d), 128.46 (d), 128.56 (d), 135.20 (s), 136.16 (s), 156.18 (s), 169.85 (s), 171.82 (s), 171.91 (s), 172.43 (s); IR ($CHCl_3$) ν 3412, 3012, 2937, 1728, 1682, 1592, 1510, 1455, 1395, 1371, 1342, 1232, 1157, 1053, 844, 698, 670 cm^{-1}; HRMS (FAB: H^+) exact mass calc. for $C_{28}H_{36}N_3O_8$ requires 542.2502, found 542.2531; *m/e* (relative intensity) 542 (7), 486 (12), 442 (4), 378 (1), 223 (9), 199 (9), 107 (4), 91 (100); Anal. Calcd. for $C_{28}H_{35}N_3O_8$: 62.10% C, 6.51% H, 7.76% N, found 61.81% C, 6.56% H, 7.64% N.

N_α-[N-(carbobenzyloxy)-α-Bn-γ-L-glutamyl]-L-asparagine **(275)**; N_α-[N-(carbobenzyloxy)-α-Bn-γ-L-glutamyl]-α-tBu-L-asparagine (0.525 g, 0.97 mmol) was dissolved in dichloromethane (11 ml) and cooled to -78 ^{o}C under positive nitrogen pressure. Trifluoroacetic acid (2.5 ml) was added

and the resulting solution warmed up to 0 °C over a period of 14 hrs. Additional trifluoroacetic acid (1.5 ml) was added and the solution stirred at 0 °C for an additional 8 hrs. At this time additional trifluoroacetic acid (2.5 ml) and dichloromethane (10 ml) was added and the resulting solution stirred at 0 °C for an additional 24 hrs. At this point TLC (100% ethyl acetate, ninhydrin stain) showed the clean formation of product and little starting material. The solvents were removed with high vacuum to give a light amber colored oil. The product was crystallized from chloroform/petroleum ether. Further recrystallization from methanol/ethyl acetate/petroleum ether afforded pure product as a white solid (0.378 g, 80%): m.p. = 137-139 °C; $[\alpha]_D$ -5.51° (c 0.49, methanol); ^{1}H NMR (CD_3OD, 500 MHz) δ 1.89-1.97 (1 H, m), 2.14-2.21 (1 H, m), 2.33 (2 H, t, J = 7.3 Hz), 2.69-2.73 (1 H, dd, J = 15.5, 6.2 Hz),), 2.73-2.78 (1 H, dd, J = 15.5, 5.2 Hz), 4.23-4.26 (1 H, dd, J = 9.3, 4.9 Hz), 4.69-4.72 (1 H, t, J = 5.9 Hz), 5.04-5.06 (1 H, d, J = 12.2 Hz), 5.08-5.11 (1 H, d, J = 12.2 Hz), 5.13-5.18 (2 H, dd, J = 15.1, 12.4 Hz), 7.28-7.34 (10 H, m); ^{13}C NMR (CD_3OD, 75.4 MHz) δ 28.24 (t), 32.86 (t), 37.73 (t), 50.41 (d), 55.07 (d), 67.71 (t), 67.96 (t), 128.80 (d), 129.00 (d), 129.16 (d), 129.27 (d), 129.46 (d), 129.57 (d), 137.20 (s), 138.08 (s), 158.65 (s), 173.47 (s), 174.23 (s), 174.46 (s), 174.99 (s); IR (KBr) ν 3500-2500 (broad), 3390, 3319, 3072, 2967, 1737, 1655, 1543, 1449, 1420, 1390, 1343, 1308, 1273, 1202, 1073, 1044, 955, 908, 844, 750, 697, 626, 597 cm^{-1}; HRMS (FAB: H^+)

exact mass calc. for $C_{24}H_{28}N_3O_8$ requires 486.1876, found 486.1892; *m/e* (relative intensity) 486 (3), 169 (8), 133 (14), 91 (100); Anal. Calcd. for $C_{24}H_{27}N_3O_8$: 59.36% C, 5.61% H, 8.66% N, found 58.11% C, 5.71% H, 8.35% N.

N-(γ-L-glutamyl)-L-asparagine (**255**); N_α-[N-(carbobenzyloxy)-α-Bn-γ-L-glutamyl]-L-asparagine (0.305 g, 0.63 mmol) was suspended in a mixture of ethanol/methanol (3 ml/2 ml) and heated until most of the solid dissolved. 10% Pd/C (0.3 g) was added followed by 1,4-cyclohexadiene (1.4 ml, 15 mmol) and the resulting mixture warmed until an exothermic reaction took place. After this exotherm the reaction mixture was stirred at R.T. for 30 min. At this time TLC (100% ethyl acetate, ninhydrin stain) showed the clean formation of product at the origin at the expense of starting material. The solvents were removed under reduced pressure at 50 °C and the residue filtered through a bed of celite eluting with water. The aqueous layer was freeze dried overnight to give product as a white solid (0.123g, 75%): m.p. = 213 °C (dec.); $[\alpha]_D$ +53.33° (c 0.75, 5 mM NaOH); ^{1}H NMR (D_2O, 300 MHz) δ 2.15-2.22 (2 H, m), 2.53 (2 H, t, J = 7.5 Hz), 2.76-2.84 (1 H, dd, J = 15.6, 8.1 Hz), 2.87-2.94 (1 H, dd, J = 15.6, 5.1 Hz), 3.88 (1 H, t, J = 6.2 Hz), 4.71-4.75 (1 H, dd, J = 7.5, 5.4 Hz); ^{13}C NMR (D_2O, 75.4 MHz) δ 25.72 (t), 30.91 (t), 36.16 (t), 49.66 (d), 53.37 (d), 173.97 (s), 174.61 (s); IR (KBr) ν 3500-2500 (broad), 3248, 3084, 2955, 2625, 1719, 1655, 1584, 1508, 1437, 1408, 1349, 1255,

1226, 1149, 1126, 1067, 991, 914, 738, 697, 638, 538, 479 cm^{-1}; HRMS (FAB: H^+) exact mass calc. for $C_9H_{16}N_3O_6$ requires 262.1039, found 262.1023.

α-tBu-L-glutamine (276); N_α(carbobenzyloxy)-α-tBu-L-glutamine (0.281 g, 8.47 mmol) was dissolved in THF (5 ml) under positive nitrogen pressure 10% Pd/C (0.28 g) was added followed by 1,4-cyclohexadiene (0.8 ml, 8.5 mmol). The mixture was warmed until a spontaneous exothermic reaction took place. After approximately 5 min. from this exotherm, TLC (100% ethyl acetate, ninhydrin stain) showed the clean formation of product (R_f = 0.02) at the expense of starting material (R_f = 0.35). The solvent was removed and the residue filtered through a bed of celite eluting with petroleum ether:ethyl acetate (50:50) and then methanol. Removal of the solvent under reduced pressure afforded product as a semisolid colorless material (0.155 g, 92%): ^1H NMR ($CDCl_3$, 300 MHz) δ 1.47 (9 H, s), 1.79 (2 H, s), 1.73-1.85 (1 H, m), 2.04-2.15 (1 H, m), 2.38 (1 H, t, J = 7.8 Hz), 3.37 (1 H, dd, J = 8.5, 4.9 Hz), 5.86 (1 H, bs), 6.21 (1 H, bs); ^{13}C NMR ($CDCl_3$, 75.4 MHz) δ 27.95 (q), 29.99 (t), 32.19 (t), 54.33 (d), 81.33 (s), 174.78 (s), 175.12 (s); HRMS (FAB: H^+) exact mass calc. for $C_9H_{19}N_2O_3$ requires 203.1396, found 203.1411; *m/e* (relative intensity) 203 (100), 147 (52), 130 (30), 101 (13), 84 (12).

N_{α}-[N_{α}-(carbobenzyloxy)-α-Bn-L-β-aspartyl]-α-tBu-L-glutamine (**277**); α-tBu-L-glutamine hydrochloride (0.332 g, 1.40 mmol) was suspended in THF (5 ml) at room temperature under positive nitrogen pressure. Triethylamine (0.12 ml, 1.4 mmol) was added and the resulting mixture stirred at room temperature for 5 min. N_{α}(carbobenzyloxy)-α-Bn-β-L-aspartic anhydride (0.971 g, 1.40 mmol) was added and the mixture stirred for 10 min. At this time TLC (100% ethyl acetate, ninhydrin stain) showed the clean formation of product (R_f = 0.43) at the expense of amine (R_f = 0.04) and anhydride (R_f = 0.64). After 1 hr. the solvent was removed under reduced pressure. Ethyl acetate was added followed by saturated sodium bicarbonate solution and the resulting mixture stirred at R.T. for 30 min to give a clear biphasic solution. The organic layer was washed with additional saturated bicarbonate solution, 10% citric acid, saturated sodium bicarbonate, water, and dried ($MgSO_4$). The solvent was removed under reduced pressure to give a white solid. The product was recrystallized from hot ethyl acetate/petroleum ether to afford a white solid (0.612 g, 81%): m.p. = 149-150 °C; $[\alpha]_D$ -15.6° (c 0.39, acetone); ^{1}H NMR ($CDCl_3$, 500 MHz) δ 1.44 (9 H, s), 1.73-1.94 (1 H, m), 2.08-2.17 (3 H, m), 2.75 (1 H, dd, J = 15.6, 3.9 Hz),), 2.93 (1 H, dd, J = 15.9, 4.6 Hz), 4.41 (1 H, dt, J = 8.5, 3.4 Hz), 4.68 (1 H, dt, J = 8.5, 4.2 Hz), 5.11 (2 H, s), 5.17 (1 H, s), 5.18 (1 H, s), 5.48 (1 H, s), 6.11 (1 H, s), 6.25 (1 H, d, J = 8.8 Hz), 6.64 (1 H, d, J = 7.3 Hz), 7.28-7.36 (10 H, m); ^{13}C NMR ($CDCl_3$, 75.4

MHz) δ 27.91 (q), 28.61 (t), 31.61 (t), 37.60 (t), 50.95 (d), 52.25 (d), 67.00 (t), 67.32 (t), 82.74 (s), 127.97 (d), 128.07 (d), 128.12 (d), 128.36 (d), 128.48 (d), 128.59 (d), 135.34 (s), 136.18 (s), 156.15 (s), 170.06 (s), 170.83 (s), 171.26 (s), 174.65 (s); IR ($CHCl_3$) ν 3412, 3012, 2937, 1725, 1678, 1606, 1501, 1454, 1371, 1336, 1304, 1220, 1156, 1060, 842, 698, 669 cm^{-1}; HRMS (FAB: H^+) exact mass calc. for $C_{28}H_{36}N_3O_8$ requires 542.2502, found 542.2479; *m/e* (relative intensity) 542 (30), 486 (15), 442 (6), 91 (100); Anal. Calcd. for $C_{28}H_{35}N_3O_8$: 62.10% C, 6.51% H, 7.76% N, found 62.55% C, 6.72% H, 7.76% N.

N_α[N_α-(carbobenzyloxy)-α-Bn-L-β-aspartyl]-L-glutamine (278); N_α[N_α-(carbobenzyloxy)-α-Bn-L-β-aspartyl]-α-tBu-L-glutamine (0.552 g, 1.02 mmol) was dissolved in dichloromethane (17 ml) and cooled to -78 °C under positive nitrogen pressure. Trifluoroacetic acid (3.9 ml, 51 mmol) was added and the resulting solution warmed up to 0°C over a period of 13 hrs. Additional dichloromethane (5 ml) and trifluoroacetic acid (3.5 ml) was added and the solution stirred at 0 °C for an additional 10.5 hrs. At this point TLC (100% ethyl acetate, ninhydrin stain) showed the clean formation of product and very little starting material. The solvents were removed with high vacuum to give a colorless oil. The product was crystallized and recrystallized from ethyl acetate/petroleum ether to give a white solid (0.484 g, 98%): m.p. = 184-186 °C; $[\alpha]_D$ -18.8° (c 0.24, DMSO); ^1H NMR

(DMSO-d_6, 500 MHz) δ 1.70-1.77 (1 H, m), 1.87-1.94 (1 H, m), 2.06-2.14 (2 H, m), 2.60 (1 H, dd, *J* = 7.8, 7.3 Hz), 2.67 (1 H, dd, *J* = 15.1, 7.4 Hz), 4.16 (1 H, dt, *J* = 8.3, 5.4 Hz), 4.49 (1 H, dt, *J* = 7.8, 5.9 Hz), 4.99 (1 H, d, *J* = 12.2 Hz), 5.04 (1 H, d, *J* = 12.7 Hz), 5.11 (2 H, s), 6.77 (1 H, s), 7.23 (1 H, s), 7.31-7.35 (10 H, m), 7.62 (1 H, d, *J* = 8.3 Hz), 8.25 (1 H, d, *J* = 7.8 Hz), 12.62 (1 H, bs); ^{13}C NMR (DMSO-d_6, 125.7 MHz) δ 27.00 (t), 31.30 (t), 36.58 (t), 50.74 (d), 51.66 (d), 65.58 (t), 66.09 (t), 127.66 (d), 127.71 (d), 127.83 (d), 127.97 (d), 128.35 (d), 128.39 (d), 135.91 (s), 136.81 (s), 155.83 (s), 168.83 (s), 171.42 (s), 173.29 (s), 173.37 (s); IR (KBr) ν 3500-2000 (broad), 3311, 3034, 1745, 1707, 1648, 1586, 1535, 1452, 1379, 1305, 1264, 1184, 1051, 1002, 744, 697, 643 cm^{-1}; HRMS (FAB: H^+) exact mass calc. for $C_{24}H_{28}N_3O_8$ requires 486.1876, found 486.1872; *m/e* (relative intensity) 486 (38), 442 (7), 352 (2), 91 (100); Anal. Calcd. for $C_{24}H_{27}N_3O_8$: 59.36% C, 5.61% H, 8.66% N, found 58.90% C, 5.81% H, 8.48% N.

Nα(β-L-aspartyl)-L-glutamine **(263)**; Nα[Nα-(carbobenzyloxy)-α-Bn-L-β-asparty]-L-glutamine (0.406 g, 0.837 mmol) was suspended in a mixture of methanol/ethanol (10 ml/5 ml). 10% Pd/ C (0.55 g) was added followed by 1,4-cyclohexadiene (1.6 ml, 17 mmol) and the resulting mixture warmed until an exothermic reaction took place. After this exotherm the reaction mixture was stirred at R.T. for 5 min. At this time TLC (100% ethyl acetate, ninhydrin stain) showed

the clean formation of product at the origin at the expense of starting material. The solvents were removed under reduced pressure and the residue filtered through a bed of celite eluting with water. The aqueous layer was freeze dried overnight to give product as colorless pellets (0.178 g, 81%): m.p. = 135 °C (dec.); $[\alpha]_D$ -0.7° (c 2.5, 1 M acetic acid); ^{1}H NMR (D_2O, 300 MHz) δ 1.93-2.03 (1 H, m), 2.14-2.24 (1 H, m), 2.36 (2 H, t, *J* = 7.5 Hz), 2.96 (1 H, d, *J* = 4.9 Hz), 2.98 (1 H, d, *J* = 2.9 Hz), 4.07 (1 H, dd, *J* = 6.6, 4.6 Hz), 4.33 (1 H, dd, *J* = 9.0, 4.9 Hz); ^{13}C NMR (D_2O, 75.4 MHz) δ 26.79 (t), 31.22 (t), 34.55 (t), 50.93 (d), 52.75 (d), 171.37 (s), 172.72 (s), 175.99 (s), 178.11 (s); HRMS (FAB: H^+) exact mass calc. for $C_9H_{16}N_3O_6$ requires 262.1039, found 262.1043; *m/e* (relative intensity) 262 (100), 190 (63), 186 (84), 167 (26), 149 (37).

2-[N-(carbobenzyloxy)]-4-cyanobutyric acid (**298**); Prepared following the method of Ressler and Ratzkin (212): colorless gel (quant. yield); ^{1}H NMR ($CDCl_3$, 500 MHz) δ 1.99-2.08 (1 H, m), 2.20-2.32 (1 H, m), 2.39-2.42 (2 H, m), 4.41-4.44 (1 H, m), 5.10 (2 H, s), 5.79 (1 H, d, *J* = 7.8 Hz), 7.31-7.37 (5 H, m), 10.39 (1 H, bs); ^{13}C NMR ($CDCl_3$, 75.4 MHz) δ 13.53 (t), 27.93 (t), 52.55 (d), 67.39 (t), 118.71 (s), 128.06 (d), 128.29 (d), 128.50 (d), 135.65 (s), 156.24 (s), 173.94 (s); IR ($CHCl_3$) ν 3421, 3026, 2954, 2609, 2250, 1720, 1509, 1453, 1422, 1344, 1228, 1051 cm^{-1}; HRMS (FAB: H^+)

exact mass calc. for $C_{13}H_{15}N_2O_4$ requires 263.1032, found 263.1031; *m/e* (relative intensity) 263 (36), 91 (100).

2-amino-4-cyanobutyric acid (**296**); 2-N-(Cbz)-4-cyanobutyric acid (1.33 g, 5.07 mmol) was dissolved in ethanol (10 ml) and 10% Pd/C (0.68 g) added followed by 1,4-cyclohexadiene (2.4 ml). The mixture was warmed until an exothermic reaction occured which caused a brief reflux. After 1 hr. at ambient temperature the solvents were removed under reduced pressure. The solid residue was filtered through celite with water and freeze dried overnight to give product as a white solid (1.2 g, 76%). Recrystallization from water/dioxane afforded pure product: m.p. = 227-229 °C [lit (212) m.p.= 227.5-229 °C]; $[\alpha]^{22}_D$ +38.8° (c 1.28, 1N acetic acid) [lit (229) $[\alpha]^{21}_D$ +32.2° (c 0.54, 1N acetic acid)]; ^1H NMR (D_2O, 500 MHz) δ 2.17-2.29 (2 H, dq, J = 7.2, 10.6 Hz), 2.69 (2 H, dt, J = 4.3, 7.5 Hz), 3.79 (1 H, t, J = 6.7 Hz) ; ^{13}C NMR (D_2O, 75.4 MHz) δ 13.24 (t), 26.00 (t), 53.04 (d), 119.79 (s), 172.74 (s) ; IR (KBr) ν 2959, 2122, 1618, 1588, 1414, 1342, 1314, 1210, 1150, 1085, 1011 cm^{-1}; HRMS (CI: H^+) exact mass calc. for $C_5H_9N_2O_2$ requires 129.066, found 129.063; *m/e* (relative intensity) 129 (100), 111 (4), 83 (42); Anal. Calcd. for $C_5H_8N_2O_2$: 46.87% C, 6.29% H, 21.86% N, found 46.85% C, 6.45% H, 21.70% N.

N_α(carbobenzyloxy)-α-Me-L-glutamine (**314**); N-(carbobenzyloxy)-L-glutamine (5.096 g, 18.20 mmol) was

dissolved in MeOH (65 ml) and a solution of Na_2CO_3 (0.96 g) in water (25 ml) added at R.T. The solution was stirred for 20 min. and the solvents removed to give a foamy white solid. DMF (70 ml) and methyl iodide (4.9 ml, 79 mmol) were added and the resulting solution warmed and stirred at R.T. overnight. At this time TLC (72:25 ethyl acetate:petroleum ether, ninhydrin) showed the formation of product. The solvents were removed under reduced pressure and the residue dissolved in ethyl acetate:water (200 ml:200 ml). Petroleum ether and 5% sodium bicarbonate solution were added and the resulting biphasic mixture stirred vigorously for 10 min. The product was filtered and washed with ethyl acetate:petroleum ether (25:75). Recrystallization from hot MeOH, ethyl acetate, and petroleum ether afforded pure product (4.42 g, 83%): m.p. = 133-134 °C [lit (126) m.p.= 139-140 °C]; $[\alpha]_D$ -20.1° (c 2.2, methanol); ^1H NMR (CD_3OD, 500 MHz) δ 1.88-1.99 (1 H, m), 2.10-2.17 (1 H, m), 2.31 (2 H, t, J = 7.6 Hz), 3.71 (3 H, s), 4.21 (1 H, dd, J = 9.0, 5.1 Hz), 5.08 (2 H, s), 7.28-7.36 (5 H, m); ^{13}C NMR (CD_3OD, 75.4 MHz) δ 26.70 (t), 30.82 (t), 51.10 (d), 53.35 (q), 66.04 (t), 127.15 (d), 127.36 (d), 127.81 (d), 135.45 (s), 156.95 (s), 172.50 (s), 175.85 (s); IR (KBr) ν 3422, 3328, 3202, 3064, 2952, 1743, 1694, 1654, 1542, 1420, 1349, 1248, 1210, 1074, 1046, 1026, 1003, 924, 885, 857, 758, 697, 642, 588 cm^{-1}; HRMS (FAB: H^+) exact mass calc. for $C_{14}H_{19}N_2O_5$ requires 295.1294, found 295.1293; m/e (relative intensity) 295 (88), 251 (9), 219

(6), 187 (7), 91 (100); Anal. Calcd. for $C_{14}H_{18}N_2O_4$: 57.14% C, 6.16% H, 9.52% N; found 57.12% C, 6.15% H, 9.43% N.

N_α(carbobenzyloxy)-L-glutarimide (**315**); Method A. Prepared following the method of Polonski (229) (14% yield). Method B. A dry flask was charged with sodium hydride (0.278 g 60% oil suspension ; 0.1668 g, 6.95 mmol) and washed with dry petroleum ether under a continuous positive nitrogen pressure. N-(carbobenzyloxy)-α-Me-L-glutamine (1.6104 g, 5.48 mmol) was added followed by THF (25 ml). The resulting mixture was stirred at room temperature until hydrogen evolution ceased (approx. 30 min.). At this time TLC (55:45 ethyl acetate:petroleum ether; ninhydrin) showed the clean formation of one product (R_f = 0.25) at the expense of starting material. The solvent was removed under reduced pressure to give an oil which was taken up in 20% potassium bisulfate (60 ml) and ethyl acetate (100 ml). The layers were separated and the aqueous layer extracted with ethyl acetate (2 X 100 ml). The organic layers were combined, dried ($MgSO_4$), and filtered. The solvent was removed under reduced pressure to give a white solid. Recrystallization from hot ethyl acetate:diethyl ether:petroleum ether and washed with petroleum ether:diethyl ether (3:2) afforded 1.328 g (93%): m.p. = 113-118 °C [lit. (126) m.p.= 122-123 °C]; $[\alpha]_D$ -21.92° (c 1.85, acetone); ^1H NMR ($CDCl_3$, 500 MHz) δ 1.88 (1 H, ddd, J = 26.4, 13.2, 4.9 Hz), 2.51-2.54 (1 H, m), 2.64-2.72 (1 H, m), 2.77-2.80 (1 H, m), 4.37 (1 H, dt, J =

6.4 Hz), 5.14 (2 H, s), 5.68 (1 H, d, J = 5.9 Hz), 7.32-7.37 (5 H, m), 8.41 (1 H, s); ^{13}C NMR ($CDCl_3$, 75.4 MHz) δ 24.99 (t), 30.94 (t), 51.89 (d), 67.09 (t), 127.96 (d), 128.10 (d), 128.36 (d), 135.18 (s), 155.89 (s), 171.13 (s), 171.39 (s); IR (KBr) ν 3351, 3256, 3098, 2954, 1708, 1534, 1458, 1366, 1338, 1297, 1249, 1193, 1084, 1064, 1037, 991, 876, 778, 734, 694 cm^{-1}; HRMS (FAB: H^+) exact mass calc. for $C_{13}H_{15}N_2O_4$ requires 263.1032, found 263.1040; m/e (relative intensity) 263 (30), 235 (4), 219 (15), 107 (48), 91 (100); Anal. Calcd. for $C_{13}H_{14}N_2O_4$: 59.52% C, 5.38% H, 10.69% N; found 59.38% C, 5.32% H, 10.62% N.

L-Glutarimide HBr (**308**); 31% HBr in acetic acid (w/v) (0.90 ml, 3.3 mmol) was added to N-(carbobenzyloxy)-L-glutarimide (0.2405 g, 0.918 mmol) and the resulting solution stirred at room temperature for 30 min under a continuous positive nitrogen pressure. After blowing nitrogen through the reaction mixture to evaporate the solvent, diethyl ether was added to precipitate the product. The mixture was stirred for 5 min. at room temperature and 5 min. at -78 °C. The product was filtered and washed once with diethyl ether and twice with acetone to afford 0.1476 g (77%): m.p. = 280 °C (dec.) [lit. (230) m.p.= 279 °C dec.]; $[\alpha]_D$ -14.9° (c 0.45, 1 M acetic acid); ^1H NMR (D_2O, 500 MHz) δ 2.22-2.31 (1 H, m), 2.45-2.51 (1 H, m), 2.89-2.92 (2 H, m), 4.42 (1 H, dd, J = 13.7, 5.4 Hz); ^{13}C NMR (D_2O, 75.4 MHz) δ 21.64 (t), 29.61 (t), 49.30 (d), 170.01 (s), 174.51 (s); IR (KBr) ν 3005, 1736,

1699, 1578, 1483, 1404, 1361, 1336, 1310, 1256, 1217, 1199, 1135, 1118, 1080, 1040, 1000, 962, 907, 840, 795, 755, 714, 677 cm^{-1}; HRMS (FAB: H^+) exact mass calc. for $C_5H_9N_2O_2$ requires 129.0664, found 129.0695; Anal. Calcd. for $C_5H_8N_2O_2$: 28.73% C, 4.34% H, 13.40% N, found 28.97% C, 4.37% H, 13.51% N.

(4*R*)-N-(*tert*-butoxycarbonyl)-4-formyl-2,2-dimethyl-3-oxazolidine (317); 3-(1,1-dimethylethyl)-4-methyl-(S)-2,2-dimethyl-3,4-oxazolidinedicarboxylate (219,220) (13.375 g, 51.64 mmol) was dissolved in dry toluene (100 ml) and cooled to -78 °C in a dry-ice acetone bath under a continuous positive nitrogen pressure. Diisobutylaluminum hydride (17.5 ml, 98.1 mmol) was cooled to -78 °C and added dropwise at a rate of approximately 1 drop every 20 sec. The solution was stirred at -78 °C for 3 hrs. at which point TLC (50:50 ethyl acetate:petroleum ether, ninhydrin stain) showed a large formation of product (R_f = 0.39) and little starting material. Cold methanol (25 ml at -65 °C) was added dropwise at -78 °C so as to avoid any major change in temperature. 1 M HCl (100 ml) was added followed by ethyl acetate (200 ml) and disodium ditartarate (saturated). After stirring for 20 min. at R.T. the layers were separated and the aqueous layer was further extracted with ethyl acetate. The organic layer was dried ($MgSO_4$) and the solvent removed under reduced pressure to give a clear light yellow oil. Chromatography on silica gel (40:60 ethyl acetate:petroleum ether, ninhydrin

stain) afforded pure product as a colorless oil (10.19 g, 86%): $[\alpha]_D$ +75.4° (c 1.57, ethyl acetate); ^1H NMR ($CDCl_3$, 500 MHz) δ 1.44-1.66 (15 H, series of singlets due to different conformations, 1.44, 1.52, 1.56, 1.61, 1.66), 4.07-4.11 (2 H, m), 4.18-4.37 (1 H, m), 9.55-9.61 (1 H, d and s two conformers, J = 2.4 Hz); ^{13}C NMR ($CDCl_3$, 75.4 MHz) δ 23.54 (q), 24.43 (q), 25.52 (q), 26.43 (q), 28.02 (q), 63.21 (t), 63.66 (t), 64.45 (d), 80.79 (s), 81.10 (s), 94.07 (s), 94.82 (s), 199.14 (d); IR ($CHCl_3$) ν 3026, 2983, 2937, 2888, 2819, 1737, 1703, 1477, 1456, 1394, 1380, 1369, 1250, 1215, 1167, 1097, 1062, 847 cm^{-1}; HRMS (FAB: H^+) exact mass calc. for $C_{11}H_{20}NO_4$ requires 230.1392, found 230.1366; m/e (relative intensity) 230 (37), 200 (87), 174 (100), 144 (40), 130 (26), 116 (70), 100 (95); Anal. Calcd. for $C_{11}H_{19}NO_4$: 57.63% C, 8.35% H, 6.11% N; found 57.62% C, 8.64% H, 5.96% N.

(4*R*)-N-(*tert*-butoxycarbonyl)-4-[(E)-3'-methoxy-3'-oxo-1'-propenyl]-2,2-dimethyl-3-oxazolidine (**318**) (4*R*)-N-(*tert*-butoxycarbonyl)-4-formyl-2,2-dimethyl-3-oxazolidine (2.3 g, 10 mmol) was dissolved in THF (30 ml) and cooled to -70 °C under a continuous positive nitrogen pressure. This solution was added dropwise to a -70 °C solution of methyl(triphenylphosphoranylidene)acetate (4.03 g, 12.1 mmol) in THF (30 ml). The mixture was allowed to warm up to R.T. over a period of 2 hrs. at which point TLC (30:70 ethyl acetate:petroleum ether, ninhydrin stain) showed the formation of product (R_f = 0.46) and little starting

material. The solvents were evaporated under reduced pressure and the residue taken up in petroleum ether to precipitate a white solid. The solid was filtered off and the solution concentrated to precipitated more solid. After several filtrations the solvent was evaporated to give a colorless oil. Chromatography on silica gel (30:70 ethyl acetate:petroleum ether, ninhydrin stain) afforded pure product as a colorless oil which solidified at -24 °C (2.58 g, 90%): trans ; m.p. = 44-46 °C [lit. (231) m.p.= 50 °C]; $[\alpha]_D$ +63.5° (c 2.63, diethyl ether); ^{1}H NMR ($CDCl_3$, 500 MHz) δ 1.42-1.64 (15 H, series of singlets due to different conformations, 1.42, 1.49, 1.51, 1.53, 1.60, 1.64), 3.73-3.75 (4 H, m), 3.78-3.81 (1 H, dt, J = 9.2, 2.8 Hz), 4.09 (1 H, t, J = 6.3 Hz), 4.41 (2/3 H, m), 4.55 (1/3 H, m), 5.90 (2/3 H, d, J = 16.0 Hz), 5.96 (1/3 H, d, J = 15.0 Hz), 6.82-6.86 (1 H, m); ^{13}C NMR ($CDCl_3$, 75.4 MHz) δ 23.50 (q), 24.59 (q), 26.37 (q), 27.21 (q), 28.30 (q), 51.51 (d), 51.62 (d), 57.94 (q), 67.08 (t), 67.27 (t), 80.15 (s), 80.66 (s), 93.96 (s), 94.44 (s), 121.77 (d), 145.99 (d), 146.29 (d), 166.49 (s); IR ($CHCl_3$) ν 3024, 2984, 2953, 2882, 1713, 1694, 1478, 1456, 1438, 1392, 1368, 1306, 1285, 1253, 1222, 1174, 1099, 1056, 977, 843 cm^{-1}; HRMS (FAB: H^+) exact mass calc. for $C_{14}H_{24}NO_5$ requires 286.1654, found 286.1653; m/e (relative intensity) 286 (32), 270 (18), 230 (100), 212 (14), 186 (42), 172 (75); Anal. Calcd. for $C_{14}H_{23}NO_5$: 58.93% C, 8.12% H, 4.91% N; found 58.95% C, 8.16% H, 4.84% N: cis.

(4*R*)-N-(*tert*-butoxycarbonyl)-4-[(E)-3'-amino-3'-oxo-1'-propenyl]-2,2-dimethyl-3-oxazolidine (**319**); (4*R*)-N-(*tert*-butoxycarbonyl)-4-[(E)-3'-hydroxy-3'-oxo-1'-propenyl]-2,2-dimethyl-3-oxazolidine (0.516 g, 1.91 mmol) was dissolved in dry diethyl ether (17 ml) and phosphorous pentachloride (0.44 g, 2.1 mmol) added at R.T. under a continuous positive nitrogen pressure. After stirring for 1 hr., the solvents were removed under high vacuum at R.T. to give a yellow oil. Diethyl ether (20 ml) was added and anhydrous ammonia bubbled in for approximately 10 min. until a thick clowdy precipitate appeared. The solvent was removed under reduced pressure to a very light yellow solid. The solid was dissolved in ethyl acetate and washed with 5% sodium bicarbonate solution. The organic layer was dried ($MgSO_4$) and the solvent removed under reduced pressure to give a white solid. Recrystallization from ethyl acetate/ petroleum ether afforded pure product (0.347 g, 68%). m.p. = 125-128 ^{o}C; $[\alpha]_D$ +58.7^{o} (c 1.03, acetone); ^{1}H NMR ($CDCl_3$, 500 MHz) δ 1.42-1.64 (15 H, series of singlets due to different conformations, 1.42, 1.48, 1.51, 1.54, 1.59, 1.64), 3.80 (1/2 H, d, J = 2.5 Hz), 3.82 (1/2 H, d, J = 2.5 Hz), 4.09 (1 H, m), 4.42 (1/2 H, m), 4.53 (1/2 H, m), 5.71 (1 H, bs), 5.82 (1 H, bs), 5.91 (1/2 H, d, J = 15.5 Hz), 6.02 (1/2 H, d, J = 15.0 Hz), 6.74 (1/2 H, d, J = 7.0 Hz), 6.77 (1/2 H, d, J = 6.0 Hz); ^{13}C NMR ($CDCl_3$, 75.4 MHz) δ 23.55 (q), 24.71 (q), 26.37 (q), 27.29 (q), 28.32 (q), 28.38 (q), 57.97 (d), 67.24 (t), 80.14 (s), 80.67 (s), 93.92 (s), 94.45 (s), 123.53 (d), 124.27 (d), 142.67 (d), 143.48 (d),

167.34 (s); IR ($CHCl_3$) ν 3528, 3412, 3010, 2985, 2937, 2881, 1689, 1650, 1592, 1478, 1456, 1394, 1379, 1368, 1248, 1220, 1170, 1099, 1057, 972, 840, 666 cm^{-1}; HRMS (FAB: H^+) exact mass calc. for $C_{13}H_{23}N_2O_4$ requires 271.1658, found 271.1655; *m/e* (relative intensity) 271 (20), 215 (100), 171 (20), 157 (37), 155 (39), 137 (72); Anal. Calcd. for $C_{13}H_{22}N_2O_4$: 57.76% C, 8.20% H, 10.36% N; found 57.60% C, 8.43% H, 10.16% N.

(4*R*)-N-(*tert*-butoxycarbonyl)-4-[(E)-3'-hydroxy-3'-oxo-1'-propenyl]-2,2-dimethyl-3-oxazolidine (**320**); (4*R*)-N-(*tert*-butoxycarbonyl)-4-[(E)-3'-methoxy-3'-oxo-1'-propenyl]-2,2-dimethyl-3-oxazolidine (0.549 g, 1.93 mmol) was dissolved in methanol (2 ml) and cooled to 0 °C. 1 M KOH (2.2 ml, 2.2 mmol) was added dropwise and the resulting solution allowed to warm to R.T. and stirred for 12 hrs. At this time TLC (40:60 ethyl acetate:petroleum ether, ninhydrin) showed the clean formation of product (R_f = 0.23, streak extending to the origin) at the expense of starting material (R_f = 0.64). The solution was acidified to pH = 7 with 0.5 M HCl and the methanol removed under reduced pressure. The resulting aqueous solution was acidified with cold 0.5 M HCl to pH = 1 to give a white precipitate which was extracted with ethyl acetate (2 X 25 ml) and dried ($MgSO_4$). Removal of the solvent under reduced pressure gave an oil which solidified as a white solid (0.476 g, 91%) : m.p. = 87-89 °C; $[\alpha]_D$ +58.7° (c 1.03, acetone); ^1H NMR ($CDCl_3$, 500 MHz) δ 1.43-1.65 (15 H, series of singlets due to different conformations,

1.43, 1.49, 1.52, 1.54, 1.60, 1.65), 3.82 (1/2 H, d, J = 2.5 Hz), 3.83 (1/2 H, d, J = 2.5 Hz), 4.11 (1 H, t, J = 7.5 Hz), 4.44 (1/2 H, m), 4.59 (1/2 H, m), 5.91 (1/2 H, d, J = 15.5 Hz), 5.97 (1/2 H, d, J = 15.5 Hz), 6.90-6.95 (1 H, m), 11.51 (1 H, bs); ^{13}C NMR ($CDCl_3$, 75.4 MHz) δ 23.34 (q), 24.35 (q), 26.15 (q), 26.99 (q), 28.11 (q), 57.75 (d), 66.82 (t), 66.97 (t), 80.21 (s), 80.83 (s), 93.92 (s), 94.37 (s), 121.58 (d), 124.27 (d), 147.71 (d), 148.00 (d), 151.349 (s), 151.96 (s), 170.40 (s); IR ($CHCl_3$) ν 3024, 2984, 2937, 2882, 1695, 1478, 1456, 1392, 1388, 1256, 1220, 1170, 1099, 1056, 978, 844 cm^{-1}; HRMS (FAB: H^+) exact mass calc. for $C_{13}H_{22}NO_5$ requires 272.1498, found 272.1458; *m/e* (relative intensity) 272 (24), 256 (13), 216 (100); Anal. Calcd. for $C_{13}H_{21}NO_5$: 57.55% C, 7.80% H, 5.16% N; found 57.52% C, 7.82% H, 5.09% N.

(4*R*)(E)-4-[N-(*tert*-butoxycarbonyl)]-5-hydroxy-2-pentenamide (**321**); (4*R*)-N-(*tert*-butoxycarbonyl)-4-[(E)-3'-amino-3'-oxo-1'-propenyl]-2,2-dimethyl-3-oxazolidine (0.068 g, 0.25 mmol) was dissolved in methanol (1 ml) and p-toluenesulfonic acid monohydrate (0.022 g, 0.12 mmol) added at R.T. After stirring the solution at R.T. for 72 hrs., TLC (95:5 ethyl acetate:methanol, ninhydrin stain) showed the formation of product (R_f = 0.36) and some remaining starting material (R_f = 0.56). The solvents were evaporated via positive nitrogen pressure nitrogen and the residue dissolved in additional methanol (0.5 ml). After 5 additional hours at R.T. the solvent was removed at R.T. and ethyl acetate added.

The organic solution was washed with 5% sodium bicarbonate solution and dried ($MgSO_4$). Removal of the solvent under reduced pressure gave crude product as a colorless oil. Chromatography on silica gel (95:5 ethyl acetate:methanol, ninhydrin stain) afforded pure product as a colorless oil. Recrystallization from chloroform:petroleum ether gave product as a white solid: m.p. = 108-109 ^{o}C; $[\alpha]_D$ +13.2^{o} (c 1.12, ethyl acetate); ^{1}H NMR (CD_3OD, 500 MHz) δ 1.44 (9 H, s), 3.57 (1 H, d, J = 6.0 Hz), 4.22-4.30 (1 H, m), 6.09 (1 H, dd, J = 15.5, 2.0 Hz), 6.73 (1 H, dd, J = 15.5, 5.5 Hz); ^{13}C NMR (CD_3OD, 75.4 MHz) δ 28.73 (q), 55.02 (d), 64.61 (t), 80.46 (s), 125.04 (d), 143.68 (d), 157.85 (s), 170.39 (s); IR (KBr) ν 3437, 3340, 3219, 2982, 2938, 2875, 1677, 1642, 1528, 1400, 1369, 1304, 1170, 1060, 1038, 1005, 973, 859, 757, 642 cm^{-1}; HRMS (FAB: H^+) exact mass calc. for $C_{10}H_{19}N_2O_4$ requires 231.1345, found 231.1346; *m/e* (relative intensity) 231 (100), 175 (31) 107 (23).

(4*R*)(E)-4-amino-5-hydroxy-2-pentenamide (**322**); (4*R*)-N-(*tert*-butoxycarbonyl)-4-[(E)-3'-amino-3'-oxo-1'-propenyl]-2,2-dimethyl-3-oxazolidine (0.172 g, 0.64 mmol) was dissolved in MeOH (5 ml) and anhydrous HCl (g) bubbled through the solution for 10 min. at R.T. After 2 hrs., TLC (100% ethyl acetate, nihydrin) showed the clean formation of product at the origin at the expense of starting material (R_f = 0.29-0.38). The solvent was removed under reduced pressure and the residue partitioned between diethyl ether:water. The

water layer was freeze dried overnight to give product as an oil; ^{1}H NMR (D_2O, 500 MHz) δ 3.77 (1 H, dd, J = 12.5, 6.5 Hz), 3.90 (1 H, dd, J = 12.5, 3.5 Hz), 4.15 (1 H, dt, J = 5.5, 5.0 Hz), 6.33 (1 H, d, J = 16.1 Hz), 6.70 (1 H, dd, J = 16.1, 6.8 Hz); ^{13}C NMR (D_2O, 75.4 MHz) δ 57.79 (t), 65.41 (d), 131.92 (d), 140.54 (d), 173.55 (s).

(4*R*)(E) Methyl 4-[N-(*tert*-butoxycarbonyl)]-5-hydroxy-2-pentenoate (**323**); (4*R*)-N-(*tert*-butoxycarbonyl)-4-[(E)-3'-methoxy-3'-oxo-1'-propenyl]-2,2-dimethyl-3-oxazolidine (0.578 g,2.03 mmol) was dissolved in acetonitrile:methanol (50:50, 2 ml) and p-toluenesulfonic acid monohydrate (0.30 g, 1.6 mmol) added at R.T. After stirring at R.T. for 45 min. TLC (60:40 ethyl acetate:petroleum ether, ninhydrin stain) showed the formation of product (R_f = 0.37) and some remaining starting material (R_f = 0.60). Sodium bicarbonate was added to bring the pH = 8-9. The organic solvents were removed under reduced pressure and the residue acidified to pH = 1-2 with 3 M HCl. The aqueous solution was extracted with ethyl acetate and the organic layer dried ($MgSO_4$). The solvent was removed under reduced pressure to give a colorless oil. Chromatography on silica gel (60:40 ethyl acetate:petroleum ether, ninhydrin stain) afforded pure product as a colorless oil: $[\alpha]_D$ +13.2° (c 1.12, ethyl acetate); ^{1}H NMR ($CDCl_3$, 500 MHz) δ 1.45 (9 H, s), 2.46 (1 H, bs), 3.31 (1 H, bs), 3.68-3.76 (5 H, m), 4.40 (1 H, m), 5.34 (1 H, d, J = 4.5 Hz), 6.01 (1 H, dd, J = 15.5, 1.5 Hz), 6.93 (1 H, dd, J = 15.7, 4.8

Hz); ^{13}C NMR ($CDCl_3$, 75.4 MHz) δ 28.29 (q), 51.60 (d), 64.36 (t), 122.15 (d), 145.55 (d), 155.50 (s), 166.42 (s); IR ($CHCl_3$) ν 3439, 3025, 2982, 2953, 1711, 1662, 1499, 1456, 1438, 1394, 1368, 1313, 1283, 1215, 1166, 1058, 978, 909, 864, 670, 532 cm^{-1}; HRMS (FAB: H^+) exact mass calc. for $C_{11}H_{20}NO_5$ requires 246.1341, found 246.1340; *m/e* (relative intensity) 246 (44), 190 (100); Anal. Calcd. for $C_{11}H_{19}NO_5$: 53.87% C, 7.81% H, 5.71% N; found 53.60% C, 7.96% H, 5.64% N.

(4*R*)(E)-4-[N-(*tert*-butoxycarbonyl)]-5-hydroxy-2-butenoic acid (**324**); Method A. (4*R*)-N-(*tert*-butoxycarbonyl)-4-[(E)-3'-hydroxy-3'-oxo-1'-propenyl]-2,2-dimethyl-3-oxazolidine (0.072 g, 0.27 mmol) was dissolved in acetonitrile:water (5:1, 2 ml) and p-toluenesulfonic acid monohydrate (0.003 g, 0.02 mmol) added at R.T. After 72 hrs. at R.T. TLC (60:40 ethyl acetate:petroleum ether, ninhydrin stain) showed the formation of product (R_f = 0.23) and some starting material remaining. 5% sodium bicarbonate solution was added until pH = 7. The acetonitrile was removed under reduced pressure and the remaining aqueous solution acidified to pH = 1-2 with 3 M HCl. The aqueous solution was extracted with ethyl acetate and the organic layer dried ($MgSO_4$). Removal of the solvent under reduced pressure afforded crude product. Chromatography on silica gel (70:30 ethyl acetate:petroleum ether, ninhydrin stain) gave pure product as a colorless oil (0.02 g, 33%). Method B. (4*R*)(E) Methyl 4-[N-(*tert*-butoxycarbonyl)]-5-hydroxy-2-pentenoate (0.014 g, 0.06 mmol)

was suspended in 1 M KOH (0.06 ml, 0.06 mmol) and methanol (6 drops at) at R.T.. After stirring at R.T. for 72 hrs., TLC (70:30 ethyl acetate:petroleum ether, ninhydrin stain) showed the formation of product (R_f = 0.24) and some remaining starting material (R_f = 0.38). The methanol was removed under reduced pressure after making certain that the solution pH = 7. 5% sodium bicarbonate was added and the aqueous solution extracted with ethyl acetate. The layers were separated and the aqueous layer acidified with 3 M HCl to pH = 1. The aqueous solution was extracted with ethyl acetate and the organic layer dried ($MgSO_4$). Removal of the solvent under reduced pressure afforded pure product which crystallized at -24 ^oC (0.012 g, 91%): m.p. = 148-150 ^oC; $[\alpha]_D$ +58.7^o (c 1.03, acetone); ^1H NMR (D_2O, 500 MHz) δ 1.47 (9 H, s), 3.61 (1 H, dd, J = 11.8, 6.8 Hz), 3.72 (1 H, dd, J = 11.5, 5.0 Hz), 4.32 (1 H, dt, J = 9.7, 4.8 Hz), 5.98 (1 H, dd, J = 16.0, 1.5 Hz), 6.53 (1 H, dd, J = 16.0, 5.0 Hz); ^{13}C NMR ($CDCl_3$, 75.4 MHz) δ 28.29 (q), 53.50 (d), 64.04 (t), 121.88 (d), 147.52 (d), 169.60 (s); IR ($CHCl_3$) ν 3422 (broad), 1702, 1654, 1560, 1420, 1165, 1060 cm^{-1}; HRMS (FAB: H^+) exact mass calc. for $C_{10}H_{18}NO_5$ requires 232.1185, found 232.1192; *m/e* (relative intensity) 232 (37), 216 (4), 176 (100); Anal. Calcd. for $C_{10}H_{17}NO_5$: 51.94% C, 7.41% H, 6.06% N; found 51.66% C, 7.68% H, 6.07% N.

APPENDIX
ABREVIATIONS FOR AMINO ACIDS

Amino Acid	Three-letter Abbreviation	One-letter Symbol
Alanine	Ala	A
Arginine	Arg	R
Asparagine	Asn	N
Aspartic Acid	Asp	D
Cysteine	Cys	C
Glutamine	Gln	Q
Glutamic Acid	Glu	E
Glycine	Gly	G
Histidine	His	H
Isoleucine	Ile	I
Leucine	Leu	L
Lysine	Lys	K
Methionine	Met	M
Phenylalanine	Phe	F
Proline	Pro	P
Serine	Ser	S
Threonine	Thr	T
Tryptophan	Trp	W
Tyrosine	Tyr	Y
Valine	Val	V

LIST OF REFERENCES

1. Carlomago, M. S., Chiariotti, L., Alifano, P., Nappo, A. G., and Bruni, C. B., *J. Mol. Biol.*, 203, 586 (1988).

2. Badet, B, Vermoote, P., and Haumont, P.-Y., *Biochemistry*, 26, 1940 (1987).

3. Koshland, D. E., and Levitzky, A., *The Enzymes*, Boyer, P. D., Ed., Academic Press, New York, pp. 539 (1974).

4. Blanche, F., Couder, M., Debusshe, L., Thibaut, D., Cameron, B., and Crouzet, J., *J. Bacteriol.*, 173, 6046 (1991).

5. McGrath, R., Vining, L. C., Sala, F., Westlake, D. W. S., *Can. J. Biochem.*, 46, 587 (1968).

6. Buchanan, J.M., *Adv. Enzymol. Relat. Areas Mol. Biol.*, 39, 91 (1973).

7. Zalkin, H., *Adv. Enzymol. Relat. Areas Mol. Biol.*, 66, 203 (1993).

8. Mei, B. and Zalkin, H., *J. Biol. Chem.*, 264, 16613 (1989).

9. Mei, B. and Zalkin, H., *J. Bacteriol.*, 172, 3512 (1990).

10. Andrulis, I. L., Chen, J., and Ray, P. N., *Mol. Cell. Biol.*, 7, 2435 (1987).

11. Tempest, D. W., and Meers, J. L., *Biochem. J.*, 117, 405 (1970).

12. Hartman, S. C., *J. Biol. Chem.*, 238, 3024 (1963).

13. Zalkin, H., *Adv. Enzymol. Relat. Areas Mol. Biol.*, 38, 1 (1973).

14. Meister, A., *Adv. Enzymol. Relat. Areas Mol. Biol.*, 62, 315 (1989).

15. Sampei, G., and Mizobuchi, K., *J. Biol. Chem.*, 264, 21230 (1989).

16. Tiedeman, A. A., Smith, J. M., and Zalkin, H., *J. Biol. Chem.*, 260, 8676 (1985).

17. Kaplan, J. B., and Nichols, B. P., *J. Mol. Biol.*, 168, 451 (1983).

18. Jah, D., Kim, Y.-C., Ishino, Y., Chen, M.-W., and Soll, D., *J. Biol. Chem.*, 265, 8059 (1990).

19. Yi, C. K., and Dietrich, L. S., *J. Biol. Chem.*, 247, 4794 (1972).

20. Crouzet, J., Cauchois, L., Blanche, F., Debussche, L, Thibaut, D., Rouyez, M.-C., Rigault, S., Mayaux, J.-F., and Cameron, B., *J. Bacteriol.*, 172, 5968 (1990).

21. Crouzet, J., Levy-Schil, S., Cameron, B., Cauchois, L., Rouyez, M.-C., Blanche, F., Debussche, L, Thibaut, D., *J. Bacteriol.*, 173, 6074 (1991).

22. Levitzki, A. and Koshland, D. E., *Biochemistry*, 10, 3365 (1971).

23. Zalkin, H. and Truitt, C. D., *J. Biol. Chem.*, 252, 5431 (1977).

24. Zalkin, H. and Murphy, T., *Biochem. Biophys. Res. Commun.*, 67, 1370 (1975).

25. Mantsala, P. and Zalkin, H., *J. Biol. Chem.*, 259, 14230 (1984).

26. Rubino, S. D., Nyunoya, H., and Lusty, C. J., *J. Biol. Chem.*, 261, 11320 (1986).

27. Humbert, R. and Simoni, R. D., *J. Bacteriol.*, 142, 212 (1980).

28. Burchall, J. J., Reichelt, E. C., and Wolin, M. J., *J. Biol. Chem.*, 239, 1794 (1964).

29. Cedar, H. and Schwartz, J. H., *J. Biol. Chem.*, 244, 4112 (1969).

30. Ravel, J. M., Norton, S. J., Humphreys, J. S., and Shive, W., *J. Biol. Chem.*, 237, 2845 (1962).

31. Reitzer, L. J. and Magasanik, B., *J. Bacteriol.*, 151, 1291 (1982).

32. McPhee, K. G., Nelson, R., and Schuster, S. M., *J. Bacteriol.*, 156, 475 (1983).

33. Ramos, F. and Wiame, J. M., *Eur. J. Biochem.*, 94, 409 (1979).

34. Surin, B. P. and Downie, J. A., *Mol. Microbiol.*, 2, 173 (1988).

35. Hongo, S., Matsumoto, T., and Sato, T., *Biochim. Biophys. Acta.*, 552, 258 (1978).

36. Huang, Y.-Z. and Knox, E. W., *Enzymes.*, 19, 314 (1975).

37. Luehr, C. A. and Schuster, S. M., *Arch. Biochem. Biophys.*, 237, 335 (1985).

38. Andrulis, I. L., Shotwell, M., Evans-Blacker, S., Zalkin, H., Siminovitch, L., and Ray, P. N., *Gene*, 80, 75 (1989).

39. Boehlein, S. K., Richards, N. G. J., and Schuster, S. M., *J. Biol. Chem.*, 269, 7450 (1994).

40. Smith, J. L., Zaluzec, E. J., Wery, J.-P., Niu, L., Switzer, R. L., Zalkin, H., and Satow, Y., *Science*, 264, 1427 (1994).

41. Kim, J. H., Krahn, J. M., Tomchick, D. R., Smith, J. L., and Zalkin, H., *J. Biol. Chem.*, 271, 15549 (1996).

42. Isupov, M. N., Obmolova, G., Butterworth, S., Badet-Denisot, M.-A., Badet, B., Polikarpov, I., Littlechild, J. A., and Teplyakov, A., *Structure*, 4, 801 (1996).

43. Tesmer, J. J. G., Klem, T. J., Deras, M. L., Davisson, V. J., and Smith, J. M., *Nat. Struct. Biol.*, 3, 74 (1996).

44. Van Heeke, G. and Schuster, S. M., *J. Biol. Chem.*, 264, 5503 (1989).

45. Van Heeke, G. and Schuster, S. M., *J. Biol. Chem.*, 264, 19475 (1989).

46. Pfeiffer, N. E., Melhaff, P. M., Wylie, D. E., and Schuster, S. M., *J. Biol. Chem.*, 262, 11565 (1987).

47. Cedar, H. and Schwartz, J. H., *J. Biol. Chem.*, 244, 4122 (1969).

48. Tso, J. Y.. Hermodson, M. A., and Zalkin, H., *J. Biol. Chem.*, 257, 3532 (1982).

49. Vollmer, S. J., Switzer, R. L., Hermodson, M. A., Bower, S. G., and Zalkin, H., *J. Biol. Chem.*, 258, 10582 (1983).

50. Sheng, S., Moraga-Amador, D., Van Heeke, G., Allison, R. D., Richards, N. G. J., and Schuster, S. M., *J. Biol. Chem.*, 268, 16771 (1993).

51. Drenth, J., Jansonius, J. N., Koebek, R., and Worthers, B. G., *The Enzymes*, 3, 485 (1971).

52. Richards, N. G. J. and Schuster, S. M., unpublished (1996).

53. Milman, H. A., Cooney, D. A., and Huang, C. Y., *J. Biol. Chem.*, 255, 1862 (1980).

54. Roberts, D. V., Enzyme Kinetics, Cambridge University Press, London (1977).

55. Markin, R. S. Luehr, C. A., and Schuster, S. M, *Biochemistry*, 20, 7226 (1981).

56. Habibzadegah-Tari, P., Ph.D. Dissertation, University of Florida (1996).

57. Felton, J., Michaelis, S., and Wright, A., *J. Bacteriol.*, 142, 221 (1980).

58. Nakamura, M., Yamada, M., Hirota, Y., Sugimoto, K., Oka, A., and Takanami, M., *Nucleic Acids Res.*, 9, 4669 (1981).

59. Scofield, M. A., Lewis, W. S., and Schuster, S. M., *J. Biol. Chem.*, 265, 12895 (1990).

60. Richards, N. G. J. and Schuster, S. M., *FEBS Lett.*, 313, 98 (1992).

61. Gibbs, R. A., Taylor, S., and Benkovic, S. J., *Science*, 258, 803 (1992).

62. Kornfield, R. and Kornfield, S., *Annu. Rev. Biochem.*, 54, 631 (1985).

63. Geiger, R. and Konig, W. in: The Peptides, Analysis, Synthesis, Biology, vol. 3 (E. Gross and Meienhofer, J., eds.) pp. 50-52, Academic Press, New York (1981).

64. Boehlein, S. K., Richards, N. G. J., Walworth, E. S., and Schuster, S. M., *J. Biol. Chem.*, 269, 26789 (1994).

65. Imperiali, B., Shannon, K. L., and Rickert, K. W., *J. Am. Chem. Soc.*, 114, 7942 (1992).

66. Imperiali, B., Shannon, K. L., Unno, M., and Rickert, K. W., *J. Am. Chem. Soc.*, 114, 7944 (1992).

67. Hendrickson, T. L., Spencer, J. R., Kato, M., and Imperiali, B., *J. Am. Chem. Soc.*, 118, 7636 (1996).

68. Stoker, P. W., O'Leary, M. H., Boehlein, S. K., Schuster, S. M., and Richards, N. G. J., *Biochemistry*, 35, 3024 (1996).

69. Boehlein, S. K., Schuster, S. M., and Richards, N. G. J., *Biochemistry*, 35, 3031 (1996).

70. Challis, B. C., and Challis, J., in: The Chemistry of Amides (J. Zabicky, ed.) pp. 759-773, Interscience, New York (1970).

71. Uflyand, I. E., Ryabukhin, Yu. I., Gorbunova, M. O., and Sheinker, V., Izv. Sev.-Kavk. Nauchn. Tsentra Vyssh. Shk., Estestv. Nauki, 78 (1990).

72. Hargreaves, M. K., Pritchard, J. G., and Dave, H. R., *Chem. Rev.*, 70, 439 (1970).

73. Remmers, L., *Chem. Ber.*, 7, 350 (1874).

74. Kay, P., *Chem. Ber.*, 26, 2848 (1893).

75. Kay, P., *Chem. Ber.*, 26, 2853 (1893).

76. Bistrzycki, A. and Ulffers, F., *Chem. Ber.*, 27, 91 (1894).

77. Ulffers, F. and von Janson, A., *Chem. Ber.*, 27, 93 (1894).

78. Smith, A. E. and Orton, K. J. P., *J. Chem. Soc.*, 93, 1242 (1908).

79. Sudborough, J. J., *J. Chem. Soc.*, 79, 533 (1901).

80. Lindemman, D., *Sitz. Akad. Wiss. Wien*, Math.-natw. Kl., 60, II. Abt., 53 (1869).

81. Hentschel, W., *Chem. Ber.*, 23, 2394 (1890).

82. Davidson, D. and Karten, M., *J. Am. Chem. Soc.*, 78, 1066 (1956).

83. Polya, J. B. and Tardrew, P. L., *J. Chem. Soc.*, 1081 (1948).

84. Polya, J. B. and Spotswood, T. M., *Rec. Trav. Chim.*, 67, 927 (1948).

85. Dunn, P., Parkes, E. A., and Polya, J. B., *Rec. Trav. Chim.*, 71, 676 (1952).

86. Wiley, R. H., Borum, O. H., and Bennett, L. L., *J. Am. Chem. Soc.*, 71, 2899 (1949).

87. Wiley, R. H., Borum, O. H., *J. Am. Chem. Soc.*, 72, 1626 (1950).

88. Cadwallader, D. E. and LaRocca, J. P., *J. Am. Pharm. Assoc.*, 45, 480 (1956).

89. Davidson, D. and Skovronek, H., *J. Am. Chem. Soc.*, 80, 376 (1958).

90. Hurd, C. D. and Prapas, A. G., *J. Org. Chem.*, 24, 388 (1959).

91. Barburao, K., Costello, A. M., Petterson, R. C., and Sander, G. E., *J. Chem. Soc. C*, 2779 (1968).

92. Pinner, A., *Chem. Ber.*, 25, 1435 (1892).

93. Titherley, A. W., *J. Chem. Soc.*, 79, 411 (1901).

94. Kuroda, Y., Saito, Y., Machida, K., and Uno, T., *Spectrochimica Acta*, 27, 1481 (1971).

95. Tarbouriech, M., *Compt. Rend.*, 137, 128 (1903).

96. Tarbouriech, M., *Compt. Rend.*, 137, 326 (1903).

97. Titherley, A. W. and Holden, T. H., *J. Chem. Soc.*, 101, 1871 (1912).

98. Dehn, W., *J. Am. Chem. Soc.*, 34, 1399 (1924).

99. Titherley, A. W., *J. Chem. Soc.*, 88, 1684 (1904).

100. Freundler, P., *Compt. Rend.*, 137, 712 (1903).

101. Thompson, Q. E., *J. Am. Chem. Soc.*, 73, 5841 (1951).

102. LaLonde, R. T. and Davis, C. B., *J. Org. Chem.*, 35, 771 (1970).

103. Wieland, V. T. and Mohr, H., *Ann. Chem.*, 599, 222 (1956).

104. Wieland, V. T. and Urbach, H., *Ann. Chem.*, 613, 84 (1958).

105. Tull, R., O'Neill, R. C., McCarthy, E. P., Pappas, J. J., and Chemerda, J. M., *J. Org. Chem.*, 29, 2425 (1964).

106. Weinstock, L. M., Karady, S., Roberts, F. E., Hoinowski, A. M., Brenner, G. S., Lee, T. B. K.,Lumma, W. C., and Sletzinger, M., *Tetrahedron Lett.*, 3979 (1975).

107. Mukaiyama, T., Ichikawa, J., and Asami, M., *Chem. Lett.*, 293 (1983).

108. Davies, J. S., Hassall, C. H., and Hopkins, K. H., *J. Chem. Soc. Perkin. Trans. I*, 2614 (1973).

109. Kantlehner, W., Fischer, P., Kugel, W., Mohring, E., and Bredereck, H., *Ann. Chem.*, 512 (1978).

110. Klinge, M., Cheng, H., Zabriskie, T. M., and Vederas, J. C., *J. Chem. Soc. Chem. Commun.*, 1379 (1994).

111. Wade, L. G., Jr., Organic Chemistry, 2nd ed., Prentice Hall, Englewood Cliffs, New Jersey (1991).

112. Gautier, M. A., *Compt. Rend.*, 67, 1255 (1868).

113. Gautier, M. A., *Ann. Chem.*, 150, 187 (1869).

114. Miller, E. H., *J. Am. Chem. Soc.*, 16, 43 (1894).

115. Seldner, R., *Amer. Chem. J.*, 17, 532 (1895).

116. Colby, C. E. and Dodge, F. D., *Amer. Chem. J.*, 13, 1 (1891).

117. Mathews, J. A., *J. Am. Chem. Soc.*, 20, 648 (1898).

118. Sumarokova, T. N., Slavinskaya, R. A., and Tember, T. A., *Zh. Org. Khim.*, 11, 2520 (1975).

119. Bergell, P., *Hoppe-Seyler's Z. Physiol. Chem.*, 51, 207 (1907).

120. Bergell, P. and Feigl, J., *Hoppe-Seyler's Z. Physiol. Chem.*, 54, 258 (1907).

121. Wiley, R. H. and Guerrant, W. B., *J. Am. Chem. Soc.*, 71, 981 (1949).

122. Toland, W. G. and Ferstandig, L. L., *J. Org. Chem.*, 23,

1350 (1958).

123. Strecker, A. *Ann. Chem.*, 103, 321 (1857).

124. Titherley, A. W., *J. Chem. Soc.*, 79, 396 (1901).

125. Rakshit, J. N., *J. Chem. Soc.*, 103, 1557 (1913).

126. Sondheimer, E. and Holley, R. W., *J. Am. Chem. Soc.*, 76, 2467 (1954).

127. Stevens, C. L. and Munk, M. E., *J. Am. Chem. Soc.*, 80, 4065 (1958).

128. Wolfe, J. F. and Trimitsis, G. B., *J. Org. Chem.*, 33, 894 (1968).

129. Rice, F. O., Greenberg, J., Waters, C. E., and Vollrath, R. E., *J. Am. Chem. Soc.*, 56, 1760 (1934).

130. Padgham, D. N. and Polya, J. B., *Australian. J. Sci.*, 13, 113 (1951).

131. Sminorva, N. V., Skoldinov, A. P., and Kocheshkov, K. A., *Doklady. Akad. Nauk. S.S.S.R.*, 84, 737 (1952).

132. Dunbar, R. E. and White, G. C., *J. Org. Chem.*, 23, 915 (1958).

133. Kato, K. and Wade, S., *Nippon. Kagaku. Zasshi.*, 83, 501 (1962).

134. King, F. E. and Kidd, D. A. A., *J. Chem. Soc.*, 3315 (1949).

135. Baker, B. R., Joseph, J. P., Schaub, R. E., and Williams, J. H., *J. Org. Chem.*, 19, 1786 (1954).

136. Kretov, A. E. and Kul'chitskaya, N. E., *Zh. Obshch. Khim.*, 26, 208 (1956).

137. von Auwers, K., *Ann. Chem.*, 309, 316 (1899).

138. Warren, W. H. and Briggs, R. A., *Chem. Ber.*, 64, 26 (1931).

139. Hagemeyer, H. J., U.S. Patent 2,656,360 (October 20, 1953).

140. Rothman, E. S., Serota, S., and Swern, D., *J. Org. Chem.*, 29, 646 (1964).

141. Bredereck, H., Gommper, R., and Bitzer, D., *Chem. Ber.*, 92, 1139 (1959).

142. Krafft, F. and Karnstens, H., *Chem. Ber.*, 25, 452 (1892).

143. Wheeler, H. W., Walden, P. T., and Metcalf, H. F., *Amer. Chem. J.*, 20, 64 (1898).

144. Gruszecki, W., Gruszecka, M., and Bradaczek, H., *Ann. Chem.*, 331 (1988).

145. Krohn, K., Franke, C., Jones, P. G., Aust, H.-J., Draeger, S., and Schulz, B., *Ann. Chem.*, 789 (1992).

146. Kikukawa, K, Kono, K., Wada, F., and Matsuda, T., *Bull. Chem. Soc. Jpn.*, 55, 3671 (1982).

147. Bowser, J. R., Williams, P. J., and Kurz, K., *J. Org. Chem.*, 48, 4111 (1983).

148. Mori, M., Kawaguchi, M., Hori, M., and Hamaoka, S., *J. Heterocycles.*, 39, 729 (1994).

149. Bates, R. B., Fletcher, F. A., Janda, K. D., and Miller, W. A., *J. Org. Chem.*, 49, 3038 (1984).

150. LeBlanc, J.-P. and Gibson, H. W., *J. Org. Chem.*, 59, 1072 (1994).

151. MaGee, D., Ramaseshan, M., and Leach, J. D., *Can. J. Chem.*, 73, 2111 (1995).

152. Berkowitz, L. M. and Rylander, P. N., *J. Am. Chem. Soc.*, 80, 6682 (1958).

153. Yoshifuji, S., Arakawa, Y., and Nitta, Y., *Chem. Pharm. Bull.*, 35, 357 (1987).

154. Sheehan, J. C. and Tullis, R. W., *J. Org. Chem.*, 39, 2264 (1974).

155. Rieche, A. and Schon, W., *Chem. Ber.*, 99, 3238 (1966).

156. Needles, H. L. and Whitfield, R. E., *J. Org. Chem.*, 31, 341 (1966).

157. Greene, T. W. and Wuts, P. G. M., Protective Groups in Organic Synthesis, 2nd ed., Wiley-Interscience, New York (1991).

158. Cahn, R. S., Ingold, C., and Prelog, V., *Angew. Chem.*

Int. Ed. Engl., 5, 385 (1966).

159. Williams, R. M., Synthesis of Optically Active α-Amino Acids, Pergamon Press, New York (1989).

160. Bada, J. L., in: Chemistry and Biochemistry of the Amino Acids, (Barrett, G. C. ed.) pp. 399-414, Chapman & Hall, London (1985).

161. Meienhofer, J., *ibid.*, pp. 297-337.

162. Csanady, G. and Medzihradszky, K., *Org. Prep. Proc. Int.*, 20, 180 (1988).

163. LeQuesne, W. J. and Young, G. T., *J. Chem. Soc.*, 1954 (1950).

164. Bergmann, M., Zervas, L., and Salzmann, L., *Chem. Ber.*, 1288 (1933).

165. Bergmann, M. and Zervas, L., *Z. Physiol. Chem.*, 221, 5 (1933).

166. Beecham, A. F., *J. Am. Chem. Soc.*, 76, 4615 (1954).

167. Scholtz, J. M. and Bartlett, P. A., *Synthesis*, 542 (1989).

168. Yoder, C. H., Copenhafer, W. C., and DuBeshter, B., *J. Am. Chem. Soc.*, 96, 4283 (1974).

169. Harris, R. K., Nuclear Magnetic Resonance Spectroscopy, Longman, London (1986).

170. Hoechst, F., FRG Patent 1,670,804, p. 264169-8 (1984).

171. Voet, D. and Voet, J. G., Biochemistry, John Wiley & Sons, New York (1990).

172. Stewart, J. J. P., *J. Comp. Chem.*, 10, 209 (1989).

173. Lee, C. M. and Kumler, W. D., *J. Am. Chem. Soc.*, 84, 565 (1962).

174. Hinderer, A. and Hess, H., *Chem. Ber.*, 107, 492 (1974).

175. Uno, T. and Machida, K., *Bull. Chem. Soc. Jpn.*, 34, 551 (1961).

176. Noe, E. A. and Raban, M., *J. Am. Chem. Soc.*, 97, 5811 (1975).

177. Laurent, A., Laurent, E., and Pellisier, N., *Tetrahedron Lett.*, 2955 (1970).

178. Steinmetz, W. E., *J. Am. Chem. Soc.*, 95, 2777 (1973).

179. Toth, G., *Acta. Chim. Acad. Sci. Hung.*, 64, 101 (1970).

180. Pine, S. H., Organic Chemistry, 5th ed., McGraw-Hill, New York (1987).

181. Carpenter, B. K., Determination of Organic Reaction Mechanisms, Wiley, New York (1974).

182. Fersht, A., Enzyme Structure and Mechanism, W. H. Freeman, New York (1985).

183. Jenks, W. P., *Chem. Rev.*, 72, 705 (1972).

184. Horvath, C. and Melander, W., *J. Chromatogr. Sci.*, 15, 394 (1977).

185. Munson, B., *Anal. Chem.*, 49, 772A (1977).

186. Lowe, G., *Tetrahedron*, 32, 291 (1976).

187. Polgar, S. and Halasz, P., *Biochem. J.*, 207, 1 (1982).

188. Bender, M. L. and Brubacher, L. J., *J. Am. Chem. Soc.*, 88, 5880 (1966).

189. Angelides, K. A. and Fink, A. L., *Biochemistry*, 17, 2959 (1978).

190. Angelides, K. A. and Fink, A. L., *Biochemistry*, 18, 2355 (1979).

191. Angelides, K. A. and Fink, A. L., *Biochemistry*, 18, 2363 (1979).

192. Khouri, H. E., Vernet, T., Menard, R., Parlati, F., Laflamme, P., Tessier, D. C., Gour-Salin, B. J., Thomas, D. Y., and Storer, A. C., *Biochemistry*, 30, 8929 (1991).

193. Menard, R., Khouri, H. E., Plouffe, C., Dupras, R., Ripoll, D., Vernet, T., Tessier, D. C., Laliberte, F., Thomas, D. Y., and Storer, A. C., *Biochemistry*, 29, 6706 (1990).

194. Dufour, E., Storer, A. C., and Menard, R., *Biochemistry*, 34, 9136 (1995).

195. Rich, D., in: Proteinase Inhibitors (A. G. Barrett and

G. Salvensen, ed.) pp. 153-173, Elsevier Science Publishers, Amsterdam (1986).

196. Drenth, J., Kalk, K. H., and Swen, H. M., *Biochemistry*, 15, 3731 (1976).

197. Kamphius, I. G., Kalk, K. H., Swarte, M. B. A., and Drenth, J., *J. Mol. Biol*, 179, 223 (1984).

198. Schroder, E., Phillips, C., Garmen, E. Harlos, K., and Crawford, C., *FEBS Lett.*, 315, 38 (1993).

199. Menard, R., Carriere, J., Laflamme, P., Plouffe, C., Khouri, H. E., Vernet, T., Tessier, D. C., Thomas, D. Y., and Storer, A. C., *Biochemistry*, 30, 8924 (1991).

200. Menard, R., Plouffe, C., Laflamme, P., Vernet, T., Tessier, D. C., Thomas, D. Y., and Storer, A. C., *Biochemistry*, 34, 464 (1995).

201. Lienhard, G. E., in: Enzyme Inhibitors as Drugs, (M. Sandler, ed.) pp. 43-51, Macmillan, London (1980).

202. Wolfenden, R., *Acc. Chem. Res.*, 5, 10 (1972).

203. Lucas, E. C. and Williams, A., *Biochemistry*, 8, 5125 (1969).

204. Sluyterman, L. A. E. and Wijdenes, J., *Biochim. Biophys. Acta*, 302, 95 (1973).

205. Lewis, C. A. and Wolfenden, R., *Biochemistry*, 16, 4890 (1977).

206. Brison, J.-R., Carey, P. R., and Storer, A. C., *J. Biol. Chem.*, 261, 9087 (1986).

207. Moon, J. B., Coleman, R. S., and Hanzlik, R. P., *J. Am. Chem. Soc.*, 108, 1350 (1986).

208. Liang, T.-C. and Abeles, R. H., *Arch. Biochem. Biophys.*, 252, 626 (1987).

209. Dufour, E., Storer, A. C., and Menard, R., *Biochemistry*, 34, 16382 (1995).

210. Gour-Salin, B. J., Storer, A. C., Castelhano, A., Krantz, A., and Robinson, V., *Enzyme Microb. Technol.*, 13, 408 (1991).

211. Petrov, K. A. and Andreev, L. N., *Russian Chem. Revs.*, 40, 505 (1971).

212. Ressler, C. and Ratzkin, H., *J. Org. Chem.*, 26, 3356 (1961).

213. Gautier, J. A., Miocque, M., and Farnoux, C. C., in: Chemistry of Amidines and Imidates (S. Patai, ed.) pp. 283-348, John Wiley & Sons, New York (1975).

214. Lee, M. and Lown, J. W., *J. Org. Chem.*, 52, 5717 (1987).

215. Roderick, W. R. and Bhatia, P. L., *J. Org. Chem.*, 28, 2018 (1963).

216. Kohler, H., *Ann. Chem.*, 134, 369 (1865).

217. Sanders, J. K. M. and Hunter, B. K., Modern NMR Spectroscopy: A Guide for Chemists, 2nd ed., Oxford University Press, New York (1993).

218. Bergmann, E. D., Ginsburg, D., and Pappo, R., *Org. React.*, 10, 179 (1959).

219. Garner, P. and Park, J. M., *J. Org. Chem.*, 52, 2361 (1987).

220. McKillop, A., Taylor, R. J. K., Watson, R. J., and Lewis, N., *Synthesis*, 31 (1994).

221. Dixon, M., *Biochem. J.*, 55, 170 (1953).

222. Williams, D. H. and Fleming, I., Spectroscopic Methods in Organic Chemistry, 4th ed., McGraw-Hill, London (1987).

223. Brent, E., in: Methods of Enzymatic Analysis (H. U. Bergmeyer, ed.) pp. 1704-1708, Academic Press, New York (1974).

224. Dewar, M. J. S., Zoebisch, E. G., Healy, E. F., and Stewart, J. J. P., *J. Am. Chem. Soc.*, 107, 3902 (1985).

225. Katsoyannis, P. G., Gish, D. T., Hess, G. P., and duVigneaud, V., *J. Am. Chem. Soc.*, 80, 2558 (1958).

226. Anderson, G. W. and Callahan, F. M., *J. Am. Chem. Soc.*, 82, 3359 (1960).

227. Bergmann, M. and Zervas, L., *Chem. Ber.*, 1192 (1932).

228. Sachs, H. and Brand, E., *J. Am. Chem. Soc.*, 75, 4610 (1953).

229. Brysk, M. M. and Ressler, C., *J. Biol. Chem.*, 245, 1156 (1970).

230. Polonski, T., *J. Chem. Soc. Perkin Trans. I*, 639 (1988).

231. Jako, I., Uiber, P., Mann, A., and Wermuth, C.-G., *J. Org. Chem.*, 56, 5729 (1991).

BIOGRAPHICAL SKETCH

Jose Guillermo Rosa Rodriguez, son of Ana Lydia Rodriguez and Jose Luis Rosa, was born in Ponce, Puerto Rico, on June 21, 1969. His education prior to college years varied from Catholic schools in Puerto Rico to public schools in Florida. In 1991 he obtained his B.S. in chemistry from the University of South Florida, as well as various awards in the field of chemistry. That same year he was granted a Patricia Roberts Harris Fellowship and became part of the Ph.D. graduate program at the University of Florida in the Organic Chemistry Division. In the spring of 1996 he was married to Lymari Montalvo and shortly after in the fall of 1996 he received his Ph.D. in chemistry from the University of Florida. His hobbies include composing and listening music, playing guitar, painting, and exercising.

I certify that I have read this study and that in my opinion it conforms to acceptable standards of scholarly presentation and is fully adequate, in scope and quality, as a dissertation for the degree of Doctor of Philosophy.

Nigel G. J. Richards, Chair
Associate Professor of
Chemistry

I certify that I have read this study and that in my opinion it conforms to acceptable standards of scholarly presentation and is fully adequate, in scope and quality, as a dissertation for the degree of Doctor of Philosophy.

Sheldon M. Schuster
Professor of Biochemistry
and Molecular Biology

I certify that I have read this study and that in my opinion it conforms to acceptable standards of scholarly presentation and is fully adequate, in scope and quality, as a dissertation for the degree of Doctor of Philosophy.

William R. Dolbier, Jr.
Professor of Chemistry

I certify that I have read this study and that in my opinion it conforms to acceptable standards of scholarly presentation and is fully adequate, in scope and quality, as a dissertation for the degree of Doctor of Philosophy.

J. Eric Enholm
Associate Professor of
Chemistry

I certify that I have read this study and that in my opinion it conforms to acceptable standards of scholarly presentation and is fully adequate, in scope and quality, as a dissertation for the degree of Doctor of Philosophy.

Gus Palenik
Professor of Chemistry

This dissertation was submitted to the Graduate Faculty of the Department of Chemistry in the College of Liberal Arts and Sciences and to the Graduate School and was accepted as partial fulfillment of the requirements for the degree of Doctor of Philosophy.

December, 1996

Dean, Graduate School